Cell Signalling in Chinese Hamster Ovary Cells Expressing Recombinant Muscarinic Receptors.

Thesis submitted for the degree of Doctor of Philosophy
at the University of Leicester.

by

Neil Thornton Burford B.Sc.(Hons).

Department of Cell Physiology and Pharmacology,
University of Leicester.

1994.

ProQuest LLC
789 East Eisenhower Parkway
P.O. Box 1346
Ann Arbor, MI 48106-1346

Contents.

page number.

Abstract.
Acknowledgements.

CHAPTER ONE. Introduction. 1

1.0 Introduction. 2
1.1 Muscarinic Receptor Subtypes. 2
1.1.1 Selective Antagonists. 3
1.1.2 Selective Agonists. 4
1.1.3 Localization and Distribution. 5
1.1.4 Molecular Structure of Muscarinic Receptors. 6
1.1.5 Muscarinic Receptor Desensitization. 8
1.2 G Proteins. 8
1.2.1 History of G Protein Discovery. 9
1.2.2 Receptor Interactions with G Proteins. 9
1.2.3 Mg^{2+} Requirements. 11
1.2.4 G Protein Activation. 12
1.2.5 Classification of $G\alpha$ Subunits and their Modulation of Effectors. 12
1.2.6 Classification of $G\beta\gamma$ Subunits and their Modulation of Effectors. 13
1.2.7 Molecular Structure of $G\alpha$ Subunits. 15
1.2.8 Molecular Structure of $G\beta\gamma$ Subunits. 16
1.3 Inositol Lipid-Specific Phospholipase C Isozymes. 17
1.3.1 PLC Isoforms. 17
1.3.2 PLC-β. 18
1.3.3 PLC-γ. 19
1.3.4 PLC-δ. 19
1.3.5 Inhibition of PLCs by PKC and PKA. 20
1.4 Inositol Phosphate Metabolites as Cellular Signals. 20
1.4.1 $Ins(1,4,5)P_3$ Metabolism. 21
1.4.2 Functions of $Ins(1,3,4,5)P_4$. 21
1.4.3 Recycling of Inositol. 22
1.4.4 $Ins(1,3,4,5,6)P_5$ and $InsP_6$. 22
1.4.5 $Ins(1,4,5)P_3$ Receptors. 23
1.4.6 $Ins(1,4,5)P_3$-Induced Calcium Release. 24
1.4.7 Calcium-Induced Calcium Release. 25

1.5 Adenylate Cyclase. 27
1.5.1 Structure. 27
1.5.2 Regulatory Properties. 27
1.5.3 Inhibition of Adenylate Cyclase. 28
1.5.4 Muscarinic Receptors and Adenylate Cyclase. 28
1.5.5 Metabolism of cAMP. 29
1.6 Aims. 29

CHAPTER TWO. General Methods. 31

2.1 Cell Lines. 32
2.2 Preparation of Plasmid DNA and Transfection Procedures. 32
2.3 Cell Culture. 33
2.4 Cell Preparation. 33
2.4.1 Intact Cell Preparation. 33
2.4.2 Membrane Preparation. 34
2.5 Cell Permeabilization. 34
2.5.1 Electroporation. 34
2.5.2 Saponin Permeabilization. 34
2.6 Protein Determinations. 34

CHAPTER THREE. Characterization of Recombinant Muscarinic Receptors in CHO-K1 Cells and Endogenously Expressed Muscarinic Receptors in SH-SY5Y Cells. 36

3.0 Introduction. 37
3.1 Methods. 37
3.1.1 Radioligand Binding Assay. 37
3.1.2 Data Analysis. 39
3.2 Results. 39
3.3 Discussion. 41

CHAPTER FOUR. Agonist Binding to Muscarinic Receptor Subtypes Expressed in CHO Cell Clones and SH-SY5Y Cells: Effects of Guanine Nucleotides, Cations and Pertussis Toxin Pretreatment. 47

4.0 Introduction. 48
4.1 Methods. 51

4.1.1 Radioligand Binding. 51
4.1.2 Data Analysis. 52
4.2 Results. 53
4.3 Discussion. 57

CHAPTER FIVE. Carbachol-Stimulated [^{35}S]GTPγS Binding in Membranes Prepared from CHO Cell Clones Expressing Recombinant Muscarinic Receptor Subtypes. 65

5.0 Introduction. 66
5.1 Methods. 68
5.1.1 Data Analysis. 68
5.2 Results. 68
5.3 Discussion. 70

CHAPTER SIX. Carbachol-Stimulated Ins(1,4,5)P_3 Mass Accumulation in CHO Cell Clones Expressing Recombinant Muscarinic Receptor Subtypes. 76

6.0 Introduction. 77
6.1 Methods. 78
6.1.1 Experimental Procedure. 78
6.1.2 Sample Preparation. 79
6.1.3 Preparation of Standards. 79
6.1.4 Preparation of Ins(1,4,5)P_3 Binding Protein from Bovine Adrenal Cortical Membranes. 80
6.1.5 Ins(1,4,5)P_3 Binding Assay. 80
6.1.6 Data Analysis. 81
6.2 Results. 81
6.3 Discussion. 85

CHAPTER SEVEN. Carbachol and Ins(1,4,5)P_3-Induced $^{45}Ca^{2+}$ Release from Permeabilized CHO Cell Clones Expressing Recombinant Muscarinic Receptors. 91

7.0 Introduction. 92
7.1 Methods. 95
7.1.1 Experimental Procedure. 95
7.1.2 Data Analysis. 96

7.2 Results. 96
7.3 Discussion. 98

CHAPTER EIGHT. Carbachol-Stimulated cAMP Accumulation in CHO Cell Clones Expressing Recombinant Muscarinic Receptors. 103

8.0 Introduction. 104
8.1 Methods. 104
8.1.1 Experimental Procedure. 104
8.1.2 Sample Preparation. 105
8.1.3 Preparation of Standards. 105
8.1.4 Preparation of cAMP Binding Protein from Bovine Adrenal Cortical Membranes. 106
8.1.5 cAMP Binding Assay. 106
8.1.6 Data Analysis. 106
8.2 Results. 107
8.3 Discussion. 110

CHAPTER NINE. Summary and Concluding Discussion. 122

Appendices. 135
Publications List. 144
Bibliography. 146

Cell Signalling in Chinese Hamster Ovary Cells Expressing Recombinant Muscarinic Receptors.

Neil Thornton Burford.

Agonist stimulation of recombinant m1, m2, and m3 muscarinic receptors, expressed in Chinese hamster ovary (CHO) cells, was compared. Carbachol binding affinity, and its modification by cations, guanine nucleotides and PTX pretreatment, was compared in washed membrane preparations of each of the CHO cell clones. Functional responses, determined by carbachol stimulation, were: [^{35}S]GTPγS binding in membranes; Ins(1,4,5)P_3 accumulation in intact cells; $^{45}Ca^{2+}$ release from permeabilized cells; and cAMP accumulation in intact cells.

m2-Transfected CHO cells were found to couple to AC, mediating inhibition of forskolin-stimulated cAMP accumulation, via PTX-sensitive G proteins. After PTX pretreatment of these cells, carbachol mediated a small potentiation of forskolin-stimulated cAMP accumulation, though with a much lower carbachol potency compared with the inhibitory response.

m1 and m3-transfected CHO cell clones were found to couple with both PTX-sensitive and PTX-insensitive G proteins, at relatively high levels of receptor expression. The PTX-insensitive G proteins mediated agonist-stimulated PLC activation and were involved in the activation of AC (though at a much lower potency). The mechanism, by which m1, m2 and m3 muscarinic receptors stimulated AC activity was not thought to be due to crosstalk via PLC activity.

The level of m3 muscarinic receptor expression, in CHO cells, was found to markedly affect both the potency, and the maximal responsiveness, with which carbachol mediated PLC activation and AC activation. Furthermore, at lower levels of receptor expression, m3 muscarinic receptors appeared to couple to a lesser extent with PTX-sensitive G proteins.

The study, therefore, concluded that comparisons of agonist-mediated responses between muscarinic receptor subtypes, expressed in CHO cells, must be performed at similar levels of receptor expression. At similar receptor densities, m1 and m3 muscarinic receptors, in CHO cells, produced very similar responses to carbachol.

Acknowledgements.

I would like to thank Professor S. R. Nahorski for his excellent supervision and encouragement. Furthermore, I would like to thank colleagues, both past and present, for their friendly help and support over the last 3 years. This thesis is based on work performed using CHO cell clones, and I am, therefore, grateful to Dr. N. Buckley for supplying them.

Finally, I would like to thank fellow post-graduates Dave and Graham; my house-mates; and Nic, for making my stay in Leicester such a happy one.

CHAPTER ONE.

GENERAL INTRODUCTION.

1.0. Introduction.

Cells, within a multicellular organism, communicate with each other by the use of chemical signals which regulate such processes as development, cell differentiation, growth and the control of cellular activity. Cells can recognize incoming chemical signals by means of receptor proteins, situated on the plasma membrane, to which the chemical molecule can bind. This detection system can be transduced and amplified within the cell cytosol by means of second messenger systems which lead to cellular responses. The work presented in this thesis tries to describe and characterize the transduction of signals induced by association of chemical signals to a distinct family of plasma membrane receptors.

1.1. Muscarinic Receptor Subtypes.

In 1914, Sir Henry Dale discovered two types of response elicited by acetylcholine, one mimicked by muscarine and one by nicotine (Dale, 1914; Dale and Ewin, 1914). This provided the basis for the classical definition of muscarinic and nicotinic receptors, which remained unchanged for 60 years. Nicotinic receptors have a central pore through which sodium and potassium ions pass, evoking responses (on stimulation) as fast as the channel opening rate (ms). Muscarinic receptor responses are more diverse and slower, ranging from 100 s of ms to seconds.

By 1980 it was realized that a single muscarinic receptor subtype could not account for muscarinic receptor-mediated actions of acetylcholine. The anti-ulcer drug pirenzepine showed discrepancies in binding affinities for muscarinic receptors from different tissues suggesting the presence of at least two receptor subtypes, M_1 and M_2 (Hammer *et al*, 1980; Hammer and Giachetti, 1982). Subsequent discrimination of binding of 4-diphenyl acetoxy-methyl piperidine methiodide (4-DAMP) to ɔM_2 receptors in heart and ileum (Barlow *et al*, 1976) led to further suggested sub-grouping of muscarinic receptors. With the production of further selective antagonists, three pharmacologically distinct muscarinic receptors were defined and called M_1, M_2 and M_3.

Application of molecular biological techniques led to the publication of genetically defined muscarinic receptor subtypes (Kubo *et al*, 1986a, b; Bonner *et al*, 1987, 1988; Peralta *et al*, 1987a,b; reviewed by Hulme *et al*, 1990). This laid to rest any doubts about the existence of distinct subtypes of muscarinic receptors and opened the way to obtaining cell lines expressing pure populations of receptors. Presently, five genetically defined subtypes have now been cloned and expressed in multiple types of cells (Richards, 1991). A nomenclature convention adopted by the ɔMuscarinic Receptor Subtype Working Party (Birdsall *et al*, 1989) is widely used and accepted where the proteins encoded by

m1 genes appear to correspond with M_1 receptors in neuronal tissues; m2 gene products to M_2 receptors found in heart and cerebellum, and m3 to M_3 receptors in smooth muscles and glandular tissues. Cloned m4 receptors were available before a pharmacologically defined M_4 receptor was characterized in tissues (Vilaro *et al,* 1991; Waelbroeck *et al,* 1990; Lazareno *et al,* 1990). mRNA for m5 receptors has been located in discreet regions of rat central nervous system (CNS) (Vilaro *et al,* 1990) and mRNA encoding muscarinic receptors in the substantia nigra pars compacta is exclusively of the m5 type (Weiner *et al,* 1990). Muscarinic agonists are known to stimulate dopamine release from substantia nigra slices (Marchi *et al,* 1991) possibly implicating a functional role for m5 receptors. Cloned m5 receptors are currently the only other means to study this receptor subtype in isolation (Caulfield, 1993).

Muscarinic receptors are members of a large superfamily of plasma membrane receptors that transduce their intracellular signals via guanine nucleotide binding proteins (G proteins) (Birnbaumer *et al,* 1990). This family of receptors share a range of similar structural features in that they are all predicted to have seven transmembrane, hydrophobic helices joined by alternating intracellular and extracellular loops, an extracellular amino-terminal domain and a cytoplasmic carboxy-terminal domain (Hulme *et al,* 1990). The intracellular, third cytoplasmic loop is known to be critical for G protein recognition and activation.

In general, m1, m3 and m5 muscarinic receptors are coupled to phospholipase C-β activation via pertussis toxin-insensitive G proteins of the G_q class (see later). m2 And m4 muscarinic receptors predominantly couple to the inhibition of adenylate cyclase activity and modulate ion channels via pertussis toxin-sensitive G proteins of the G_i class (Caulfield, 1993). The interactions between these subtypes and effectors appear not to be exclusive, especially when receptor-effector interactions have been established in various transfected cell lines (reviewed by Richards, 1991). Muscarinic receptor structure, G proteins and receptor-effector coupling is addressed in more detail later in this chapter.

1.1.1. Selective Antagonists.

Muscarinic receptor research has been hindered by the lack of selective antagonists which will distinguish one receptor subtype from the other four. Antagonist potency can be defined by radioligand binding studies or by functional studies using Schild analysis (Arunlakshana and Schild, 1959). A particular receptor subtype can be defined by the rank order of potency of a series of selective antagonists. This profile of affinity for various selective antagonists may vary in different tissues, especially if multiple subtypes of receptor are expressed. Antagonist affinity profiles are, therefore, given more credence in tissues where only a single receptor subtype is expressed *eg* M_2 receptors in the heart, or a cloned receptor subtype expressed in cell lines which do not normally express

muscarinic receptors (Buckley *et al*, 1989; Dorje *et al*, 1991; Richards, 1991). (Table 1.1). Antagonist affinities for any one receptor subtype can vary 3-fold between studies from different laboratories suggesting that caution should be taken when comparing antagonist affinities between receptors in different systems. Changes in ionic strength and composition of buffers used for binding assays can dramatically influence the subtype selectivity of antagonists (Pedder *et al*, 1991). Reassuringly, the selectivity of various selective antagonists for muscarinic receptors expressed in tissues are maintained in most of the cloned muscarinic receptors (Richards, 1991).

Pirenzepine differentiates M_1 receptors (high affinity) from M_2, M_3 and m5 receptors (low affinity) (Doods *et al*, 1987; Dorje *et al*, 1991). However, M_1 and M_4 receptors have similar affinities for pirenzepine (as determined by functional studies) (Caulfield and Brown, 1991) and less than ten fold selectivity between m1 and m4 receptors (Wess *et al*, 1991a; Hulme *et al*, 1990). Himbacine is currently the only antagonist that can differentiate between M_4 (high affinity) and M_1 receptors (low affinity) (Lazareno *et al*, 1990).

Methoctramine binds to M_2 receptors with high affinity but is low in affinity for M_3 receptors (Michel and Whiting, 1988). Therefore, M_2 receptors can be characterized by their high affinity for methoctramine and low affinity for pirenzepine and 4-DAMP (Barlow *et al*, 1976). One drawback of using methoctramine is the reported allosteric effect observed at concentrations in excess of 1 μM (seen as a decrease in [^{3}H] N-methyl scopolamine (NMS) dissociation rate) (Giraldo *et al*, 1988). A number of compounds including gallamine appear to bind to an allosteric site on muscarinic receptors. Gallamine does not follow the mass action predictions of competitive interactions and furthermore alters the rates of dissociation of competitive ligands (Jones *et al*, 1992).

M_3 receptors have a high affinity for 4-DAMP and para flouro-hexahydro-silo difenidol (pF HHSiD) (Lambrecht *et al*, 1988) and a low affinity for pirenzepine and methoctramine.

M_4 receptors (as described above) have a high affinity for himbacine (Lazareno *et al*, 1992) and a moderate affinity for pirenzepine. Other selective antagonists do not distinguish M_4 receptors from M_2 or M_3 receptors.

m5 Receptors have been characterized in cells expressing the recombinant receptor (Dorje *et al*, 1991) and show very low affinity for some AFDX-116 (11[[2-[(diethylamino)methyl]-1-piperidinyl]acetyl]-5,11-dihydro-6H-pyrido[2,3-b][1,4]benzodiazepine-6-one) analogues compared with other receptor subtypes.

1.1.2. Selective Agonists.

No particularly selective agonists have been described, but a number of possible candidates exist including McN-A-343 ((4-Hydroxy-2-butynyl)-1-trimethylammonium-

Table 1.1. Selected antagonist potencies from functional or radioligand binding experiments on muscarinic receptor subtypes.
Data was collated (by Caulfield, 1993) from a number of different groups and is expressed as a range of pK_B (negative logarithm of dissociation constant) values.

Receptor gene:	m1	m2	m3	m4	m5
Subtype:	M_1	M_2	M_3	M_4	
Selective antagonists					
Pirenzepine	7.9-8.5	6.3-6.7	6.7-7.1	7.1-8.1	6.2-7.1
AFDX 116	6.4-6.9	7.1-7.2	5.9-6.6	6.6-7.0	6.6
Methoctramine	7.1-7.6	7.8-8.3	6.3-6.9	7.4-8.1	6.9-7.2
4-DAMP	8.9-9.2	8.0-8.4	8.9-9.3	8.9-9.4	9.0
pFHHSiD	7.2-7.5	6.0-6.9	7.8-7.9	7.5	7.0
Himbacine	7.0-7.2	8.0-8.3	6.9-7.4	8.0-8.8	6.3
AFDX 384	7.3-7.5	8.2-9.0	7.2-7.8	8.0-8.7	6.3

m-chlorocarbinilate chloride) which is reputedly M_1-selective (Eltze, 1988; Mei *et al*, 1991; Hu and El-Fakahany, 1990). Interest in the development of selective M_1 receptor agonists has grown in view of the suggestion that M_1 receptors are involved in memory function and the finding that basal forebrain and septal cholinergic inputs to the hippocampus and cerebral cortex are severely disrupted in senile dementia of the Alzheimer type.

Strategies for the detection of a compound with subtype selectivity have involved screens which look at the potency of an agonist in producing a functional response. Unfortunately, this says nothing quantitative about either the agonist s binding affinity for the receptor or its efficacy. Therefore, data generated in such systems do not represent constants that can be applied to agonists binding to receptors in other systems. Radioligand binding approaches can produce estimates of binding affinities but still do not define the efficacy of agonists (Caulfield, 1993). Another possible confounding factor results from changes in receptor-G protein stiochiometry from tissue to tissue. Indeed, many agonists tend to display differences in intrinsic activity depending on the preparation used to study receptor pharmacology (Hoyer and Boddeke, 1993).

1.1.3. Localization and Distribution.

Studies with complementary deoxyribose nucleic acid (cDNA) sequences able to hybridize with parts of muscarinic receptor messenger ribose nucleic acid (mRNA), either in Northern blots of mRNA in tissues, or with *in situ* hybridization, have resulted in a considerable extension of knowledge of the anatomical localization of muscarinic receptors (see Buckley, 1990 for review). However, hybridization studies may be misleading when the site of mRNA production (*ie* the cell body) is remote from the site of expression of receptor protein (*e.g.* on remote dendrites of neurons). The introduction of specific muscarinic receptor antibodies and their use in localization studies will increase the knowledge of sites of expression of each subtype (Levey *et al*, 1991). In the brain , m1-m5 receptor mRNA is expressed and m1-m5 receptor antibody immunoreactivity has been shown in a series of studies (reviewed by Caulfield, 1993). However, attributing functions to these subtype localizations in the brain is still not possible. Localization studies in the periphery will probably be more rewarding in terms of defining functional roles to muscarinic receptor subtypes in isolated tissues. m1 And m3 receptor protein has been found in exocrine glands (Dorje *et al*, 1991b). m3 Receptor mRNA is found extensively in smooth muscle and m3 receptor protein has been located in urinary bladder, lung and ileum along with m2 receptor protein. Only m2 receptor protein is found in the mammalian heart. m2 And m4 receptor protein has been detected in lung (Dorje *et al*, 1991b). Although the new antibodies have produced encouraging and interesting results, it is clearly too early to make firm judgements on receptor localization,

other than in a few tissues (*e.g.* heart). As yet, m5 receptors have not been identified in peripheral tissues (Caulfield, 1993).

Another use for specific muscarinic receptor antibodies will be in defining functional roles of muscarinic receptors in tissues, especially where multiple subtypes are present. Luthin and co-workers have shown that specific m2 receptor antibodies can precipitate solubilized complexes of m2 muscarinic receptor and G protein from rat heart. The G protein α subunits can then be identified by probing with G_α specific antibodies to determine the G proteins that couple with these m2 muscarinic receptors (Matesic *et al*, 1989).

1.1.4. Molecular Structure of Muscarinic Receptors.

G protein-coupled receptors share a range of similar structural features including predicted seven transmembrane (TM), hydrophobic α helices joined by alternating intracellular and extracellular loops (as previously described). All muscarinic receptors contain a very large third intracellular loop (i3) which, except for membrane-proximal portions, displays virtually no sequence identity among the different subtypes. In contrast, the five muscarinic receptor subtypes display a high degree of sequence homology in the TM domains (Hulme *et al*, 1990).

Ligand binding to muscarinic receptors is thought to occur in a pocket formed by the seven TM domains (Hulme *et al*, 1990; Wess, 1993) and this is consistent with other members of the G protein-coupled receptor superfamily (*e.g.* adrenoceptors) (Strader *et al*, 1989). Conclusions drawn from mutagenesis studies are consistent with three dimensional molecular modelling studies of muscarinic receptors which suggest that the binding site for agonists is located in a narrow cleft defined by several TM domains about 15 A away from the extracellular surface (Wess, 1993). A conserved aspartate (Asp) residue located in TM III is thought to be an important site of ion-ion interactions for the positively charged amino head group present in virtually all muscarinic receptor ligands. In fact this Asp residue is found in all receptors that bind biogenic amine ligands.

Sequence analysis shows that the seven TM domains of all muscarinic receptors contain a series of conserved serine (Ser), threonine (Thr) and tyrosine (Tyr) residues, most of which do not occur in other G protein-coupled receptors. Point mutation studies have shown that replacement of hydroxyl groups present in the side chains of these amino acids (by replacement with alanine (Ala) or phenylalanine (Phe)) resulted in mutant receptors that displayed affinities for the agonists acetylcholine and carbachol that were 10-60 times smaller than those shown by the wild-type receptor. These mutations had little effect on antagonist binding affinities, suggesting that antagonists bind to different subsites of muscarinic receptors than agonists (Wess *et al*, 1991b). Helical wheel projection models predict that the majority of the conserved Thr and Tyr residues that are

critical for acetylcholine binding face the central binding cavity enclosed by the seven TM domains (Wess, 1993).

Considerable evidence suggests that a conserved Asp residue present in TM II plays a pivotal role in mediating the conformational change associated with receptor activation. For instance, substitution of Asp^{71} or Asp^{122} with asparagine (Asn) in M_3 receptors produced mutant receptors that displayed high affinity for carbachol, but decreased efficacy and potency, respectively, in agonist-induced phosphoinositide (PI) metabolism (Fraser *et al*, 1989). Mutational modification of this residue in various adrenoceptors (Strader *et al*, 1988; Wang *et al*, 1991) and dopamine receptor subtypes (Neve *et al*, 1991) was shown to abolish or markedly reduce the efficiency of receptor-G protein coupling. Thr, Tyr and proline (Pro) residues, found in the TM regions of all the muscarinic receptor subtypes, have also been found to be important in receptor activation, by mutation studies (Wess, 1993).

Ligand binding to many members of the G protein-coupled family of receptors (including muscarinic receptors) is modulated allosterically by monovalent cations ($Na^+ \geq Li^+ > K^+$), leading to a synergistic activation of effectors with guanine nucleotides (Limbird *et al*, 1982). Substitution of Asp^{79} (of TM II) with Asn eliminates allosteric modulation of agonist binding to mutant α_2-adrenoceptors, by sodium ions (Hurstman *et al*, 1990).

Functional studies with hybrid m2/m3 muscarinic receptors have shown that the specificity of G protein coupling is largely dependent on the first 16-21 amino acids of the i3 loop (Wess *et al*, 1989,1990a). Other areas of receptor-G protein interaction are present in the carboxy-terminal portion of the i3 loop and in the i2 loop (Wang *et al*, 1991). Within the i3 loop, the region proximal to TM V shows a series of amino acids which are conserved with respect to m1, m3 and m5 versus m2 and m4 receptors. The use of chimeric m2/m3 receptors have shown that m2 receptors with the i3 loop of m3 couple to phosphoinositide (PI) metabolism via a PTX-insensitive G protein. Conversely, m3 receptors with the i3 loop of m2 couple to the inhibition of adenylate cyclase (Wess *et al*, 1990a). The amino and carboxy-terminal regions of the i3 loop are predicted to form amphipathic α-helical extensions of uncharged and positively charged amino acids, thought to be of primary importance for recognition and activation of G proteins (Cheung *et al*, 1992). Mastoparan (a wasp venom peptide) can activate G proteins (Higashijima *et al*, 1990) and is thought to form an amphipathic helix when it binds to phospholipid membranes, thus mimicking the i3 loop of muscarinic receptors (Wakamatsu *et al*, 1983).

Recent evidence (Maggio *et al*, 1993) suggests that muscarinic receptors and β_2-adrenoceptors (Kobilka *et al*, 1988), behave in a fashion analogous to two subunit receptors. Truncated m2 and m3 receptors (TM1-V) and (TM VI and VII), when co-expressed in COS-7 cells, resulted in the эreconstitution of functional muscarinic receptors. These findings suggest that muscarinic receptors are composed of two

independently folding domains which, after their insertion into the lipid bilayer, are able to recognize each other and form a functional complex (reviewed by Wess, 1993). The physiological significance of this phenomenon in terms of dimerization of receptor domains deserves further functional studies.

1.1.5. Muscarinic Receptor Desensitization.

Muscarinic receptors, as with many members of the G protein-coupled receptor family, undergo desensitization, internalization and down-regulation following prolonged exposure to agonists (Moro *et al*, 1993). Phosphorylation of these receptors is now thought to initialize desensitization. Cerebral but not atrial muscarinic receptors can be phosphorylated by protein kinase C (PKC). Atrial muscarinic receptors are better substrates of cAMP-dependent protein kinase (PKA) than cerebral muscarinic receptors (Haga *et al*, 1993). This form of agonist-independent phosphorylation may be the mechanism by which m1 muscarinic receptors can be heterologously desensitized by prolonged exposure of β_2-adrenoceptors to isoproterenol, when both receptor subtypes are expressed in CHO cells (Lee and Fraser, 1993). In this study, PKA was found to phosphorylate specific, central regions of the i3 loop of m1 muscarinic receptors. Point mutation studies found that this region is crucial for the initiation of desensitization, internalization and down-regulation of the m1 muscarinic receptor and also the m3 muscarinic receptor (Maeda *et al*, 1993; Lameh *et al*, 1992).

Recently, it has been shown that recombinant, human m3 receptors (expressed in CHO cells) were phosphorylated rapidly in an agonist-dependent manner by a serine kinase distinct from PKA, Ca-calmodulin-sensitive protein kinase and PKC (Tobin and Nahorski, 1993). This phosphorylation may be an important event in the rapid, partial desensitization of PI hydrolysis observed in this cell clone (Wojcikiewicz *et al*, 1993). Agonist-dependent, rapid phosphorylation of m2 muscarinic receptors has also been observed (Kameyama *et al,* 1993) via a muscarinic receptor kinase (mAChR kinase) which is very similar to β-adrenergic receptor kinase (βARK). Phosphorylation mediated by these kinases were found to be regulated by G proteins in a dual manner; stimulation by βγ and inhibition by αβγ (Haga *et al*, 1993; Kameyama *et al,* 1993).

1.2. G Proteins.

Several families of cell surface receptors have been characterized that transduce ligand binding events into an intracellular signal, via different mechanisms of signal transduction. Ligand-gated ion channels, such as the nicotinic acetylcholine and $GABA_A$ (γ-aminobutyric acid) receptor, change conformation on interaction with agonists forming

a pore through which ions may cross the plasma membrane. This mechanism of signal transduction produces very rapid responses. For instance, the nicotinic receptors begin to respond within 20 μs of addition of acetylcholine (Katz and Miledi, 1965). Another mechanism of signal transduction is one where receptors have intrinsic protein tyrosine kinase activity (*e.g.* insulin receptors) which generally regulate relatively slow responses (for review see White and Kahn, 1994). Another mechanism of signal transduction is one where a ligand-activated receptor communicates with effector molecules via a guanine nucleotide binding protein (G protein).

Signal transducing G proteins occur in two forms; the ɔsmall G proteins are generally found as single polypeptides consisting of approximately 200 amino acids (*e.g.* p21ras (Downward, 1990)) and function in the regulation of cell growth, protein secretion and intracellular vesicle interactions; the heterotrimeric G proteins consist of α, β and γ subunits and are associated with cell surface receptors all of which share a characteristic topological structure consisting of seven transmembrane domains. Muscarinic receptor subtypes (as previously described) are members of this superfamily of receptors which now consists of over one hundred members. Receptor activation modulates G protein activation which exchange guanosine 5 -diphosphate (GDP) (bound to the α subunit) for guanosine 5 -triphosphate (GTP). α-GTP is then thought to dissociate from the βγ complex and modulate effector systems. An intrinsic GTPase activity of the α subunit then cleaves off the terminal phosphate group and α-GDP and βγ recombine, completing the cycle (described in more detail in subsequent sections).

1.2.1. History of G protein Discovery.

Rodbell and his collaborators (Rodbell *et al*, 1971a;b) provided the first evidence that a receptor and effector protein could communicate via a G protein. The identification of phototransducin (Wheeler and Bilensky, 1977) and the S49 cell mutant ɔcyc⁻ (Bourne *et al*, 1975) (which lacks G_s), which affected those aspects of adenylate cyclase activity that are GTP-dependent (Ross and Gilman, 1977), increased research interest in this area. By 1980, transducin and G_s had been purified (Godchaux and Zimmerman, 1979; Kuhn, 1980; Bitensky *et al*, 1981; Stryer *et al*, 1981). Cloning and sequencing techniques have successfully identified and classified 16, 4 and 7 mammalian genes encoding α, β and γ subunits, respectively (Conklin and Bourne, 1993; Simon *et al,* 1991).

1.2.2. Receptor Interactions with G Proteins.

The ternary complex model of agonist-receptor-G protein interactions (DeLean *et al*, 1980) was originally developed to account for several features of ligand binding. First, agonists but not antagonists were able to distinguish between a high and a low affinity

state of the receptor. Second, the proportion and relative affinity of ligands for these two states of the receptor was observed to vary with the intrinsic activity of the agonist. Thirdly, guanine nucleotides appeared to convert high affinity binding sites to low affinity binding sites.

GDP bound to a G protein α subunit normally dissociates slowly, but agonist binding to the receptor catalyzes a conformational change in the G protein increasing the rate of GDP dissociation and its substitution with GTP. Aluminium fluoride (AlF_4^-) can be used as a pharmacological tool to activate G proteins by binding alongside GDP, on the α subunit and mimicking the terminal phosphate group of GTP (Bigay *et al*, 1985).

Agonist binding to receptors results in a conformational change in the receptor protein which represents activation of the receptor. The activated receptor has a high affinity for a conformation of the G protein in which its α and $\beta\gamma$ subunits are associated and the guanine nucleotide binding site on the α subunit is empty (see Figure 1.1). Although only the α subunit undergoes guanine nucleotide exchange, the $\beta\gamma$ complex plays a crucial role in presenting it to the receptor (Florio and Sternweis, 1989). The ternary complex is normally short-lived as an endogenous guanine nucleotide would bind to the site on the α subunit within milliseconds. However, in washed membrane preparations where guanine nucleotides are omitted, the ternary complex can be stabilized and measured.

An agonist binds more tightly to the active conformation of its receptor, which in this case is the ternary complex. Therefore, stabilization of the ternary complex under the experimental conditions described above, results in a proportion of the receptors binding agonist with a high affinity. If guanine nucleotides are added (GDP, GTP or stable analogues) the transition state is lost and the affinity of agonist binding is weakened. This hypothesis forms the basis for current understanding of shallow agonist displacement binding curves in competition binding isotherms at G protein-coupled receptors which become uniphasic and of lower affinity in the presence of guanine nucleotides (Waelbroeck *et al*, 1982; Evans *et al*, 1985). The heterogeneity of agonist binding sites in the absence of guanine nucleotides is a manifestation of high and low affinity states distinguished by agonists but not by antagonists. Partial agonists are intermediate in their ability to stabilize ternary complexes and this ability seems to be closely correlated with their intrinsic activities (Evans *et al*, 1985).

Recent studies (reviewed by Lefkowitz *et al*, 1993), using mutated adrenoceptors which have constitutive activity, suggest that the classical ternary complex model requires expansion to accommodate an isomerization of the receptors from an inactive to an active state which couple to G proteins. Constitutive activity of these mutant adrenoceptors can be measured by functional studies in the absence of agonist, or by high affinity agonist binding to receptors in the absence of G proteins (*ie* after solubilization and purification) (Samama *et al*, 1993). The intrinsic activity of an agonist can vary dramatically depending on the tissue in which the receptors are expressed (Hoyer *et al*, 1993). A given agonist can

display a range of intrinsic activities depending on the extent of receptor reserve and the particular effector system being studied.

It seems likely that the intrinsic efficacy of an agonist will depend on the ability of agonists to isomerize the receptor into an active state. One study has shown that pilocarpine (a muscarinic receptor partial agonist), in a reconstituted system with purified atrial muscarinic receptors and purified atrial G_i, was less efficacious than the full agonist carbachol. This difference in activity was the result of a decrease in affinity of the receptor-ligand complex for G_i, as opposed to differences in their relative abilities to activate the G protein (measured by GTPase activity) (Tota and Schimerlik, 1990).

Initially, antagonists (which bind to receptors with a single affinity) were thought to bind indiscriminately and fail to alter the existing equilibrium between G protein conformations (Taylor, 1990). The allosteric ternary complex model suggests that antagonists may revert the isomerized, activated state of the receptor to the inactive state, thereby uncoupling the receptor from the G protein. Evidence for this theory comes from the finding that antagonists can block basal responses in the absence of endogenous agonists (reviewed by Schutz and Freissmuth, 1992). Also, complexes of muscarinic receptors and G proteins, formed in the presence of agonist, remain stable after removal of agonist and subsequent solubilization and purification from cardiac membranes. Dissociation of the receptor from the G protein occurs when the antagonist atropine is added, following removal of agonist (Matesic and Luthin, 1991). This demonstrated that antagonists destabilize receptor-G protein complexes.

1.2.3. Mg^{2+} Requirements.

Neither activation of the G protein, nor formation of high affinity receptor-G protein complexes occur in the absence of magnesium ions (Mg^{2+}) (Birnbaumer *et al*, 1990; Hulme *et al*, 1983). Mg^{2+} at concentrations of 5-100 mM stimulate the rate of binding of guanosine 5 -O-(3-thiotriphosphate) (GTPγS) to both G_s and G_i (Northup *et al*, 1982; Bokoch *et al*, 1984; Sternweis *et al*, 1981; Hanski *et al*, 1981) and this is directly correlated with the rate of GDP dissociation, stimulated by Mg^{2+} in G_i (Higashijima *et al*, 1987). Interestingly, G protein βγ subunits increase G_α affinity for GDP thus stabilizing the inactive state. Hormone stimulation of G_s occurs at 10 μM Mg^{2+} (Iyengar and Birnbaumer, 1982). Ligand activation thereby lowers the Mg^{2+} requirement to obtain G protein activation. Hence, under physiological conditions, receptor activation changes the affinity of a regulatory Mg^{2+}-binding site from millimolar (and hence is unoccupied at the normal 0.5mM concentration of cytosolic free Mg^{2+}) to micromolar, causing it to become saturated by the cytosolic free Mg^{2+}. This system has been termed the ɔMg switch (Birnbaumer *et al*, 1990). Nanomolar concentrations of Mg^{2+} are also required for the intrinsic GTPase activity of G_α subunits.

1.2.4. G Protein Activation.

Binding of GTP or its stable analogues (GTPγS or guanylyl-imidodiphosphate (GppNHp)) is the step that leads to G protein activation. The α-GTP complex dissociates from the βγ complex (Iyengar *et al*, 1988) and complexes with effector molecules modulating their activity. A contentious point is whether the α-GTP complex actually leaves the membrane environment or whether it anchors to the membrane (Mumby *et al*, 1990). It seems unlikely that the α-GTP complexes leave the membrane as the resulting dilution factor would be detrimental to the signalling and amplification process.

1.2.5. Classification of G_α Subunits and Their Modulation of Effectors.

G_α subunits show a high degree of amino acid similarity and can be divided into four classes (see figure 1.2).

$G_{s\alpha}$ class

$G\alpha_s$ and $G\alpha_{olf}$ are both capable of activating adenylyl cyclase to increase intracellular adenosine 3 ,5 -cyclic monophosphate (cAMP) levels (Graziano *et al*, 1987). $G\alpha_s$ is distributed ubiquitously whereas $G\alpha_{olf}$ is restricted to specific neural tissues and is enriched in neurons in the olfactory epithelium. A number of splice variants occur in $G\alpha_s$ resulting in two short forms and two long forms (Birnbaumer *et al*, 1990). Both $G\alpha_{olf}$ and $G\alpha_s$ contain a site which can be ADP-ribosylated by cholera toxin (CTX) (inhibiting the intrinsic GTPase activity of α_s), but both subtypes lack susceptibility to be ADP-ribosylated by pertussis toxin (PTX). $G\alpha_s$ is also implicated in modulating certain Ca^{2+} channels after β_1-adrenoceptor activation (Yatini *et al*, 1987).

$G_{i\alpha}$ class

Members of this class of G protein α subunits (with the exception of $G\alpha_z$) contain sites susceptible to modification by PTX (Simon *et al*, 1991; Gierschik, 1992) which catalyzes the transfer of an adenosine diphosphate (ADP)- ribose moiety from b-nicotinamide-adenine-dinucleotide (NAD^+) to the α subunit, resulting in uncoupling of the modified G protein from receptors. G_i class α subunits are, therefore, expected to mediate activation of PTX-sensitive processes. $G\alpha_i$ and $G\alpha_o$ have been shown to function in regulating ion channels (Caulfield, 1993; Birnbaumer, 1990). $G\alpha_i$ subtypes lower

intracellular cAMP levels in reconstituted systems (Parker *et al*, 1991; Taussig *et al*, 1993). The $\beta\gamma$ dimer resulting from G_i activation may act synergistically with $G\alpha_i$, in some systems, lowering cAMP levels by binding with activated $G_{s\alpha}$ subunits (Birnbaumer *et al*, 1990). A PTX-sensitive G protein has also been implicated in phospholipase C activation (Ashkenazi *et al*, 1987) but the recent observation that $\beta\gamma$ dimers of PTX-sensitive G proteins can activate PLC-β2 directly, suggests that $G_{i\alpha}$ subunits may not be implicated in the activation of this effector. This finding (which is discussed in more detail later in this introduction) contradicts an earlier statement whereby PTX-sensitive processes are expected to be regulated by $G_{i\alpha}$ subunits. Care must therefore be taken when implicating a functional role of $G_{i\alpha}$ subunits based on PTX-sensitivity of effector responses. $G\alpha_{t1}$ (rod transducin) couples rhodopsin to the activation of retinol phosphodiesterase (Chabre and Deterre, 1989). $G\alpha_z$ is found primarily in neurons and bears some resemblance to the $G_{i\alpha}$ class of G proteins. $G\alpha_z$ is , however, PTX-insensitive and its function remains obscure.

$G_{q\alpha}$ class

The members of this class of α subunits vary in their tissue specificity but seem to couple receptors to the activation of PLC-β isozymes in a PTX-insensitive manner (Wu *et al*, 1992; Taylor *et al*, 1991; Smrcka *et al*, 1991). $G\alpha_q$ and $G\alpha_{11}$ are widely distributed whereas $G\alpha_{14}$ is found primarily in stromal and epithelial cells. $G\alpha_{15}$ is found in murine B-lymphocytes and $G\alpha_{16}$ in human T lymphocytes. $G\alpha_{16}$ has a much higher affinity for PLC-β2 than other members of this class; this corresponds with the relatively high expression levels of PLC-β2 in cells of hematopoeitic origin (Wu *et al*, 1993).

$G_{12\alpha}$ class

Both $G\alpha_{12}$ and $G\alpha_{13}$ mRNAs are expressed ubiquitously but little is known of their function except that they are potentially insensitive to ADP-ribosylation by PTX.

1.2.6. Classification of $G_{\beta\gamma}$ Subunits and Their Modulation of Effectors.

The four forms of $G\beta$ subunits cloned to date (each comprised of about 340 amino acids) cannot form dimers with each kind of G_γ subunit (75 amino acids in length). $G_{\beta1}$ can associate with $G_{\gamma1}$ or $G_{\gamma2}$, whereas $G_{\beta2}$ can associate with $G_{\gamma2}$ but not with $G_{\gamma1}$. $G_{\beta3}$ is unable to associate with either $G_{\gamma1}$ or $G_{\gamma2}$ (Clapham and Neer, 1993). G_γ subunits differ in their modification by prenyl groups; $G_{\gamma1}$ is farnesylated whereas $G_{\gamma2}$ is geranyl geranylated (reviewed by Spiegal *et al*, 1991). These modifications enable $\beta\gamma$ subunits to

anchor to the plasma membrane. Palmitoylation and myristoylation has also been observed in various α subunits (Parenti *et al*, 1993).

Before 1987, the sole function of βγ subunits was thought to be their ability to present Gα subunits to the cell surface receptors. βγ activation of the cardiac K^+ channel (I_{KAch}) was one of the first studies implicating an effector role for βγ (Logothetis *et al*, 1987). More recently, it has become less clear as to whether this ion channel is regulated by βγ directly, or is a secondary effect of phospholipase A_2 (PLA_2) activity (Kim *et al*, 1989). Little is known of the regulation of PLA_2 activity by G proteins.

βγ activation of the yeast mating response provided further evidence for an effector role of βγ subunits (Whiteway *et al*, 1989).

Identification of four recombinant mammalian adenylate cyclases (AC) and their expression in Sf9 insect cells along with recombinant, individual G protein subunits showed that type I (calmodulin-sensitive) AC was activated by GTPγS bound $G\alpha_s$ and inhibited by $G_{\beta\gamma}$. Types II and IV (calmodulin-insensitive) AC were modestly activated by $G\alpha_s$ but with the further addition of $G_{\beta\gamma}$ produced a 5-6 fold increase in activity (Tang and Gilman, 1991). Co-expression of a mutationally active α_s with AC II converted agonists that act through ɔinhibitory receptors (coupled to G_i) into stimulators of cAMP synthesis (Federman *et al*, 1992). $G_{\beta\gamma}$ neither activates nor inhibits type III AC (Tang and Gilman, 1991).

Phospholipase C (PLC) exists in several isoforms some of which are regulated by $G_{\beta\gamma}$ proteins (such as PLC-$\beta_{1\text{-}3}$). $G\alpha_q$ or $G\alpha_{11}$ stimulate PLC activity in the order of PLC-β_1 ≥PLC-β_3 >> PLC-β_2, which differs from the order of PLC-β_3> PLC-β_2 > PLC-β_1 for $G_{\beta\gamma}$-dependent activation (Park *et al*, 1993). PLC-β_4 is not modulated by $G_{\beta\gamma}$ (Clapham and Neer, 1993). Unlike $G_{\beta\gamma}$ stimulation of AC, which requires the presence of activated $G\alpha_s$, $G_{\beta\gamma}$ stimulation of PLC-β isoforms does not require the presence of activated $G\alpha_q$ (Park *et al*, 1992). The presence of PLC-β_2 in hematopoietic cell lines may explain PTX-sensitive PLC activation in these cells (Katz *et al*, 1992).

Simon and co-workers (Wu *et al*, 1993) have demonstrated that specific combinations of β and γ subunits are required for PLC-β_2 activation and for synergistic activation of PLC-β_2 with $G\alpha_{16}$. They suggested that Gβ subunits may play a role in determining the relative specificity of the $G_{\beta\gamma}$ complex for effector activation while the G_γ subunit may be important for determining the affinity of the $G_{\beta\gamma}$ complex for specific Gα proteins.

$G_{\beta\gamma}$ may also modulate receptor function by controlling the location of receptor-specific protein kinases that lead to receptor phosphorylation and desensitization. $G_{\beta\gamma}$ can induce a ten fold increase in the agonist-dependent phosphorylation of purified muscarinic m2 and β_2- adrenergic receptors by similar protein kinases (MAChR Kinase and βARK, respectively) (Kameyama *et al*, 1993; Haga *et al*, 1993; Clapham and Neer, 1993). $G_{\beta\gamma}$ may remain bound to receptors after the α subunit has been dissociated (by receptor activation) allowing the kinase to bind to the receptor-$G_{\beta\gamma}$ complex. Therefore, another

functional role for $G_{\beta\gamma}$ is their ability to regulate receptors by controlling their phosphorylation and subsequent desensitization.

PLC-β1 increases GTPase activity of $G\alpha_q$ / $G\alpha_{11}$ subunits by fifty fold (Ross and Berstein, 1993) suggesting that effectors may act as GTPase activating proteins (GAPs). Such GAP molecules were initially identified for the ɔsmall G protein p21 ^{ras} (Hall, 1992). This GAP activity of PLC-β1 explains the discrepancy that the turn off rate of $G\alpha_q$ activity was too slow *in vitro* to be physiological (Bourne and Stryer, 1992). GAP activity may increase the turnover rate of activated $G\alpha$ subunits and thus amplify the signal generated by receptor activation. $G_{\beta\gamma}$ (in a recombinant system) has been shown to increase $G\alpha_o$ GTPase activity (Bauer *et al*, 1992). In addition, phosducin (a retinal protein)(Clapham and Neer, 1993) reduced the stimulation of $G\alpha_o$ GTPase activity which is caused by βγ subunits by modulating the ability of $G_{\beta\gamma}$ to interact with $G\alpha_o$.

1.2.7. Molecular Structure of Gα Subunits.

The different $G\alpha$ subunits (35-52 KDa) share 50 to 90 % sequence identity. $G\alpha$ subunits have 5 highly conserved G regions which are found in all known GTPases. 3-Dimensional modelling has been applied to the $G\alpha$ subunits (Masters *et al*, 1986) using information gained from X-ray crystallography of two ɔsmall G proteins, p21^{ras} (Milburn *et al*, 1990) and a bacterial elongation factor, Tu (EF-TU) (Jurnak, 1985). The molecular structure of $G\alpha$ subunits appears rather complex. Evidence to date suggests that the areas of interaction between plasma membrane bound proteins (*i.e.* βγ, receptors and effectors) and $G\alpha$ subunits occurs on one side of the $G\alpha$ subunit (Conklin and Bourne, 1993), whereas the guanine nucleotide binding pocket is located on the opposite (cytoplasmic) side of the protein. The plasma membrane facing side of $G\alpha$ subunits are thought to consist of the amino-terminal, carboxy-terminal and G5 region and several mutation studies and antibody studies have implicated these regions in receptor and βγ coupling to $G\alpha$ subunits (reviewed by Conklin and Bourne, 1993).

Sites of Interaction of βγ with Gα Subunits.

The amino-terminal region of $G\alpha$ subunits is thought to be crucial for interactions with βγ subunits. Myristoylation of the amino-terminal region of $G\alpha_o$ greatly enhanced its affinity for βγ (Linder *et al*, 1991). Also, a monoclonal antibody against the amino-terminal region of $G\alpha_{t1}$ caused its dissociation from βγ (Mazzoni and Hamm, 1989). βγ appears to interact with other areas of $G\alpha$ subunits (possibly the hα2 region) and with the receptor itself, as the receptor catalyzed release of GDP from the βγ.α-GDP heterotrimer is more efficient than from α-GDP alone (Florio and Sternweis, 1989). Also, βγ increases $G\alpha_s$ affinity for GDP by about 100-fold (Higashijima *et al*, 1987).

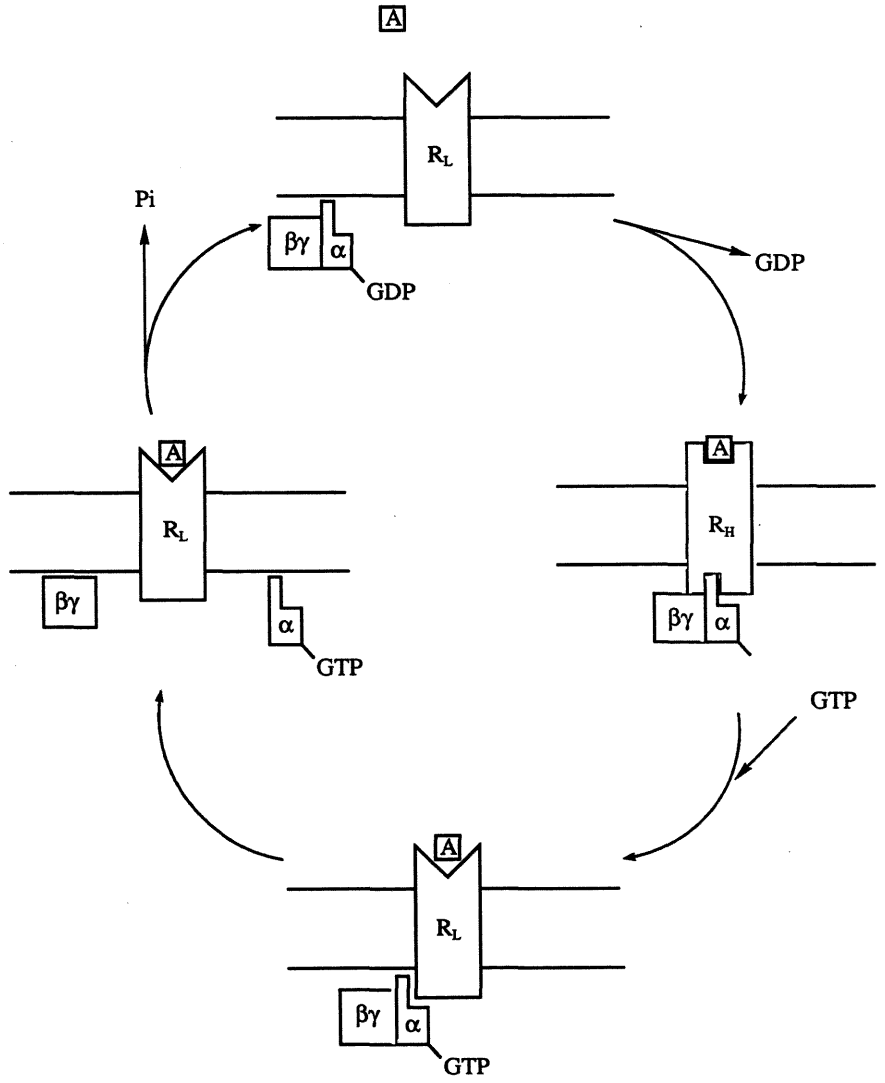

Figure 1.1. Receptor interactions with G proteins.

The figure shows interactions between agonist (A), receptor (R) and G protein ($\alpha\beta\gamma$) as described in detail in the text. R_L = low affinity conformation of the receptor for agonist. R_H = high affinity conformation of the receptor for agonist (the ternary complex).

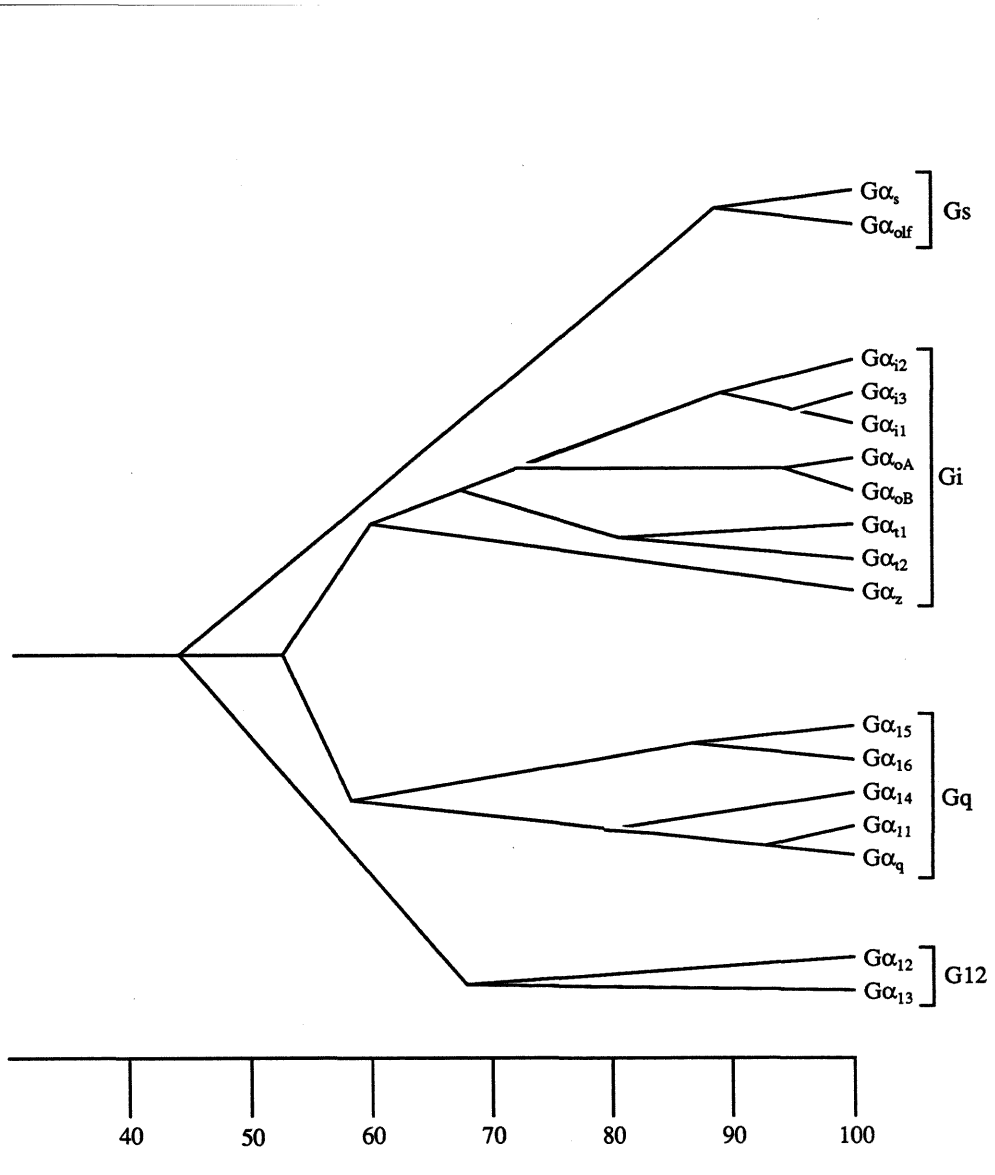

Figure 1.2. Relationship among mammalian Gα subunits.
The α subunits are grouped by amino acid sequence identity and branches indicate approximate values calculated for each pair of sequences (Simon *et al*, 1991).

Sites of Interaction of Receptors with Gα Subunits.

The carboxy-terminus, amino-terminus and G5 region have all been implicated as contact points for receptor interactions. Covalent modification by PTX-catalyzed ADP-ribosylation of a cysteine residue near the carboxy-terminus (of PTX-sensitive Gα subunits) and peptide specific antibodies directed against the carboxy-terminus, uncouple G proteins from receptors (West *et al*, 1985; Gutowski *et al*, 1991). In studies using chimeric Gα subunits, replacement of the final 4, 5 or 9 amino acids of $G\alpha_q$ with $G\alpha_{i2}$ resulted in chimeras that mediated PLC activation when activated by D_2-dopamine receptors and A_1 adenosine receptors (both normally coupling to G_i) (Conklin *et al*, 1993). The carboxy-terminus of Gα subunits may also be involved in G protein activation. The activated receptor seems to alter the carboxy-terminus in a way that relieves a carboxy-terminal-dependent restraint on GDP release (Conklin and Bourne, 1993). A conformational change in this region of $G\alpha_{t1}$ on binding to photorhodopsin made it inaccessible to PTX (Hamm, 1990).

The putative G5 region of Gα subunits is an attractive potential site for receptor-catalyzed release of GDP. Mutational replacement of a conserved cysteine in this region of $G\alpha_o$ reduces its affinity for GDP by 10-fold (Conklin and Bourne, 1993).

A role for the amino-terminal region of Gα subunits being involved in receptor interactions is made complicated by its interactions with βγ subunits (which also seem to interact with receptors) and its close proximity to the carboxy-terminal region. An amino-terminal $G\alpha_{t1}$ peptide inhibited interaction of G_t with photorhodopsin in a manner whereby the peptide did not cause dissociation of the $G\alpha_{t1}$ from βγ (Hamm *et al*, 1988).

Sites of Interaction of Effectors with Gα Subunits.

Distinct regions of $G\alpha_s$ have been implicated in $G\alpha_s$ binding to AC (Berlot and Bourne, 1992). These regions (distal hα2, insert 2-loop L7 and insert 4-loop L9 (see Conklin and Bourne , 1993)) are all putatively positioned on the plasma membrane facing side of the Gα subunit. The hα2 region, which has connections with the guanine nucleotide binding pocket, may be important in communicating the GAP activity of PLC-β1.

1.2.8. Molecular Structure of βγ Subunits.

The Gβ subunits (35-36 KDa) share more than 80 % amino acid identity. The amino-terminal region is predicted to form an amphipathic α-helix. The remainder of the protein consists of seven repeating subunits, each about 43 amino acids long (Clapham and Neer,

1993). The function of these repeating regions is not yet known. The Gγ subunits (6-10 KDa) are far more heterogeneous sharing less than 50% homology.

1.3. Inositol Lipid-Specific Phospholipase C Isozymes.

On binding to their cell surface receptors, many extracellular signalling molecules including hormones, peptide growth factors, neurotransmitters and immunoglobulins elicit intracellular responses by activating inositol phospholipid-specific phospholipase C (PLC). Activated PLC catalyzes the hydrolysis of phosphatidylinositol 4,5 bisphosphate (PIP_2) to generate diacylglycerol (DAG) and inositol 1,4,5 trisphosphate ($Ins(1,4,5)P_3$). DAG is the physiological activator of protein kinase C (PKC) and $Ins(1,4,5)P_3$ induces the release of Ca^{2+} from internal stores. This bifurcating signal transduction mechanism is now known to regulate a large array of cellular processes, including metabolism, secretion, contraction, neural activity and proliferation (Berridge, 1993; Cockcroft and Thomas, 1992; Nishizuka, 1992).

1.3.1. PLC Isoforms.

16 amino acid sequences (14 mammalian enzymes and 2 *Drosophila* enzymes) have been deduced from nucleotide sequences of their corresponding cDNAs (reviewed by Rhee and Choi, 1992). These can be separated into three types β, γ and δ on the basis of sequence homology. Overall sequence homology between these subtypes is low but two regions, X (approximately 70 amino acids) and Y (approximately 240 amino acids) are highly conserved and thought to represent the catalytic site of the enzymes. The catalytic activities of all three types of PLC are dependent on Ca^{2+}. The carboxy-terminal half of the Y region has been suggested to be the binding site for Ca^{2+} on the basis of the fact that the amino acid sequence of this region is homologous to those of the Ca^{2+}-binding domains of PKC and cytosolic phospholipase A_2 (Clark *et al,* 1991). All PLC isoforms contain an amino-terminus of approximately 300 amino acids. Whereas PLC-β and PLC-δ contain short sequences of 50-70 amino acids separating the X and Y regions, PLC-γ has a long sequence of 400 amino acids which contains the so-called *src* homology (SH2 and SH3) domains (domains first identified as non-catalytic regions common to a variety of *src* family tyrosine kinases) (Koch *et al*, 1991). The carboxyl-terminal sequence following the Y region is approximately 450 amino acids long in PLC-β but much smaller in PLC-γ and almost non-existent in PLC-δ (Cockcroft and Thomas, 1992).

Single polypeptide PLC isoforms with molecular masses of 62-68 KDa have been purified, but cloning and sequencing data has shown no regions corresponding to the X and Y domains in these putative PLC-α enzymes. Recent studies have shown that PLC-α

cDNA actually encodes a thiol:protein-disulphide oxidoreductase that carries no PLC activity (Rhee *et al*, 1989).

1.3.2. PLC-β.

The PLC-β family contains three members PLC-β1, β2 and β3, all present in mammalian cells. Demonstrations that GTP is required for agonist-stimulated PLC conversion of PIP_2 to $Ins(1,4,5)P_3$ (Cockcroft and Gomperts, 1985) initially suggested a G protein involvement in this second messenger system analogous to the adenylate cyclase second messenger system. It was more recently shown that the α subunits of the Gq class of G proteins are specific activators of the β-type PLC isozymes (Taylor *et al*, 1991; Smrcka *et al*, 1991). Co-transfection of cDNAs corresponding to PLC-β1 and to $G\alpha_q$ or $G\alpha_{11}$ into Cos-7 cells markedly increased total inositol phosphates in the presence of aluminium fluoride. On the other hand, transfection of cDNA s encoding $G\alpha_z$, $G\alpha_{oA}$, $G\alpha_{oB}$ and $G\alpha_t$ did not increase inositol phosphate formation suggesting that PTX-sensitive G protein α subunits were not involved in PLC-β1 activation (Wu *et al*, 1992). This was somewhat surprising considering the widely reported phenomenon that pretreatment of cells with PTX led to inhibition of inositol phosphate formation (Ashkenazi *et al*, 1987; Richards, 1991). Recent studies have found that $G\alpha_q$ does not activate PLC-β2 very efficiently compared to PLC-β1 (Park *et al*, 1992). $G\alpha_{16}$, however, has a high specificity for PLC-β2 suggesting that different PLC-β isoforms may be regulated by different Gqα-family subunits (Park *et al*, 1993; Wu *et al*, 1993). Co-localization of $G\alpha_{16}$ and PLC-β2 in cells of hematopoietic origin supports this view. In the last year, many groups have found that PLC-β isoforms can be stimulated by βγ subunits originating from both PTX-insensitive and PTX-sensitive G proteins (Katz *et al*, 1992; Wu *et al*, 1993; Park *et al*, 1993; Carozzi *et al*, 1993). The α subunits of Gq class G proteins (except for $G\alpha_{16}$) have therefore been shown to activate PLC-β isozymes in the order of PLC-β1≥ PLC-β3>> PLC-β2, which differs from the order of PLC-β3> PLC-β2> PLC-β1 for βγ-dependent activation.

As described in a previous section m1, m3 and m5 muscarinic receptor subtypes are thought to couple to PLC via Gq class G proteins. Coupling of M_1 muscarinic receptors to PLC-β1 via $G\alpha_{q/11}$ has been shown when each of these species were reconstituted in lipid vesicles (Berstein *et al*, 1992). In this study it was found that PLC-β1 stimulated the hydrolysis of $G_{q/11}$-bound GTP at least 50-fold. They suggested that PLC-β1 is a GAP (as described previously). GAP activity of effector molecules has important implications in determining the rate of responses during receptor activation and amplification of the signal (Taylor, 1990; Ross and Berstein, 1993).

M_2 receptors which were initially found to couple with PTX-sensitive G proteins (G_i family) can also produce stimulation of PLC activity (Ashkenazi *et al*, 1987) in a variety

of cells (Richards, 1991) in a PTX-sensitive manner. Receptor-stimulated PLC activity in cells of hematopoietic origin such as neutrophils, macrophages and human HL-60 granulocytes also seem to be susceptible to PTX treatment (Cockcroft, 1987; Fain, 1990; Park *et al*, 1993). βγ activation of PLC-β2 may explain PTX-sensitive PLC activity. PTX-pretreatment could inhibit the dissociation of free βγ subunits from PTX-sensitive G proteins, thus reducing PLC activity. An alternative explanation is that an, as yet, unidentified PTX-sensitive G protein may be the activator of PLC.

1.3.3. PLC-γ

The PLC-γ family is comprised of γ1 and γ2. PLC-γ2 isoforms predominate in spleen, B-cells, HL-60 cells and lung, whereas PLC-γ1 is widely distributed in many tissues (Cockcroft and Thomas, 1992). Polypeptide growth factors mediate their effects by binding to, and activating, cell surface receptors that have a similar molecular topology, including a cytoplasmic region that contains a tyrosine kinase domain. Despite the structural similarities between their receptors, PI signalling does not appear to be universal. Binding of platelet-derived growth factor (PDGF), epidermal growth factor (EGF) and nerve growth factor (NGF) to their respective receptors induces PI turnover whereas insulin and colony-stimulating factor (CSF-1) appear to have no effect on PI turnover. Treatment of a number of cell types with EGF, PDGF or NGF led to an increase in the phosphorylation of PLC-γ1 (but not of PLC-β1 or PLC-δ1) with the increased phosphorylation occurring on both serine and tyrosine residues (Rhee and Choi, 1992). The receptor-PLC-γ1 association is mediated by a high affinity interaction between the SH2 region of PLC-γ1 and a specific tyrosine autophosphorylated site of the receptor (Koch *et al*, 1991). The major sites of PLC-γ1 phosphorylation by the receptors for EGF, PDGF and NGF appear to be identical and are Tyr-771, Tyr-783 and Tyr-1254 (Kim *et al*, 1991). A conformational change induced by these phosphorylation events may present the normally cytosolic PLC-γ1 to the membrane, positioning the X and Y catalytic regions closer to its substrate.

Recently it has been discovered that m5 muscarinic receptors expressed in CHO cells, on addition of carbachol, induce an increased phosphorylation of endogenous PLC-γ. This reaction was dependent on the presence of extracellular Ca^{2+}. Tyrosine kinase inhibitors and Ca^{2+}-channel antagonists both attenuated PI metabolism suggesting another possible mechanism for muscarinic receptor stimulation of PI metabolism (Gusovsky *et al*, 1993).

1.3.4. PLC-δ

Three mammalian subtypes of this PLC isozyme have been identified (δ1, δ2 and δ3). Neither the receptors nor the transducer that are coupled to any of the PLC-δ members are

known.

1.3.5. Inhibition of PLC s by PKC and PKA.

Evidence suggests that activation of PKC or PKA attenuates receptor-coupled PLC activity in certain types of cell, thus providing a negative feedback pathway (Cockcroft and Thomas, 1992). Phosphorylation of EGF (at Thr-654) by PKC has been shown to reduce phosphorylation of PLC-γ1 by its tyrosine kinase (Decker *et al*, 1990). Increases in PKC activity can also lead to direct phosphorylation of serine residues in PLC-β1 (Ryu *et al*, 1990). They suggested that phosphorylation of PLC-β1 by PKC may alter its interaction with Gq.

1.4. Inositol Phosphate Metabolites as Cellular Signals.

In 1953, Hokin and Hokin observed that acetylcholine enhanced phospholipid turnover. Almost thirty years later it was found that neurotransmitter-stimulated calcium release correlated best with enhanced hydrolysis of PIP_2 (Michell, 1982). In 1983, Streb *et al* directly showed that low micromolar concentrations of Ins $(1,4,5)P_3$ triggered a rapid release of calcium in permeabilized pancreatic cells. Subsequently, many groups have shown that $Ins(1,4,5)P_3$ applied to a variety of permeabilized cell preparations stimulates calcium release from non-mitochondrial stores presumed to be located in a part of the endoplasmic reticulum or in specialized organelles called calciosomes (reviewed by Berridge and Irvine, 1984; Berridge and Irvine, 1989).

It is now well established that a large number of receptors can activate PLC isoforms whose catalytic hydrolysis of phosphatidylinositol 4,5-bisphosphate (PIP_2) gives rise to *sn* 1,2-diacylglycerol (DAG) and D-*myo*-inositol 1,4,5-trisphosphate ($Ins(1,4,5)P_3$) which perform second messenger roles in cells. It is also possible that PLC isoforms act on other inositol phospholipids liberating DAG and two inositol phosphates (inositol 1,4-bisphosphate ($Ins(1,4)P_2$) from phosphatidylinositol 4-phosphate (PIP) and inositol 1-phosphate ($Ins(1)P_1$) from phosphatidylinositol) both devoid of any known second messenger action. DAG can also be synthesized by the actions of phospholipase D (PLD) and PLC on phosphatidylcholine. This may be a secondary generation of DAG ensuing from the activation of PKC together with increases in cytoplasmic calcium levels by PLC-induced hydrolysis of PIP_2 (Figure 1.3).

DAG is the known physiological activator of protein kinase C (PKC) which in turn phosphorylates and thereby regulates the activities of a number of intracellular enzymes (Azzi *et al*, 1992). DAG is metabolized by a number of enzymes эswitching off PKC activity and leading to the recycling of various phospholipids, triacylglycerol and

phosphatidic acid (PA) (which may also have a potential messenger role (Moolenar *et al*, 1986)).

Ins (1,4,5)P_3 interacts with receptors on vesicular membranes causing calcium release from intracellular stores which in turn produces a large array of cellular responses.

1.4.1. Ins(1,4,5)P_3 Metabolism.

Metabolism of Ins(1,4,5)P_3 regulates three important aspects of cell signalling: 1) its rapid metabolism by enzymes controls the cellular Ins(1,4,5)P_3 concentration and hence the response level of cells to receptor stimulation; 2) metabolism also involves recycling of inositol essential for the synthesis and maintenance of the inositol phospholipids; 3) metabolism of Ins(1,4,5)P_3 results in the synthesis of inositol 1,3,4,5-tetrakisphosphate (Ins(1,3,4,5)P_4) which may play an important role as a signalling mediator.

Ins(1,4,5)P_3 is metabolized by two key enzymes, 5-phosphatase and 3-kinase. Which of these enzymes is most active physiologically is cause for some debate. Enzyme kinetic studies suggest that 3-kinase is operating close to its V_{max}, under physiological conditions, whereas 5-phosphatase seems to operate well below its V_{max}. The contributions of these two enzymes to Ins(1,4,5)P_3 metabolism is complicated due to the high concentrations of agonist used to amplify responses so that sufficient metabolites can be measured after labelling with ^{3}H-inositol. By raising Ins(1,4,5)P_3 to levels that are somewhat high for cells *in vivo*, the 5-phosphatase will become increasingly active due to its ɜreserve capacity for Ins(1,4,5)P_3 (Shears, 1991). 3-kinase catalyzes the addition of a phosphate group to Ins(1,4,5)P_3 producing Ins(1,3,4,5)P_4. This reaction is energy consuming (requiring ATP). 5-phosphatase removes a specific phosphate group by hydrolysis from Ins(1,4,5)P_3 producing inositol 1,4-bisphosphate (Ins (1,4)P_2). Both of these enzymes are dependent on calcium concentration in the cytosol and can be phosphorylated by PKC and Ca-calmodulin-dependent protein kinase II suggesting that these Ins(1,4,5)P_3 -metabolizing enzymes may be modulated by a feedback mechanism.

1.4.2. Functions of Ins(1,3,4,5)P_4.

The co-existence of two enzymes capable of metabolizing Ins(1,4,5)P_3, the apparent energy cost of the 3-kinase pathway and the short half-life of cellular Ins(1,3,4,5)P_4, have all contributed to speculation that Ins(1,3,4,5)P_4 has some specific function as a second messenger. Several reports (reviewed by Downes and MacPhee, 1990) have shown that Ins(1,3,4,5)P_4 potentiates Ins(1,4,5)P_3-induced calcium release and enhancement of calcium sequestration by calcium storage organelles. D-Ins(1,3,4,5)P_4 but not L-Ins(1,3,4,5)P_4 is also a weak, but full agonist at Ins(1,4,5)P_3 receptors in permeabilized SH-SY5Y cells, mediating a similar maximal release of loaded $^{45}Ca^{2+}$ but with a 15-fold

lower apparent affinity (Wilcox *et al*, 1993). The dominant notion, however, is that Ins(1,3,4,5)P_4 acts in concert with Ins(1,4,5)P_3 to prolong agonist-stimulated calcium signals (Morris *et al*, 1987; Irvine *et al*, 1988). Agonist stimulation (via Ins(1,4,5)P_3 generation) mediates calcium release in two phases. The initial calcium response is large and transient and thought to represent calcium release from intracellular stores. This is followed by a prolonged phase of calcium release which is dependent on the presence of extracellular calcium (*e.g*. Lambert and Nahorski, 1990). This led to the hypothesis of the capacitance model (Putney, 1986) which argues that the empty state of Ins(1,4,5)P_3-sensitive calcium stores activates an influx pathway that replenishes the stores (see Putney and Bird, 1993 for recent review). Ins(1,3,4,5)P_4 has been proposed to mediate this conductance of calcium from the plasma membrane into intracellular stores (Irvine *et al*, 1988; Irvine, 1990). Many studies reporting synergistic effects of Ins(1,3,4,5)P_4 on intracellular calcium mobilization have not always convincingly addressed the problems of Ins(1,4,5)P_3 contamination of Ins(1,3,4,5)P_4 used, back conversion of Ins(1,3,4,5)P_4 into Ins(1,4,5)P_3 by endogenous 3-phosphatase activity in the cells, or indirect effects of Ins(1,3,4,5)P_4 by protection of Ins(1,4,5)P_3 from 5-phosphatase metabolism. Evidence suggests that Ins(1,3,4,5)P_4 may mediate its putative physiological effects via specific high affinity IP_4-binding sites detected in certain tissues (Challiss *et al*, 1990; Wilcox *et al*, 1993; Bradford and Irvine, 1987; Enyedi and Williams, 1988).

1.4.3. Recycling of Inositol.

Ins(1,3,4,5)P_4 is a high affinity substrate for 5-phosphatase resulting in cleavage of the phosphate group at position 5 to form (Ins(1,3,4)P_3. Both Ins(1,4)P_2 and Ins(1,3,4)P_3 have no detectable activity in cells and hence their production signifies the termination of activity by Ins(1,4,5)P_3 and, putatively, Ins(1,3,4,5)P_4. Further degradation of these inositol phosphates by 1-phosphatase, 4-phosphatase and 3-phosphatase leads to the accumulation of Ins(3)P_1, Ins(4)P_1 and Ins(1)P_1. The enzyme inositol monophosphatase then completes the recycling process by liberating free inositol which can then be incorporated to form phosphotidylinositol (Shears, 1991) (Figure 1.4). Lithium may reduce the recycling of free inositol required to sustain phosphatidylinositol synthesis by uncompetitively inhibiting the enzyme inositol monophosphatase (Nahorski *et al*, 1991). It is not yet certain whether this action of lithium is related to its use as a treatment for manic depressive illness.

1.4.4. Ins (1,3,4,5,6)P_5 and InsP_6.

Ins(1,3,4,5,6)P_5 and InsP_6 were two of the earliest inositol phosphates to be identified, primarily because they are highly concentrated in avian erythrocytes and plant seeds,

Figure 1.3. Pathway of receptor-mediated breakdown of PtdIns and PtdCho.

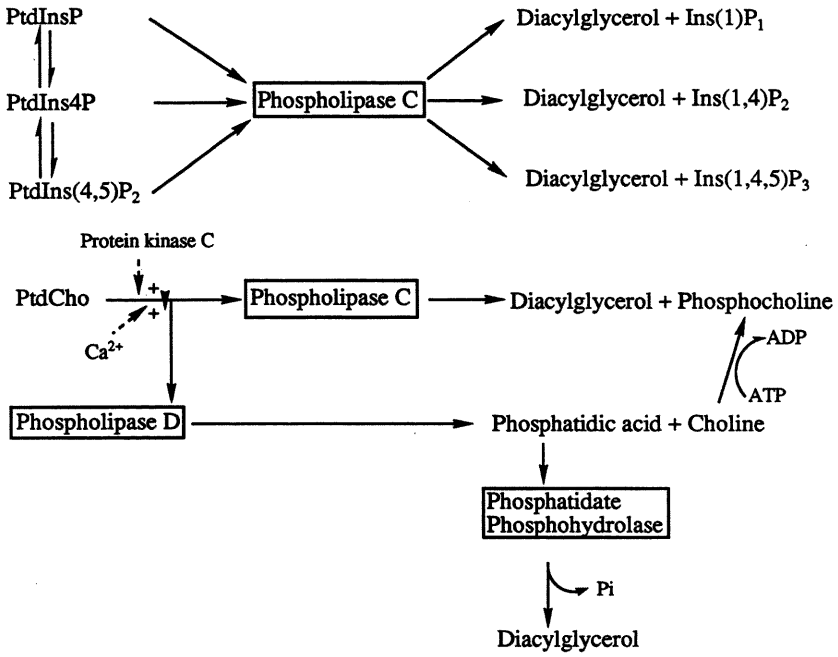

Figure 1.4. Metabolism of $Ins(1,4,5)P_3$.

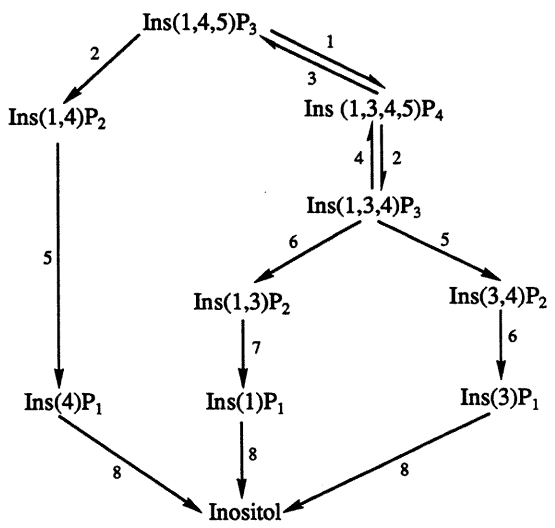

1 = 3-kinase; 2 = 5-phosphatase; 3 = 3-phosphatase; 4 = 5-kinase; 5 = 1-phosphatase; 6 = 4-phosphatase; 7 = 3-phosphatase; 8 = monophosphatase.

respectively. Ins(1,3,4,5,6)P_5 has the specialized ability to reduce the affinity of haemoglobin for oxygen in erythrocytes from birds, thus participating in oxygen distribution in avian tissues. InsP_6 forms an iron chelate that augment Fe^{2+}-mediated oxygen reductions and blocks the formation of hydroxyl radicals in plant seeds. Ins(1,3,4,5,6)P_5 and InsP_6 have been detected in a wide variety of cells at concentrations of 5-15 μM (Downes and MacPhee, 1990) but there has been little progress in understanding their intracellular roles. Detection of Ins(1,3,4,5,6)P_5 and InsP_6 upon receptor activation have produced conflicting results in many studies (reviewed by Shears, 1991) and deserves further investigation. The synthesis of these inositol phosphates is thought to be mediated by a variety of kinase enzymes with Ins(1,3,4)P_3 being a possible initial substrate.

1.4.5. Ins(1,4,5)P_3 Receptors.

The availability of high-specific activity radiolabelled Ins(1,4,5)P_3 in the mid 1980s and the development of a radioligand binding assay has allowed localization and biochemical characterization of specific Ins(1,4,5)P_3 receptors. High affinity binding sites for radiolabelled Ins(1,4,5)P_3 were originally discovered in liver and neutrophils (Spat *et al*, 1986) and were followed by similar reports in rat cerebellum (Willcocks *et al*, 1987), adrenal cortex and rat brain (Challiss *et al*, 1988). The high affinity binding site displays strict stereospecificity (Willcocks *et al*, 1987) with D-Ins(1,4,5)P_3 being greater than 3000-fold more potent than the L-isomer in adrenal cortex (Challiss *et al*, 1990).

The Ins(1,4,5)P_3 receptor was characterized in 1979 as a protein called P_{400} that was enriched in Purkinje cells of the mouse cerebellum (Mikoshiba *et al*, 1979). In 1988 two groups independently purified the receptor as IP_3 binding protein (Supattapone *et al*, 1988) and P_{400} (Maeda *et al*, 1988) which were shown to be immunologically identical (Maeda *et al*, 1990). Cloning the cDNA for the mouse cerebellar Ins(1,4,5)P_3 receptor (Furuichi *et al*, 1989) and subsequent transfection of the cDNA into cell lines resulted in enhanced Ins(1,4,5)P_3 binding activity and also Ca^{2+}-releasing activity, suggesting that the cloned cDNA actually encodes a protein having both Ins(1,4,5)P_3-binding and Ca^{2+} channel activities, *ie*, an Ins(1,4,5)P_3-gated Ca^{2+} channel (Miyawaki *et al*, 1990). This protein is comprised of 2749 amino acids and has a large amino-terminal cytoplasmic domain (consisting of the ligand binding domain and a regulatory domain) and six or eight membrane spanning domains near the carboxy-terminus (figure 1.5). Deletion of any small fragment within this region abolishes any Ins(1,4,5)P_3 binding activity (Mignery and Sudhof, 1990). The cerebellar Ins(1,4,5)P_3 receptor protein has some sequence homology in its transmembrane regions with the skeletal muscle ryanodine receptor which is a calcium release channel in the muscle sarcoplasmic reticulum and considered to be important in excitation-contraction coupling (Berridge, 1993). Cross

linking experiments (Maeda *et al*, 1991) have provided evidence that (like the ryanodine receptors) the Ins(1,4,5)P_3 receptor is a homotetramer which is capable of binding four Ins(1,4,5)P_3 molecules. Analysis of the kinetics of Ins(1,4,5)P_3-induced Ca^{2+} release suggests that the mechanism of channel opening is co-operative, producing Hill coefficient values of greater than three (Meyer *et al*, 1988). However, incorporation of the Ins(1,4,5)P_3 receptor into planar lipid bilayers has shown that the Ins(1,4,5)P_3 receptor Ca^{2+} channel exhibits four sub-conductance levels suggesting that Ins(1,4,5)P_3 molecules open the channel in an additive manner (Watras *et al*, 1991). Discrepancies between groups might be attributed to the different tissues used (rat basophilic leukaemia cells versus the reticulum of canine cerebellum) and the possible heterogeneity of Ins(1,4,5)P_3 receptors expressed in these tissues.

Alternative splicing of two segments called SI and SII can produce various forms of the Ins(1,4,5)P_3 receptor. The SI segment consists of 45 nucleotides located within the ligand binding domain of the receptor. The SII region consists of 120 nucleotides divided into three further splicing subsegments A, B and C and lies within the regulatory domain between two possible phosphorylation sites (Figure 1.5). Isoforms carrying at least one of the subsegments are expressed only in the CNS while the fully deleted SII form is expressed ubiquitously (Mikoshiba, 1993). Other forms of Ins(1,4,5)P_3 receptors can originate from separate genes and hence the original Ins(1,4,5)P_3 receptor is now called the cerebellar type or type 1 receptor as opposed to the type 2 Ins(1,4,5)P_3 receptor which has a significantly higher affinity for Ins(1,4,5)P_3 and types 3 and 4 which have been partially sequenced (Sudhof *et al*, 1991; Ross *et al*, 1992). Such heterogeneity is also seen with the ryanodine receptor family which presently consists of three members (Berridge, 1993). The presence of multiple forms of Ins(1,4,5)P_3 and ryanodine receptors raises the possibility that intracellular Ca^{2+} signalling may involve multiple pathways with different regulatory properties dependent on different Ins(1,4,5)P_3 transduction pathways.

1.4.6. Ins(1,4,5)P_3-Induced Calcium Release.

A sub-maximal concentration of Ins(1,4,5)P_3 might be expected to produce a sub-maximal opening of the calcium channels, with the result being a slower efflux of calcium, but leading ultimately to the same net release. However, sub-optimal doses of Ins(1,4,5)P_3 cause a rapid release of a fraction of the releasable calcium, the remainder becoming accessible at higher doses (Mullam *et al*, 1989; Taylor and Potter, 1990). This response was called ɔquantal calcium release and several hypotheses have been created to explain the mechanism.

One hypothesis suggested that different Ins(1,4,5)P_3-sensitive calcium stores were differentially sensitive to Ins(1,4,5)P_3 and that calcium was released from stores in an ɔall or nothing manner (Parker and Ivorra, 1990). Evidence for differential sensitivity of

Figure 1.5. Amino acid sequence structure of the Ins(1,4,5)P_3 receptor showing the three functional domains.

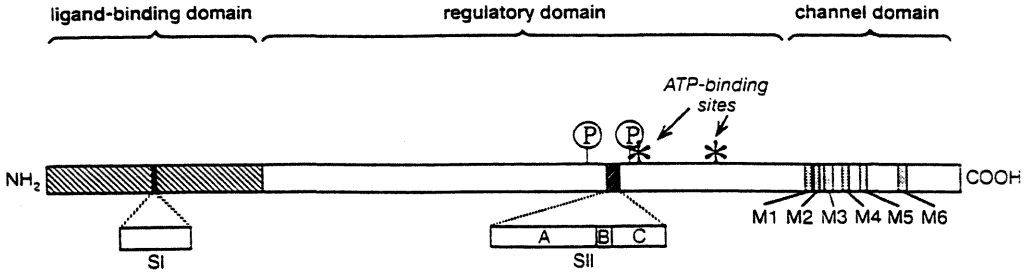

P = phosphorylation sites.
SI and SII isoforms are produced by alternative RNA splicing.
M1-M6 = putative transmembrane spanning regions.

calcium stores came from spatial analysis of calcium release triggered by applying increasing doses of Ins(1,4,5)P_3 to *Xenopus oocytes*, revealing the existence of ɔhot spots (Parker and Yao, 1991). These responses may arise due to the heterogeneity of Ins(1,4,5)P_3 receptors or possible post-translational modifications such as phosphorylation by PKA, PKC or calcium-calmodulin-dependent protein kinase II (Mikoshiba, 1993). Ins(1,4,5)P_3 receptors do not appear to desensitize rapidly. However, chronic stimulation of muscarinic acetylcholine receptors can reduce Ins(1,4,5)P_3 receptor concentrations in human neuroblastoma cells (Wojcikiewicz *et al*, 1992).

Another possible mechanism to explain quantal release is that intra-luminal calcium concentration may play a role in the release of calcium by Ins(1,4,5)P_3 (Irvine, 1990), by binding to a putative calcium binding site on the luminal face of the Ins(1,4,5)P_3 receptor or via a luminal protein associated with the Ins(1,4,5)P_3 receptor. The biphasic nature of Ins(1,4,5)P_3-induced calcium responses can be explained by a ɔsteady state theory involving two allosteric sites, the Ins(1,4,5)P_3 binding site and the putative intra-luminal calcium binding site. In this system, high concentrations of calcium in the stores increases the sensitivity of Ins(1,4,5)P_3-induced calcium release. As the calcium stores empty, calcium binding to the Ins(1,4,5)P_3 receptor would also fall resulting in a decreased sensitivity of the store for Ins(1,4,5)P_3 (Irvine, 1990; Missiaen *et al*, 1992a; Missiaen *et al*, 1992b, Nunn and Taylor, 1992).

The calcium release process is unaffected by a variety of calcium channel blockers but sensitive to agents such as cinnarizine and flunarizine and the potassium channel inhibitor tetraethylammonium (TEA). The latter observation led to the finding that K^+ uptake counteracts the calcium release from Ins(1,4,5)P_3-sensitive stores maintaining electrical neutrality (Berridge and Irvine, 1989).

1.4.7. Calcium-Induced Calcium Release.

Both ryanodine receptors and Ins(1,4,5)P_3 receptors have a common sensitivity to cytosolic calcium. Ryanodine receptors in skeletal muscle are activated by a small influx of calcium ions through voltage-operated calcium channels (VOCC s) triggering an explosive release of stored calcium from the sarcoplasmic reticulum. Ins(1,4,5)P_3-induced calcium release can be manifest as a sudden and near-maximal release of calcium if the level of Ins(1,4,5)P_3 is gradually increased through injection or by flash photolysis of caged Ins(1,4,5)P_3 (Parker and Yao, 1991). Above a certain threshold, small hot spots resulting from localized release of calcium suddenly transformed into all or nothing responses that appeared as expanding circular or spiral waves of calcium mobilization (Lechleiter and Clapham, 1992). This all or nothing response seems to arise through a positive feedback effect whereby calcium stimulates its own release. Ins(1,4,5)P_3-induced calcium flux, using a cerebellar microsomal fraction incorporated into a lipid bilayer,

showed a bell-shaped curve for channel open probability depending on calcium concentrations, suggesting that Ins(1,4,5)P_3-induced calcium release is regulated by cytosolic calcium (Bezprozvanny *et al*, 1991). Calcium seems to maximally activate Ins(1,4,5)P_3-induced calcium release at a concentration of 300 nM after which calcium becomes inhibitory. Therefore, Ins(1,4,5)P_3-induced calcium release is initially enhanced by resting cytosolic calcium concentrations (approximately 100 nM) but after calcium accumulates, due to release from intracellular stores, a negative feedback system operates inhibiting further Ins(1,4,5)P_3-induced calcium release. Switching from positive to negative feedback systems may involve the Ins(1,4,5)P_3 receptor switching from a low affinity state, which can gate calcium, to an inactive high affinity state (Pietri *et al,* 1990). Once the concentration of calcium returns to its resting level, the inactive, high affinity state converts back to the active, low affinity state. This mechanism may account for repetitive calcium spiking and calcium oscillations seen in many cells (Berridge, 1993). Many studies have shown that injection of Ins(1,4,5)P_3 into *Xenopus oocytes* leads to calcium waves propagating through the cytoplasm. It is now thought that calcium-induced calcium release acting via Ins(1,4,5)P_3 receptors may account for such calcium waves via a co-operative interaction between calcium and Ins(1,4,5)P_3. Heparin, which inhibits the binding of Ins(1,4,5)P_3 to its receptor, prevented the migration of calcium waves induced by the poorly metabolized Ins(1,4,5)P_3 triphosphorothioate analogue ($InsP_3S_3$). Injection of calcium (without causing elevations in Ins(1,4,5)P_3) also failed to trigger calcium waves. In the presence of $InsP_3S_3$, however, endogenously released or locally injected calcium elicited calcium waves (DeLisle and Welsh, 1992).

Further levels of complexity arise, when studying calcium-induced calcium release, in that PLC isozymes are also activated by calcium, therefore, levels of Ins(1,4,5)P_3 will rise in the presence of calcium. Furthermore, calcium will activate combinations of Ins(1,4,5)P_3 receptors and ryanodine receptors (if both receptors are present in the cells) leading to a complex array of possible calcium signals.

An ATP binding site on the purified Ins(1,4,5)P_3 receptor has been identified (Maeda *et al*, 1991). Snyder s group (Ferris *et al*, 1990) showed that between 1-10 μM, ATP increased maximal Ins(1,4,5)P_3-induced calcium release by 50 % with no change in Ins(1,4,5)P_3 potency. The enhancing effects of ATP diminished between 100-1000 μM. This suggests a physiological role of ATP in Ins(1,4,5)P_3-induced calcium release. They hypothesized that diminishing local ATP concentrations coincide with filling of calcium stores by the calcium ATPase which may enhance Ins(1,4,5)P_3-induced release of calcium, an effect that would decline as ATP returns to physiological levels. Therefore, ATP, like calcium, may induce calcium release and play a role in oscillations of intracellular calcium concentrations. Cytosolic levels of ATP do not seem to alter greatly during receptor stimulation and measurement of localized ATP concentrations is not yet possible.

1.5. Adenylate Cyclase.

It is well established that adenylate cyclase is activated and inactivated via G_s and G_i G proteins, respectively. Adenylate cyclase converts ATP to cAMP which then activates cAMP-dependent protein kinases resulting in a diverse array of responses.

1.5.1. Structure.

Little was known about the structure of adenylate cyclase until the cloning of a cDNA encoding one of these proteins (Kropinski *et al,* 1989). Six mammalian cDNAs have now been cloned (I-VI). The most common motifs in these proteins include a short amino-terminal region and two cytoplasmic domains (each about 40 KDa), C_1 and C_2, punctuated by two intensely hydrophobic stretches (M_1 and M_2). These hydrophobic regions are thought to contain six transmembrane helices anchoring the protein to the plasma membrane (Tang and Gilman, 1992). The nucleotide binding site is not yet known but is thought to be located in portions of the C_1 and C_2 domains (designated C_{1a} and C_{2a}) which are highly conserved among the mammalian enzymes and with a series of membrane-bound guanylate cyclases (Chinkers and Garkers, 1991). Adenylate cyclases cloned from the brain are known to be about 120 KDa in size, however, estimates of molecular weight *in vivo* have been estimated to be 200-250 KDa (Neer *et al,* 1980) suggesting that these enzymes may form dimers (actually a tetramer of C_{1a} and C_{2a}-like domains).

1.5.2. Regulatory Properties.

All of the mammalian isoforms of AC are activated by $G\alpha_s$ and forskolin (Tang and Gilman, 1992). Type I AC is found predominantly in the brain and is activated by Ca^{2+}-calmodulin (Krupinski *et al,* 1989). More recent evidence suggests that this isoform can also be inhibited by $\beta\gamma$ subunits of G proteins (Tang and Gilman, 1991). Such an action is unlikely to occur in vivo from Gs $\beta\gamma$ subunits due to the relative weakness of $\beta\gamma$ activity compared with $G\alpha_s$ activity. It seems more likely that $\beta\gamma$ subunits from G_i/G_o (which are more highly expressed in the brain) could modulate inhibition of type I AC.

Conversely, type II and type IV AC (Feinstein *et al*, 1991; Gao and Gilman, 1991) are activated by $\beta\gamma$ subunits in the presence of $G\alpha_s$ (Tang and Gilman, 1991). It has also been observed that α_2-adrenoceptors (which normally mediate inhibition of AC via G_i), when transfected into HEK-293 cells, mediate inhibition of AC as predicted. After co-transfection of α_2-adrenoceptors and type II AC into these cells, stimulation of these receptors resulted in increased cAMP levels (following PTX treatment of the cells)

(Federman *et al*, 1992). Type II and IV AC are found in the brain and in some peripheral tissues and are structurally similar. Neither of these isoforms are modulated by Ca^{2+}-calmodulin.

Type III AC (Bakalyar and Reed, 1990) is abundantly found in olfactory tissue and, like type I AC, is activated by Ca^{2+}-calmodulin.

Type V and VI AC (Ishikawa *et al*, 1992; Premont *et al*, 1992) are found in the heart, brain and other peripheral tissues and are not modulated by Ca^{2+}-calmodulin. Neither types III, V or VI AC appear to be effected by $\beta\gamma$ subunits (Tang and Gilman, 1992).

1.5.3. Inhibition of Adenylate Cyclase.

A long standing controversy has been whether $G\alpha_i$ subunits actually inhibit AC or whether $\beta\gamma$ subunits released by activation of G_i inhibit $G\alpha_s$ activity. Brain $G\alpha_i$ was shown to inhibit AC only modestly and at concentrations thought to be rather high physiologically (Katada *et al*, 1984). Further evidence for $\beta\gamma$ modulation of effectors was accumulating from studies on cardiac K^+ channels and the discovery of $\beta\gamma$ involvement in the yeast mating response (as reviewed by Bourne, 1989). The more recent finding that $\beta\gamma$ can inhibit type I AC in the presence of $G\alpha_s$ (Tang and Gilman, 1991) increased the evidence in favour of AC inhibiton being a $\beta\gamma$-mediated effect. However, a large body of evidence does suggest that $G\alpha_i$ subunits can also actively inhibit AC. First, inhibition of adenylate cyclase by hormones and / or guanine nucleotides is easily seen in membranes of the $G\alpha_s$-deficient S49 lymphoma mutant *cyc*$^-$. Second, activation of any G protein-coupled receptor should theoretically lead to release of $\beta\gamma$ subunits, and hence, inhibition of AC. Finally, constitutively active mutants of $G\alpha_i$ ($G\alpha_{i1}$, $G\alpha_{i2}$ and $G\alpha_{i3}$) transiently expressed in HEK-293 cells can inhibit AC (Wong *et al*, 1992). More recently still, myristoylation of recombinant $G\alpha_i$ has been shown to be required for activity (Taussig *et al*, 1993).

1.5.4. Muscarinic Receptors and Adenylate Cyclase.

It is well known that m2 and m4 muscarinic receptors couple to the inhibition of AC via G_i proteins whereas the odd numbered subtypes preferentially couple to PI hydrolysis via G_q-activation of PLC. However, m1 and m3 (but not m5) muscarinic receptors have also been shown to increase cAMP levels on stimulation by agonists (as reviewed by Baumgold, 1992). Controversy exists as to whether this stimulation of cAMP accumulation is due to $\beta\gamma$ stimulation of AC; activation of $G\alpha_s$ or via a mechanism secondary to PI hydrolysis such as Ca^{2+} and / or PKC activation of AC.

1.5.5. Metabolism of cAMP.

Phosphodiesterases (PDEs) control the metabolism of cAMP. Accumulation of cAMP can be attenuated by muscarinic stimulation via increased activation of PDE in 1321N1 human astrocytoma cells, which express M_3 receptors (Hughes *et al*, 1984). This attenuation of cAMP accumulation is PTX-insensitive and may be due to an increase in intracellular Ca^{2+} activating a Ca^{2+}-dependent PDE in these cells.

1.6. Aims.

The aims of this study were to investigate signal transduction mechanisms produced by stimulation of recombinant muscarinic receptor subtypes, expressed as homogeneous populations, in Chinese hamster ovary (CHO) cells. Such studies are often complicated in tissues which commonly express multiple subtypes of muscarinic receptors. By investigating agonist-stimulated second messenger responses from single subtypes of muscarinic receptors in the same cell type, which presumably have the same compliment of G proteins and effectors, comparisons could be made between different muscarinic receptor subtypes. This may lead to a better understanding as to why three muscarinic receptor subtypes seem to couple to the same effector, *i.e.* PLC activation (m1, m3 and m5) and the other two to inhibition of adenylate cyclase (m2 and m4).

In the present study, PLC activation was measured in two ways; firstly, by measuring $Ins(1,4,5)P_3$ accumulation in intact and permeabilized CHO cell clones; and secondly, by measuring the release of loaded $^{45}Ca^{2+}$ from permeabilized CHO cell clones.

Adenylate cyclase activity was measured indirectly by measuring cAMP accumulation in intact CHO cell clones.

Previous studies have shown that interactions between effectors and a given muscarinic receptor subtype are not always exclusive, especially in cells expressing recombinant receptors (Richards, 1991). This promiscuity may be due to cell type or the relatively high expression levels of recombinant receptors expressed in these cell clones compared to physiologically relevant levels. The effect of expression levels of muscarinic receptors on coupling to effectors was investigated in this study to try and clarify this situation.

By measuring agonist-stimulated responses in PTX-treated and untreated CHO cell clones, it was hoped that the responses mediated via PTX-sensitive and PTX-insensitive

G proteins could be defined. A major aim of this study was to investigate whether changes in levels of receptor expression affected any promiscuous coupling of the different muscarinic receptor subtypes with PTX-sensitive and PTX-insensitive G proteins.

Agonist-stimulated activation of G proteins in CHO cell membranes was also measured using [^{35}S]GTPγS, the non-hydrolyzable analogue of GTP. Agonist-stimulated [^{35}S]GTPγS binding was measured to gain insight into the nature of G protein activation in PI-linked receptors (m1 and m3 muscarinic receptors) and in AC-linked receptors (m2 muscarinic receptors).

Tissue studies using cardiac membranes (washed free of guanine nucleotides), which express only M_2 muscarinic receptors, have shown that guanine nucleotide modification of agonist binding(≅GTP-shifts) appear to be large (Waelbroeck *et al*, 1982; Matesic *et al*, 1989). Guanine nucleotide modification of agonist binding to PI-linked receptors has not been as well characterized, partly because of the lack of tissues available which express homogeneous populations of these receptors. Interestingly, where such studies have been carried out using PI-linked receptors, either in tissues or using recombinant receptors expressed in cells, the GTP-shift is somewhat smaller (Evans *et al*, 1985; Flynn *et al*, 1989; Wess *et al*, 1990a), or not present at all (Wess *et al*, 1990b) due to the fact that the agonist binding curves are less shallow than those seen with AC-linked receptors, in the absence of guanine nucleotides. This may represent a fundamental difference between coupling of these receptors to G proteins and deserves further investigation.

Finally, comparison of carbachol occupancy-response curves would give some indication of the efficiency of coupling of the different receptor subtypes to the various effectors measured in CHO cells. Of particular interest is the relative efficiency of coupling of m1 and m3 receptors to PLC activation and to mobilization of intracellular Ca^{2+}. Are there differences in these responses that necessitate the requirement for two receptor subtypes which couple to the same effector protein? Equally important is the effect that receptor expression levels have on the various carbachol occupancy-response curves. It would be of interest to see whether changes in receptor expression levels would evoke the agonist-stimulated responses expected by classical receptor theory.

CHAPTER TWO.

GENERAL METHODS.

2.1 Cell Lines.

Chinese hamster ovary (CHO-K1) cells were sub-cloned from the parent cell line CHO cells derived from the ovary of an adult Chinese hamster. The cells require proline due to the absence of the gene for proline synthesis. CHO-K1 cells are epithelial in morphology but undergo morphological changes in response to cholera toxin (Guerrant *et al*, 1974; Peterson *et al*, 1991).

SH-SY5Y cells were sub cloned from the parent cell line SK-N-SH which were established from a neuroblastoma metastasis from a 4-year old female Caucasian. The SH-SY5Y cells are neuroblast-like as opposed to another sub-clone of SK-N-SH cells called SH-EP1 cells which are non-neuronal (Ross and Biedler, 1985). SH-SY5Y cells were a kind gift from Dr. J. Biedler, Sloane Kettering Institute, New York, USA.

2.2 Preparation of Plasmid DNA and Transfection Procedures.

Chinese hamster ovary (CHO-K1) cells (which do not endogenously express muscarinic receptors) transfected with cDNA encoding either m1, m2 or m3 muscarinic receptors were a kind gift from Dr N.J. Buckley from the National Institute for Medical Research, Mill Hill, London. The methodology for preparation of plasmid DNA and transfection procedures were previously described (Buckley, Bonner, Buckley and Brann, 1989), and is briefly outlined below.

m1, m2 And m3 cDNAs were inserted into the Okayama/Berg pCD expression vector (Okayama and Berg, 1983). Cells were transfected using the modified calcium phosphate procedure described by Chen and Okayama (1987) where a pCDneo vector was co-expressed so that transfected cells could be selected for on the basis of neomycin resistance. After selection with growth medium containing 400 μg / ml of the neomycin analogue G418, transfected cells were diluted out so that single colonies could be isolated, grown separately and assayed for [^{3}H] N-methyl scopolamine (NMS) binding capacity. Three of these cell clones were received from Dr.N. Buckley. CHO cell clones expressing m1 or m2 or m3 muscarinic receptors were characterized pharmacologically (see chapter 3) and renamed CHO-m1, CHO-m2 and CHO-m3 cells, respectively.

A CHO cell clone was developed independently within the department by Dr A.B. Tobin and V. Toth. The coding sequence for the human m3 muscarinic receptor (obtained from cDNA obtained from Dr N. Buckley) was sub-cloned into a mammalian expression vector (pMX-neo) that drives constitutive expression from a retroviral murine sarcoma virus long terminal repeat (MSV-LTR). The resulting vector termed pVT-1 (see Figure 2.1) was transfected into CHO-K1 cells (obtained from Dr. N. Buckley, Mill Hill, London) using the calcium phosphate precipitation procedure essentially as described by

Sambrook, Fritsch and Maniatis (1989). Following selection of transfected cells in growth medium supplemented with 300 μg / ml neomycin, individual colonies were isolated using cloning cylinders, grown separately and assayed for [^{3}H]NMS binding capacity. One CHO cell clone developed in this way expressed m3 muscarinic receptors at a relatively lower receptor density than in CHO-m3 cells. This new clone was named CHO-vt9.

A CHO clone expressing a higher density of m2 muscarinic receptors than CHO-m2 cells was sub-cloned from CHO-m2 cells by Dr S. Lazerino from the National Institute for Medical Research, Mill Hill, London. This clone was kindly sent to this department towards the end of this study and named CHO-slm2.

2.3 Cell Culture.

CHO-K1 cells expressing recombinant muscarinic receptor subtypes were grown in 175 cm^3 culture flasks containing 30 ml of growth medium. Growth medium consisted of alpha minimal essential media (αMEM) supplemented with 10 % new-born calf serum, 100 IU / ml penicillin, 100 μg / ml streptomycin and 2.5 μg / ml fungizone. Cells were incubated in a 5% CO_2, humidified incubator at 37 °C. Media was replaced twice weekly and cells were passaged weekly (approximately a 1 in 50 dilution) using trypsin (0.5 g / l) / EDTA (0.2 g / l) in modified Pucks saline.

SH-SY5Y human neuroblastoma cells were grown identically using minimal essential media (MEM) supplemented with 10 % foetal calf serum, 100 IU / ml penicillin, 100μg / ml streptomycin, 2 mmol / l L-glutamine and 2.5 μg / ml fungizone. Cells were passaged weekly (approximately a 1 in 8 dilution) in the same manner as the CHO cell clones.

2.4 Cell Preparation.

2.4.1 Intact Cell Preparation.

CHO cell clones and SH-SY5Y cells were grown to confluence and harvested using 10 mM HEPES, 0.02% EDTA and 0.9% NaCl, pH 7.4. Cells were then pelleted and washed twice in the assay buffer required for use in experiments before being pelleted and resuspended in buffer at the protein concentration required (see methods sections at the beginning of each chapter for details).

2.4.2 Membrane Preparation.

Cells were grown to confluence and harvested using 10 mM HEPES, 0.02% EDTA and 0.9% NaCl, pH 7.4. Cells were then pelleted and washed in ice-cold buffer consisting of 10 mM HEPES, 10 mM EDTA, pH 7.4. Cells were then homogenized using a polytron

tissue disrupter (level 6, 6 x 3 s bursts). Crude membranes were pelleted in a refrigerated centrifuge at 40 000 g for 10 min at 4 °C and then washed and pelleted twice more in cold assay buffer. Membranes were finally resuspended in assay buffer at the protein concentration required for use in experiments (see methods sections at the beginning of each chapter for details).

2.5. Cell Permeabilization.

Cells were harvested at confluence using 10 mM HEPES, 0.02% EDTA and 0.9% NaCl, pH 7.4 and resuspended in cytosol-like buffer (CLB) (see Appendix 1). Cells were pelleted and washed twice in 10 ml of ice-cold CLB to remove any remaining EDTA (from the harvesting process).

2.5.1 Electroporation.

Each flask of cells was finally resuspended in 0.8 ml of ice-cold CLB and permeabilized with three discharges of a 3 μF capacitor with a field strength of 3.75 KV / cm and a time constant of 0.1 msec (Gene Pulsar, Biorad, Richmond, CA). The permeabilized cell suspensions were then diluted in 5 ml of ice-cold CLB, centrifuged at 500 g for 2 min and finally resuspended in ice-cold CLB at the protein concentration required (see individual method sections for details).

2.5.2. Saponin Permeabilization.

Each flask of cells was finally resuspended in 2 ml of ice-cold CLB. 200 μl of saponin (1 mg / ml stock solution) was added to the cell suspension and mixed gently for 30 s. Cells were then pelleted (500 g for 2 min) and resuspended in ice-cold CLB at the protein concentration required (see chapter 7 methods).

2.6. Protein Determinations.

Protein assays were performed as a modification of the method of Lowry (Lowry *et al*, 1951). Protein standards were prepared from bovine serum albumin (BSA) diluted in 0.1 M NaOH to give a range of concentrations from 0 to 300 μg of protein / ml. 500 μl of each standard were aliquoted into separate test tubes in duplicate along with 50 μl of sample + 450 μl of 0.1 M NaOH (a 1 in 10 dilution of the sample). 2.5 ml of solution E was added to each test tube. Solution E consisted of 100 ml of solution A (2 % Na_2CO_3 in 0.1 M NaOH) + 1 ml of solution B (1 % $CuSO_4$) + 1 ml of solution C (2 % Na^+K^+-tartrate). 250 μl of solution D (a 1 in 4 dilution of Folin / Ciocalteus phenol reagent in

distilled water) was added to each test tube after 10 min and each tube was vortex mixed. 30 min later, absorbance readings at 750 nm were determined and sample absorbance was converted to protein concentration by comparison with the absorbance values for the protein standards.

Figure 2.1. Diagram of the pVT-1 expression vector.

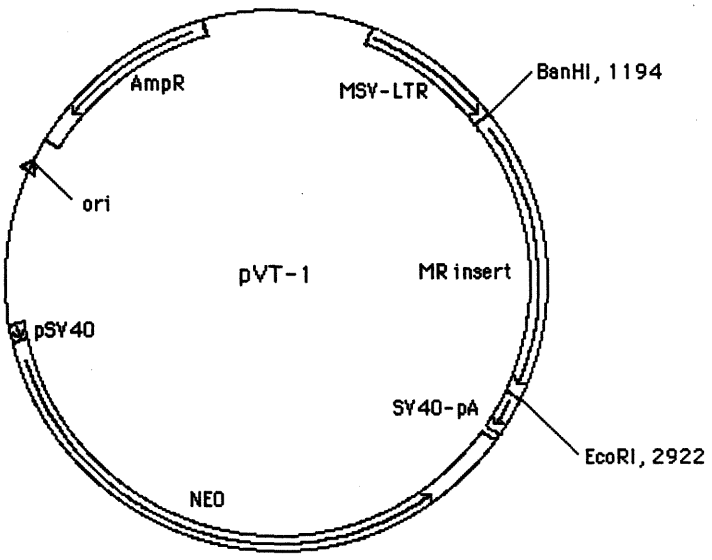

AmpR = ampicillin resistance; MSV-LTR = murine sarcoma virus long terminal repeat; BanHI and EcoRI = restriction sites; MR insert = muscarinic receptor sequence; SV40-pA = simian virus poly A tail; NEO = neomycin resistance; pSV40 = simian virus promoter; ori = origin of replication.

CHAPTER THREE.

CHARACTERIZATION OF RECOMBINANT MUSCARINIC RECEPTORS IN CHO-K1 CELLS AND ENDOGENOUSLY EXPRESSED MUSCARINIC RECEPTORS IN SH-SY5Y CELLS.

3.0 Introduction.

The pharmacological and biochemical characterization of individual muscarinic receptor subtypes has been hindered by the general lack of a homogeneous population of muscarinic receptors found endogenously in tissues.

The discovery and cloning of five genetically-defined muscarinic receptor subtypes which have been expressed in multiple cell types in the past five years (Richards, 1991; Hulme *et al*, 1990; Caulfield, 1993) has resulted in systems whereby individual muscarinic receptor subtypes can be studied in isolation.

Chinese hamster ovary cell-clones, each transfected with cDNA encoding either m1, m2 or m3 muscarinic receptors, were a kind gift from Dr. N. Buckley (M.R.C. Mill Hill, London). The aim of this study was to characterize the subtypes of muscarinic receptors expressed in the CHO cell clones in terms of their expression levels and their affinity profiles for a range of selective muscarinic antagonists. No single selective muscarinic antagonist can adequately distinguish one muscarinic receptor subtype from the other four. Therefore, a particular muscarinic receptor subtype must be defined with dissociation constants for a range of selective antagonists (Jones *et al*, 1992; Hulme *et al*, 1990; Caulfield, 1993; Buckley *et al*, 1989; Dorje *et al*, 1991; Lazareno *et al*, 1990).

SH-SY5Y human neuroblastoma cells, which endogenously express muscarinic receptors, were characterized in an identical manner to the CHO-cell clones. The nature of the muscarinic receptor subtype(s) expressed in SH-SY5Y cells has been subject to controversy (for review see Lambert and Nahorski, 1990b). Previous studies using selective muscarinic antagonist affinity profiles have suggested that SH-SY5Y cells express M_1 receptors alone (Serra *et al*, 1988); a mixed population of M_1 and M_2 receptors (Adem *et al*, 1987); a mixed population of M_1, M_2 and M_3 receptors (Kukkonen *et al*, 1992); or a homogeneous population of M_3 receptors (Lambert *et al*, 1989).

3.1 Methods.

Cells were grown to confluence, harvested and resuspended in Krebs / HEPES assay buffer, pH 7.4 (see appendix 2) for experiments using intact cells. Membranes were prepared (as described in Chapter 2) and resuspended in 10 mM HEPES, 1 mM $MgCl_2$, 100 mM NaCl, pH 7.4.

3.1.1. Radioligand Binding Assay.

Saturation binding experiments using intact cells or membranes (in their respective assay buffers) were conducted by incubating cells or membranes with a range of

concentrations of [^{3}H] N-methyl scopolamine (NMS) (84 Ci / mmol) (0.03 - 3.00 nM) in a 1 ml final assay volume for 60 min at 37 °C, by which time equilibrium binding was achieved. Final protein concentrations (μg / ml) used in experiments using intact cells were 148 ± 18 (SH-SY5Y, n=5), 115 ± 18 (CHO-m1, n=3), 135 ± 10 (CHO-m2, n=4), 26 ± 2 (CHO-m3, n=3) and 186 ± 30 (CHO-slm2, n=3). Final protein concentrations (μg / ml) used in experiments using membranes were 128 ± 8 (CHO-m1, n=3), 523 ± 23 (CHO-m2, n=3), 20 ± 2 (CHO-m3, n=3) and 181 ± 19 (CHO-vt9, n=4). Binding was terminated by filtration using Whatman GF/B filters.

[^{3}H]NMS saturation binding experiments in cell membranes were performed using identical conditions to those in intact cells except that filters were pre-soaked in distilled water containing 1% BSA and 1% Sigmacote siliconizing fluid for two hours. Filters were then rinsed in distilled water and left to dry overnight before use (as described by Harden *et al*, 1983). It was found in Chapter 4 that pretreating the filters in this way decreased non-specific binding of [^{3}H]NMS (filter blank). The agonist carbachol at high concentrations was found to displace [^{3}H]NMS non-specific binding to a greater extent than 1 μM atropine thereby slightly altering the shape of the displacement curves. This was particularly marked in CHO-m2 membranes where carbachol displacement of [^{3}H] NMS binding to the filter blank became a significant proportion of total [^{3}H] NMS binding in membranes which have a low density of muscarinic receptors.

In experiments where intact cells or membranes were used, filters were dampened with cold assay buffer just prior to filtration of the samples. Samples were filtered (by vacuum filtration using a Brandel cell harvester) and the filters were then washed twice with 3 ml of cold binding buffer. Filters were transferred to separate vials and 4 ml of scintillation cocktail (Optiphase X) was added. Samples were then left for greater than 12 hours before being counted for radioactivity by liquid scintillation spectrometry. Non-specific binding was determined in the presence of 1 μM atropine. In all experiments, protein concentrations were modified so that [^{3}H]NMS bound was less than 20 % of total radiolabel added. Non-specific binding was normally 10 % or less of total [^{3}H]NMS bound (data not shown).

Competition binding experiments were performed in intact cells using the same incubation conditions as above. Cells were incubated with a single concentration of [^{3}H]NMS (approximately 0.4 nM) and increasing concentrations of a selective muscarinic receptor antagonist. Selective antagonists used were pirenzepine (10^{-4} - 10^{-10} M), methoctramine (10^{-4} - 10^{-10} M) and 4-DAMP (4-diphenylacetoxy-N-methyl piperidine methiodide) (10^{-4} - 10^{-10} M). Incubations were terminated as described above. In all experiments protein concentrations were modified so that [^{3}H]NMS bound was less than 20 % of total bound.

3.1.2 Data Analysis.

[^{3}H]NMS saturation binding data for each experiment was analysed by Scatchard analysis (Scatchard, 1949) to determine maximal binding capacity (B_{max}), equilibrium dissociation constant (K_D) and Hill coefficient (nH) values. Competition binding experiments were analysed using the computer program ALLFIT (De Lean *et al*, 1978) which calculates IC_{50} and Hill coefficient values. IC_{50} values were then adjusted to inhibition dissociation constant (K_i) values by the method of Cheng and Prusoff (1973) taking into account the concentration of competing radioligand.

A K_i value for pirenzepine binding to CHO-vt9 cells was obtained by using the [^{3}H]NMS dissociation constant (K_D) for CHO-m3 cells (see Table 3.2.1) due to the absence of [^{3}H]NMS saturation binding data to muscarinic receptors in CHO-vt9 cells. As both of these cell lines express recombinant m3 muscarinic receptors then the K_D values for [^{3}H] NMS binding should be the same and can be incorporated into the Cheng / Prusoff equation.

3.2 Results.

[^{3}H]NMS equilibrium binding in CHO-m3 cells and SH-SY5Y cells was achieved after a 30 min incubation period at 37 ^{o}C. Equilibrium binding was maintained for a further 60 min without any significant loss of binding (data not shown). All experiments using [^{3}H]NMS were therefore carried out using a 60 min incubation at 37 ^{o}C.

Saturation binding data obtained from experiments using intact CHO cell clones and SH-SY5Y cells are shown in Table 3.2.1 and show that [^{3}H]NMS binding to the different muscarinic receptor subtypes was relatively non-selective with dissociation constants ranging between 0.09 nM and 0.19 nM. Hill coefficient values of unity were produced suggesting that [^{3}H]NMS bound to each muscarinic receptor subtype with a single affinity.

CHO-m1 cells expressed an intermediate density of m1 muscarinic receptors (367 $\pm$ 26 fmol / mg protein). Later studies (*i.e.* Chapters 5-8) were performed using CHO-m1 cells that expressed a higher density of m1 muscarinic receptors (approximately 1-2 pmol of receptor / mg protein). Original CHO-m1 cell stocks were lost due to a clerical error whereby records of stocks of CHO-m1 cells taken from the liquid nitrogen store were not maintained and stocks taken were not replenished later. The high expressing CHO-m1 clone was kindly donated by Dr N. Buckley 6 months after the initial CHO-m1 clone was sent. Both the intermediate and high expressing CHO-m1 clones are thought to originate from the same initial stock of CHO-m1 cells and the muscarinic receptors expressed by both clones bound pirenzepine with an identical high affinity.(data not shown). The other

cell lines were grown up from a single source of frozen down stocks of cells and their expression levels of muscarinic receptors were maintained throughout the three year period of study (data not shown).

B_{max} determinations showed that CHO-m3 cells expressed a relatively high density of m3 muscarinic receptors (1397 ± 84 fmol / mg of protein).

CHO-m2 cells expressed a low density of m2 muscarinic receptors (76 ± 11 fmol / mg protein). The CHO-m2 subclone (CHO-slm2) expressed 5-fold more m2 muscarinic receptors than CHO-m2 cells (366 ± 68 fmol / mg protein).

SH-SY5Y cells expressed a low density of muscarinic receptors (165 ± 40 fmol / mg protein).

[^{3}H]NMS saturation binding in membranes produced similar K_D values between CHO cell clones and SH-SY5Y cells though in all cases [^{3}H]NMS bound with a slightly higher affinity to muscarinic receptors in membrane preparations than in intact cells (see Table 3.2.1).

B_{max} values were significantly higher in membranes compared with intact cells especially in membranes from CHO-m3 cells (see Table 3.2.1). Membranes prepared from CHO-vt9 cells were found to express 7-fold fewer m3 muscarinic receptors (430 ± 43 fmol / mg protein) than CHO-m3 cell membranes (3043 ± 165 fmol / mg protein).

Due to the inability of [^{3}H]NMS to distinguish between different muscarinic receptor subtypes, three selective antagonists were used in competition experiments with a single concentration of [^{3}H]NMS (approximately 0.4 nM). Each of the selective antagonists, pirenzepine, methoctramine and 4-DAMP produced inhibition binding curves in these cell lines with Hill coefficient values of unity (see Table 3.2.2). This clearly showed that only single muscarinic receptor subtypes could be identified pharmacologically in each of these cell lines. These results were expected in the CHO cell clones which do not endogenously express muscarinic receptors but do express a single recombinant muscarinic receptor subtype. The SH-SY5Y cells endogenously express muscarinic receptors and these results suggest that only a single muscarinic receptor subtype can be identified pharmacologically in these cells.

Pirenzepine is reported to have a selectively higher affinity for M_1 muscarinic receptors than for M_2, M_3 or m5 muscarinic receptor subtypes (Caulfield, 1993). Pirenzepine had a significantly higher affinity for the recombinant muscarinic receptors expressed in CHO-m1 cells compared with the other cell lines (see Table 3.2.2). Pirenzepine had a 14-fold and 17-fold lower affinity for m3 muscarinic receptors

expressed in CHO-m3 cells and CHO-vt9 cells, respectively, than for m1 receptors. m2 Muscarinic receptors expressed in CHO-m2 cells had a 43-fold lower affinity for pirenzepine compared with m1 receptors. Similarly, SH-SY5Y cells had a 45-fold lower affinity for pirenzepine than m1 receptors expressed in CHO-m1 cells.

Pirenzepine was relatively non-selective (2 to 3-fold) between the m2 receptors expressed in CHO-m2 cells and m3 receptors expressed in CHO-m3 cells and CHO-vt9 cells.

Methoctramine is reported to bind with a higher affinity to M_2 muscarinic receptors compared with M_3 muscarinic receptors (Michel and Whiting, 1988). Methoctramine had a significantly higher affinity for m2 receptors expressed in CHO-m2 cells than for muscarinic receptors expressed in all other cell lines. Methoctramine bound with a 3-fold lower affinity for m1 receptors compared with m2 receptors in CHO cells. m3 Muscarinic receptors expressed in CHO-m3 cells and muscarinic receptors expressed in SH-SY5Y cells bound methoctramine with a 47-fold and 85-fold lower affinity, respectively, than did m2 receptors expressed in CHO-m2 cells. Methoctramine was relatively non-selective (less than 2-fold) between m3 receptors expressed in CHO-m3 cells and muscarinic receptors expressed in SH-SY5Y cells.

4-DAMP is reported to have a higher affinity for M_3 receptors than for M_2 receptors (Barlow *et al*, 1976). 4-DAMP bound to muscarinic receptors in all cell types with a relatively higher affinity and was relatively non-selective (less than 2-fold) for m1 and m3 receptors expressed in CHO cells and muscarinic receptors expressed in SH-SY5Y cells. 4-DAMP bound to m2 receptors expressed in CHO-m2 cells with a 6-fold lower affinity than for m3 receptors expressed in CHO-m3 cells.

3.3 Discussion.

The different CHO-cell clones (with the possible exception of CHO-m1 cells) were found to stably express muscarinic receptors over the three year period of this study. The increased expression of muscarinic receptors in CHO-m1 cells that occurred after 6 months, coincided with the receipt and usage of a new stock of CHO-m1 cells from Dr. N. Buckley. The changes in B_{max} (determined by [^{3}H]NMS saturation binding) observed in all cell lines studied, between experiments using intact cells and experiments performed using membranes, could have resulted from various differences in assay conditions. The use of siliconized filters in experiments using membranes compared with untreated filters in experiments using intact cells probably increased the percentage of specifically bound radiolabel as was shown with the binding of the muscarinic agonist [*methyl*-^{3}H] oxotremorine to muscarinic receptors in cardiac membranes (Harden *et al*, 1983). During

preparation of the membranes, soluble proteins will be lost resulting in an increased ratio of receptors to protein present. For every mg of protein, the number of receptors would be increased resulting in an increased B_{max} compared with intact cells. The different binding buffers used for experiments using intact cells and membrane preparations might well explain the marginal affinity differences observed for [^{3}H]NMS binding and the binding of other antagonists (Hulme *et al*, 1990) and may also have more subtle effects on the proportion of specific [^{3}H]NMS bound.

The expression levels of muscarinic receptors expressed in CHO-m2 and CHO-m3 cell membranes were found to be very similar to values obtained by Buckley *et al* (1989) from whom these CHO clones were obtained. However, Buckley *et al* (1989) observed that the CHO-m1 clone expressed only 180 ± 43 fmol of receptor / mg protein compared with the present study where m1 receptors were expressed initially at 556 ± 19 fmol / mg protein, which later increased to 1-2 pmol / mg protein. The reason for the apparent increase in m1 muscarinic receptor expression in our CHO-m1 cells may be due to an accidental selection of a high-expressing subclone of the original CHO-m1 population. A similar subclone (CHO-slm2) was derived intentionally by Dr. Lazareno from the original CHO-m2 cell stocks.

In the present study, CHO cells expressing homogeneous populations of recombinant m1, m2 or m3 receptors have been characterized on the basis that each muscarinic receptor subtype has a distinct pharmacological profile based on the rank order of affinity of a series of selective antagonists (Jones *et al*, 1992; Hulme *et al*, 1990; Caulfield, 1993; Buckley *et al*, 1989; Dorje *et al*, 1991; Lazareno *et al*, 1990; Richards; 1991). The selective muscarinic receptor antagonists pirenzepine, methoctramine and 4-DAMP produced [^{3}H]NMS displacement binding curves with Hill coefficient values close to unity in each of the CHO cell clones and in SH-SY5Y cells. Therefore, each of these cell lines appear to express a homogeneous population of muscarinic receptors.

The Hill coefficient values for methoctramine binding to muscarinic receptors expressed in CHO-m1 and CHO-m2 cells were slightly higher than unity suggesting that methoctramine may bind to an allosteric site on muscarinic receptors as has been observed in other studies (Giraldo *et al*, 1988). The allosteric nature of methoctramine has been observed at concentrations above 1 μM and results in a decrease in the dissociation rate of [^{3}H]NMS. However, in the present study, the relative steepening of the antagonist displacement curve occurred at lower concentrations of methoctramine (below 100 nM) and were, therefore, unlikely to be caused by the allosteric nature of methoctramine.

Pirenzepine binds preferentially to M_1 muscarinic receptors compared with M_2, M_3 or m5 receptors (Hammer *et al*, 1980; Hulme *et al*, 1990; Caulfield, 1993). In the present

study, pirenzepine produced an affinity profile of m1 > m3 ≥ m2 in the CHO cell clones which is consistent with the pirenzepine affinity profile obtained by Buckley *et al* (1989) and Dorje *et al* (1991) in CHO cell membranes expressing recombinant muscarinic receptor subtypes. In the present study the affinity values for pirenzepine binding to m1, m2 and m3 receptors expressed in CHO cells were not significantly different to the range of antagonist affinities collated in an extensive review of muscarinic receptor research by Caulfield (1993). Pirenzepine bound to m1 receptors expressed in CHO-m1 cells with a pK_B (negative logarithm of dissociation constant) of 7.94 compared with the range of affinities for pirenzepine binding to $m1/M_1$ receptors collated from various studies (Caulfield, 1993) of 7.9-8.2. The pK_B values for pirenzepine binding to m3 and m2 receptors in CHO-m3 and CHO-m2 cells, respectively, were 6.78 and 6.28 compared with the pK_B values for pirenzepine binding to $m3/M_3$ receptors and $m2/M_2$ receptors of 6.7-7.1 and 6.3-6.5, respectively (Caulfield, 1993).

Methoctramine is a useful antagonist for discriminating between M_2 receptors (high affinity binding) and M_3 receptors (low affinity binding) (Michel and Whiting, 1988). In the present study methoctramine had an affinity profile for the muscarinic receptors expressed in CHO-cell clones of m2 > m1 > m3. This is consistent with the methoctramine affinity profile obtained in CHO-cell membranes expressing recombinant muscarinic receptors (Buckley *et al*, 1989; Dorje *et al*, 1991). Methoctramine bound to m2, m1 and m3 receptors expressed in CHO cells, in the present study, with pK_B values of 7.62, 7.14 and 5.95, respectively. The range of pK_B values for methoctramine binding to $m2/M_2$, $m1/M_1$ and $m3/M_3$ receptors, reviewed by Caulfield (1993), were 7.8-8.3, 7.1-7.6, and 6.3-6.9, respectively. Although the affinities of the m2 and m3 muscarinic receptor subtypes for methoctramine were comparatively slightly weaker (less than 3-fold), the affinity profile strongly suggests that CHO-m2, CHO-m1 and CHO-m3 cells express m2, m1 and m3 receptors, respectively.

4-DAMP binds preferentially to M_3 receptors compared with M_2 receptors (Barlow *et al*, 1976). In the present study 4-DAMP had an affinity profile for the muscarinic receptors expressed in CHO cell clones of m1 ≃ m3 > m2. This 4-DAMP affinity profile is similar to the one obtained by Dorje *et al* (1991) in CHO cell membranes expressing recombinant muscarinic receptor subtypes (m3 ≃ m1 > m2) whereby both m1 and m3 receptors have a similar affinity for 4-DAMP, but 4-DAMP has a lower affinity for m2 receptors. In the present study, 4-DAMP bound to m1, m3 and m2 receptors in CHO cells with pK_B values of 8.79, 8.65, and 7.9, respectively. The range of pK_B values for 4-DAMP binding to $m1/M_1$, $m3/M_3$ and $m2/M_2$ receptors, collated from the literature by Caulfield (1993) were 8.9-9.2, 8.9-9.3 and 8.0-8.4, respectively. The affinities of the muscarinic receptors expressed in CHO-m1, CHO-m3 and CHO-m2 cells for 4-DAMP

were slightly weaker in comparison.

Selective muscarinic receptor antagonist binding affinities tend to vary by approximately 3-fold between different studies by different groups (see Caulfield, 1993 for review). These variations in binding affinities are probably caused by changes in assay conditions between different studies (Hulme *et al*, 1990; Peddar *et al,* 1991). Therefore, comparisons of individual selective antagonist binding affinities between groups can lead to errors in characterizing the muscarinic receptor subtype present, especially if the antagonist used has only a ten-fold selectivity between subtypes. The rank order of affinity of a series of selective antagonists for muscarinic receptor subtypes is, therefore, a more accurate determination of the receptor subtype present.

For the pharmacological data obtained with cloned muscarinic receptors to be physiologically relevant, the receptors must have similar antagonist binding properties when expressed endogenously in tissues and in transfected cell lines. Fortunately, this appears to be the case (Jones *et al*, 1992; Caulfield, 1993; Lazareno *et al*, 1990). Similarly, there does not seem to be any major discrepancies between muscarinic receptor antagonist affinities determined in radioligand binding studies and apparent muscarinic receptor antagonist affinities in corresponding functional experiments, indicating that the characteristics of antagonist binding sites probably reflects the characteristics of the corresponding coupled receptors (Mitchelson *et al*, 1989; Caulfield, 1993; Richards, 1991).

The affinity profiles of pirenzepine, methoctramine and 4-DAMP for m1 receptors are very similar to those which have been obtained for m4 receptors (Lazareno *et al*,1990; Caulfield, 1993). CHO-m1 cells had been transfected with the cDNA encoding m1 receptors only and no further characterization of these muscarinic receptors was thought necessary. However, if the same affinity profile was obtained in tissues expressing endogenous muscarinic receptors, further characterization would be necessary to distinguish whether the muscarinic receptors were of the m1 subtype or the m4 subtype. Currently, the only selective antagonist capable of distinguishing these two receptor subtypes is himbacine which has an approximately 10-fold greater affinity for m4 receptors than for m1 receptors (Lazareno *et al*, 1990; Caulfield, 1993).

Comparison of the binding affinities and Hill coefficients of the binding curves obtained with pirenzepine, methoctramine and 4-DAMP for the muscarinic receptors expressed in SH-SY5Y cells and for the muscarinic receptors expressed in CHO-m1, CHO-m2 and CHO-m3 cells, suggests that SH-SY5Y cells express a predominant (if not homogeneous) population of M_3 muscarinic receptors. The low affinity binding of methoctramine to muscarinic receptors expressed in CHO-m3 cells and in SH-SY5Y cells

relative to CHO-m1 and CHO-m2 cells is convincing evidence that both CHO-m3 cells and SH-SY5Y cells express the same subtype of muscarinic receptors. This conclusion is in agreement with studies by Lambert *et al* (1989) which were performed using the same stock of SH-SY5Y cells as the present study.

SH-SY5Y cells expressed 8-fold fewer M_3 receptors than CHO-m3 cells. This is assuming that the protein content of CHO cells and SH-SY5Y cells are similar because receptor densities were expressed as fmol of receptor / mg protein.

Wall *et al* (1991) used muscarinic receptor subtype-selective antisera to determine the subtypes of muscarinic receptors expressed in SH-SY5Y cells. They found that SH-SY5Y cells expressed predominantly m3 receptors (74%) with lower levels of m1 (5%) and m2 (8%) receptors. Another group has also detected mRNA encoding m1, m2 and m3 muscarinic receptors in SH-SY5Y cells (Kukkonen *et al*, 1992). These studies may explain the differences in pharmacological characterization of the muscarinic receptors expressed in SH-SY5Y cells observed by different groups (Serra *et al*, 1988; Adem *et al*, 1987; Lambert *et al*, 1989). Pharmacological characterization of muscarinic receptor subtypes can be relatively insensitive to a small population of one subtype of receptor (less than 10%) in the presence of another receptor subtype which predominates. In effect, the antagonist binding characteristics of the small population of muscarinic receptor subtype can be masked by the antagonist binding characteristics of the predominant muscarinic receptor subtype. Therefore, in the present study, the presence of small populations of M_1 and/or M_2 receptors in SH-SY5Y cells cannot be excluded despite the fact that the selective muscarinic receptor antagonist affinity profiles suggest that a homogeneous population of M_3 receptors is expressed. Kukkonen *et al* (1992) have shown that mRNA for m1, m2 and m3 muscarinic receptors can be detected in SH-SY5Y cells. However, binding studies could only verify the presence of two affinity sites for pirenzepine and for 4-DAMP in SH-SY5Y cells, and the affinity for the high affinity sites could change dramatically depending on the batch of SH-SY5Y cells used. Functional studies, *i.e.* antagonist inhibition of agonist-stimulated Ca^{2+} mobilization, also showed a differential affinity for pirenzepine but the relative proportions of high and low affinity sites of the receptors could not be accurately measured (Kukkonen *et al*, 1992). They suggested from these results that SH-SY5Y cells expressed a mixed population of M_1 and M_3 muscarinic receptors and that a co-expression of M_1, M_2 and M_3 muscarinic receptors in SH-SY5Y cells was theoretically difficult to show by means of binding experiments with the presently available selective antagonists.

Variations in muscarinic receptor subtype expression in SH-SY5Y cells may explain the diversity of results obtained from pharmacological characterization of these cells by different groups. Variations in muscarinic receptor subtype expression in SH-SY5Y cells may be caused by differences in culture conditions or from differing sources of SH-SY5Y

cells used. It may, therefore, be necessary to repeat such antagonist affinity profiles periodically in SH-SY5Y cells; not to determine quantitative assessments of the proportions of muscarinic receptor subtypes present; but to, at least, be aware of the possible presence of different muscarinic receptor subtypes which may affect muscarinic agonist-induced responses in SH-SY5Y cells. Similarly, the total expression level of muscarinic receptors in SH-SY5Y cells should be monitored as a precautionary measure. If such changes do occur, then it would strongly suggest that SH-SY5Y cells may change their expression level of muscarinic receptors, or the relative subtypes present; either with changes in passage number; or at different levels of confluency. Such factors may be very important and recent observations suggest that the degree of SH-SY5Y cell differentiation can markedly influence muscarinic agonist-induced responses (unpublished), possibly relating to changes in expression levels of muscarinic receptor number and/or subtype.

Table 3.2.1.

[^{3}H]NMS saturation binding in intact CHO cell clones and in membranes preparations of CHO cell clones.

K_D (log molar values) represents the dissociation constant from individual experiments. **nH** represents the Hill number and B_{max} represents the maximal binding capacity in fmol of receptor / mg protein. Numbers in parenthesis represent the number of individual experiments performed. All data is expressed as the mean ± standard error of values obtained from the individual experiments.

[^{3}H]NMS saturation binding in intact cells.

	K_D	B_{max}	nH	n
CHO-m1*	-10.07 ± 0.05	367 ± 26	0.98 ± 0.09	(3)
CHO-m2	-9.72 ± 0.06	76 ± 11	1.07 ± 0.03	(4)
CHO-m3	-9.84 ± 0.10	1397 ± 84	1.07 ± 0.07	(3)
SH-SY5Y	-9.85 ± 0.12	165 ± 40	0.96 ± 0.02	(5)
CHO-slm2	-9.76 ± 0.04	366 ± 68	1.05 ± 0.06	(3)

[^{3}H]NMS saturation binding in membranes.

	K_D	B_{max}	nH	n
CHO-m1*	-9.90 ± 0.07	556 ± 19	0.95 ± 0.02	(3)
CHO-m2	-9.34 ± 0.05	99 ± 25	1.03 ± 0.03	(3)
CHO-m3	-9.55 ± 0.04	3043 ± 165	0.98 ± 0.02	(3)
CHO-vt9	-9.47 ± 0.03	430 ± 43	0.97 ± 0.02	(3)

* A later stock of CHO-m1 cells produced B_{max} values (in intact cells) of approximately 1-2 pmol of receptor / mg protein (see **3.3 Results** for details).

Table 3.2.2.

Antagonist binding parameters derived from [^{3}H]NMS displacement experiments in intact CHO cell clones.

K_i (log molar values) represents the inhibition constant obtained using the Cheng-Prusoff equation and the [^{3}H]NMS K_D values from Table 3.2.1. To deduce a K_i value for CHO-vt9 cells the [^{3}H]NMS K_D value for CHO-m3 cells was used. nH represents the Hill number and numbers in parenthesis represent the number of individual experiments. All data is represented as the mean ± standard error of values obtained from the individual experiments.

		CHO-m1	CHO-m2	CHO-m3	SH-SY5Y	CHO-vt9
	K_i	-7.94 ± 0.03	-6.28 ± 0.13	-6.78 ± 0.05	-6.31 ± 0.01	-6.69 ± 0.02
Pirenzepine	nH	0.89 ± 0.03	0.98 ± 0.05	0.98 ± 0.01	1.08 ± 0.04	0.98 ± 0.01
	n	(3)	(3)	(3)	(3)	(3)
	K_i	-7.14 ± 0.08	-7.62 ± 0.06	-5.95 ± 0.08	-5.69 ± 0.09	
Methoctramine	nH	1.16 ± 0.05	1.20 ± 0.09	1.02 ± 0.04	1.02 ± 0.05	
	n	(3)	(5)	(5)	(3)	
	K_i	-8.79 ± 0.01	-7.90 ± 0.19	-8.65 ± 0.12	-8.61 ± 0.09	
4-DAMP	nH	0.89 ± 0.03	0.93 ± 0.02	0.98 ± 0.03	1.06 ± 0.03	
	n	(3)	(3)	(3)	(3)	

CHAPTER FOUR.

AGONIST BINDING TO MUSCARINIC RECEPTOR SUBTYPES EXPRESSED IN CHO CELL CLONES AND SH-SY5Y CELLS: EFFECTS OF GUANINE NUCLEOTIDES, CATIONS AND PERTUSSIS TOXIN PRETREATMENT.

4.0 Introduction.

Agonists unlike antagonists tend to bind to G protein-coupled receptors with multiple affinity states (see chapter 1). A high agonist affinity state of the receptor is thought to be the 'active' conformation of the receptor as described by the ternary complex model of agonist-receptor-G protein interactions (DeLean *et al*, 1980; Taylor, 1990). In its active conformation, the receptor is thought to be bound to a G protein which has the guanine nucleotide binding site on its α subunit empty, *i.e.* at the transition between GDP dissociation and GTP association. A low agonist affinity state of the receptor is thought to exist when the receptor is either not bound to a G protein, or when it is bound to a G protein where the guanine nucleotide binding site on the α subunit is occupied by either GDP or GTP (or their analogues). The active conformation of the receptor is normally short-lived because a guanine nucleotide will quickly bind to the α subunit of the G protein. High affinity agonist binding can be preserved when experiments are carried out in washed membranes in the absence of guanine nucleotides. Experiments normally involve the use of a single concentration of a radiolabelled antagonist and increasing concentrations of unlabelled agonist. In this manner the agonist will displace the radiolabelled antagonist producing a displacement curve which is equivalent to an agonist binding curve. Direct binding of a radiolabelled agonist is often not possible due to the low binding affinity of agonists compared with antagonists. Bound radiolabelled agonist would be lost in the filtration procedure due to its lower affinity for, and hence, its rapid dissociation from the receptors.

Agonist displacement curves produced in the presence of a radiolabelled antagonist are often shallow with slope factor values less than unity. Slope factor values of less than unity suggest the presence of more than one affinity state of the receptor subtype or the presence of more than one receptor subtype (each with a different affinity for the agonist). This is why cell lines expressing single receptor subtypes are useful because they allow investigation of multiple agonist affinity states of an individual receptor subtype. Tissue studies can lead to misinterpretations of agonist binding studies due to the presence of multiple receptor subtypes. On addition of guanine nucleotides the agonist displacement curve will shift to a lower affinity and the slope of the curve will increase towards a slope factor value of unity as a proportion of the high affinity agonist binding sites are converted to low affinity agonist binding sites by guanine nucleotide binding to G protein α subunits.

The formation of high affinity guanine nucleotide-sensitive agonist binding appears to correlate with the intrinsic activity of agonists, *i.e.* a partial agonist will produce a smaller component of high affinity agonist binding than full agonists, thus producing a

comparatively smaller GTP-shift (Evans *et al*, 1985b; Taylor, 1990). The GTP-shift has, therefore, been taken as an indication of the efficacy of agonists in a particular system.

More recently, the ternary complex model of agonist-receptor-G protein interaction has been modified to take into account the activities of constitutively active recombinant mutant receptors expressed in cell lines (Lefkowitz *et al*, 1993; see also chapter 1). These activities include; 1) demonstrable activity of the mutant receptors even in the absence of agonist; 2) increased agonist activity coinciding with increases in affinity of the agonist for the constitutively active mutant receptors; and 3) increased affinity of an agonist for the constitutively active mutant receptors even under circumstances where no receptor-G protein coupling could occur. The 'allosteric ternary complex model' (Lefkowitz *et al*, 1993; Samama *et al*, 1993) proposes that the receptor exists in two states, the isomerization of one state to the other occurring in the absence of agonist but at a relatively low level, resulting in constitutive activity. Agonists may catalyze the isomerization of the inactive state of the receptor to the activated state thus allowing the receptors to interact with G proteins leading to increased "activity". The ability of an agonist to induce this isomerization from the inactive to the active conformation of the receptor may represent the intrinsic activity of that particular agonist, *i.e.* a partial agonist will be less successful than the full agonist at inducing the active conformation of the receptor. Presumably, G protein activation causes the isomerization of the active conformation of the receptor back to the inactive conformation, thus explaining GTP-shifts. The allosteric ternary complex model, therefore, provides an explanation for the correlation between proportions of high affinity guanine-nucleotide-sensitive agonist binding sites observed in radioligand binding studies, and agonist efficacy.

Agonist binding to G protein-linked receptors can be modulated by cations as well as by guanine nucleotides. Neither activation of the G protein nor formation of guanine nucleotide-sensitive high affinity receptor-G protein complexes occur in the absence of Mg^{2+} (or other divalent cations such as Mn^{2+}) (Birnbaumer *et al*, 1990; Hulme *et al*, 1983) in M_1 receptors (Flynn et al, 1989) and M_2 receptors (Wei and Sulakhe, 1980; Hulme *et al*, 1983. Mg^{2+} increases the rate of GDP dissociation from the G protein α subunit, thus allowing association of GTP and subsequent activation of the G proteins (Higashijima *et al*, 1987; Shiozaki and Haga, 1992). Agonist binding to the receptors lowers the Mg^{2+} requirement to obtain G protein activation and hence, under physiological conditions, changes the affinity of a regulatory Mg^{2+}-binding site from millimolar (and hence is unoccupied at the normal 0.5 mM concentration of cytosolic free Mg^{2+}) to micromolar, causing it to become saturated by the cytosolic free Mg^{2+} (Birnbaumer *et al*, 1990). In washed membrane preparations it is, therefore, important to add back Mg^{2+} to the incubation buffer in order to observe high affinity agonist binding to the receptor.

Monovalent cations (especially Na^+ and NH_4^+) modulate agonist binding to M_2 receptors (and many other G protein-linked receptors) in a similar manner to guanine nucleotides, causing agonist affinity to decrease (Hosey, 1983) and promoting cholinergic agonist-mediated inhibition of AC (Jakobs *et al,* 1979). Site-directed mutagenesis studies in α_2 adrenoceptors have found that replacement of Asp-79 with Asn-79 (which lies in the second putative transmembrane spanning domain), entirely eliminates allosteric regulation of ligand binding by monovalent cations, without perturbing the selectivity of adrenergic binding (Horstman *et al,* 1990). The high degree of conservation of this aspartate residue in all G protein-coupled receptors suggests that a similar site may be found in muscarinic receptor subtypes.

Agonist binding to G protein-coupled receptors can be modulated by pertussis toxin (PTX)(Evans *et al,* 1985) if the G proteins to which the receptors couple are sensitive to PTX-mediated ADP-ribosylation. It is generally agreed that ADP-ribosylation by PTX prevents the interaction of the agonist-activated receptor with the GDP-liganded G protein thus preventing formation of the ternary complex (and high affinity agonist binding) (Gierschik, 1992). By treating the various CHO cell clones with PTX it was hoped that high affinity agonist binding to muscarinic receptors could be categorized as being mediated by an interaction of the receptors with either PTX-sensitive or PTX-insensitive G proteins. In this respect it was of interest to see whether PTX-sensitive high affinity agonist binding could be seen in CHO cells expressing m3 muscarinic receptors (which couple primarily to PTX-insensitive G proteins of the $G_{q/11}$ family when activating PLC) and if any PTX sensitivity was correlated with the expression level of this receptor subtype in CHO cells.

Mammalian cardiac tissue appears to express a homogeneous population of M_2 muscarinic receptors and studies using cardiac membranes (washed free of guanine nucleotides) have been reported that show large 'GTP shifts' in agonist binding curves (Waelbroeck *et al*, 1982; Matesic *et al*, 1989). PI-linked muscarinic receptors (m1, m3 and m5) have not been well characterized in terms of guanine nucleotide modification of agonist binding due to the lack of homogeneous populations of these muscarinic receptor subtypes expressed in tissues. Interestingly, where such studies have been carried out using PI-linked muscarinic receptors, either in tissues (particularly rat brain) or using recombinant receptors expressed in cells, the GTP shift is somewhat smaller (Richards, 1991; Evans *et al*, 1985; Flynn *et al*, 1989; Wess *et al*, 1990a) or not present at all (Wess *et al*, 1990b). It is possible that differences in cell type used may be a factor as to why GTP shifts differ between agonist binding curves in cells expressing M_2 receptors (mainly performed in cardiac membranes) and agonist binding in cells expressing either m1/M_1 or

m3 receptors (in various brain regions and in various cloned cell types). It is equally possible that the differences in guanine nucleotide modification of agonist binding between AC-linked receptors and PI-linked receptors may represent different mechanisms of coupling of these receptor subtypes with their respective G proteins.

In this study, guanine nucleotide modification of agonist binding was performed in CHO cells expressing either m1, m2 or m3 muscarinic receptors, and in SH-SY5Y cells which endogenously express M_3 receptors in order to gain further insight into the effects of guanine nucleotides on agonist binding to these receptors, using identical binding conditions.

4.1. Methods.

Membranes were prepared (as previously described in Chapter 2) from CHO-m1, CHO-m2, CHO-m3, CHO-vt9 and SH-SY5Y cells. The initial binding buffer consisted of 10 mM HEPES, 1mM $MgCl_2$, pH 7.4. Binding buffer was modified several times by addition and subtraction of various concentrations of NaCl and $MgCl_2$.

4.1.1. Radioligand Binding

Saturation binding experiments using a range of concentrations of [^{3}H]NMS (specific activity 84 Ci / mmol) (0.03-3.00 nM) were performed in binding buffers of various composition.

Membranes were co-incubated with [^{3}H]NMS concentrations in a 1 ml final assay volume for 60 min at 37 °C. Bound and free radioligand were then separated by filtration using Whatman GF/B filters. Filters were washed twice with 3 ml of cold binding buffer during the filtration procedure. Filters were then transferred to 4 ml of scintillation cocktail (Optiphase X) and left for at least 12 hours before being counted by liquid scintillation spectrometry. Non-specific binding was determined in the presence of 1 μM atropine. 100 μM GppNHp (a poorly hydrolysed guanine nucleotide analogue) was co-incubated in [^{3}H]NMS saturation binding studies with CHO-m3 cell membranes and with SH-SY5Y cell membranes to see whether it had any effect on [^{3}H]NMS binding.

Competition binding studies using a single concentration of [^{3}H]NMS (approximately 0.4 nM) and increasing concentrations of the muscarinic receptor agonist carbachol (3 x 10^{-8}-10^{-2}M) were performed in CHO-m3 and SH-SY5Y cell membranes. Binding buffer consisted of 10 mM HEPES, 1 mM $MgCl_2$, pH 7.4. Incubation and filtration procedures were carried out identically to those described above. Maximal GTP modification of carbachol binding to muscarinic receptors in CHO-m3 and SH-SY5Y cell membranes was

determined by using two concentrations of carbachol (10 μM and 30 μM), a single concentration of [^{3}H]NMS (approximately 0.4 nM) and increasing concentrations of GTP (10^{-9}-10^{-4}M) in the incubation mixture. Different concentrations of Na^+ and Mg^+ ions in the binding buffer led to enhanced GTP modification of agonist binding in CHO-m3 membranes.

Carbachol competition binding curves generated using CHO-m1, CHO-m2, CHO-m3 and CHO-vt9 cell membranes were performed in a binding buffer consisting of 10 mM HEPES, 1 mM $MgCl_2$, 100 mM NaCl, pH 7.4 in the presence and absence of 100 μM GTP. In some cases cells were pretreated with pertussis toxin (PTX) by adding 100 ng / ml PTX to the cell growth media for 20 hours prior to membrane preparation.

Incubations were carried out as above and bound and free radioligand were separated by filtration. Whatman GF/B filters were pre-soaked in distilled water containing 1 % BSA and 1 % Sigmacote siliconizing fluid for two hours. Filters were then rinsed with distilled water and left to dry overnight. Filters were dampened with cold binding buffer just prior to filtration of the samples. Samples were then filtered as described above. Pretreating the filters in this way decreased non-specific binding (NSB) of [^{3}H]NMS. The agonist carbachol at high concentrations was found to displace [^{3}H]NMS NSB to a greater extent than 1 μM atropine thereby slightly altering the shape of the displacement curves. This was particularly marked in CHO-m2 cell membranes (which have a low muscarinic receptor density) where carbachol displacement of [^{3}H]NMS NSB became a relatively large proportion of total [^{3}H]NMS bound (approximately 25 %). By reducing the [^{3}H]NMS NSB by pretreating the filters and by wetting the filters in a high salt buffer just prior to filtration of the samples, carbachol displacement of [^{3}H]NMS NSB was reduced to less than 2 % of total [^{3}H]NMS binding (Harden *et al*, 1983). Increasing the protein concentrations of the membranes increased the amount of total [^{3}H]NMS binding without effecting NSB (data not shown). Increasing the protein concentrations of the membranes reduced carbachol-displacement of [^{3}H]NMS NSB to insignificant levels. Protein concentrations of membranes were only raised to the point where no more than 20 % of the radiolabel added was bound.

4.1.2 Data Analysis.

K_D, B_{max} and Hill slope values were obtained from Scatchard analysis of saturation binding data. IC_{50} values and slope factors were derived from competition binding studies, using the computer program ALLFIT (DeLean *et al*, 1978). K_{50} values were obtained from IC_{50} values using the Cheng-Prusoff equation (Cheng and Prusoff, 1973). Statistical significance was set at $p \leq 0.05$ using unpaired T-test analysis.

4.2 Results.

Agonist Binding in Membranes Prepared from SH-SY5Y Cells and CHO-m3 Cells.

[^{3}H]NMS binding to m3 muscarinic receptors, expressed in SH-SY5Y and CHO-m3 cell membranes, reached an equilibrium after 30 min incubation in binding buffer consisting of 10 mM HEPES, 1 mM $MgCl_2$, pH 7.4, at 37 °C (Figure 4.2.1). Incubations continued for a further 60 min did not result in any significant loss of [^{3}H]NMS binding. Radioligand binding studies using [^{3}H]NMS, either in saturation binding studies or in displacement studies with carbachol, were subsequently incubated at 37 °C for 60 min.

[^{3}H]NMS saturation binding studies to muscarinic receptors in SH-SY5Y and CHO-m3 cell membranes were analysed by Scatchard analysis (Figure 4.2.1 inset). In SH-SY5Y cell membranes, the maximum specific binding capacity (B_{max}) of [^{3}H]NMS was 460 ± 20 fmol / mg of membrane protein. and the dissociation constant (log K_D) was -10.13 ± 0.07. In CHO-m3 cell membranes [^{3}H]NMS bound to muscarinic receptors with a B_{max} of 1592 ± 85 fmol / mg of membrane protein and a log K_D of -10.11 ± 0.07. Both membrane preparations produced binding curves with Hill slope values of unity. The presence of 100 μM GppNHp (an analogue of GTP) did not significantly effect B_{max}, K_D or Hill slope values in both SH-SY5Y and CHO-m3 cell membranes (Figure 4.2.1 inset).

Carbachol displacement binding curves in SH-SY5Y and CHO-m3 cell membranes were fitted assuming the presence of a single affinity state of the receptors. K_{50} (log molar) values of -5.14 ± 0.07 and -5.33 ± 0.06 with slope factors of 0.56 ± 0.07 and 0.47 ± 0.03 were produced in SH-SY5Y and CHO-m3 cell membranes, respectively.

In the presence of 100 μM GTP, carbachol K_{50} values were increased 3-4 fold and the slope factor values were increased towards unity, in both SH-SY5Y and CHO-m3 cell membranes with K_{50} (log molar) values of-4.62 ± 0.02 and -4.71 ± 0.08, and slope factor values of 0.71 ± 0.04 and 0.77 ± 0.08, respectively) (Figure 4.2.2).

GTP (100 μM) maximally reduced carbachol (10 and 30 μM) displacement of [^{3}H]NMS binding in both CHO-m3 and SH-SY5Y cell membranes (see Figure 4.2.3). Slope factor values in the presence of a maximally effective concentration of GTP (100 μM) were still significantly lower than unity in both cell types suggesting that a small proportion of high affinity agonist binding sites remained.

It is widely reported that Mg^{2+} and Na^+ ions modify agonist binding to G protein-linked receptors (Birnbaumer *et al*, 1990; Hulme *et al*, 1983). Effects of Mg^{2+} and Na^+ ions on carbachol displacement binding curves were studied in CHO-m3 cell membranes

to try and induce optimal binding conditions to observe GTP-induced modifications.

Effects of $Mg^{2\pm}$ on Agonist Binding to Muscarinic Receptors Expressed in CHO-m3 Cell Membranes.

Saturation binding studies using [^{3}H]NMS were not performed at varying concentrations of Mg^{2+}. Total specific binding of an approximately K_D concentration of [^{3}H]NMS (0.4 nM) in displacement binding studies was not affected, either in the absence of $MgCl_2$, or in the presence of 1mM $MgCl_2$, suggesting that Mg^{2+} did not affect the binding affinity of the radiolabelled antagonist (data not shown). 1 mM $MgCl_2$ did not have any significant effect on the carbachol displacement binding curve in the absence of guanine nucleotides (with a K_{50} (log molar) value of -5.19 ± 0.12 and a slope factor value of 0.46 ± 0.10) compared to experiments performed in the absence of $MgCl_2$ (K_{50} (log molar) value of -4.94 ± 0.15 and slope factor of 0.37 ± 0.02) (Figure 4.2.4). In the absence of added $MgCl_2$, 100 μM GTP produced a very small increase in the slope factor value (0.57 ± 0.12) without affecting the K_{50} (log molar) for carbachol (-4.95 ± 0.13), compared to experiments performed in the absence of added GTP. In the presence of 1 mM $MgCl_2$, 100 μM GTP increased the K_{50} (log molar) value for carbachol binding by 2-fold (to -4.88 ± 0.02) and increased the slope factor value to 0.71 ± 0.08, compared to carbachol binding curves produced in the absence of GTP (Figure 4.2.4). 10 mM $MgCl_2$ did not have any further modulatory effect on GTP modification of carbachol binding in CHO-m3 cell membranes (data not shown).

Effects of $Na^{\pm}$ on Agonist Binding to Muscarinic Receptors. Expressed in CHO-m3 Cell Membranes.

Effects of Na^+ on agonist binding curves were performed in the presence of 1 mM $MgCl_2$. The presence of NaCl in the binding buffer decreased the affinity of [^{3}H]NMS for m3 receptors in CHO-m3 cell membranes, in a dose-dependent manner (see Table 4.2.1). 100 mM NaCl produced a 5-fold reduction in the affinity of [^{3}H]NMS without significantly affecting the maximal binding capacity. NaCl dose-dependently reduced the affinity of carbachol for m3 receptors in CHO-m3 cell membranes both in the absence and presence of guanine nucleotides (Figure 4.2.5 and Table 4.2.2). Slope factor values were also increased both in the absence and presence of guanine nucleotides. In the presence of both 100 mM NaCl and 100 μM GTP, the carbachol displacement curve was shifted to one which had a slope factor value not significantly different from unity (0.95 ± 0.01) with a K_{50} (log molar) value of -4.03 ± 0.03.

Further studies on carbachol displacement binding were performed in binding buffer

consisting of 10 mM HEPES, 1 mM $MgCl_2$ and 100 mM NaCl, pH 7.4.

GTP and PTX Modification of Agonist Binding to Muscarinic Receptors Expressed in CHO Cell Membranes.

Using the above conditions and filtering the samples using siliconized filters (see Methods), the effects of GTP and PTX pretreatment on carbachol displacement curves were studied in CHO-m1, CHO-m2, CHO-m3 and CHO-vt9 cell membranes.

Pretreatment of CHO cells with 100 ng / ml PTX for 20 hours prior to membrane preparation had no effect on total [^{3}H]NMS binding (at K_D concentrations of [^{3}H]NMS) in carbachol competition binding experiments (data not shown). This concentration of PTX proved to be maximally effective at uncoupling m2 receptors from G proteins as described in [^{35}S]GTPγS binding studies in Chapter 5.

CHO-m2 Cell Membranes.

CHO-m2 cell membranes in the absence of PTX pretreatment or GTP produced very shallow carbachol binding curves (slope factor value of 0.42 ± 0.02 with a K_{50} (log molar) value of -5.99 ± 0.22) suggesting the presence of multiple carbachol affinity states of the m2 muscarinic receptors. 100 μM GTP significantly increased the slope of the carbachol displacement binding curve ($p < 0.05$, unpaired T-test) producing slope factor values approaching unity (0.71 ± 0.09) and causing a 10-fold increase in the K_{50} for carbachol (Figure 4.2.6. and Table 4.2.3). Pretreatment of CHO-m2 cells with 100 ng / ml of PTX for 20 hours prior to membrane preparation resulted in a large modification of the carbachol binding curve in a similar manner to that seen with 100 μM GTP. The slope factor value after PTX pretreatment was no longer significantly different from unity ($p>0.05$ for an unpaired T-test). The presence of GTP in PTX pretreated CHO-m2 cell membranes had no additional effect on the carbachol displacement binding curve (Figure 4.2.6 and Table 4.2.3).

CHO-m1 Cell Membranes.

In CHO-m1 cell membranes, carbachol binding curves in the absence of GTP or PTX pretreatment had slope factor values of unity suggesting that only a single, low carbachol affinity state of the m1 muscarinic receptors could be identified (K_{50} (log molar) values of-3.70 ± 0.01) (Figure 4.2.6 and Table 4.2.3). GTP and PTX pretreatment had no significant effect on either the K_{50} or slope factor values of carbachol binding curves in CHO-m1 cell membranes. The low affinity state of m1 muscarinic receptors (*i.e.* in the presence of a saturating concentration of GTP) was approximately 18-fold and 2-3-fold

lower in affinity for carbachol than the low affinity state of m2 and m3 muscarinic receptors, respectively.

CHO-m3 Cell Membranes.

In CHO-m3 cell membranes, carbachol binding curves in the absence of GTP or PTX pretreatment were initially shallow (slope factor values of 0.65 ± 0.02) (Figure 4.2.7 and Table 4.2.3) but not as shallow as those seen in CHO-m2 cell membranes. Addition of 100 μM GTP significantly increased the slope factor ($p < 0.05$ for an unpaired T-test) to a value not significantly different from unity. The K_{50} (log molar) of -4.40 ± 0.08 was increased by 2.5-fold in the presence of GTP. PTX pretreatment of CHO-m3 cells in the absence of GTP resulted in a 2-fold increase in the K_{50} value for carbachol binding. The slope factor value was also increased (0.78 ± 0.05) but proved not to be significantly different from the control binding curve ($p = 0.069$ for an unpaired T-test). Addition of 100 μM GTP in PTX pretreated CHO-m3 cell membranes resulted in a 1.5-fold increase in the K_{50} for carbachol binding with the slope factor increasing to a value which was not significantly different from unity. The slope factor values for carbachol displacement binding curves between PTX pretreated cell membranes in the presence and absence of GTP were not significantly different ($p = 0.064$ for an unpaired T-test) (Figure 4.2.7 and Table 4.2.3). The carbachol binding affinity for m3 receptors (in CHO-m3 cell membranes) in the presence of 100 μM GTP was approximately 11-fold lower than for m2 receptors (in CHO-m2 cell membranes) under identical conditions.

CHO-vt9 Cell Membranes.

In CHO-vt9 cell membranes, carbachol displacement binding curves under control conditions were slightly shallow (slope factor values of 0.87 ± 0.02; K_{50} (log molar values) -4.11 ± 0.05), but significantly steeper than binding curves produced in CHO-m3 cell membranes under identical conditions (Figure 4.2.7 and Table 4.2.3). Addition of 100 μM GTP significantly increased the slope factor ($p < 0.05$, unpaired T-test) to values which were not significantly different from unity and produced a 1.9-fold increase in the K_{50} value. PTX pretreatment of CHO-vt9 cells had no significant effect on the carbachol binding curve in CHO-vt9 cell membranes compared to control values. Addition of 100 μM GTP to PTX pretreated cell membranes produced a 2.2-fold increase in the K_{50} of the carbachol binding curve and the slope factor was increased significantly ($p < 0.05$, unpaired T-test) to a value which was not significantly different from unity (Figure 4.2.7 and Table 4.2.3). K_{50} values for carbachol binding to m3 muscarinic receptors, expressed at different receptor densities, in CHO-m3 and CHO-vt9 cell membranes, in the presence of GTP, were not significantly different.

4.3. Discussion.

The present study has shown that endogenously expressed M_3 muscarinic receptors in SH-SY5Y cell membranes and recombinant m3 muscarinic receptors expressed in CHO cell membranes bound carbachol with two affinities (low and high) in the absence of guanine nucleotides. The high agonist affinity state of the receptor was sensitive to guanine nucleotides which caused a proportion of the high affinity binding sites to shift to low affinity binding sites, thus increasing the K_{50} values and the slopes of the carbachol displacement binding curves. The radiolabelled muscarinic antagonist [^{3}H]NMS bound to muscarinic receptors with a single affinity and was unaffected by GppNHp (an analogue of GTP).

Carbachol binding affinity values and slope factor values were very similar between the two cell types despite the probable differences in G protein pools in SH-SY5Y cells compared with CHO cells, and the higher density of muscarinic receptors expressed in CHO-m3 cells.

Interestingly, in both cell types, a maximally effective concentration of GTP (100 μM) was unable to convert all of the high affinity agonist binding sites to low affinity agonist binding sites, because slope factor values in the presence of GTP were still significantly lower than unity. Attention was therefore directed to modifying the incubation buffer in order to achieve 'optimal' guanine nucleotide-modification of agonist binding in CHO-m3 cell membranes expressing m3 muscarinic receptors.

The low agonist affinity state of the receptor is thought to represent a combination of conditions *i.e.* receptor not coupled to G protein; receptor and G protein coupled with GDP bound to the G protein α subunit; or the activated receptor whereby the G-protein has bound GTP and the α subunit-GTP complex has dissociated from the receptor (Taylor, 1990). An estimate of the intrinsic activity of agonists can be deduced by comparisons of occupancy curves (using the low affinity agonist binding sites) and response curves for the agonist. By creating conditions whereby a single population of low affinity carbachol binding sites for the muscarinic receptor subtypes could be detected, it was hoped that the intrinsic activity of carbachol to mediate second messenger responses in CHO cells expressing different subtypes of muscarinic receptors, investigated in later studies, could be assessed.

In the present study, addition of Mg^{2+} to the incubation buffer did not affect total binding of the antagonist [^{3}H]NMS to m3 muscarinic receptors, expressed in CHO-m3 cell membranes, at an approximate K_D concentration of 0.4 nM suggesting that Mg^{2+} did not significantly effect the binding affinity of the antagonist. Wei and Sulakhe (1980) have also shown that Mg^{2+} did not affect the affinity of binding of the antagonist atropine

to cardiac (M_2) muscarinic receptors.

In the present study, high affinity agonist binding was detected in CHO-m3 cell membranes even in the absence of added Mg^{2+}. Addition of 1 mM $MgCl_2$ to the incubation buffer had no significant effect on the agonist binding curve in the absence of guanine nucleotides. This was somewhat surprising considering the extensive literature that suggests that divalent cations increase the proportion of high affinity agonist binding sites in M_2 muscarinic receptors (Wei and Sulakhe, 1980; Hulme *et al*, 1983; Birnbaumer *et al*, 1990; Shiozaki and Haga, 1992) and were required to observe any high affinity agonist binding to M_1 muscarinic receptors, in rabbit hippocampal membranes (Flynn *et al*, 1989). However, in the present study $MgCl_2$ was required to observe guanine nucleotide modification of carbachol binding suggesting that divalent cations may play a role in activating the receptor-G protein complex. Shiozaki and Haga (1992) also showed that $MgCl_2$ was necessary for carbamylcholine to influence the binding of guanine nucleotides in a reconstituted system consisting of m2 muscarinic receptors (derived from porcine atria) and G proteins (purified from porcine cerebrum). In the presence of 10 mM $MgCl_2$, the apparent affinity for GDP was decreased 20-fold by the addition of carbamylcholine. No such effect of carbamylcholine was observed in the absence of $MgCl_2$. A similar finding was observed by Higashijima *et al* (1987) who went on to show that the steady-state rate of GTP hydrolysis was strictly correlated with the rate of dissociation of GDP from G_α.

Na^+ produced a dose-dependent reduction in the affinity of [^{3}H]NMS for m3 muscarinic receptors expressed in CHO-m3 cell membranes without affecting maximal binding capacity. Similar effects have been observed in other studies where the general consensus suggests that changes in the ionic strength of the buffer may be the cause of lowering antagonist affinity rather than a specific effect of Na^+ (Birdsall *et al*, 1979; Harden *et al*, 1983; Wei and Sulakhe, 1980). NaCl dose-dependently reduced the binding affinity of carbachol for m3 muscarinic receptors expressed in CHO-m3 cell membranes and increased the slope of the agonist binding curve, both in the absence and presence of guanine nucleotides. Na^+ has been shown to modulate ligand binding to M_2 muscarinic receptors (Hosey, 1983) and promote cholinergic agonist-mediated inhibition of AC (Jakobs *et al*, 1979) in a manner synergistic with GTP. The present study suggests that Na^+ acts in an additive manner with guanine nucleotides to increase the proportion of low affinity agonist binding to m3 muscarinic receptors and may, therefore, mediate its effect by an interaction with a molecular site distinct from that of guanine nucleotides.

Studies which have investigated carbachol-stimulated [^{35}S]GTPγS binding to G proteins in cardiac membranes expressing M_2 muscarinic receptors, have found that NaCl (100 mM) can enhance the relative agonist-stimulated [^{35}S]GTPγS binding by

preferentially reducing basal [^{35}S]GTPγS binding (Hilf and Jakobs, 1992; Hilf *et al*, 1989). Similar studies in HL60 cell membranes, which express formyl-methionyl-leucyl-phenylalanine (FMLP) peptide receptors (coupled via a PTX-sensitive G protein(s) to PLC activation), have shown that 100 mM NaCl reduced the proportion of high affinity FMLP (agonist) binding sites in favour of low affinity binding sites; produced a coincidental reduction in the potency of FMLP to stimulate a high affinity GTPase; but in contrast markedly enhanced the degree of FMLP-stimulated GTPase activity (Gierschik *et al*, 1989). These results suggest that monovalent cations (particularly Na^+) regulate the interaction of FMLP peptide receptors with both the chemotactic agonist and the G protein by acting on a single site, possibly located on the receptor itself. The marked reduction in basal GTPase activity (Gierschik *et al,* 1989) and basal [^{35}S]GTPγS binding (Hilf and Jakobs, 1992; Hilf *et al*, 1989) in the presence of either NaCl and after PTX-catalyzed ADP-ribosylation of the G proteins, suggests that G proteins interact with and are activated by receptors even in the absence of agonists and that Na^+ uncouples the G protein(s) from unoccupied, but nevertheless active receptors.

Horstmann *et al* (1990) identified an amino acid residue (Asp-79) in the putative second transmembrane spanning region of the α_2-adrenoceptor which is highly conserved amongst many G protein-coupled receptors. Replacement of Asp-79 with Asn-79 entirely eliminated allosteric regulation of ligand binding by monovalent cations. Aspartate residues located in the second and third transmembrane domains of G protein-coupled receptors seem to be important determinants for observing high affinity agonist binding sites and for activating G proteins (Fraser *et al, 1989;*Wang *et al, 1991*). Conformational changes in the receptor may be conveyed by Na^+ interacting with one or more of these aspartate residues, leading to a reduction in high affinity agonist binding sites and an increased response to the agonist. It is still unclear, however, what physiological significance Na^+ has in modulating agonist binding and receptor-G protein coupling. The extracellular concentration of Na^+ remains relatively constant (at 140 mM) and, therefore, would exert maximal modifications of agonist binding under physiological conditions. This is why the possibility of Na^+ acting as an intracellular mediator cannot be ruled out.

In the present study, 100 μM GTP was able to modify agonist binding to m3 muscarinic receptors producing carbachol binding curves that bound with a single low affinity, in the presence of 1mM $MgCl_2$ and 100 mM NaCl.

A proportion of low affinity agonist binding sites were detected in membranes prepared from each of the CHO cell clones, in the absence of added guanine nucleotides. Such mixtures of low and high affinity agonist binding sites in the absence of added guanine nucleotides are common amongst G protein-coupled receptors.

The question arises as to the nature of the proportion of low agonist affinity binding

sites observed using muscarinic receptor subtypes in washed membranes where guanine nucleotides are omitted. One explanation might be that some of the receptors fail to couple with G proteins, therefore, binding agonists with low affinity. Such a scenario may occur if the receptor population exceeds the population of G proteins to which that receptor population couples. Similarly, the affinity of coupling of the receptor with a particular G protein may be low so that only a proportion of receptors and G proteins are coupled under equilibrium binding conditions. In this event, a proportion of low agonist affinity binding sites might be expected, even in the absence of added guanine nucleotides. Mei *et al* (1989) suggested that the proportion of high affinity agonist binding sites in B82 (murine fibroblast) cell membranes, expressing recombinant m1 muscarinic receptors, was decreased as receptor expression increased (Mei *et al*, 1989). They suggested that at higher levels of receptor expression the proportion of receptors exceeded G proteins to which they could couple resulting in a proportion of 'spare' receptors with low agonist binding affinity. A second possible explanation for the proportion of low agonist affinity binding sites observed in the absence of added guanine nucleotides may be that endogenous guanine nucleotides may still be present in the membrane preparation. Agonist binding experiments have traditionally used washed membrane preparations in order to deplete endogenous levels of guanine nucleotides and thus observe GTP shifts in the presence of added guanine nucleotides. Intact cells and even permeabilized cell suspensions (in the case of SH-SY5Y cells)(Wojcikiewicz *et al*, 1990a) contain relatively high concentrations of guanine nucleotides (greater than 50 μM) so that no further GTP shift of the agonist binding curve is observed on addition of excess concentrations of guanine nucleotides (Wojcikiewicz *et al*, 1990b). Experiments have not been carried out to measure the guanine nucleotide content in the washed membrane preparations used in this study. Endogenous guanine nucleotides (GTP or GDP) may induce a proportion of the muscarinic receptors to adopt a low affinity agonist binding conformation when coupled to G proteins.

CHO-m2 cell membranes (expressing m2 receptors at a density of 99 ± 25 fmol / mg protein) initially produced a shallow carbachol displacement binding curve indicating the presence of more than one affinity state of the m2 receptors. GTP modified the curve increasing the proportion of low agonist affinity binding sites and decreasing the proportion of high agonist affinity sites, a modification commonly called the 'GTP shift', resulting in an increase in the K_{50} for carbachol and an increase in the slope factor value towards unity. A similar modification of carbachol binding occurred after pretreatment of the cells with PTX (100 ng / ml, 20 hr), suggesting that the high agonist affinity state of the receptors represented an interaction of PTX-sensitive G proteins (G_i or possibly G_o) with the receptors which was abolished after PTX-catalyzed ADP-ribosylation of the G proteins (Gierschik, 1992). Many studies have shown similar modification of agonist

binding to M_2/m2 muscarinic receptors, in tissues (heart, cerebellum, brain stem) and in cloned cells, by guanine nucleotides (*e.g.* Wess *et al*, 1990a; Waelbroeck *et al*, 1982; Matesic *et al*, 1989; Korn *et al*, 1983; Gurwitz *et al*, 1985) and by PTX (Wess *et al*, 1990a; Evans *et al*, 1985a)

CHO-m1 cell membranes (expressing m1 muscarinic receptors at a density of 556 ± 19 fmol / mg protein) produced no high affinity carbachol binding under these conditions and, therefore, produced no subsequent modification of the curve in the presence of either GTP or PTX pretreatment. CHO-m1 cells, however, did show large Ins(1,4,5)P_3 mass accumulation and Ca^{2+} mobilization responses to the high efficacy agonist, carbachol (though at a higher receptor density) (see chapters 6 and 7).

Previous studies have hypothesized that the efficacy of an agonist at a given muscarinic receptor subtype depends on the ratio of its affinities for high and low agonist affinity sites (Evans *et al*, 1985b). In the present study, the high efficacy agonist carbachol failed to produce any high affinity agonist binding sites (under particular conditions) and, therefore, fails to support this hypothesis. Many studies on M_1 muscarinic receptors, particularly in rat forebrain, have shown that guanine nucleotides have little, if any effect on agonist binding affinity (Korn *et al*, 1983; Watson *et al*, 1986; Vickroy *et al*, 1983; Gurwitz *et al*, 1985; reviewed by Richards, 1991). However, other investigators have observed guanine nucleotide-sensitive high affinity agonist binding to M_1 receptors in rabbit hippocampal membranes (Flynn *et al*, 1989) and m1 muscarinic receptors expressed in cloned cells (Brann *et al*, 1987; Lai *et al*, 1988). The reasons for this lack of high affinity agonist binding to m1 muscarinic receptors are not known. One possible explanation may be that receptor-G protein interactions may be lost in the preparation of the membranes. Obviously, this was not the case with the CHO-m2 cell membranes where agonist binding was modulated by GTP and PTX pretreatment. The m1 muscarinic receptors in CHO-m1 cells, however, may couple to different G proteins (*i.e.* G_q) which may more readily dissociate when membranes are prepared.

A further possibility is that the assay conditions may favour the conversion of high affinity binding sites to low affinity binding sites in the case of the m1 muscarinic receptors expressed in CHO cell membranes. Perhaps the concentration of Na^+ in the assay buffer may induce a complete conversion of the high affinity agonist binding state to the low affinity state of the receptor, in the case of the m1 muscarinic receptors. Agonist binding curves in CHO-m1 cell membranes in the absence of added Na^+ were not performed in this study.

CHO-m3 cell membranes (expressing m3 muscarinic receptors at a density of 1-2 pmol / mg protein) produced a complex carbachol displacement binding curve in the

absence of added guanine nucleotides, suggesting the presence of more than one affinity state of the receptor. However, the curve was not as shallow as that seen in CHO-m2 cell membranes, a trend that has been observed by other groups (Evans *et al*, 1985a; Wess *et al*, 1990a; Keen and Nahorski, 1988). The more complex nature of agonist binding curves observed with receptors that couple to AC (m2) rather than PLC (m1, m3) suggests that the two affinity states of the m2 receptors lie further apart than in PI-linked m1 and m3 receptors. Alternatively, m1 and m3 muscarinic receptors in the preparation of the CHO cell membranes may be more readily disrupted in terms of their ability to couple with specific G proteins than the m2 muscarinic receptors, resulting in somewhat artifactual agonist binding curves.

In the present study, two-site curve fitting programmes were not used to analyse the agonist binding curves to m3 muscarinic receptors. It was thought that such analysis would be highly speculative due to the fact that the low and high agonist affinity states differed by less than 100-fold. Manipulating the data given by two-site analysis, by entering small variations in the apparent affinity states of the m3 receptors (entered into the program as constants) produced variations in the relative proportions of each affinity state present without significantly affecting the overall K_{50} for carbachol or the slope factor of the binding curve. Therefore, it was thought to be more appropriate to give the one-site analysis of the agonist binding curves, expressing their affinity and slope factor values.

In the presence of GTP, the carbachol binding curve in CHO-m3 membranes was significantly shifted to the right compared to the carbachol binding curve produced in the absence of added guanine nucleotides, producing a slope factor value not significantly different from unity. This suggests that guanine nucleotide-sensitive high agonist affinity sites were all converted to low affinity sites in the presence of GTP. Interestingly, PTX-pretreatment of CHO-m3 cells resulted in a small but not statistically significant modification of the carbachol binding curve in a similar manner to added GTP. GTP had no significant affect on the agonist binding curve in CHO-m3 cells pretreated with PTX suggesting that PTX pretreatment reduced the proportion of guanine nucleotide-sensitive high affinity binding sites. M_3 muscarinic receptors probably couple preferentially to PLC via the PTX-insensitive G protein family G_q. The present study suggests that m3 muscarinic receptors expressed in CHO cells may also couple to PTX-sensitive G proteins due to the reduction of high affinity agonist binding sites observed in CHO-m3 cell membranes after PTX pretreatment.

CHO-vt9 cell membranes (expressing m3 muscarinic receptors at a density of 430 ± 43 fmol / mg protein) produced carbachol displacement binding curves with slope factor

values that were only marginally less than unity. The presence of GTP significantly shifted the curve to a slope factor value of unity, suggesting the presence of only a small proportion of guanine nucleotide-sensitive high agonist affinity sites in CHO-vt9 cell membranes. PTX pretreatment of the cells had no effect on the agonist binding curves either in the absence or presence of added GTP. Therefore, it would seem that lowering the receptor density of m3 receptors in CHO-vt9 cells compared with CHO-m3 cells, resulted in a loss of guanine nucleotide and PTX-sensitive high agonist affinity binding sites. Expressed in another way, the present study suggests that increasing the m3 receptor density in CHO cells may result in a promiscuous coupling of receptors with PTX-sensitive G proteins that is not seen at lower levels of receptor expression. Although the idea of high receptor expression levels leading to promiscuous coupling with G proteins is gaining momentum in the literature, this study provides the first evidence (although tentative) for G protein promiscuity with m3 muscarinic receptors, derived from agonist binding studies. Other groups have studied the PTX-sensitivity of high affinity agonist binding in cells expressing m3 receptors, but neither group showed any coupling of this receptor to PTX-sensitive G proteins (Wess *et al*, 1990a; Evans *et al*, 1985a). Wess *et al* (1990a) expressed the m3 receptor in A9L cells at a density of 618 fmol / mg protein, whereas Evans *et al*,(1985a) studied the endogenously expressed M_3 receptor in 1321N1 human astrocytoma cells (receptor density not stated). It is possible that the level of expression of m3 receptors in these cell lines may not have been adequate to achieve a promiscuous coupling of the receptors with PTX-sensitive G proteins. Alternatively, these cell types may not express the correct ratio of PTX-sensitive G proteins to receptors necessary to observe interactions between these proteins.

In the present study, as m3 receptor expression was increased, the proportion of high affinity binding sites also increased. This is in contrast to the study by Mei *et al* (1989) who suggested that the proportion of high affinity agonist binding sites in B82 (murine fibroblast) cell membranes, expressing recombinant m1 muscarinic receptors, was decreased as receptor expression increased. This observation, they suggested, could be explained by the presence of "spare receptors" which did not couple to G proteins. In the present study, however, the majority of high affinity agonist binding sites observed in CHO-m3 cell membranes appeared to be PTX-sensitive indicating a coupling of m3 muscarinic receptors with PTX-sensitive G proteins at high levels of receptor expression. Perhaps the m1 muscarinic receptors in B82 cell membranes did not couple with PTX-sensitve G proteins at higher levels of receptor expression thus exhibiting different agonist binding curves at different levels of receptor expression than those observed in the present study in CHO cells expressing m3 muscarinic receptors.

If the increased proportion of high affinity agonist binding in CHO-m3 cell

membranes compared with CHO-vt9 cell membranes was due to increased coupling with PTX-sensitive G proteins, then the proportion of guanine nucleotide-sensitive, PTX-insensitive high affinity agonist binding was small, and in the case of the CHO-m1 cell membranes, absent. This may be due to buffer conditions (which may not suit high affinity binding of carbachol with m1 and m3 receptors). Alternatively, interactions between m1/m3 receptors and $G_{q/11}$ family G proteins may be preferentially disrupted by membrane preparation of the CHO cell clones. Alternatively, the lack of PTX-insensitive high affinity agonist binding to m1 and m3 receptors in CHO cell membranes may represent a fundamental difference between agonist interactions with muscarinic receptors coupled to AC and muscarinic receptors coupled to PLC.

In the presence of 100 μM GTP, carbachol showed significant selectivity for the muscarinic receptor subtypes expressed in CHO cell membranes; being approximately 10-fold more selective for m2 receptors than for m3 receptors and approximately 2-fold more selective for m3 receptors than for m1 receptors. There was no significant difference between the affinity of carbachol for the low affinity state of the m3 receptors expressed in CHO-m3 and CHO-vt9 cell membranes. The selectivity of carbachol for the m2 muscarinic receptor subtype over both m1 and m3 receptors has also been observed by Hulme *et al* (1990) by displacement of [^{3}H]NMS binding with carbachol in intact CHO cells. The determination of agonist affinity for different muscarinic receptor subtypes by radioligand binding studies, although not entirely accurate, gives a good approximation of the relative affinity of agonists such as carbachol for the different muscarinic receptor subtypes. However, comparisons of agonist potency to elicit functional responses between different muscarinic receptor subtypes must be viewed with caution because the expression level of each receptor subtype can markedly affect the apparent potency of the agonist (Schwarz *et al,* 1993;Caulfield, 1993;also see subsequent chapters). Therefore, although it appears that carbachol has a higher selectivity for m2 receptors over m1 and m3 receptors, the net responses of cells coexpressing these receptor subtypes will depend on the intrinsic activity of the agonist to modulate a particular effector pathway via each receptor subtype, and the expression level of each subtype present.

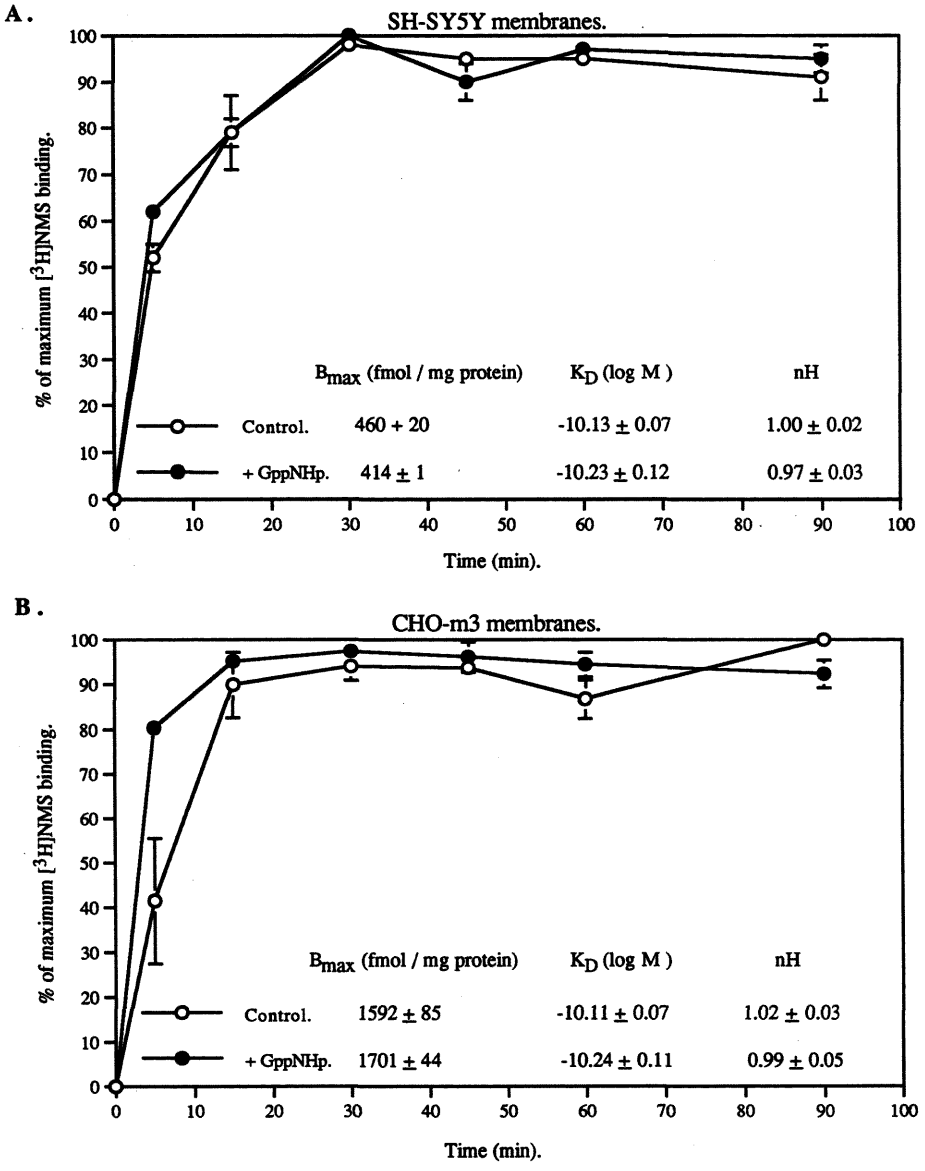

Figure 4.2.1. Time courses for equilibrium binding of 0.3 nM [^{3}H]NMS to m3 muscarinic receptors in **A**. SH-SY5Y and **B**. CHO-m3 cell membranes in 10 mM HEPES, 1 mM $MgCl_2$, pH 7.4 at 37 °C in the presence and absence of 100 μM GppNHp. **Inset:** shows Scatchard analysis of [^{3}H]NMS saturation binding experiments under identical conditions using a 60 min incubation period. Maximal specific binding capacity (B_{max} in fmol / mg protein), equilibrium dissociation constant (log K_D) values and Hill coefficient (nH) values for [^{3}H]NMS binding are expressed as mean ± standard error values of three independent experiments.

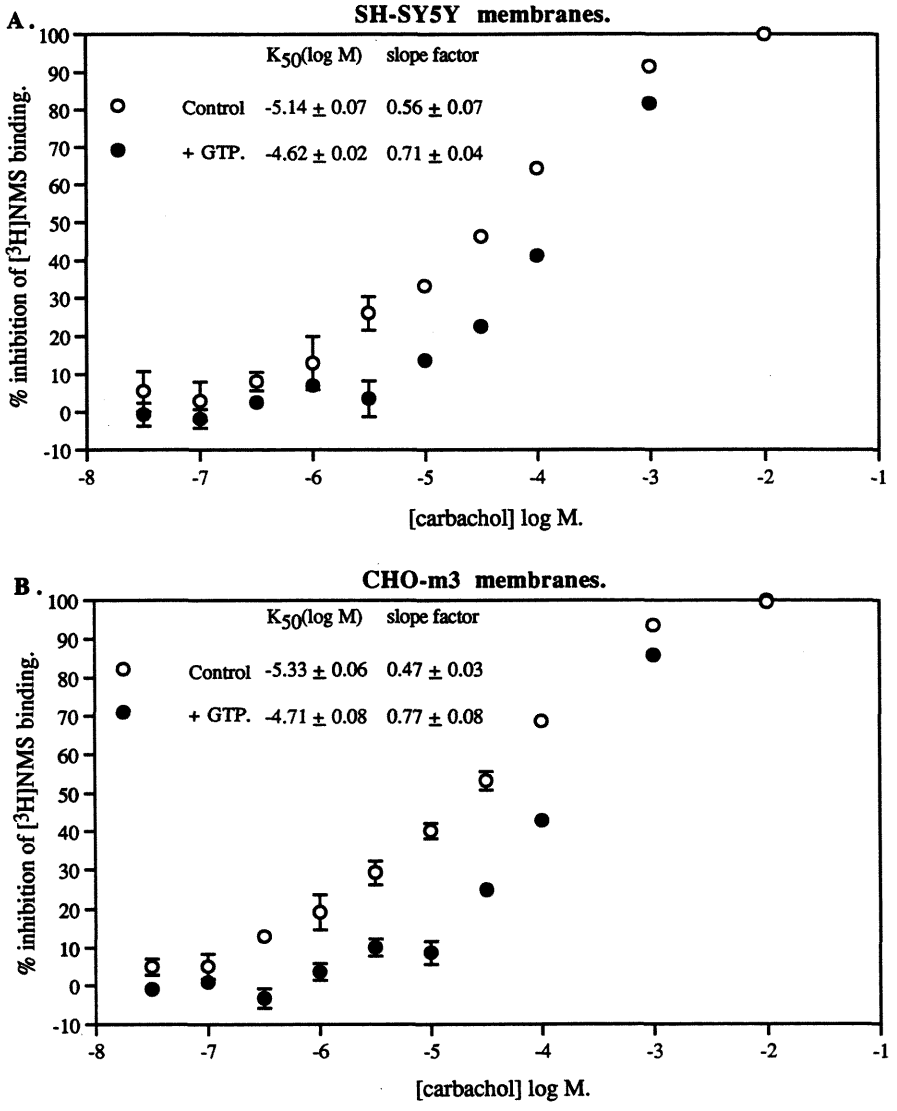

Figure 4.2.2. Carbachol competition binding with [^{3}H]NMS (approximately 0.4 nM) to muscarinic receptors in **A**. SH-SY5Y membranes and **B**. CHO-m3 membranes in 10 mM HEPES, 1 mM $MgCl_2$, pH 7.4 in the presence and absence of 100 µM GTP.Binding curves represent mean ± standard error values of untransformed data (not taking into account small changes in [^{3}H]NMS concentration) from 3 independent experiments. **Inset:** Carbachol binding inhibition constant (log M K_{50}) values (derived from IC_{50} values using the Cheng-Prusoff equation) and slope factor values expressed as mean ± standard error values of three independent experiments.

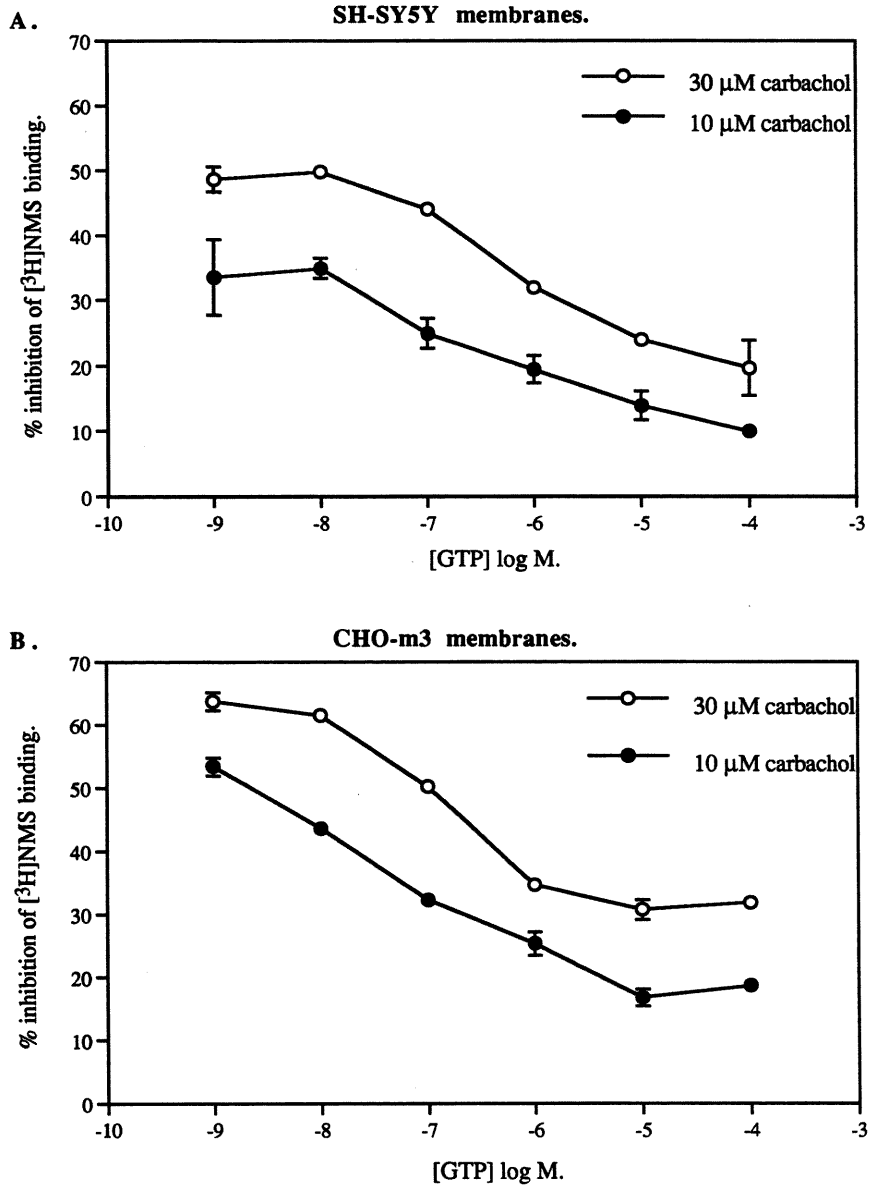

Figure 4.2.3. Effect of increasing concentrations of GTP on carbachol displacement of [^{3}H]NMS binding (approximately 0.4 nM) in **A** .SH-SY5Y cell membranes and **B** .CHO-m3 cell membranes, in 10 mM HEPES, 1 mM $MgCl_2$, pH 7.4. Binding curves represent mean ± standard error values of untransformed data (not taking into account small changes in [^{3}H]NMS concentration) from three independent experiments.

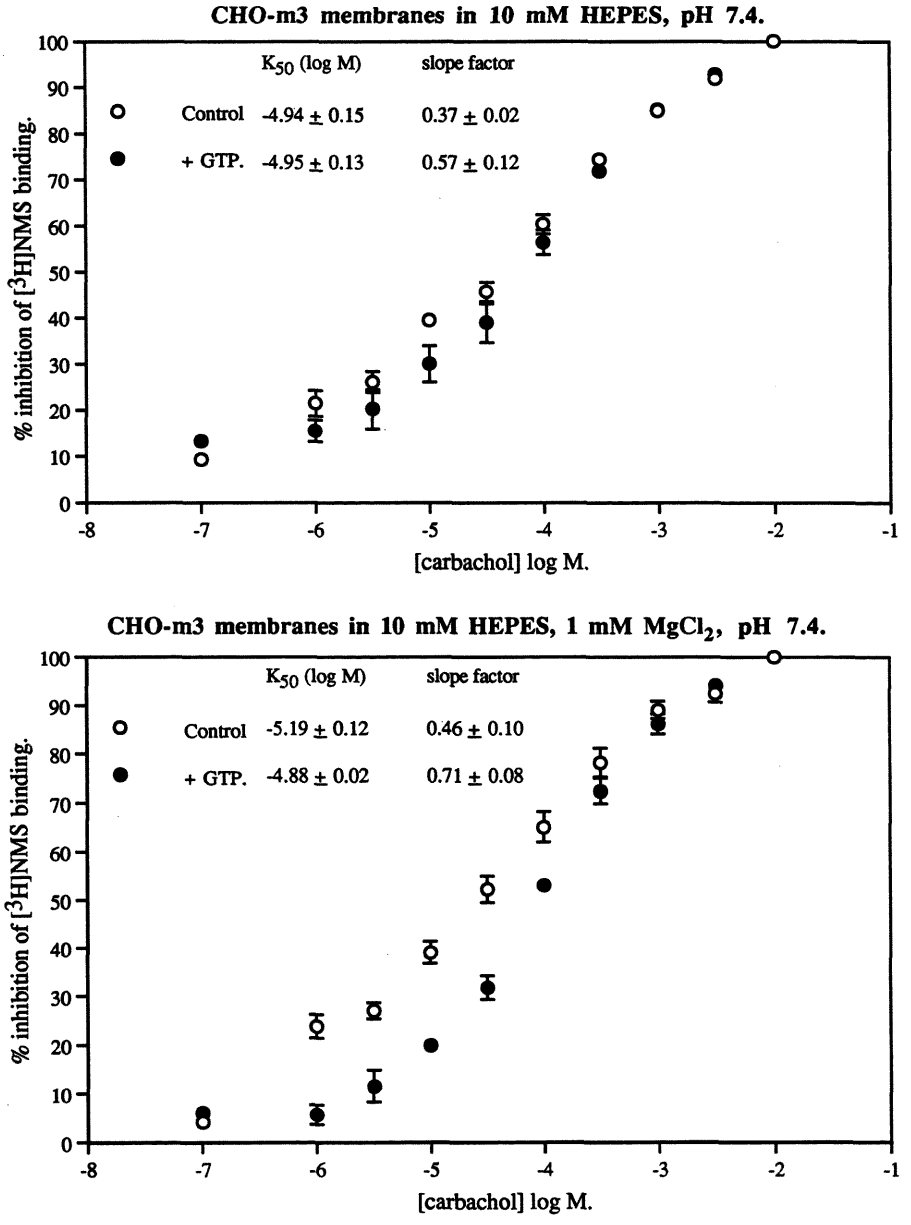

Figure 4.2.4. Effect of Mg^{2+} ions on carbachol displacement of [^{3}H]NMS binding (approximately 0.4 nM) to m3 muscarinic receptors in CHO-m3 cell membranes, in the presence and absence of 100 µM GTP. Binding curves show mean ± standard error values of untransformed data (not taking into account small changes in [^{3}H]NMS concentration) from three independent experiments. **Inset** : Carbachol binding inhibition constant (log. M K_{50}) values (derived from IC_{50} values using the Cheng-Prusoff equation) and slope factor values are expressed as mean ± standard error values of three independent experiments.

Table 4.2.1.

Effect of Na^+ ions on [^{3}H]NMS saturation binding to m3 muscarinic receptors in CHO-m3 cell membranes. Binding buffer consisted of 10 mM HEPES, 1 mM $MgCl_2$ and various concentrations of NaCl, pH 7.4. Equilibrium dissociation constant (log M $\mathbf{K_D}$) values, maximal specific binding capacity ($\mathbf{B_{max}}$ in fmol mg / protein) values and Hill coefficient (**nH**) values were derived from Scatchard analysis of [^{3}H]NMS saturation binding data. Data is represented as mean $\pm$ standard error values of three independent experiments. * = significantly different from 0 mM Na^+ value ($p < 0.05$, unpaired T-test).

[NaCl]	K_D (log M)	B_{max}	nH
0 mM	-10.11 $\pm$ 0.07	1592 $\pm$ 85	1.02 $\pm$ 0.03
30 mM	-9.76 $\pm$ 0.05 *	1271 $\pm$ 309	1.03 $\pm$ 0.03
100 mM	-9.41 $\pm$ 0.04 *	1212 $\pm$ 279	1.02 $\pm$ 0.01

Figure 4.2.5. Effect of Na^+ ions on carbachol displacement of [^{3}H]NMS binding to m3 muscarinic receptors in CHO-m3 membranes, in the presence and absence of 100 μM GTP. Binding curves represent the mean ± standard error values of untransformed data (not taking into account small changes in [^{3}H]NMS concentration) from three independent experiments.

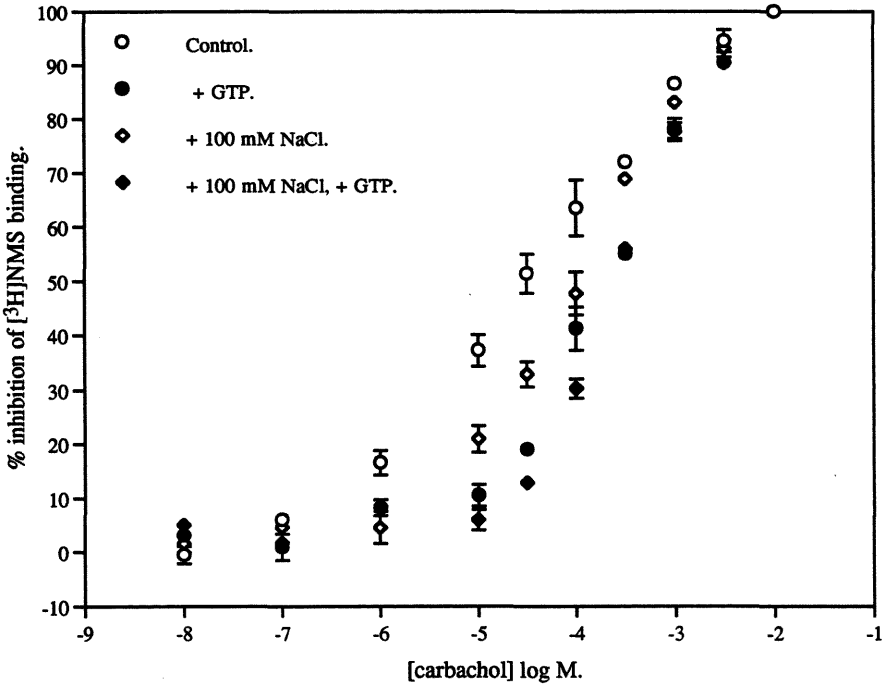

Table 4.2.2. Carbachol inhibition constant (log M K_{50}) values (derived from IC_{50} values using the Cheng-Prusoff equation) and slope factor values, for carbachol displacement of [^{3}H]NMS binding to m3 muscarinic receptors in CHO-m3 cell membranes, in the presence and absence of 100 μM GTP. Binding buffer consisted of 10 mM HEPES, 1 mM $MgCl_2$ and various concentrations of NaCl, pH 7.4. Data is expressed as the mean ± standard error values of three independent experiments.

[NaCl]		K_{50}(log M)	slope factor
0 mM	Control	-5.51 ± 0.16	0.42 ± 0.00
	+ GTP	-4.75 ± 0.03	0.74 ± 0.02
30 mM	Control	-4.91 ± 0.03	0.53 ± 0.04
	+GTP	-4.43 ± 0.04	0.76 ± 0.05
100 mM	Control	-4.39 ± 0.03	0.62 ± 0.02
	+ GTP	-4.03 ± 0.03	0.95 ± 0.01

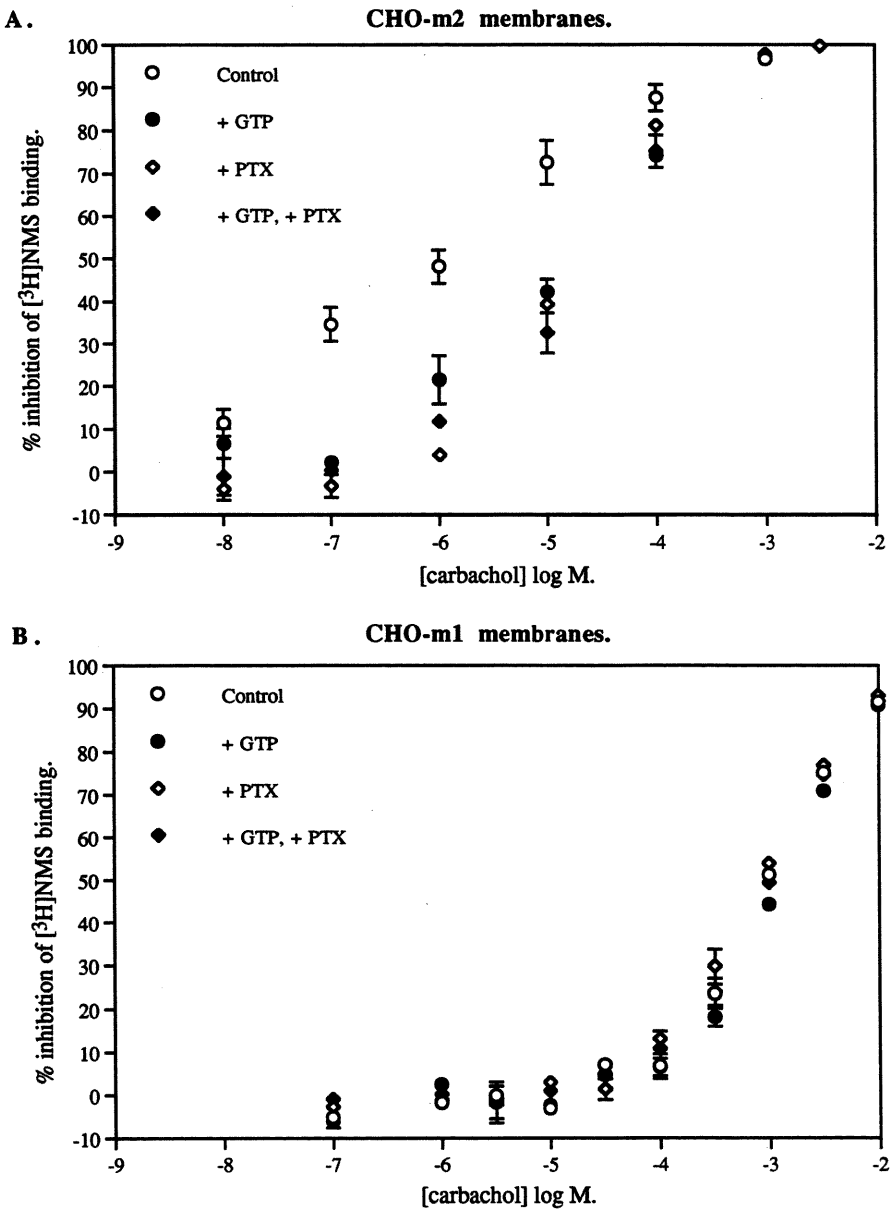

Figure 4.2.6. Carbachol competition binding with [^{3}H]NMS (approximately 0.4 nM) in **A.** CHO-m2 and **B.** CHO-m1 cell membranes, in binding buffer consisting of 10 mM HEPES, 1 mM $MgCl_2$, 100 mM NaCl, pH 7.4. Membranes were incubated in the presence and absence of 100 µM GTP before and after PTX pretreatment of cells (100 ng / ml for 20 h). Incubations were for 60 min at 37 °C and were terminated by filtration onto siliconized Whatman GF/B filters. Binding curves show mean ± standard error values of untransformed data (not taking into account small changes in the [^{3}H]NMS concentration) from three independent experiments.

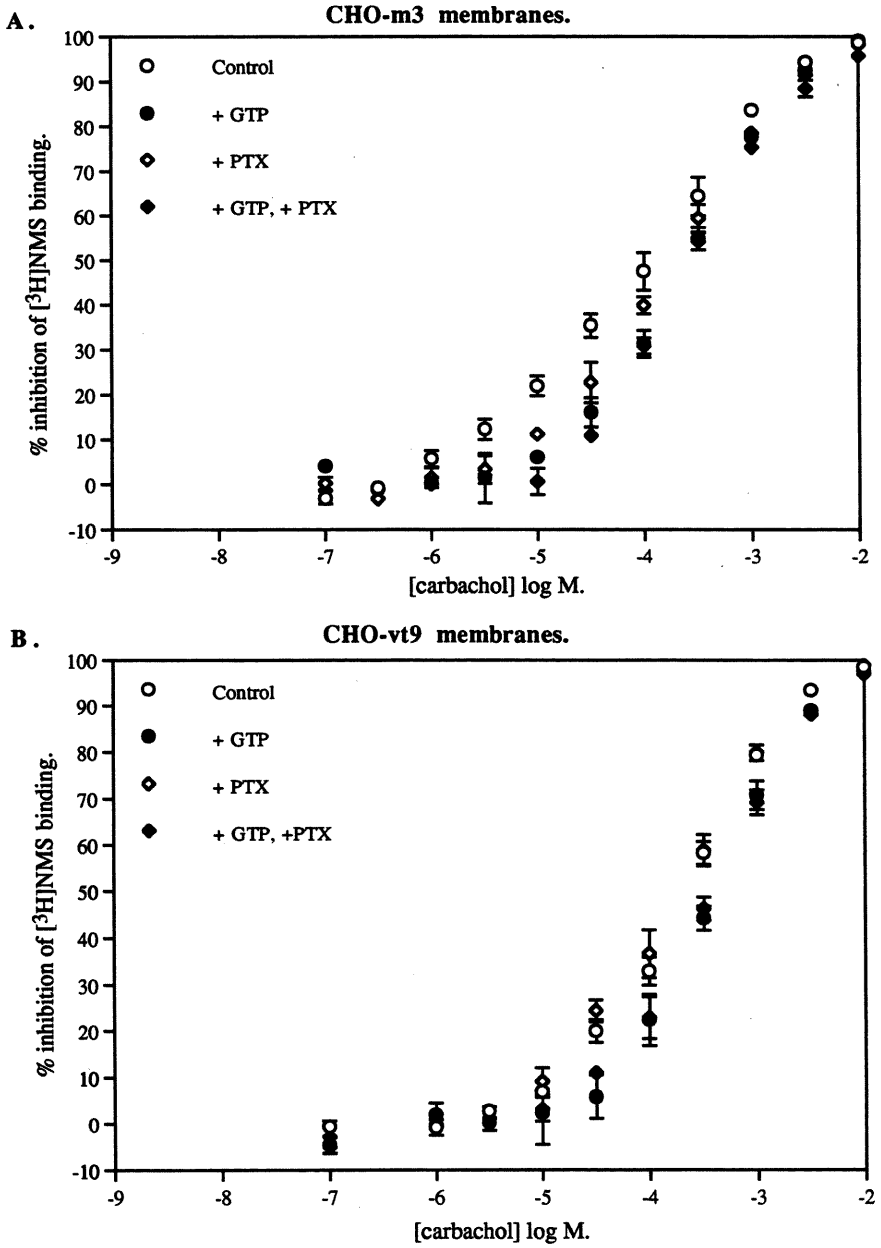

Figure 4.2.7. Carbachol competition binding with [^{3}H]NMS (approximately 0.4 nM) in **A**. CHO-m3 and **B**. CHO-vt9 cell membranes, in binding buffer consisting of 10 mM HEPES, 1 mM $MgCl_2$, 100 mM NaCl, pH 7.4. Membranes were incubated in the presence and absence of 100 μM GTP before and after PTX pretreatment of cells (100 ng / ml for 20 h). Incubations were for 60 min at 37 °C and were terminated by filtration onto siliconized Whatman GF/B filters. Binding curves show mean ± standard error values of untransformed data (not taking into account small changes in the [^{3}H]NMS concentration) from three independent experiments.

Table 4.2.3.

Carbachol binding parameters derived from [^{3}H]NMS displacement experiments in CHO-K1 cell membranes expressing m1, m2 or m3 muscarinic receptors.

K_{50} (log M) represents the inhibition constant for carbachol obtained using the Cheng-Prusoff equation. Numbers in parenthesis represent the number of individual experiments. All data represent the mean ± standard error values obtained from individual experiments. * represents a significant difference in slope factor values of $p < 0.05$ (unpaired T-test) compared with control. ** represents a significant difference in slope factor values of $p < 0.01$ (unpaired T-test) compared with control. [a] = significant difference ($p < 0.05$, unpaired T-test) from CHO-m2 membranes + GTP. [b] = significant difference ($p < 0.05$, unpaired T-test) from CHO-m3 membranes + GTP.

	K_{50}	slope factor	n
CHO-m2 membranes			
Control	-5.99 ± 0.22	0.42 ± 0.02	(5)
+ GTP	-4.95 ± 0.12	0.71 ± 0.09 *	(6)
+ PTX	-5.08 ± 0.01	0.91 ± 0.03 **	(3)
+ GTP / + PTX	-4.95 ± 0.07	0.83 ± 0.04 **	(3)
CHO-m3 membranes			
Control	-4.40 ± 0.08	0.65 ± 0.02	(4)
+ GTP	-4.00 ± 0.09 [a]	0.90 ± 0.05 *	(4)
+ PTX	-4.13 ± 0.03	0.78 ± 0.05	(4)
+ GTP / + PTX	-3.93 ± 0.03	0.91 ± 0.04 **	(4)
CHO-vt9 membranes			
Control	-4.11 ± 0.05	0.87 ± 0.02	(3)
+ GTP	-3.83 ± 0.07 [a]	1.00 ± 0.04 *	(3)
+ PTX	-4.12 ± 0.03	0.82 ± 0.01	(3)
+ GTP / + PTX	-3.78 ± 0.05	0.93 ± 0.03	(3)
CHO-m1 membranes			
Control	-3.70 ± 0.01	1.03 ± 0.06	(4)
+ GTP	-3.59 ± 0.02 [a,b]	1.06 ± 0.03	(4)
+ PTX	-3.79 ± 0.04	0.95 ± 0.05	(4)
+ GTP / + PTX	-3.70 ± 0.04	1.00 ± 0.05	(4)

Carbachol showed significant selectivity ($p < 0.05$, unpaired T-test analysis) for the different subtypes of muscarinic receptors expressed in CHO cell membranes in the presence of 100 μM GTP *i.e.* the low affinity state of the receptors of:

$$m2 >> m3 > m1$$

CHAPTER FIVE.

CARBACHOL-STIMULATED [^{35}S]GTPγS BINDING IN MEMBRANES PREPARED FROM CHO CELL CLONES EXPRESSING RECOMBINANT MUSCARINIC RECEPTOR SUBTYPES.

5.0. Introduction.

The binding of an agonist to G protein-coupled receptors results in activation of the G proteins, promoting the dissociation of GDP (Higashijima *et al*, 1987) and the subsequent binding of GTP. The G protein α subunits (with GTP bound) then dissociate from the βγ subunits and modulate effector molecules (such as AC and PLC). An intrinsic GTPase activity of the G protein α subunits finally breaks down the bound GTP to GDP, thus inactivating the Gα subunits and causing reassociation of the α subunits with βγ subunits to reform the heterotrimeric G proteins (Taylor, 1990).

GTPγS is a metabolically stable analogue of GTP which binds to G protein α subunits, causing them to dissociate from βγ complexes and modulate their effector molecules. GTPγS is only poorly hydrolysed by the GTPase activity of the α subunit, thereby rendering the α subunit irreversibly activated. In this respect, GTPγS has been shown to irreversibly stimulate or inhibit AC activity, and to stimulate PLC activation via their respective G proteins (Katada *et al*, 1984b; Harden *et al*, 1988; Safrany and Nahorski, 1994). GTPγS-stimulated responses tend to have an initial lag phase, when compared with hormone-stimulated responses. This is thought to be due to the relatively slow rate at which GTPγS exchanges with guanine nucleotides on G protein α subunits in the absence of receptor agonists. Co-stimulation with hormone and GTPγS results in an enhanced response, greater than the response produced in the presence of hormone alone. The lag phase of the response is also abolished, or greatly reduced (Katada *et al*, 1984b; Safrany and Nahorski, 1994). Hormone binding to receptors will greatly increase the rate of GDP dissociation from the G protein α subunits, thus allowing rapid association of GTPγS, and subsequent activation of the response (Taylor, 1990).

Agonist-stimulated GTPγS binding to G protein α subunits can be measured in membranes using [^{35}S]GTPγS, which will bind to the G proteins and can be separated from free [^{35}S]GTPγS by vacuum filtration. In this way, agonist-stimulated [^{35}S]GTPγS binding can be used to define the potency and intrinsic activity of agonists, by using [^{35}S]GTPγS binding as a measurable response.

Many studies have investigated agonist-stimulated [^{35}S]GTPγS binding in tissues, *e.g.* cardiac membranes expressing M_2 muscarinic receptors (Hilf and Jakobs, 1992; Hilf *et al*, 1989); in cell lines, *e.g.* HL 60 human leukaemia cells which express receptors for the chemotactic peptide fMet-Leu-Phe (FMLP)(Gierschik *et al*, 1991); in cells expressing recombinant receptors, *e.g.* CHO cells expressing recombinant muscarinic receptors (Lazareno *et al*, 1993); and in reconstituted systems, *e.g.* purified muscarinic receptors with purified G_i reconstituted in phospholipid vesicles (Kurose *et al*, 1986). From these studies it has become clear that certain pre-requisites must be met before agonist-stimulated [^{35}S]GTPγS binding could be observed. Mg^{2+} was required to observe

[^{35}S]GTPγS binding and at higher concentrations (*i.e.* maximally effective at approximately 500 μM) to observe agonist-stimulated [^{35}S]GTPγS binding (Hilf *et al*, 1989). Similar Mg^{2+} requirements have been reported for guanine nucleotide regulation of agonist binding (see Chapter 4). Mg^{2+} has also been shown to be necessary for agonists to influence the binding of guanine nucleotides, by increasing the rate of GDP dissociation, thus enhancing GDP-GTP exchange and subsequent GTP hydrolysis (Higashijima *et al*, 1987; Shiozaki and Haga, 1992). It is, therefore, standard procedure to perform [^{35}S]GTPγS binding studies in the presence of excess $MgCl_2$ (approximately 10 mM).

The second important requirement to enhance agonist-stimulated [^{35}S]GTPγS binding is the presence of GDP in the reaction mixture. GDP appears to reduce basal binding of [^{35}S]GTPγS to a greater extent than agonist-stimulated [^{35}S]GTPγS binding, thus increasing the proportion of agonist-stimulated [^{35}S]GTPγS binding as a percentage above basal [^{35}S]GTPγS binding (Hilf and Jakobs, 1992; Lorenzen *et al*, 1993; Hilf *et al*, 1989; Gierschik *et al*, 1991; Lazareno *et al*, 1993). The possible reasons for this GDP requirement are discussed in the discussion section of this chapter.

The third requirement to enhance agonist-stimulated [^{35}S]GTPγS binding is NaCl. In cardiac membranes, 150 mM NaCl reduced basal binding of [^{35}S]GTPγS and produced an approximate 10-fold increase in the EC_{50} value for carbachol-stimulated [^{35}S]GTPγS binding without effecting the maximal increase in absolute [^{35}S]GTPγS binding (Hilf *et al*, 1989; Hilf and Jakobs, 1992). As a consequence of reduced basal binding the relative carbachol-stimulated [^{35}S]GTPγS binding was increased in the presence of NaCl. NaCl has also been shown to modulate agonist binding to receptors (see chapter 4) and this has been shown to coincide with a marked reduction of the potency of agonist (fMet-Leu-Phe)(FMLP) to stimulate a high-affinity GTPase in HL 60 cell membranes (Gierschik *et al*, 1989). In contrast, the degree of FMLP-stimulated GTPase activity was markedly enhanced in the presence of Na^+. These results suggested that monovalent cations (particularly Na^+) regulate agonist-receptor-G protein interactions. The reduction in basal [^{35}S]GTPγS binding (Hilf *et al*, 1989) and the reduction in basal GTPase activity (Gierschik *et al*, 1989) in the presence of Na^+ suggests that G proteins interact with and are activated by receptors even in the absence of agonists and that Na^+ uncouples unoccupied receptors from G protein interaction and activation.

In the previous chapter, a possible coupling of m3 muscarinic receptors to both PTX-insensitive and PTX-sensitive G proteins , in CHO-m3 cell membranes, was tentatively suggested on the basis of modification of agonist displacement binding curves by PTX pretreatment of cells. The study also suggested that the degree of interaction of these receptors with PTX-sensitive G proteins increased with increased expression of the receptor (Chapter 4). In the present study, it was hoped that a more accurate assessment of muscarinic receptor-G protein interactions could be achieved by investigating agonist-

stimulated binding of [^{35}S]GTPγS to G proteins in CHO cell membranes expressing recombinant muscarinic receptors.

5.1. Methods.

Membranes were prepared from CHO cell clones (see chapter 2) and resuspended in buffer consisting of 10 mM HEPES, 10 mM $MgCl_2$, 100 mM NaCl, pH 7.4 at a final protein concentration of 50 μg / ml. Incubations were conducted in a 1 ml final assay volume at 37 °C for 60 min by which time carbachol-stimulated [^{35}S]GTPγS binding was maximal over basal [^{35}S]GTPγS binding. Incubations were conducted in the presence of 3 μM GDP (except where indicated) and 70 pM [^{35}S]GTPγS (specific activity 1202 Ci / mmol), (approximately 200 000 dpm) in the presence and absence of 500 μM carbachol. Non-specific binding was determined in the presence of 10 μM unlabelled GTPγS. Reactions were terminated by vacuum filtration using a Brandel cell harvester and Whatman GF/B filters. Filters were pretreated with 1 % BSA and 1 % Sigmacote siliconizing fluid (as described in chapter 4). Pretreated filters were dampened with cold binding buffer just prior to filtration of the samples. After filtration, the filters were transferred to 4 ml of scintillation cocktail (Optiphase X) and left for at least 12 hr before being counted for radioactivity by liquid scintillation spectrometry. PTX pretreatment of cells involved supplementing the cell growth media with 100 ng / ml PTX for 20 hr prior to membrane preparation.

5.1.1 Data Analysis.

Data was expressed as carbachol-stimulated [^{35}S]GTPγS binding in specific dpm / 50 μg protein. Statistical significance between control and PTX-treated data was set at $p \leq 0.05$ using paired T-test analysis.

5.2. Results

Effect of GDP on Carbachol-Stimulated [^{35}S]GTPγS Binding in CHO Membranes Expressing Recombinant Muscarinic Receptors.

Time course studies in the presence of 3 μM GDP showed that maximal carbachol-stimulated [^{35}S]GTPγS binding over basal occurred after a 60 min incubation (Figure 5.2.1) in CHO-m1, CHO-m2 and CHO-m3 cell membranes. All further experiments were therefore incubated for 60 min.

Carbachol-stimulated [^{35}S]GTPγS binding was not detected above basal binding in the absence of GDP in each of the CHO cell clones. Co-incubation of increasing

concentrations of GDP with approximately 70 pM [^{35}S]GTPγS in the presence and absence of 500 μM carbachol were conducted to establish an optimal window of carbachol-stimulated [^{35}S]GTPγS binding over basal. Increasing GDP concentration from 10^{-8}M to 3 x 10^{-4}M led to a dose-dependent reduction in total [^{35}S]GTPγS binding in each cell membrane preparation (Figure 5.2.2.a, 5.2.3.a and 5.2.4.a). However, carbachol-stimulated [^{35}S]GTPγS binding increased as a percentage of basal binding with increasing concentrations of GDP (Figure 5.2.2.b, 5.2.3.b and 5.2.4.b). Addition of GDP resulted in a reduction in basal [^{35}S]GTPγS binding without reducing carbachol-stimulated [^{35}S]GTPγS binding in CHO-m3 membranes (Figure 5.2.4.a), or possibly enhancing carbachol-stimulated [^{35}S]GTPγS binding in CHO-m2 and CHO-m1 cells (Figures 5.2.2.a and 5.2.3.a). A final concentration of 3μM GDP was used in further studies, as this concentration of GDP produced a relatively large window of carbachol-stimulated [^{35}S]GTPγS binding above basal levels in each of the membrane preparations. Further increases in GDP concentration appeared to reduce the window of carbachol-stimulated [^{35}S]GTPγS binding above basal levels in CHO-m1 cell membranes (Figure 5.2.3.a). Also, with increasingly higher GDP concentrations, the differences between basal and carbachol-stimulated [^{35}S]GTPγS binding became less clearly defined as total binding decreased. Using these binding conditions CHO-m2, CHO-m3, CHO-vt9 and CHO-m1 cell membranes produced maximal carbachol-stimulated [^{35}S]GTPγS binding as a percentage of basal levels of; 137 ± 3 (n=7), 125 ± 2 (n=7), 108 ± 1 (n=3) and 136 ± 5 (n=4), respectively (Figure 5.2.5), with basal values (specific dpm / 50 μg protein) being 14898 ± 1187, 11541 ± 974, 13195 ± 1152 and 13153 ± 2219, respectively.

Effect of PTX Pretreatment on Agonist-Stimulated [^{35}S]GTPγS Binding in CHO Membranes Expressing Recombinant Muscarinic Receptors.

PTX-pretreatment of each cell clone (100 ng / ml, 20 hr) resulted in a 70-80 % reduction in basal [^{35}S]GTPγS binding compared to control basal levels (data not shown). Carbachol-stimulated [^{35}S]GTPγS binding above basal levels in PTX-pretreated CHO-m2 cell membranes was reduced to approximately 3 % of the carbachol-stimulated [^{35}S]GTPγS binding above basal levels observed in untreated CHO-m2 cell membranes (from 5908 ± 531 dpm / 50 μg protein to 239 ± 125 dpm / μg protein) (Figure 5.2.6). Carbachol-stimulated [^{35}S]GTPγS binding was no longer statistically significantly different from basal values after PTX-pretreatment ($p > 0.05$, by paired T-test).

PTX-pretreatment of CHO-m1 cells resulted in a significant reduction in carbachol-stimulated [^{35}S]GTPγS binding above basal levels from 4804 ± 247 dpm / 50 μg protein (n=4) to 2520 ± 151 dpm / 50 μg protein (n=4) ($p< 0.01$, by paired T-test); a reduction to approximately 52 % of the carbachol-stimulated [^{35}S]GTPγS binding observed in

untreated CHO-m1 cell membranes. After PTX-pretreatment, carbachol-stimulated [^{35}S]GTPγS binding remained significantly higher than basal levels of [^{35}S]GTPγS binding ($p < 0.001$, by paired T-test). Experiments performed in CHO-m1 cells pretreated with 300 ng / ml PTX for 20 hr were not significantly different from experiments carried out using cells pretreated with 100 ng / ml PTX for 20 hr, suggesting that the initial dose of PTX used was maximally effective in this study (data not shown).

PTX-pretreatment of CHO-m3 cells resulted in a significant reduction in carbachol-stimulated [^{35}S]GTPγS binding above basal levels from 3126 ± 214 dpm / 50 μg protein (n=7) to 1192 ± 131 dpm / 50 μg protein (n=7) ($p < 0.01$, by paired T-test); a reduction to approximately 39 % of the carbachol-stimulated [^{35}S]GTPγS binding observed in untreated CHO-m3 cell membranes. After PTX-pretreatment, carbachol-stimulated [^{35}S]GTPγS binding remained significantly higher than basal levels of [^{35}S]GTPγS binding ($p < 0.001$, by paired T-test).

PTX-pretreatment of CHO-vt9 cells resulted in a small reduction in carbachol-stimulated [^{35}S]GTPγS binding above basal levels from 1224 ± 235 dpm / 50 μg protein (n=3) to 851 ± 258 dpm / 50 μg protein (n=3) which proved not to be statistically significant ($p = 0.088$, by paired T-test). In each of three experiments, however, carbachol-stimulated [^{35}S]GTPγS binding after PTX pretreatment was, on average, 66% of carbachol-stimulated [^{35}S]GTPγS binding in untreated cells. The lack of statistical significance of this response may lie in the fact that small reductions are being assessed in a system where the window for carbachol-stimulated [^{35}S]GTPγS binding above basal levels is only small (approximately 8%). Additional repetitions of these experiments may be required to define more clearly the effect of PTX pretreatment on carbachol-stimulated [^{35}S]GTPγS binding in CHO-vt9 cell membranes. After PTX-pretreatment, carbachol-stimulated [^{35}S]GTPγS binding in CHO-vt9 cell membranes remained significantly higher than basal levels of [^{35}S]GTPγS binding ($p \leq 0.05$, by unpaired T-test).

5.3. Discussion.

In the present study, carbachol-stimulated [^{35}S]GTPγS binding to G proteins was used as a measurement of receptor-mediated activation of G proteins by different muscarinic receptor subtypes. The nature of the G proteins to which the muscarinic receptors couple could also be defined by their sensitivity to PTX pretreatment.

The reduction in total [^{35}S]GTPγS binding observed after PTX pretreatment of the CHO cell clones (70-80%) suggests that a large proportion of the G proteins to which [^{35}S]GTPγS binds are PTX-sensitive G proteins. Similar observations have also been observed in other studies either in CHO cell membranes (Lazareno *et al*, 1993), HL 60 cell membranes (Gierschik *et al*, 1991; Gierschik *et al*, 1989) or in a reconstituted system (Kurose *et al*, 1986). In contrast, PTX pretreatment had no effect on control [^{35}S]GTPγS

binding in porcine atrial membranes while at the same time reducing carbachol-stimulated [^{35}S]GTPγS binding by approximately 70% (Hilf *et al*, 1989).

It has previously been shown that ADP-ribosylation of G proteins by PTX interferes specifically with receptor-G protein interactions without modifying the intrinsic functions of the G protein *i.e.* GTPase activity, GTPγS binding and subunit dissociation (Haga *et al*, 1985; Enomoto and Asakawa, 1986; Huff and Neer, 1986; Katada *et al*, 1986). The large reduction in basal [^{35}S]GTPγS binding observed in the present study after PTX pretreatment of the CHO cell clones, therefore, suggests a number of possibilities. The 70-80% reduction in basal [^{35}S]GTPγS binding may represent a proportion of PTX-sensitive G proteins that were coupled to receptors (endogenous and/or recombinant) in the absence of a receptor agonist. Thus, unoccupied receptors may not be completely silent with regard to G protein activation. Evidence for this theory has come from the findings that reconstitution of the purified β-adrenoceptor into lipid vesicles containing purified G_s significantly enhanced GTPase activity of G_s, even in the absence of a receptor agonist (Cerione *et al*, 1984). Similarly, studies with mutant β-adrenoceptors have led to an extended version of the ternary complex model of agonist-receptor-G protein interactions whereby the receptor can interchange between two isomerization states, one active and one inactive, the rate of interchange to the active form being governed by agonist binding (Samama *et al*, 1993). Based on these findings it appears reasonable to suggest that unoccupied receptors may interact with and activate G proteins. Uncoupling the unoccupied receptors from the PTX-sensitive G proteins with PTX pretreatment will, therefore, lead to a reduction in total [^{35}S]GTPγS binding as was observed in the present study. In opposition to this view is the fact that Na^+ ions are believed to uncouple G proteins from unoccupied receptors, thereby resulting in a reduction in basal [^{35}S]GTPγS binding (Hilf *et al*, 1989; Gierschik *et al*, 1989). As NaCl (100 mM) was present in the incubation buffer, it was surprising to see such a dramatic apparent constitutive activity of PTX-sensitive G protein-coupled receptors.

Expression of recombinant m2 muscarinic receptors (in CHO-m2 cell membranes), which couple to PTX-sensitive G proteins, did not produce an increased basal activity of [^{35}S]GTPγS binding compared with expression of m3 muscarinic receptors (in CHO-vt9 cell membranes), which were found not to couple significantly with PTX-sensitive G proteins. If a large proportion of basal binding of [^{35}S]GTPγS was due to constitutively active PTX-sensitive G protein-coupled receptors then it might have been expected to increase with increased expression of PTX-sensitive G protein-coupled receptors (*i.e.* m2 muscarinic receptors). This was clearly not the case.

Basal [^{35}S]GTPγS binding was identical in each of the CHO cell clones despite the

varying expression levels of the muscarinic receptors present. Increasing m3 muscarinic receptor number from approximately 300-400 fmol / mg protein (CHO-vt9 cell membranes) to greater than 1000 fmol / mg protein (CHO-m3 cell membranes) had no significant effect on the basal binding of [^{35}S]GTPγS. Thus, increasing the number of unoccupied m3 muscarinic receptors in these CHO cell clones seemed to have no significant effect on G protein activation in the absence of a receptor agonist. Another possible explanation for the large reduction in basal [^{35}S]GTPγS binding after PTX-pretreatment may be that ADP-ribosylation of PTX-sensitive G proteins may indeed modify [^{35}S]GTPγS binding to uncoupled PTX-sensitive G proteins; an explanation that is generally opposed by the evidence of the available literature (Haga *et al*, 1985; Enomoto and Asakawa, 1986; Huff and Neer, 1986; Katada *et al*, 1986; Gierschik, 1992).

Agonist-stimulated [^{35}S]GTPγS binding in CHO clone membranes was either very small or absent unless experiments were carried out in the presence of GDP. With increasing GDP concentrations, basal [^{35}S]GTPγS binding was dose-dependently inhibited. Carbachol-stimulated [^{35}S]GTPγS binding, however, was relatively unaffected by GDP concentration. Therefore, with increasing concentrations of GDP, carbachol-stimulated [^{35}S]GTPγS binding was increased as a percentage above basal binding. The requirement for GDP to observe agonist-stimulated [^{35}S]GTPγS binding is widely reported in a number of studies carried out in different cell lines expressing different G protein-coupled receptors (Hilf and Jakobs, 1992; Lorenzen *et al*, 1993; Hilf *et al*, 1989;Gierschik *et al*, 1991; Lazareno *et al*, 1993). In each case added GDP enhanced agonist-stimulated [^{35}S]GTPγS binding by reducing basal binding to a greater extent. Lazareno *et al* (1993) have shown that GDP dose-dependently shifts the agonist dose-response curve for [^{35}S]GTPγS binding to the right for m1 and m3 muscarinic receptors expressed in CHO cell membranes (probably correlating with the reduction in agonist binding affinity that results from the presence of guanine nucleotides).

A requirement for GDP suggests that a proportion of G proteins in the membrane preparation were guanine nucleotide-free, because exogenous GDP would not be necessary if the G proteins were already coupled to endogenous GDP. It is thought that guanine nucleotide-free G proteins will interact with [^{35}S]GTPγS in an agonist-independent manner. Agonist stimulation is believed to increase the rate of GDP dissociation from the G protein allowing GTP to bind (Higashijima *et al*, 1987; Shiozaki and Haga, 1992). Thus, it appears that exogenous GDP is required to couple with G proteins in the membrane preparations so that they may then be activated by agonist stimulation of the receptors. At the same time, exogenous GDP will reduce the total binding of [^{35}S]GTPγS. Hilf *et al* (1989) have shown that the requirement for GDP to

observe carbachol-stimulated [^{35}S]GTPγS binding cannot be replaced by the metabolically stable analogue GDPβS in cardiac membranes. One possible explanation for this anomaly is that GDPβS may not readily dissociate from the G protein upon receptor activation and, therefore, prevent [^{35}S]GTPγS binding. Studies have not been reported which substantiate this possible explanation.

GDP was shown to be quickly metabolized in HL60 cell membranes incubated at 30 °C (Wieland *et al*, 1992) and required exogenous GDP to observe FMLP-stimulated [^{35}S]GTPγS binding. Experiments carried out at 0°C, however, reduced the metabolism of endogenous GDP so that agonist-stimulated [^{35}S]GTPγS binding could be observed in the absence of exogenous GDP (Wieland *et al*, 1992).

Together these results suggest that receptor activation of G proteins requires the GDP-liganded form of the G protein, allowing receptor-induced exchange of bound GDP for GTPγS. In membrane preparations, bound GDP can be rapidly released (and degraded) resulting in guanine nucleotide-free G proteins to which GTPγS will bind independently of agonist-activated receptors.

The actual increase in [^{35}S]GTPγS binding observed in each CHO cell clone, in the presence of 500 μM carbachol, was not solely related to receptor expression levels but also to the particular receptor subtype present. CHO-m2 cell membranes expressing m2 muscarinic receptors at a relatively low receptor density (approximately 100 fmol / mg protein) produced the largest increase in agonist-stimulated [^{35}S]GTPγS binding despite high expression levels of m1 and m3 muscarinic receptors (> 1000 fmol / mg protein) in CHO-m1 and CHO-m3 cell membranes, respectively. CHO-vt9 cell membranes which expressed at least 3-fold fewer m3 muscarinic receptors than CHO-m3 cell membranes, produced an agonist-induced maximal [^{35}S]GTPγS binding response that was approximately 3-fold lower than in CHO-m3 cell membranes suggesting that the number of m3 receptors in CHO-vt9 cells was not sufficient to produce a maximal activation of the coupled G proteins in response to 500 μM carbachol.

Agonist-stimulated [^{35}S]GTPγS binding, as a percentage above basal, may not necessarily identify that one particular muscarinic receptor subtype is more efficiently coupled to their respective G proteins. The experimental conditions (and particularly the concentration of [^{35}S]GTPγS used) may preferentially bind [^{35}S]GTPγS to certain families of G proteins. It has been observed that G_i proteins bind GTPγS with a greater affinity than do G_s proteins (Bokoch *et al*, 1984). Therefore, although it appears that m2 muscarinic receptors couple more efficiently to G proteins than do m1 or m3 muscarinic receptors, the experiment may reflect a preferential binding of [^{35}S]GTPγS to a particular type of G protein (*e.g.* G_i) over other G protein species (*e.g.* $G_{q/11}$),which may be involved in coupling with the other muscarinic receptor subtypes. The use of

approximately 70 pM [^{35}S]GTPγS in the present study, may cause a relatively selective binding of [^{35}S]GTPγS with PTX-sensitive G proteins compared with PTX-insensitive G proteins. To increase the proportion of carbachol-stimulated [^{35}S]GTPγS binding to $G_{q/11}$ proteins, higher concentrations of [^{35}S]GTPγS may be required to label all of the lower affinity G protein sites. Further modification of the assay conditions may increase the carbachol-stimulated [^{35}S]GTPγS binding in CHO cell clone membranes as a percentage of basal. For instance, by increasing the protein concentration of membranes used and the GDP concentration used, the proportion of agonist-induced [^{35}S]GTPγS binding may be increased without reducing absolute binding to a level where resolution becomes affected. By increasing the agonist-stimulated portion of [^{35}S]GTPγS binding, dose-response curves to carbachol could be constructed allowing an assessment of the apparent potency and degree of amplification that occurs between agonist binding to the various muscarinic receptor subtypes and subsequent G protein activation.

Carbachol-stimulated [^{35}S]GTPγS binding to m2 receptors in CHO-m2 cell membranes was completely abolished after PTX pretreatment of the cells, suggesting that m2 muscarinic receptors couple with only PTX-sensitive G proteins in CHO cells. Both m1 and m3 muscarinic receptors expressed in CHO cells at relatively high receptor densities produced carbachol-stimulated [^{35}S]GTPγS binding that was partially but significantly PTX-sensitive, suggesting that both PTX-sensitive and PTX-insensitive G proteins can couple with these receptors in CHO cell membranes.

A comparison of PTX-sensitive agonist-stimulated [^{35}S]GTPγS binding with PTX-sensitive high affinity agonist binding (see chapter 4) in CHO-m3 cell membranes strengthens the hypothesis that at high expression levels, m3 muscarinic receptors can couple with PTX-sensitive G proteins. A similar comparison was not applicable for m1 muscarinic receptors due to the lack of any high affinity agonist binding observed in CHO-m1 cell membranes (see chapter 4).

PTX-pretreatment did not significantly reduce carbachol-stimulated [^{35}S]GTPγS binding in CHO-vt9 cell membranes in the present study , though further repetitions of the experiment may eventually show a small element of PTX-sensitive carbachol-stimulated[^{35}S]GTPγS binding in CHO-vt9 cell membranes. Equally, PTX-sensitive high affinity carbachol binding was not observed in CHO-vt9 cell membranes (see chapter 4).

The lack of PTX-insensitive high affinity agonist binding to PI-linked muscarinic receptors, and the relatively poor efficiency of coupling of PI-linked muscarinic receptors with G proteins, in CHO cell membranes, suggests the possibility that, in membranes, coupling of m1 and m3 muscarinic receptors with PTX-insensitive G proteins may be weakened. Functional studies involving m1 and m3 receptor stimulation were conducted

in intact or permeabilized cells (see chapters 6-8), and it is not known whether efficient coupling of m1 and m3 muscarinic receptors with PLC activation, remains in membrane preparations of the CHO cell clones. Agonist-stimulated PLC activation has previously been reported in membrane preparations of cells (Gutowski *et al*, 1991), but functional studies, to test whether muscarinic receptor-PLC coupling is maintained in membrane preparations of CHO-m1, CHO-m3 and CHO-vt9 cells, need to be performed.

The present data does, however, strengthen the hypothesis that m3 muscarinic receptors become increasingly promiscuously coupled with PTX-sensitive G proteins, in CHO cell membranes, with increasing expression of the receptor subtype. The results also suggest that m1 muscarinic receptors, when highly expressed in CHO cell membranes can also couple with both PTX-sensitive and PTX-insensitive G proteins.

Figure 5.2.1. Time course for maximal (500 μM) carbachol stimulation of [^{35}S]GTPγS binding over basal in CHO-m2, CHO-m3 and CHO-m1 cell membranes.

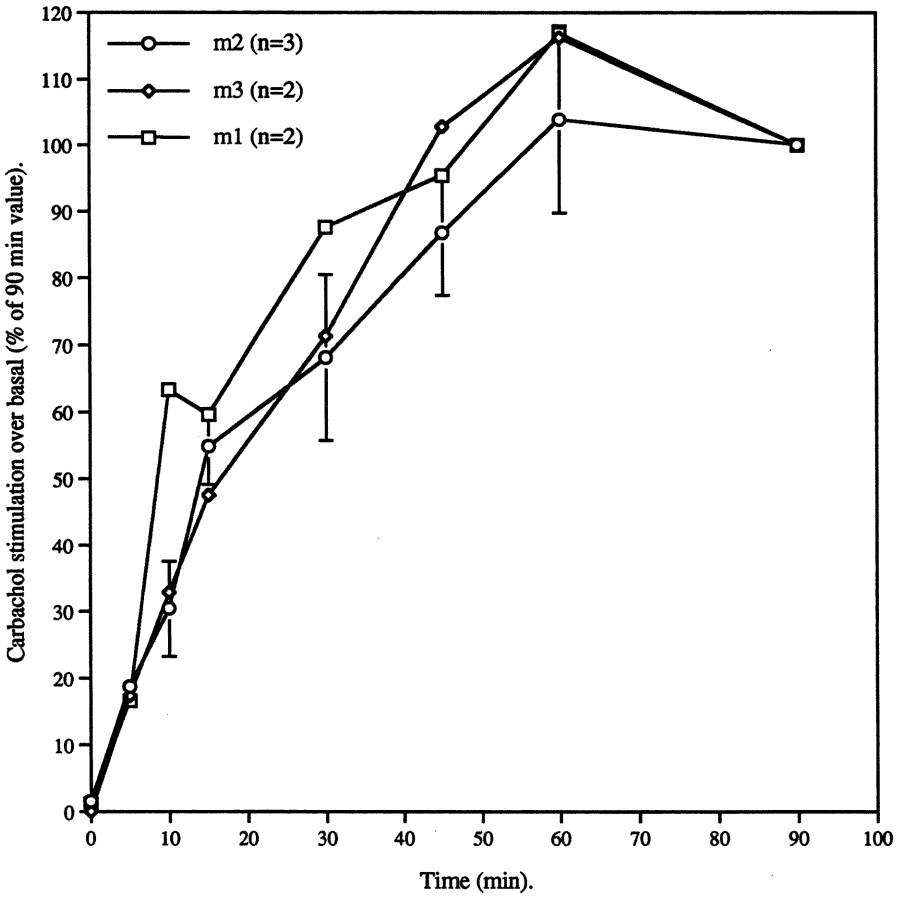

Binding buffer consisted of 10 mM HEPES, 10 mM $MgCl_2$ and 100 mM NaCl, pH 7.4. Membranes (50 μg / ml) were co-incubated with 3μM GDP, 70 pM [^{35}S]GTPγS in the presence and absence of 500 μM carbachol. Non specific binding was determined in the presence of 10 μM unlabelled GTPγS.

Figure 5.2.2.a. Effect of GDP concentration on basal and carbachol-stimulated [^{35}S]GTPγS binding in CHO-m2 cell membranes (n=2).

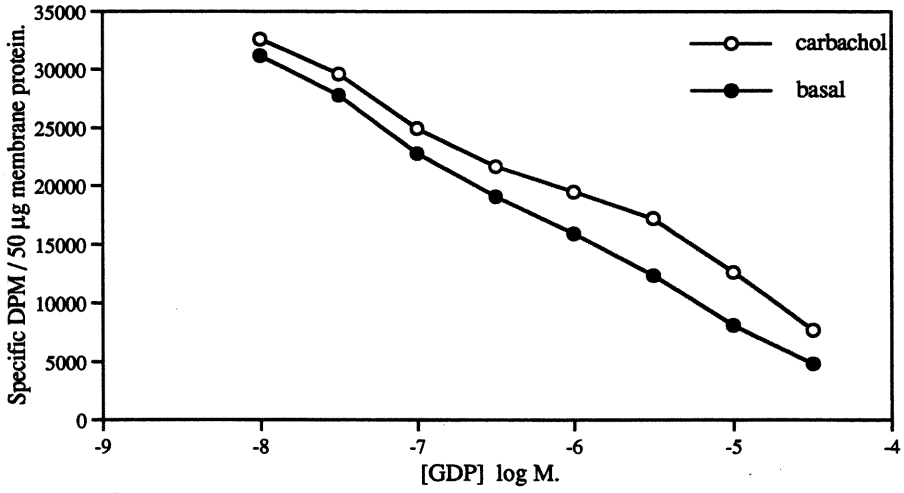

Figure 5.2.2.b. Effect of GDP concentration on carbachol-stimulated [^{35}S]GTPγS binding above basal levels in CHO-m2 cell membranes (n=2).

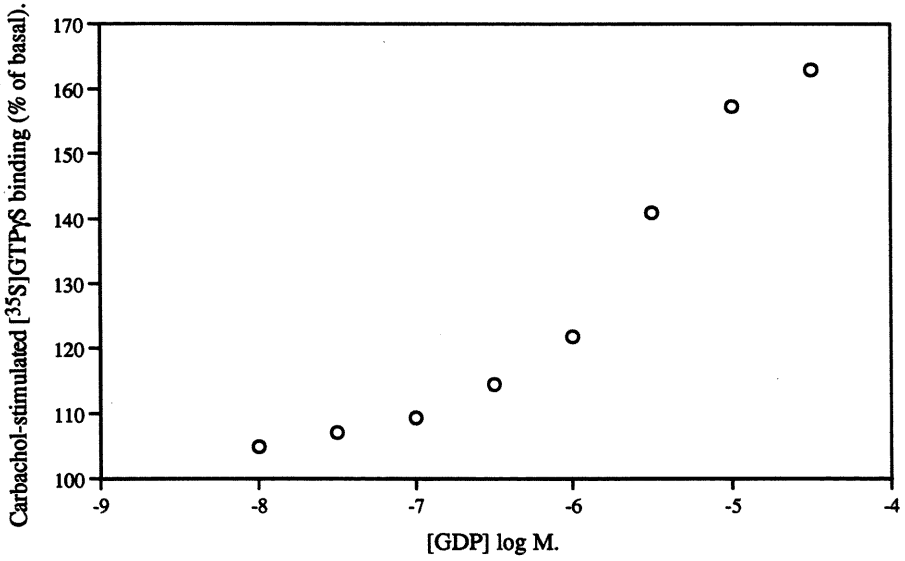

CHO-m2 cell membranes (50 µg protein / ml) were co-incubated with increasing concentrations of GDP, approximately 70 pM [^{35}S]GTPγS in the presence and absence of 500 µM carbachol, for 60 min at 37 °C, as described in 5.1 Methods.

Figure 5.2.3.a. Effect of GDP concentration on basal and carbachol-stimulated [^{35}S]GTPγS binding in CHO-m1 cell membranes (n=2).

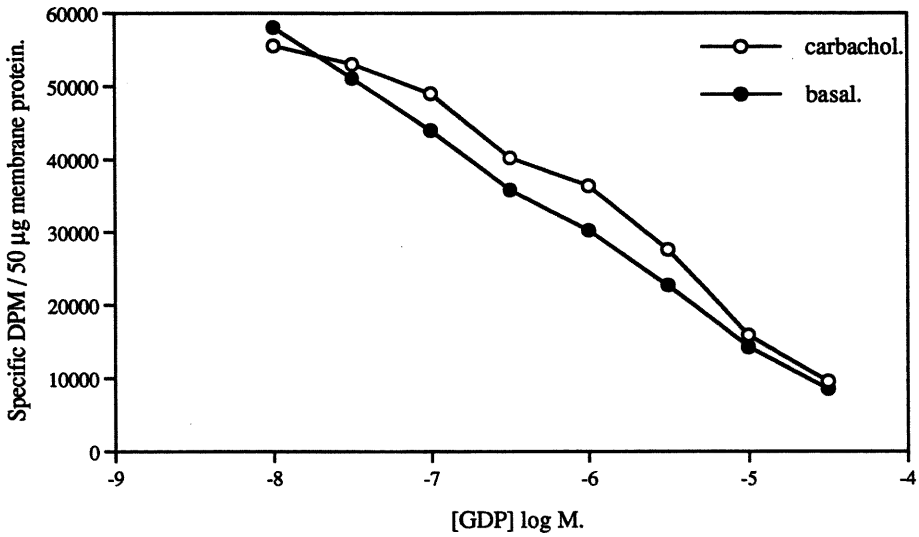

Figure 5.2.3.b. Effect of GDP concentration on carbachol-stimulated [^{35}S]GTPγS binding above basal levels in CHO-m1 cell membranes (n=2).

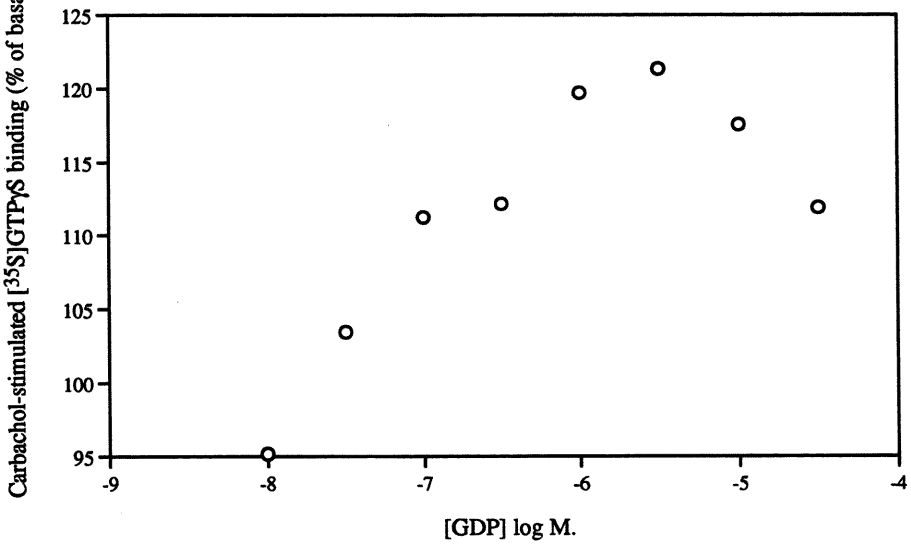

CHO-m1 cell membranes (50 µg protein / ml) were co-incubated with increasing concentrations of GDP, approximately 70 pM [^{35}S]GTPγS in the presence and absence of 500 µM carbachol, for 60 min at 37 °C, as described in 5.1 Methods.

Figure 5.2.4.a. Effect of GDP concentration on basal and carbachol-stimulated [^{35}S]GTPγS binding in CHO-m3 cell membranes (n=2).

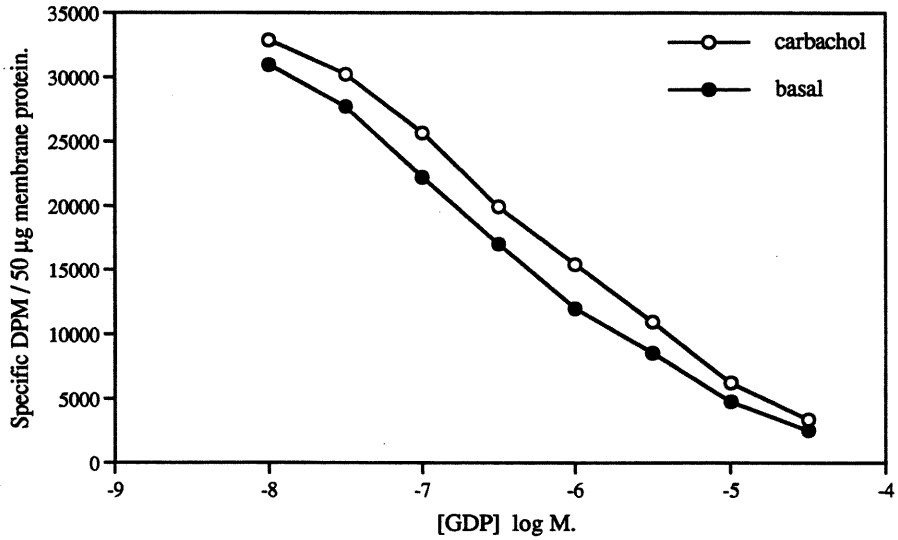

Figure 5.2.4.b. Effect of GDP concentration on carbachol-stimulated [^{35}S]GTPγS binding above basal levels in CHO-m3 cell membranes (n=2).

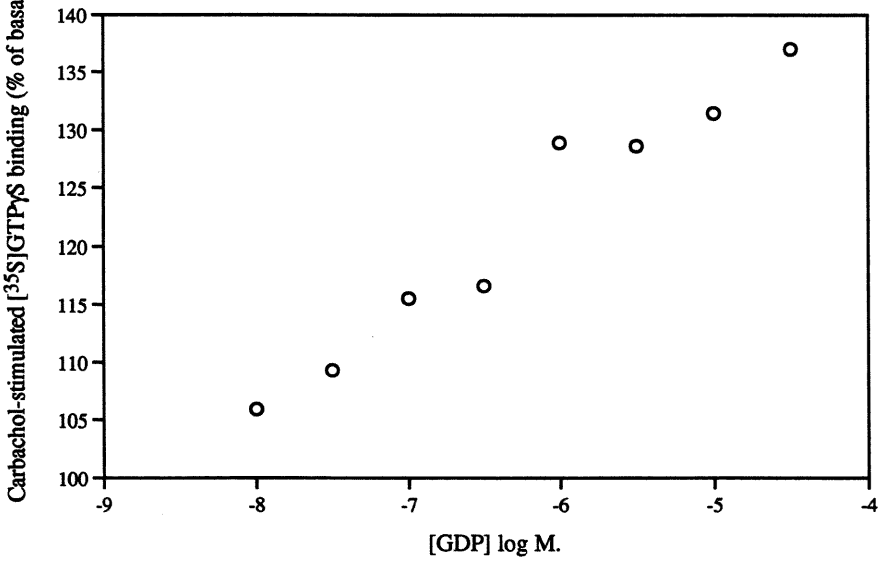

CHO-m3 cell membranes (50 µg protein / ml) were co-incubated with increasing concentrations of GDP, approximately 70 pM [^{35}S]GTPγS in the presence and absence of 500 µM carbachol, for 60 min at 37 ^{o}C, as described in 5.1 Methods.

Figure 5.2.5. Maximal carbachol stimulation of [^{35}S]GTPγS binding above basal levels in CHO-m2, CHO-m3, CHO-vt9 and CHO-m1 cell membranes.

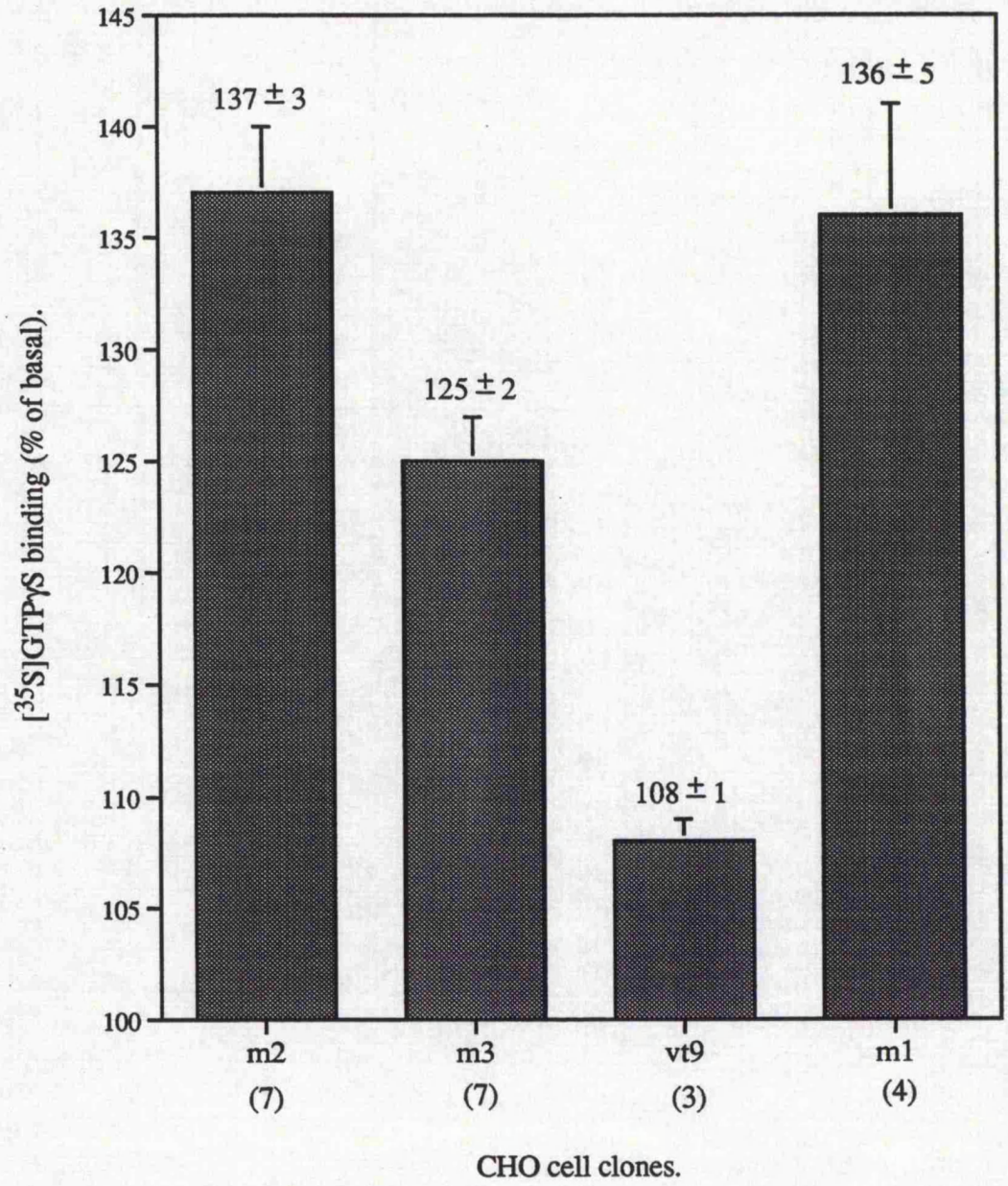

Membranes (50 µg protein / ml) from the different CHO cell clones were co-incubated with 3 µM GDP and approximately 70 pM [^{35}S]GTPγS in the presence and absence of 500 µM carbachol as described in 5.1. Methods. **Figure 5.2.5.** shows the mean ± standard error of carbachol-stimulated [^{35}S]GTPγS binding as a % of basal levels. The number of experiments performed for each cell clone are shown in parenthesis on the x-axis.

Figure 5.2.6. Effect of PTX pretreatment on carbachol-stimulated [^{35}S]GTPγS binding above basal levels in CHO cell clones.

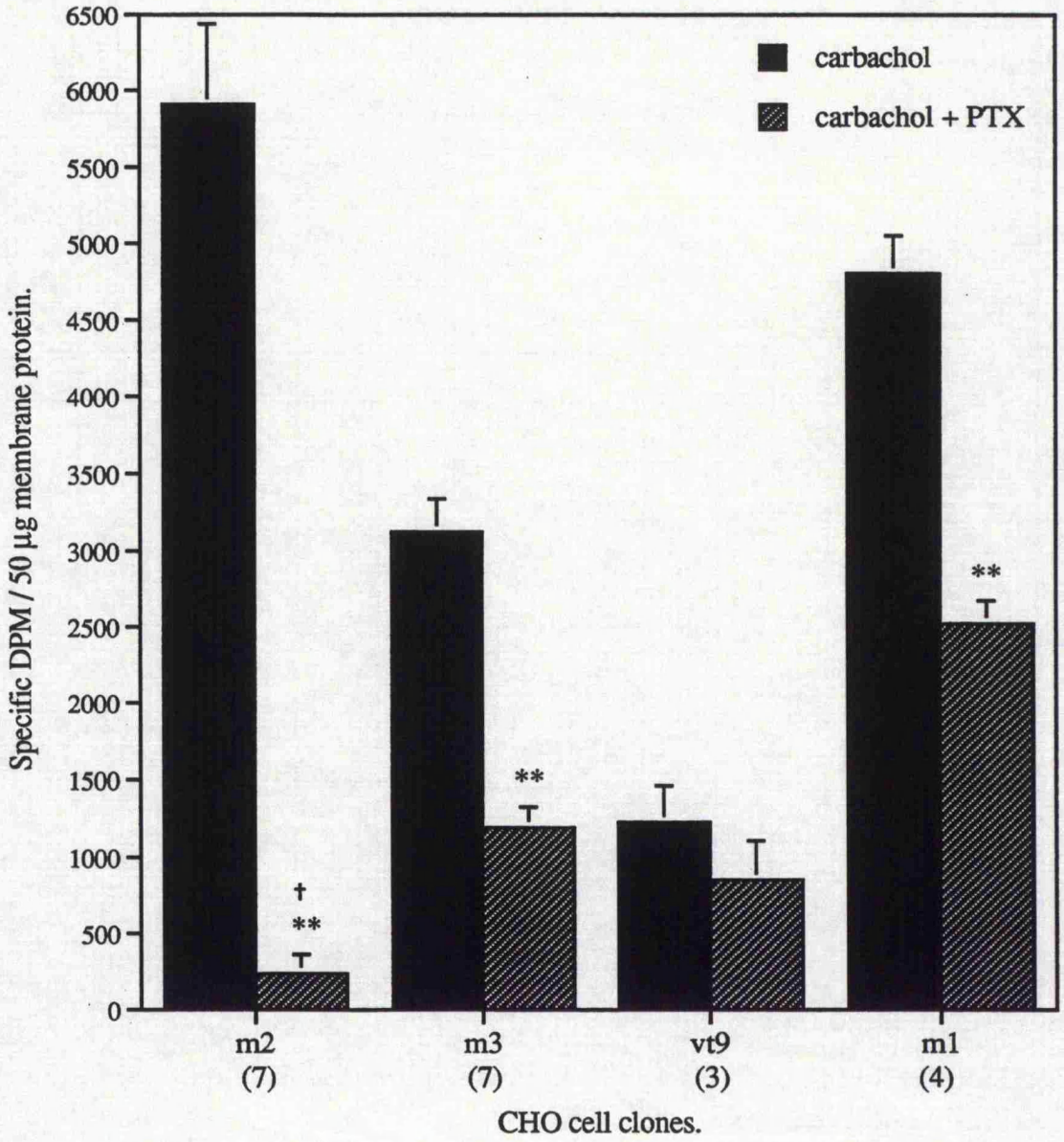

CHO cell membranes (50 µg protein / ml) were co-incubated with 3 µM GDP and approximately 70 pM [^{35}S]GTPγS in the presence and absence of 500 µM carbachol as described in 5.1 Methods. PTX pretreatment involved adding 100 ng / ml PTX to the growth medium of the cells for 20 hr prior to membrane preparation. **Figure 5.2.6.** shows the effect of PTX pretreatment on the proportion of specific [^{35}S]GTPγS binding that was stimulated by carbachol, above basal levels. The graph shows the mean ± standard error of values derived from a number of individual experiments (shown in parenthesis on the x-axis). Values are given in the text (5.2 Results). Paired T-test analysis of the data are also shown.

** represents $p \leq 0.01$ for comparisons of carbachol-stimulated [^{35}S]GTPγS binding before and after PTX pretreatment, in each of the CHO cell clones.

† represents $p > 0.05$ for comparisons with basal levels of [^{35}S]GTPγS binding.

CHAPTER SIX.

CARBACHOL-STIMULATED INS(1,4,5)P_3 MASS ACCUMULATION IN CHO CELL CLONES EXPRESSING RECOMBINANT MUSCARINIC RECEPTOR SUBTYPES.

6.0. Introduction.

m1, m3 and m5 Muscarinic receptor activation predominantly leads to PLC activation leading to the generation of Ins(1,4,5)P_3 and DAG from PIP_2 (reviewed by Caulfield, 1993; Hulme *et al*, 1990; Richards, 1991). This PLC activation is thought to be mediated by G proteins of the $G_{q/11}$ family which are insensitive to PTX-catalyzed ADP-ribosylation (reviewed by Simon *et al*, 1991) acting on PLC-β isoforms (preferentially PLC-β_1) (Rhee and Choi, 1992; Smrcka *et al*, 1991; Taylor *et al*, 1991; Wu *et al*, 1992). Indeed, cloned m1 muscarinic receptors have been shown to activate PLC-β_1 in the presence of pure $G_{q/11}$, reconstituted in phospholipid vesicles (Berstein *et al*, 1992).

As well as $G_q\alpha$ subunits, βγ subunits have been found to activate PLC-β isoforms in the order of PLC-β_3 > PLC-β_2 > PLC-β_1 (Park *et al*, 1993). Furthermore, Gusovsky *et al*, (1993) have recently found that carbachol activation of m5 receptors, transfected in CHO cells, increased the tyrosine phosphorylation of PLC-γ and that a tyrosine kinase inhibitor partially reduced carbachol-evoked total inositol phosphates. Therefore, further study is required to obtain a clear understanding of the G proteins and the PLC isoforms involved in muscarinic receptor-mediated Ins(1,4,5)P_3 generation.

Many studies have measured PLC activity by measuring the accumulation of total inositol phosphates in cells, in the presence of lithium (Li^+). Li^+ (10 mM) uncompetitively blocks the monophosphatase enzymes which dephosphorylate the inositol monophosphates, thus preventing recycling of inositol into the lipids (Nahorski *et al*, 1991). The trapping of inositol monophosphates also acts as an amplification signal for measuring PLC activity. However, it is not known whether a fraction of the total inositol phosphates produced may be derived directly from phosphatidylinositol and/or phosphatidylinositol phosphate (PIP), via a possible Ca^{2+}-activation of PLC isoforms distinct from PLC-β. By measuring Ins(1,4,5)P_3 accumulation, phosphatidylinositol bisphosphate (PIP_2) hydrolysis can be directly measured.

m2 And m4 muscarinic receptors couple predominantly to the inhibition of adenylate cyclase via PTX-sensitive G proteins (G_i and possibly G_o) (Caulfield, 1993; Hulme *et al*, 1990; Matesic *et al*, 1991) but recombinant m2 receptors expressed in cloned cell lines have also been found to couple (though less efficiently) to PLC activation by a mechanism that can be inhibited by PTX-catalyzed ADP-ribosylation (Ashkenazi *et al*, 1987; Lai *et al*, 1991; Katz *et al*, 1992). It was difficult to determine from these studies whether the receptor-mediated PTX-sensitive PLC activation was due to the relatively high expression of m2 receptors in these cloned cell lines compared to expression levels in tissues, and whether the activation of PLC was via βγ subunits released from PTX-sensitive G proteins

or via "crosstalk" resulting from another PTX-sensitive G protein-mediated effector mechanism (*i.e.* inhibition of AC). Co-transfection of COS-7 cells with PLC-β_1 and $G\alpha_o$ did not increase inositol phosphate formation, which was in contrast to the co-transfection of COS-7 cells with PLC-β_1 and $G\alpha_q$ or $G\alpha_{11}$ (Wu *et al*, 1992). This suggests that the PTX-sensitive activation of PLC observed upon activation of m2 muscarinic receptors was unlikely to be due to direct interaction of $G\alpha_o$ with PLC-β_1.

Receptor-mediated PTX-sensitive PLC activation has also been observed in cells particularly of hematopoietic origin suggesting an involvement of PTX-sensitive G proteins in the activation of PLC (for references see Park *et al*, 1993). These cells tend to possess a large proportion of the PLC-β_2 isoform which is susceptible to $\beta\gamma$ stimulation.

In the present study, it was hoped to determine the nature of the G proteins that couple the different muscarinic receptors to PLC activation by measuring the agonist-mediated accumulation of Ins(1,4,5)P_3 in the intact CHO cell clones before and after PTX-pretreatment. In this way it was hoped that a possible functional significance could be applied to the proportion of PTX-sensitive agonist-stimulated [^{35}S]GTPγS binding observed in CHO cells expressing either m1 or m3 muscarinic receptors (see chapter 5). The study also hoped to elucidate any possible differences that may exist between Ins(1,4,5)P_3 production elicited by agonist stimulation of m1 and m3 muscarinic receptors expressed at similar receptor densities in CHO cells. It was also of interest to see how changes in the expression of m3 muscarinic receptors in CHO cells affected Ins(1,4,5)P_3 production.

6.1. Methods.

6.1.1. Experimental Procedure.

CHO cell clones were harvested as described in chapter 2 and resuspended in Krebs-HEPES buffer, pH 7.4 (see appendix 2). In experiments where permeabilized cells were used, cells were electroporated as described in chapter 2 and resuspended in cytosol-like buffer (see appendix 1). Cell suspensions were then incubated in a waterbath at 37 °C (for intact cell experiments) or at room temperature (for permeabilized cell experiments, allowing comparison with $^{45}Ca^{2+}$ release studies (see chapter 7)), for 30 min, to allow basal Ins(1,4,5)P_3 levels to settle; basal levels of Ins(1,4,5)P_3 tended to increase in cells during the harvesting procedure. 90 µl of cells in suspension were added (at time zero) to tubes containing 10 µl of either buffer or carbachol, at either 37 °C (intact cells) or room temperature (permeabilized cells). In some cases, cells were pretreated with PTX by adding 100 ng / ml PTX to the growth media of cells, for 20 hr prior to cell harvesting. Reactions were terminated by the addition of 100 µl of (1M) Trichloro-acetic acid (TCA).

TCA lyzed the cells, denatured proteins and reduced the pH to a level where no further enzyme activity could take place. Samples were then kept on ice for a short period (approximately 1 hr) before being prepared for the binding assay, described later. At this stage, 100 µl of (1 M) TCA was also added to 90 µl aliquots of cell suspensions. These aliquots were then centrifuged at 11 000 rpm for 4 min, at room temperature, and the subsequent pellets were each resuspended in 100 µl of (0.1 M) NaOH and left overnight at 4 °C. The following day, protein assays were performed (see chapter 2) to deduce the protein concentration / tube for each sample.

6.1.2. Sample Preparation.

Samples generated from experiments were centrifuged at 11 000 rpm for 4 min and 160 µl of supernatant was removed and added to tubes containing 40 µl of (10 mM) EDTA and 200 µl of a mixture of 1,1,2-Trichlorotrifluoroethane (Freon) and Tri-n-octylamine (1:1). The EDTA sequestered free Ca^{2+} from the samples which would otherwise inhibit the binding of Ins(1,4,5)P_3 (generated from the samples) to the Ins(1,4,5)P_3 binding protein in the binding assay. EDTA also enhanced the separation of the phases, after addition of Freon / Tri-n-octylamine. The Freon / Tri-n-octylamine was used to extract the TCA from the samples. The resulting mixture was vortex mixed and left for 15 min before being centrifuged at 11 000 rpm for 4 min. This resulted in the separation of two phases; the lower phase consisted of the Freon / Tri-n-octylamine plus the extracted TCA; the upper phase consisted of the water soluble fraction containing inositol phosphates. 100 µl of the upper phase was removed from each sample and added to tubes containing 50 µl of (25 mM) $NaHCO_3$ which corrected the pH of the sample to pH 7.8. This pH was optimal for the Ins(1,4,5)P_3 binding assay. The prepared samples were then kept at 4 °C until Ins(1,4,5)P_3 binding assays were performed.

6.1.3. Preparation of Standards.

Unlabelled D-myo inositol (1,4,5) trisphosphate (Ins(1,4,5)P_3) was diluted in buffer that had been extracted in the same way as the samples prepared in **6.1.2** above. A range of concentrations of Ins(1,4,5)P_3 were created from 1200 nM down to 1.2 nM. Non-specific binding was determined in the presence of 10 000 nM unlabelled Ins(1,4,5)P_3. A four-fold dilution of these standards in the final assay volume resulted in a range of concentrations from 300 nM (36 pmol / tube) to 0.3 nM (0.036 pmol / tube) being produced.

6.1.4. Preparation of Ins(1,4,5)P_3 Binding Protein from Bovine Adrenal Cortical Membranes.

8-10 Bovine adrenal glands were collected fresh from the abattoir and placed on large petri dishes, on ice. They were then dampened with preparation buffer consisting of 1.68 g / l $NaHCO_3$, 0.15 g / l dithiothreitol (DTT) made up in ice-cold distilled water with the pH adjusted to 8.0 with concentrated hydrochloric acid (HCl). Fat and connective tissue were removed from the glands which were then halved, demedullated and the cortex scraped into a pre-weighed beaker on ice. 8-10 Bovine adrenal glands produced approximately 60-80 g of scraped cortex which was then homogenised in preparation buffer using a Polytron tissue disrupter (level 6 for 10 x 5 s bursts). The homogenate was then spun in a refrigerated centrifuge at 3000 g for 10 min at 4 °C. The supernatant was removed and kept while the pellet was rehomogenized and respun at 3000 g for 10 min at 4 °C. The supernatant was removed and combined with the previous supernatant and spun at 38 000 g for 20 min at 4 °C. This time the pellet was kept, resuspended in preparation buffer and respun at 38 000 g for 10 min at 4 °C. The pellet was then resuspended in 60 ml of preparation buffer and a protein assay was performed (see chapter 2). Ins(1,4,5)P_3 binding protein was then diluted to 15-18 mg / ml, aliquoted and stored at -20 °C until required.

6.1.5. Ins(1,4,5)P_3 Binding Assay.

The Ins(1,4,5)P_3 binding assay (Challiss *et al*, 1990) is a competition assay between a single concentration of radiolabelled Ins(1,4,5)P_3 and concentrations of unlabelled Ins(1,4,5)P_3 generated in the samples or present in the standards. Both radiolabelled and unlabelled Ins(1,4,5)P_3 compete for Ins(1,4,5)P_3 receptors present in the Ins(1,4,5)P_3 binding protein. Bound and free radioligand can then be separated by filtration. A competition curve can be constructed using the range of standards against a single concentration of radiolabelled Ins(1,4,5)P_3. Radioactivity bound in the presence of samples can be converted using this curve to give a concentration of Ins(1,4,5)P_3 generated by each sample.

Each assay tube contained 30 µl of standard / sample, 30 µl of Tris (100 mM)/ EDTA (4 mM), pH 8.0 and 30 µl of [^{3}H]Ins(1,4,5)P_3 (approximately 0.8 nM final concentration) (specific activity 34 Ci / mmol) (made up in distilled water). Tris / EDTA was used to sequester free Ca^{2+} from the assay mixture thus preventing inhibition of Ins(1,4,5)P_3 binding to the Ins(1,4,5)P_3 receptors found in the binding protein. Incubations were started at 4 °C by the addition of 30 µl of Ins(1,4,5)P_3 binding protein. Incubations were carried out for one hr at 4 °C before being terminated by filtration.

GF/B filters were dampened with ice-cold wash buffer consisting of 3.03 g / l TRIS base, 0.4 g / l $NaHCO_3$ and 0.37 g / l EDTA, pH 7.8. The wash buffer composition was

identical to that of the assay mixture. 4 ml of ice-cold wash buffer was added to each assay tube and the contents of each tube was then filtered rapidly. Filters were then transferred to 4 ml of scintillation cocktail (Optiphase X) and left for at least 12 hours before being counted for radioactivity by liquid scintillation spectrometry.

6.1.6. Data Analysis.

A standard curve was constructed from the DPM given for the standard data (see appendix 4) and sample Ins(1,4,5)P_3 accumulation (in DPM) was converted to pmol / tube from the standard curve. Ins(1,4,5)P_3 mass was then converted to pmol / mg protein using the protein concentrations deduced from protein assays. This value was then multiplied by the dilution factor (12.5) which resulted from preparation of the samples, to give the concentration of Ins(1,4,5)P_3 generated in the experiments. Carbachol dose-response curves were analysed by GraphPAD INPLOT (GraphPAD Software Inc., San Diego, CA) to give EC_{50} values and statistical significance was set at $p \leq 0.05$ by unpaired T-test analysis.

6.2. Results.

CHO-m2 Cells.

Incubation of CHO-m2 cell suspensions with 1 mM carbachol for periods up to 20 min did not produce any significant increase in Ins(1,4,5)P_3 accumulation above basal levels, which were maintained at approximately 50 pmol / mg protein (Figure 6.2.1.).

Time Course Profiles for Carbachol-Stimulated Ins(1,4,5)P_3 Accumulation in CHO-m1, CHO-m3 and CHO-vt9 Cell Clones.

Incubation of CHO-m1, CHO-m3 and CHO-vt9 cell suspensions with 1 mM carbachol produced similar profiles of Ins(1,4,5)P_3 accumulation over a 20 min period. The profile consisted of a rapid elevation in Ins(1,4,5)P_3 accumulation reaching a peak at approximately 10 s after the incubation of cells with 1 mM carbachol. This peak response was short-lived, returning to a plateau phase of Ins(1,4,5)P_3 accumulation after approximately 1 min of incubation with carbachol. This plateau phase of Ins(1,4,5)P_3 accumulation was significantly greater than basal Ins(1,4,5)P_3 accumulation for at least 19 min, in the continued presence of carbachol.

Stimulation of m1 muscarinic receptors in CHO-m1 cells with 10 μM and 1 mM carbachol, resulted in a peak accumulation of Ins(1,4,5)P_3 at 10 s of 327 ± 7 pmol / mg

protein and 593 ± 84 pmol / mg protein, respectively (Figure 6.2.2). At the 20 s time point, 1 mM carbachol-stimulated Ins(1,4,5)P_3 accumulation was significantly reduced compared with the 10 s time point. However, at the 20 s time point, Ins(1,4,5)P_3 accumulation induced by 1 mM and 10 μM carbachol, were not significantly different, being 286 ± 19 and 294 ± 32 pmol / mg protein, respectively (Figure 6.2.2). Ins(1,4,5)P_3 accumulation after 10 min incubation, corresponding to the plateau phase of Ins(1,4,5) accumulation, was 170 ± 10 pmol / mg protein and 215 ± 50 pmol / mg protein in the presence of 10 μM and 1 mM carbachol, respectively. Basal levels of Ins(1,4,5)P_3 accumulation decreased marginally over a 20 min period from 54 ± 12 pmol / mg protein to 33 ± 6 pmol / mg protein.

Stimulation of m3 muscarinic receptors expressed in CHO-m3 cells with 10 μM and 1 mM carbachol, for 10 s, resulted in a peak accumulation of Ins(1,4,5)P_3 which was not significantly different, the values being 494 ± 58 pmol / mg protein and 555 ± 52 pmol / mg protein, respectively (Figure 6.2.3.). The plateau phase of Ins(1,4,5)P_3 accumulation, after 10 min incubation with 10 μM and 1 mM carbachol, was 133 ± 8 pmol / mg protein and 168 ± 18 pmol / mg protein, respectively. Basal levels of Ins(1,4,5)P_3 decreased marginally over a 20 min period from 39 ± 5 pmol / mg protein to 28 ± 2 pmol / mg protein.

Stimulation of m3 muscarinic receptors expressed in CHO-vt9 cells with 1 mM carbachol resulted in a peak accumulation of Ins(1,4,5)P_3, at 10 s, of 252 ± 44 pmol / mg protein (Figure 6.2.4.). This peak response was significantly lower than that seen in CHO-m3 cell suspensions. At the 20 s time point, 1 mM carbachol-stimulated Ins(1,4,5)P_3 accumulation (238 ± 55 pmol / mg protein) was not significantly different to the accumulation obtained at the 10 s time point. In CHO-m1 and CHO-m3 cells, 1 mM carbachol-stimulated Ins(1,4,5)P_3 accumulation, at the 20 s time point, was significantly reduced compared with their respective 10 s time point values. 10 μM carbachol did not produce a significantly higher Ins(1,4,5)P_3 accumulation at 10 s (87 ± 26 pmol / mg protein) than it did at 10 min (55 ± 14 pmol / mg protein) in CHO-vt9 cells. At 10 min, 1 mM carbachol produced a plateau phase of Ins(1,4,5)P_3 accumulation of 109 ± 32 pmol / mg protein in CHO-vt9 cells. Basal levels of Ins(1,4,5)P_3 in CHO-vt9 cells decreased marginally over a 20 min period from 80 ± 5 pmol / mg protein to 39 ± 10 pmol / mg protein.

Dose-Response Relationships for Carbachol-Stimulated Ins(1,4,5)P_3 Accumulation in CHO-m1, CHO-m3 and CHO-vt9 Cell Clones.

Before carbachol dose-response curves could be performed at exact time points, before and after PTX pretreatment, it was necessary to determine whether PTX pretreatment affected the Ins(1,4,5)P_3 mass accumulation profile. Time course studies in the presence of 1 mM carbachol, in PTX pretreated CHO-m1 and CHO-m3 cells resulted in an identical profile of peak and plateau Ins(1,4,5)P_3 accumulation compared with untreated cells (Figure 6.2.5.).

Carbachol dose response curves were performed in CHO-m1, CHO-m3 and CHO-vt9 cell suspensions at 10 s and at 10 min incubation with increasing concentrations of carbachol, in the presence and absence of PTX pretreatment. Maximal, carbachol-stimulated Ins(1,4,5)P_3 mass accumulation was significantly greater ($p \leq 0.05$, by unpaired T-test analysis) at 10 s than at 10 min, in each of the cell lines. These time points correspond with the peak and plateau phases of carbachol-stimulated Ins(1,4,5)P_3 accumulation, respectively. Basal levels of Ins(1,4,5)P_3 were marginally greater at 10 s than at 10 min. This was probably due to minor Ins(1,4,5)P_3 formation, caused by turbulence, on addition of the cell suspensions to the incubation tubes. Pretreatment of the CHO cell clones with PTX had no significant affect on basal or carbachol-stimulated Ins(1,4,5)P_3 accumulation in CHO-m1 (Figure 6.2.6 and Table 6.2.1), CHO-m3 (Figure 6.2.7 and Table 6.2.2) or CHO-vt9 (Figure 6.2.8 and Table 6.2.3) cell suspensions.

At 10 s incubation, maximal carbachol-stimulated Ins(1,4,5)P_3 accumulation was 384 $\pm$ 40 pmol / mg protein and 430 $\pm$ 30 pmol / mg protein in CHO-m1 and CHO-m3 cell suspensions, respectively. Maximal, carbachol stimulation of m3 muscarinic receptors, expressed in CHO-vt9 cell suspensions, produced significantly lower levels of Ins(1,4,5)P_3 accumulation (224 $\pm$ 32 pmol / mg protein) at 10 s, compared with CHO-m1 and CHO-m3 cell suspensions. After 10 min incubation with carbachol, maximal Ins(1,4,5)P_3 responses were reduced by 50 % and 65-70 % of values seen at 10 s in CHO-m1 and CHO-m3 cell suspensions, respectively. However, maximal responses at 10 min were not significantly different in CHO-m1 cells (196 $\pm$ 33 pmol / mg protein) compared with CHO-m3 cells (153 $\pm$ 33 pmol / mg protein) due to the relatively large experimental error.

Maximal Ins(1,4,5)P_3 responses in CHO-vt9 cells at 10 min incubation with carbachol (124 $\pm$ 25 pmol / mg protein) were not significantly different to those seen in CHO-m3 cells. This is in contrast to the 10 s time point, where maximal carbachol-stimulated Ins(1,4,5)P_3 accumulation in CHO-vt9 cells, was approximately 50 % of the maximal carbachol-stimulated Ins(1,4,5)P_3 accumulation produced in CHO-m3 cells. However, it should be noted that basal levels of Ins(1,4,5)P_3 formation at 10 min, in CHO-vt9 cell

suspensions were approximately 20 pmol / mg protein higher than the basal levels of $Ins(1,4,5)P_3$ formation observed in CHO-m3 cell suspensions, at the same time point.

Comparisons of Carbachol Potency to Elicit $Ins(1,4,5)P_3$ Accumulation in CHO-m1, CHO-m3 and CHO-vt9 Cell Clones.

The potency of carbachol to stimulate $Ins(1,4,5)P_3$ accumulation, in CHO-m1 cell suspensions, was increased approximately 2.8-fold at 10 min (EC_{50} (log M) -5.60 ± 0.12 , n=4), compared with 10 s incubations (-5.16 ± 0.06, n=4). The potency of carbachol to stimulate $Ins(1,4,5)P_3$ accumulation in CHO-m3 cell suspensions, was not significantly different at 10 s (EC_{50} (log M) -5.58 ± 0.12, n=4) or 10 min (-5.80 ± 0.15, n=4). Carbachol was marginally more potent (approximately 2.6-fold) at stimulating $Ins(1,4,5)P_3$ accumulation in CHO-m3 cell suspensions compared to CHO-m1 cell suspensions at the 10 s time point. The potency of carbachol to stimulate $Ins(1,4,5)P_3$ accumulation in CHO-vt9 cell suspensions at 10 s (EC_{50} (log M) -4.49 ± 0.05, n=4) and at 10 min (-5.05 ± 0.18, n=4) was significantly reduced compared with the potency of carbachol to stimulate $Ins(1,4,5)P_3$ accumulation in CHO-m3 cell suspensions.

In the absence of PTX-pretreatment, EC_{50} (log M) values for carbachol-stimulated $Ins(1,4,5)P_3$ accumulation were approximately 3.6-fold lower at 10 min than at 10 s in CHO-vt9 cell suspensions. After PTX pretreatment, EC_{50} values at the different time points were no longer significantly different. The differences in EC_{50}, in the absence of PTX may be partly explained by the relatively small responses observed in CHO-vt9 cell suspensions after 10 min incubation with carbachol, and hence the large error in determining an EC_{50} value.

Carbachol-Stimulated $Ins(1,4,5)P_3$ Accumulation in Permeabilized CHO-m1 Cells.

Carbachol-stimulated $Ins(1,4,5)P_3$ accumulation was also investigated in CHO-m1 cell suspensions that had been electrically permeabilized in a cytosol-like buffer (see 6.1 Methods) which was also used in chapter 7 to investigate $Ins(1,4,5)P_3$ and carbachol-stimulated $^{45}Ca^{2+}$ mobilization. Peak carbachol-stimulated accumulation of $Ins(1,4,5)P_3$ was achieved at approximately 30 s (189 ± 54 pmol / mg protein, n=3 and 144 ± 25 pmol / mg protein, n=3, with 1 mM and 10 μM carbachol, respectively) followed by a more gradual attenuation of $Ins(1,4,5)P_3$ accumulation than that seen in intact CHO-m1 cell suspensions (Figure 6.2.9.a). In the continued presence of carbachol, $Ins(1,4,5)P_3$ formation was still significantly above basal levels after 20 min incubation (44 ± 19 pmol / mg protein and 28 ± 4 pmol / mg protein, with 1 mM and 10 μM carbachol, respectively, compared with basal levels of 13 ± 2 pmol / mg protein, n's=3). PTX-pretreatment of

CHO-m1 cells did not affect the profile of carbachol-stimulated Ins(1,4,5)P_3 formation in electroporated CHO-m1 cell suspensions (Figure 6.2.9.b).

Carbachol dose-response curves were constructed at the 30 s time point (Figure 6.2.10) and showed a maximal response of 120 ± 5 pmol / mg protein, from basal levels of 28 ± 7 pmol / mg protein (n's=3). Carbachol-stimulated Ins(1,4,5)P_3 accumulation at a 30 s incubation period was not significantly different in permeabilized CHO-m1 cells and PTX-pretreated, permeabilized CHO-m1 cells. Carbachol, at 30 s incubation, stimulated Ins(1,4,5)P_3 formation in permeabilized CHO-m1 cell suspensions with an EC_{50} (log M) value of -5.46 ± 0.14, which was very similar to the EC_{50} values obtained for carbachol-stimulated Ins(1,4,5)P_3 formation in intact CHO-m1 cell suspensions (either at 10 s or 10 min).

6.3. Discussion.

The results of the present study show that m2 muscarinic receptors expressed in CHO cells at a density of approximately 100 fmol / mg protein did not significantly activate PLC in the presence of carbachol. Studies where m2 receptor activation has led to PLC activation were generally carried out using high expression levels of the m2 receptor in cloned cell lines (Ashkenazi *et al*, 1987; Lai *et al*, 1991; Katz *et al*, 1992). Similarly, 5-HT_{1A} receptor stimulation can also lead to inhibition of AC and activation of PLC at high levels of expression, both via a PTX-sensitive mechanism (Raymond *et al*, 1992). At higher levels of receptor expression in CHO cells, a weak coupling of m2 muscarinic receptors to PLC activation may become more apparent, perhaps by increasing the amount of free $\beta\gamma$ subunits available to interact with PLC-β_2 or PLC-β_3.

The time course profile of Ins(1,4,5)P_3 accumulation induced by carbachol stimulation of m1 and m3 muscarinic receptors in CHO cells, was similar to the profile of carbachol-stimulated Ins(1,4,5)P_3 accumulation observed in intact SH-SY5Y cells (Lambert *et al*, 1991), and in rat cerebellar granule cells (Whitham *et al*, 1991) both of which are thought to express an endogenous population of M_3 receptors. Similar profiles of carbachol-stimulated Ins(1,4,5)P_3 generation have also been observed in CHO-m3 cells (Tobin *et al*, 1992).

The initial rapid accumulation of Ins(1,4,5)P_3 is thought to be responsible for the rapid release of Ca^{2+} from intracellular stores via Ins(1,4,5)P_3 receptors which possess an intrinsic Ca^{2+} channel (for reviews see Berridge and Irvine, 1989; Berridge, 1993; Putney and Bird, 1993).

The plateau phase of Ins(1,4,5)P_3 accumulation observed in many cell types is less well understood. The plateau phase of Ins(1,4,5)P_3 accumulation appears to mirror an often present plateau elevation of intracellular free Ca^{2+} levels upon agonist stimulation.

This plateau elevation in intracellular free Ca^{2+} is thought to be mediated by Ca^{2+} entry across the plasma membrane, a process that can be mimicked by injection of $Ins(1,4,5)P_3$ into cells and completely blocked by the presence of the $Ins(1,4,5)P_3$ receptor antagonist heparin (Putney and Bird, 1993; Bird *et al*, 1992).In other studies Ca^{2+} entry required the presence of both $Ins(1,4,5)P_3$ and $Ins(1,3,4,5)P_4$ (Morris *et al*, 1987) leading to the notion that $Ins(1,3,4,5)P_4$ also plays a significant role in Ca^{2+} entry (Irvine, 1992). The plateau elevation in intracellular free Ca^{2+} can be blocked by removing extracellular free Ca^{2+} with EGTA (Meldolesi *et al*, 1991; Wojcikiewicz and Nahorski, 1993). The carbachol-mediated plateau phase of $Ins(1,4,5)P_3$ accumulation in SH-SY5Y cells and in CHO-m3 cells also appears to be partially inhibited in the absence of extracellular Ca^{2+}, suggesting a Ca^{2+}-regulation of PLC activation via a Ca^{2+} entry mechanism (Lambert *et al*, 1991; Wojcikiewicz *et al*, 1994).

A possible mechanism for the presence of two distinct phases of agonist-mediated $Ins(1,4,5)P_3$ accumulation has come to light using the CHO-m3 cell clones.

Total inositol phosphate accumulation in CHO-m3 cells in response to carbachol is also biphasic, the initial rate of accumulation (over the first 10 s) being approximately 15 times greater than the latter rate (between 30-300 s) (Wojcikiewicz *et al*, 1993; 1994). This response is mirrored in CHO-m3 cells by a biphasic PIP_2 hydrolysis and the corresponding biphasic $Ins(1,4,5)P_3$ generation. The peak phase of $Ins(1,4,5)P_3$ generation can be desensitized by a 5 min pre-incubation with carbachol, a desensitization event that has no significant effect on the plateau phase of carbachol-stimulated $Ins(1,4,5)P_3$ generation (Tobin *et al*, 1992). This evidence suggested that the biphasic nature of m3 muscarinic receptor-mediated PLC activation was a result of a rapid, partial desensitization event occurring after about 10 s. Such a desensitization event may result if PIP_2 levels were rapidly depleted so that PLC activity could not be maintained at its initial level due to lack of substrate. More recently, a rapid phosphorylation of the m3 muscarinic receptors in CHO cells has been observed in response to carbachol with a time course that apparently mimics that of the desensitization event (Tobin and Nahorski, 1993; Tobin *et al*, 1993). This agonist-dependent phosphorylation appears to occur via a serine kinase distinct from PKA, Ca^{2+}-calmodulin-dependent protein kinase and PKC, and may, therefore, be a member of the rapidly growing family of G-protein-linked receptor kinases. Whether the rapid, partial desensitization of the m3 muscarinic receptor-mediated PLC activation in CHO cells results from a rapid phosphorylation of the m3 receptor in response to carbachol remains to be established. Whatever the mechanism, it would follow that the m1 muscarinic receptor-mediated stimulation of PLC activity is regulated in a similar manner, as the biphasic nature of $Ins(1,4,5)P_3$ accumulation was also apparent in the CHO-m1 cells in the present study.

Carbachol-stimulated Ins(1,4,5)P_3 accumulation in CHO-m1, CHO-m3 and CHO-vt9 cells was unaffected by pretreatment of the cells with a maximally effective concentration of PTX, suggesting that PTX-sensitive G proteins coupled to m1 or m3 muscarinic receptors (see chapter 5) played no functional role in receptor-mediated PLC activation in CHO cells.

The PTX-insensitive stimulation of PLC activity mediated via m1 and m3 muscarinic receptors is strongly suspected to be coupled via G proteins of the $G_{q/11}$ family, whose expression in CHO cells has been shown to be down-regulated by several hours of agonist stimulation of m1 muscarinic receptors (Mullaney *et al*, 1993). In SH-SY5Y cells (which express endogenous M_3 muscarinic receptors), carbachol-stimulated total inositol phosphate generation and intracellular free Ca^{2+} levels were also unaffected by PTX pretreatment (Lambert and Nahorski, 1990c).

Carbachol-stimulated Ins(1,4,5)P_3 accumulation in CHO-m1 cells was maintained in permeabilized CHO-m1 cells suspended in a cytosol-like buffer. Although the time course profile of carbachol-stimulated Ins(1,4,5)P_3 accumulation was different in the permeabilized cell preparation compared with intact cells, and the maximal, carbachol-induced stimulation of Ins(1,4,5)P_3 accumulation was reduced by approximately 60-70 %, the potency of carbachol to elicit PLC activation was largely unaffected. This suggests that electroporation of CHO cells in a cytosol-like buffer, where Ca^{2+} was buffered to levels of approximately 100 nM, did not prevent receptor-mediated PLC activation.

Addition of guanine nucleotides to the cytosol-like buffer may have increased the responsiveness of electroporated CHO-m1 cells to receptor activation by increasing the maximal response and/or shifting the carbachol dose-response curve to the left, as has been observed in permeabilized SH-SY5Y cells (Wojcikiewicz *et al*, 1990; Safrany and Nahorski, 1994). However, in the present study, the EC_{50} for carbachol-induced Ins(1,4,5)P_3 accumulation was similar between intact CHO-m1 cells and permeabilized CHO-m1 cells, suggesting that the guanine nucleotide content of permeabilized CHO-m1 cells was adequate to maintain effective receptor-G protein-mediated stimulation of PLC. The reduced maximal response to carbachol, in permeabilized CHO-m1 cells may have been due to a reduction in the intrinsic activity of PLC under these assay conditions (particularly the reduction in Ca^{2+} concentration) compared to in intact cells, or an increased rate of metabolism of the generated Ins(1,4,5)P_3. Receptor-G protein coupling may also have been affected by the experimental conditions, but it might be expected that this would have produced a shift in the EC_{50} value for the carbachol-stimulated response.

CHO cell clones expressing either m1 or m3 muscarinic receptors at similar receptor densities (1-2 pmol / mg protein, see chapter 3) produced very similar carbachol-stimulated Ins(1,4,5)P_3 accumulation dose-response curves at both peak and plateau

phases of Ins(1,4,5)P_3 formation. The small potency difference between the peak phases of carbachol-stimulated Ins(1,4,5)P_3 accumulation in CHO-m1 and CHO-m3 cells correlate with the small differences in carbachol affinity for the low affinity state of m1, compared with m3 muscarinic receptors, expressed in CHO-m1 and CHO-m3 cell membranes, respectively (see Chapter 4). Carbachol had a slightly higher affinity for m3 muscarinic receptors and has a slightly higher potency for Ins(1,4,5)P_3 accumulation, in CHO-m3 cells, compared with m1 muscarinic receptors in CHO-m1 cells. The carbachol potency difference between m1 and m3 muscarinic receptors, therefore, also explains the time course responses obtained in CHO-m3 cells compared with CHO-m1 cells, in response to 10 μM carbachol. Whereas 10 μM carbachol produced maximal responses in CHO-m3 cells, the same concentration of carbachol produced sub-maximal responses in CHO-m1 cells.

These results are similar to those obtained by a number of other groups, in CHO cells, which showed a 2 to 3-fold selectivity of carbachol for m3 muscarinic receptors compared with m1 muscarinic receptors (Hu *et al*, 1991; Schwarz *et al*, 1993; Richards, 1991. However, Buck and Fraser (1990) observed a 17-fold higher affinity of carbachol for m3 muscarinic receptors compared with m1 muscarinic receptors, in [^{3}H]QNB displacement experiments. All of these other studies assessed PLC activity by measuring total inositol phosphate accumulation in the presence of Li^+. Hu *et al* (1991) found that the 2 to 3-fold affinity difference between m1 and m3 muscarinic receptors, in CHO cells, correlated with a 2 to 3-fold higher potency of carbachol for stimulating total inositol phosphate generation in CHO cells expressing m3 muscarinic receptors, compared to m1 muscarinic receptors, expressed at similar densities. The maximal responses to carbachol were not significantly different between CHO cells expressing m1 or m3 receptors (Hu *et al*, 1991). Therefore, the present study, although using a different method for measuring PLC activity, produced very similar results to those described by Hu *et al* (1991), in terms of comparisons of carbachol affinity and potency of PLC activation, between m1 and m3 muscarinic receptors expressed in CHO cells, at similar receptor densities. Buck and Fraser (1990), however, found that carbachol stimulation of m1 muscarinic receptors in CHO cells, produced a maximal total inositol phosphate response which was twice that observed in CHO cells expressing m3 muscarinic receptors, when expressed at similar receptor densities. They suggested, therefore, that m1 muscarinic receptors coupled more efficiently to PLC activation than did m3 muscarinic receptors (Buck and Fraser, 1990). In the present study, no such differences between m1 and m3 receptor-stimulation was observed suggesting that both m1 and m3 muscarinic receptor subtypes couple with the same efficiency to PLC activation.

In the present study the plateau phase of Ins(1,4,5)P_3 accumulation was approximately

52 % of the peak carbachol-stimulated Ins(1,4,5)P_3 response in CHO-m1 cells, whereas the plateau phase of Ins(1,4,5)P_3 accumulation was approximately 35 % of the peak carbachol-stimulated Ins(1,4,5)P_3 response in CHO-m3 cells. Although not statistically significant, the trend suggests that at comparable receptor densities, m1 muscarinic receptors may produce a larger response than m3 muscarinic receptors during the sustained phase of carbachol-stimulated Ins(1,4,5)P_3 accumulation. Whether this trend reflects a difference in the sensitivity of m1 and m3 muscarinic receptors to be desensitized may become apparent in the near future.

CHO-vt9 cells and CHO-m3 cells expressed m3 muscarinic receptors at a density of 300-400 fmol / mg protein and 1-2 pmol / mg protein, respectively (see chapter 3). Both the maximal Ins(1,4,5)P_3 accumulation response to carbachol at 10 s, and the potency of the response to carbachol were reduced in CHO-vt9 cells compared with CHO-m3 cells suggesting that the receptor number in CHO-vt9 cells was reduced below a threshold required to maintain the response observed in CHO-m3 cells. Therefore, by manipulating receptor number, carbachol appeared to act as a partial agonist in CHO-vt9 cells and as a full agonist in CHO-m3 cells, in terms of mediating the peak phase of Ins(1,4,5)P_3 accumulation.

The effect of changes in m3 muscarinic receptor expression in CHO cells on the plateau phase of carbachol-stimulated Ins(1,4,5)P_3 accumulation was less clear. The relatively large standard error values for the carbachol-mediated plateau phase of Ins(1,4,5)P_3 accumulation and the differences in the basal levels of Ins(1,4,5)P_3 accumulation between CHO-m3 and CHO-vt9 cells, makes a quantitative assessment of the changes in carbachol-mediated plateau phase Ins(1,4,5)P_3 accumulation difficult.

The potency of the Ins(1,4,5)P_3 mass response to carbachol in CHO-vt9 cells was reduced compared to CHO-m3 cells. However, the maximal plateau response to carbachol appeared not to be significantly reduced in CHO-vt9 cells compared with CHO-m3 cells. This suggests that the threshold number of m3 muscarinic receptors required to activate the maximal plateau phase of Ins(1,4,5)P_3 generation in CHO cells may be less than that required to produce the maximal peak phase of Ins(1,4,5)P_3 generation. Speculatively, these result might be explained if the agonist-mediated desensitization of PLC activation was also affected by the expression levels of m3 muscarinic receptors present.

Hypothetically, carbachol stimulation of m3 muscarinic receptors in CHO m3 cells should result in a greater activation of G proteins (as observed in chapter 5) resulting in the production of greater concentrations of free $\beta\gamma$ subunits than in CHO-vt9 cells which express fewer m3 muscarinic receptors. $\beta\gamma$ subunits are thought to be essential for co-ordinating the phosphorylation of m2 muscarinic receptors following agonist stimulation (Kameyama *et al*, 1993). It is not yet known whether $\beta\gamma$ subunits are required to mediate phosphorylation of the other muscarinic receptor subtypes. If this is indeed the case then

phosphorylation of the m3 muscarinic receptors in CHO-vt9 cells might be expected to be less than that seen in CHO-m3 cells. This theory can be extended to suggest that the partial desensitization event in CHO-vt9 cells may be less than that observed in CHO-m3 cells. This might explain the lack of affect of reducing m3 muscarinic receptor expression on the plateau phase of $Ins(1,4,5)P_3$ accumulation compared with the 50 % reduction observed during the peak phase of $Ins(1,4,5)P_3$ accumulation.

The different expression levels of m3 muscarinic receptors in CHO-vt9 and CHO-m3 cells might also be expected to produce differences in $Ins(1,4,5)P_3$ accumulation, if PIP_2 depletion was thought to be involved in the generation of two phases of carbachol-stimulated $Ins(1,4,5)P_3$ accumulation. In this way, lowering m3 muscarinic receptor expression would act in a similar manner to reducing the concentration of carbachol used. By reducing either receptor expression or carbachol concentration, it might be expected that PLC activation would also be reduced, therefore, PIP_2 levels would be depleted at a slower rate. If PIP_2 depletion leads to reduced PLC activity due to substrate depletion, then the initial phase of receptor-mediated $Ins(1,4,5)P_3$ accumulation would be expected to last for a longer time in a system where fewer receptors are expressed, or where lower concentrations of the agonist are used. Experiments need to be conducted in detail to assess this possibility, but the present study does suggest that lower levels of receptor expression (*i.e.* CHO-vt9 cells), or reduced concentrations of the agonist carbachol, may prolong the initial phase of $Ins(1,4,5)P_3$ accumulation in CHO cells, when the 10 s and 20 s time points, from time course studies, were compared.

Above all, the present study shows that comparisons of second messenger responses between different receptor subtypes must be carried out, not only in the same cell line, but also at comparable receptor densities. Apparent differences in agonist-mediated responses between different receptor subtypes in the same cell may be a consequence of differential receptor expression rather than actual differences in the subtype of receptor expressed.

Figure 6.2.1. Time course of carbachol-stimulated $Ins(1,4,5)P_3$ accumulation in CHO-m2 cell suspensions.

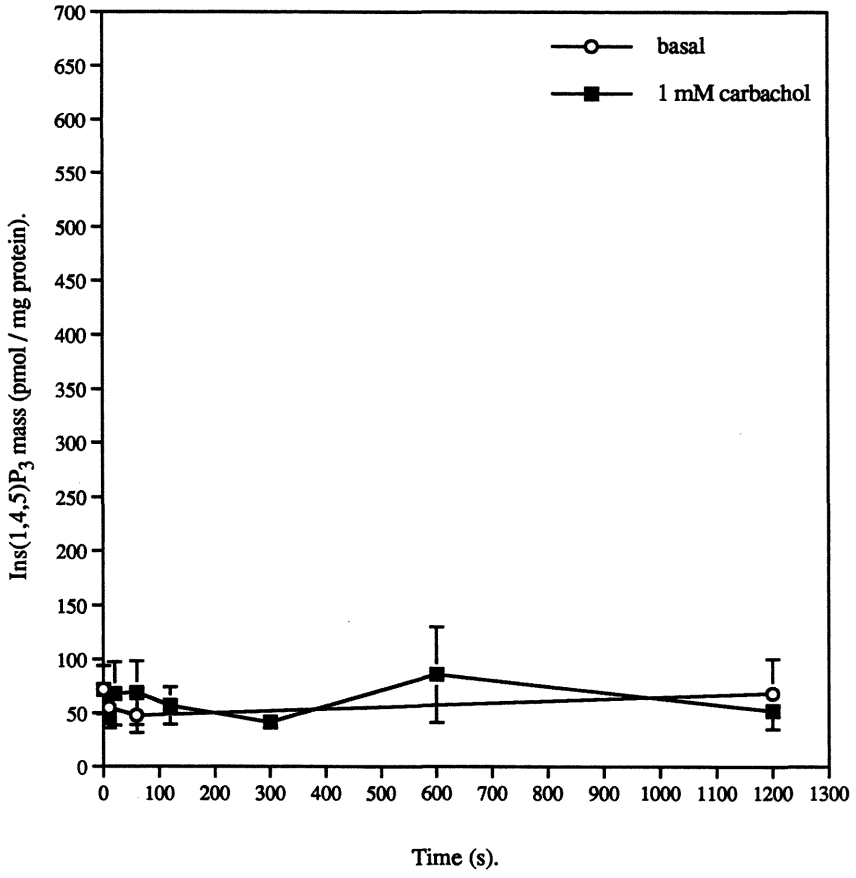

CHO-m2 cell suspensions were incubated with 1 mM carbachol in a waterbath at 37 °C in Krebs / HEPES buffer, pH 7.4. Incubations were terminated by the addition of 1 M TCA. Sample preparation and $Ins(1,4,5)P_3$ binding assays were performed as described in 6.1 Methods. The graph shows mean ± standard error values of 3 independent experiments.

Figure 6.2.2. Time course for carbachol-stimulated Ins(1,4,5)P_3 accumulation in CHO-m1 cell suspensions.

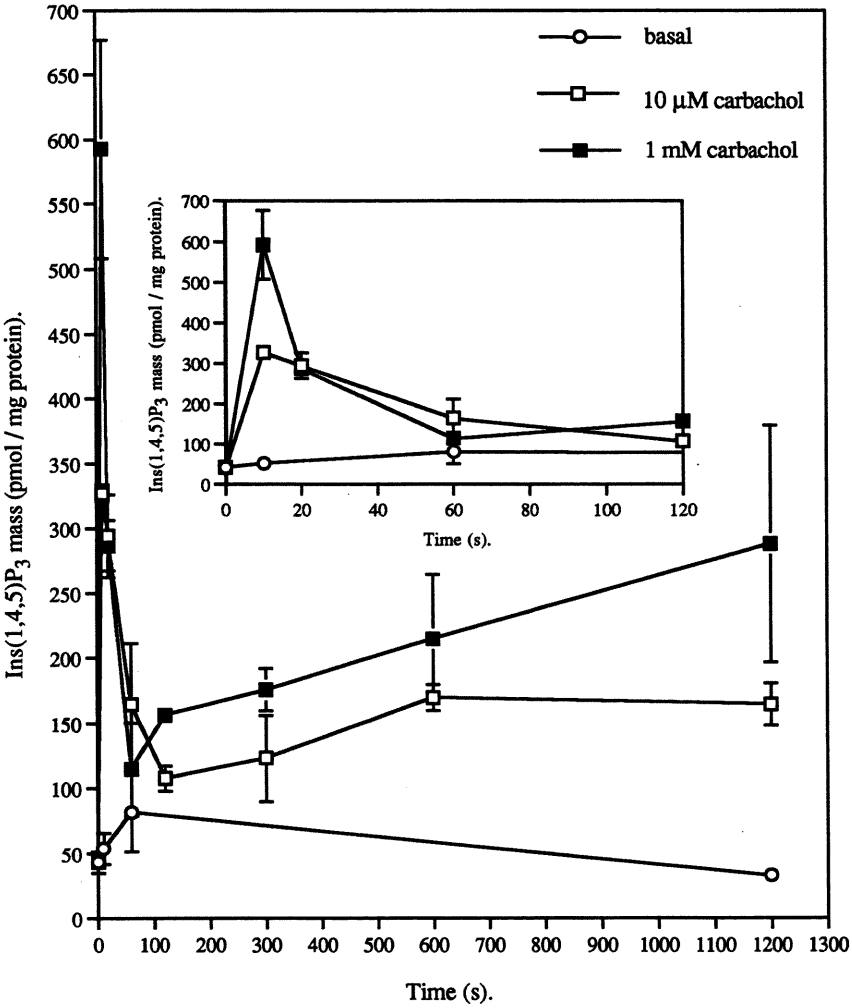

CHO-m1 cell suspensions were incubated with 10 μM and 1 mM carbachol in a waterbath at 37 °C in Krebs / HEPES buffer, pH 7.4. Incubations were terminated by the addition of 1 M TCA. Sample preparation and Ins(1,4,5)P_3 binding assays were performed as described in 6.1 Methods. The graph shows mean ± standard error values of 3 independent experiments. The inset graph is an expanded version of the main graph over the first 2 min of incubation.

Figure 6.2.3. Time course of carbachol-stimulated Ins(1,4,5)P_3 accumulation in CHO-m3 cell suspensions.

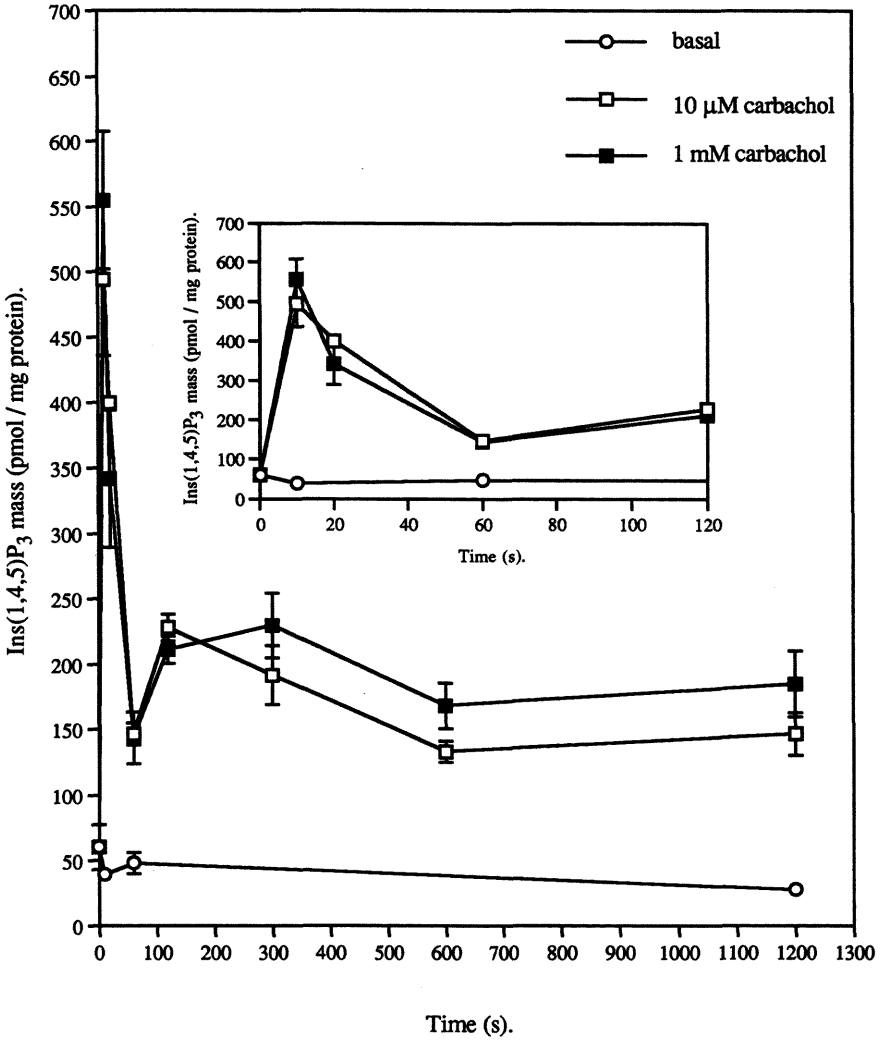

CHO-m3 cell suspensions were incubated with 10 μM and 1 mM carbachol in a waterbath at 37 °C in Krebs / HEPES buffer, pH 7.4. Incubations were terminated by the addition of 1 M TCA. Sample preparation and Ins(1,4,5)P_3 binding assays were performed as described in 6.1 Methods. The graph shows mean ± standard error values of 3 independent experiments. The inset graph is an expanded version of the main graph over the first 2 min of incubation.

Figure 6.2.4. Time course for carbachol-stimulated Ins(1,4,5)P_3 accumulation in CHO-vt9 cell suspensions.

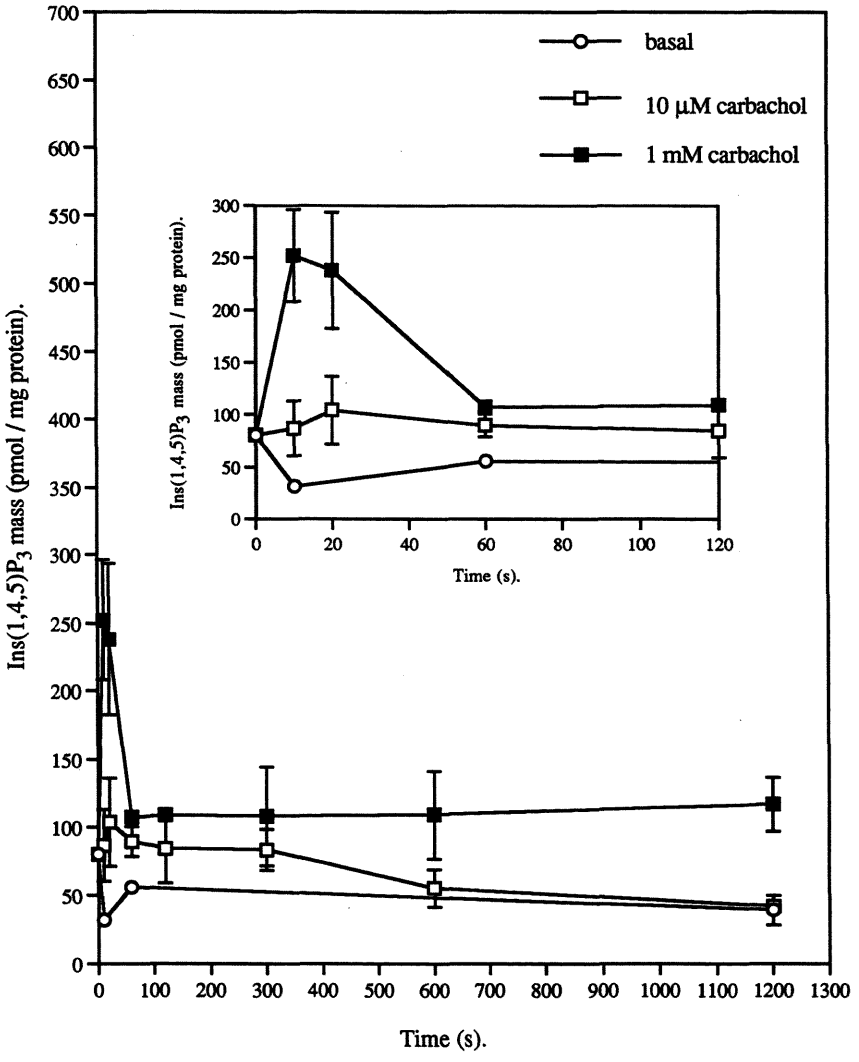

CHO-vt9 cell suspensions were incubated with 10 μM and 1 mM carbachol in a waterbath at 37 °C in Krebs / HEPES buffer, pH 7.4. Incubations were terminated by the addition of 1 M TCA. Sample preparation and Ins(1,4,5)P_3 binding assays were performed as described in 6.1 Methods. The graph shows mean ± standard error values of 3 independent experiments. The inset graph is an expanded version of the main graph over the first 2 min of incubation.

Figure 6.2.5. Time course of carbachol-stimulated Ins(1,4,5)P_3 accumulation in PTX pretreated CHO-m1 and CHO-m3 cell suspensions.

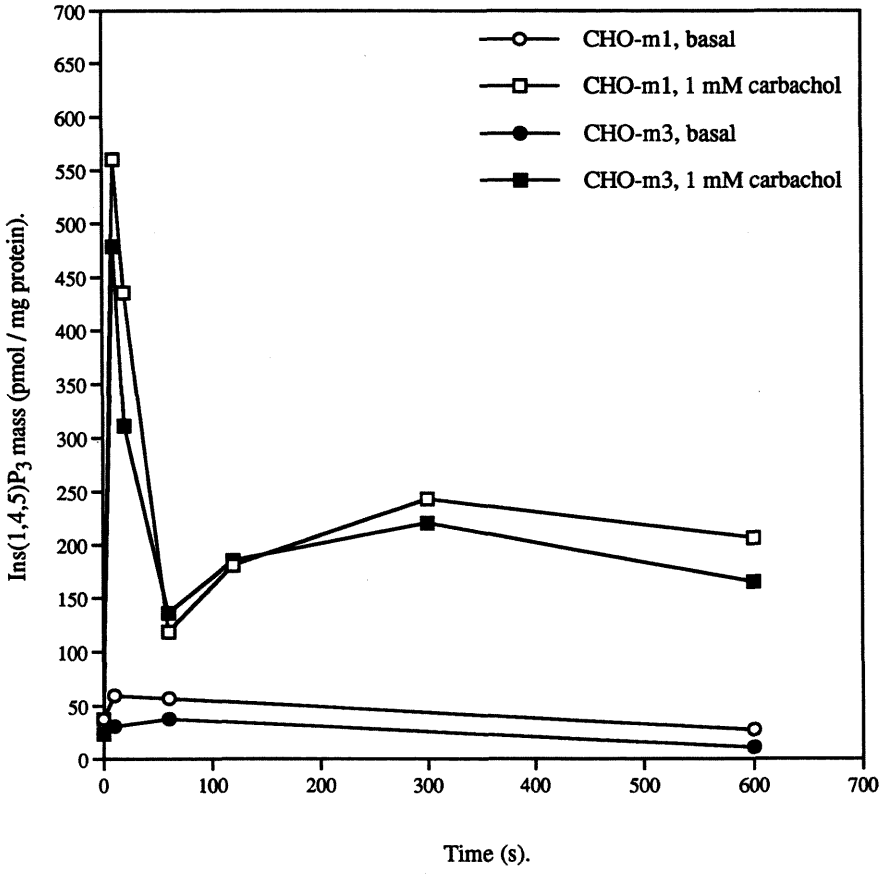

CHO-m1 and CHO-m3 cells were pretreated with 100 ng / ml PTX for 20 hr prior to cell harvesting. Cell suspensions were incubated with 1 mM carbachol in a waterbath at 37 °C in Krebs / HEPES buffer, pH 7.4. Incubations were terminated by the addition of 1 M TCA. Sample preparation and Ins(1,4,5)P_3 binding assays were performed as described in 6.1 Methods.The graph shows values from a single experiment.

Figure 6.2.6. Carbachol dose-response curves for Ins(1,4,5)P_3 accumulation at 10 s and 10 min, in CHO-m1 and PTX pretreatred CHO-m1 cell suspensions.

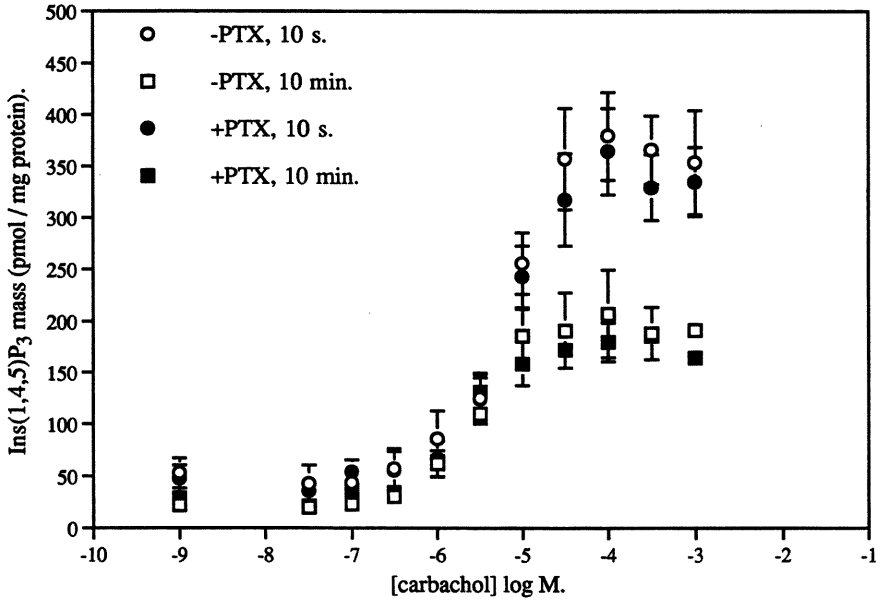

Experiments were performed in a waterbath at 37 °C and incubations were terminated by the addition of 1M TCA. Samples were prepared and assayed as described in 6.1 Methods. **Figure 6.2.6** shows the mean ± standard error values for points derived from 4 individual experiments with untreated and PTX pretreated CHO-m1 cell suspensions. **Table 6.2.1** shows the mean ± standard error values resulting from analysis of individual dose-response curves .Min. and max. represent minimum (basal) and maximal carbachol-stimulated Ins(1,4,5)P_3 mass response, respectively. EC_{50} values represent the molar concentration of carbachol which produced 50 % of the maximium response. (n) represents the number of individual experiments performed. * represents $p \leq 0.05$ for unpaired T-test analysis of data at the 10 min point compared with data at the 10 s time point.

Table 6.2.1.		**- PTX**	**+ PTX**
10 s	min.(pmol / mg protein)	47 ± 12	39 ± 8
	max.(pmol / mg protein)	384 ± 40	348 ± 35
	EC_{50} (log M values)	-5.16 ± 0.06	-5.19 ± 0.03
	(n)	(4)	(4)
10 min	min.(pmol / mg protein)	18 ± 6	26 ± 6
	max.(pmol / mg protein)	196 ± 33 *	180 ± 7 *
	EC_{50} (log M values)	-5.60 ± 0.12 *	-5.65 ± 0.31 *
	(n)	(4)	(4)

Figure 6.2.7. Carbachol dose-response curves for Ins(1,4,5)P_3 accumulation at 10 s and 10 min, in CHO-m3 and PTX pretreated CHO-m3 cell suspensions.

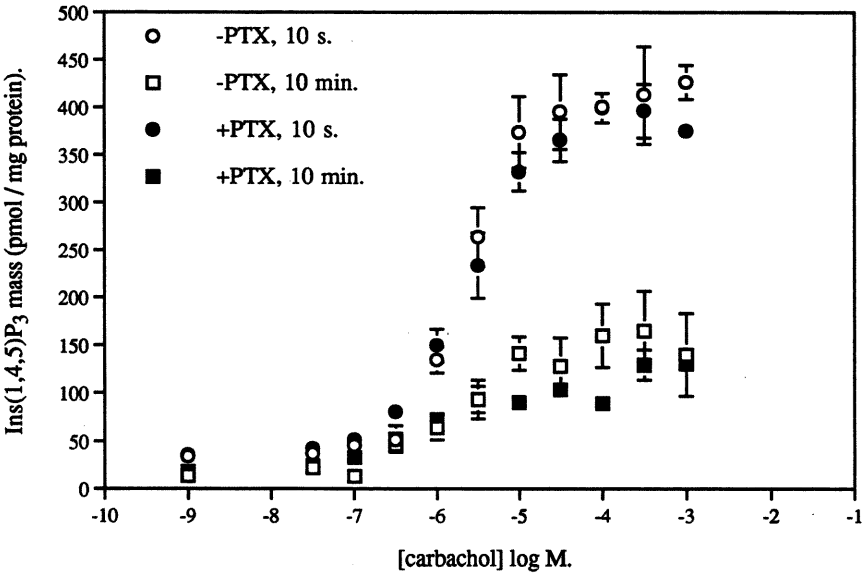

Experiments were performed in a waterbath at 37 °C and incubations were terminated by the addition of 1M TCA. Samples were prepared and assayed as described in 6.1 Methods. **Figure 6.2.7.** shows the mean ± standard error values for points derived from 4 individual experiments in untreated and PTX pretreated CHO-m3 cell suspensions. **Table 6.2.2.** shows the mean ± standard error values resulting from analysis of individual dose-response curves . Min. and max. represent minimum (basal) and maximal carbachol-stimulated Ins(1,4,5)P_3 mass response, respectively. EC_{50} values represent the molar concentration of carbachol which produced 50 % of the maximium response. (n) represents the number of individual experiments performed. * represents $p \leq 0.05$ for unpaired T-test analysis of data at the 10 min time point compared with data at the 10 s time point.

Table 6.2.2.		**- PTX**	**+ PTX**
10 s	min.(pmol / mg protein)	33 ± 9	37 ± 2
	max.(pmol / mg protein)	430 ± 30	397 ± 19
	EC_{50} (log M values)	-5.58 ± 0.12	-5.61 ± 0.15
	(n)	(4)	(4)
10 min	min.(pmol / mg protein)	13 ± 4	18 ± 4 *
	max.(pmol / mg protein)	153 ± 33 *	101 ± 7 *
	EC_{50} (log M values)	-5.80 ± 0.15	-6.28 ± 0.26
	(n)	(4)	(4)

Figure 6.2.8. Carbachol dose-response curves for $Ins(1,4,5)P_3$ accumulation at 10 s and 10 min, in CHO-vt9 and PTX pretreated CHO-vt9 cell suspensions.

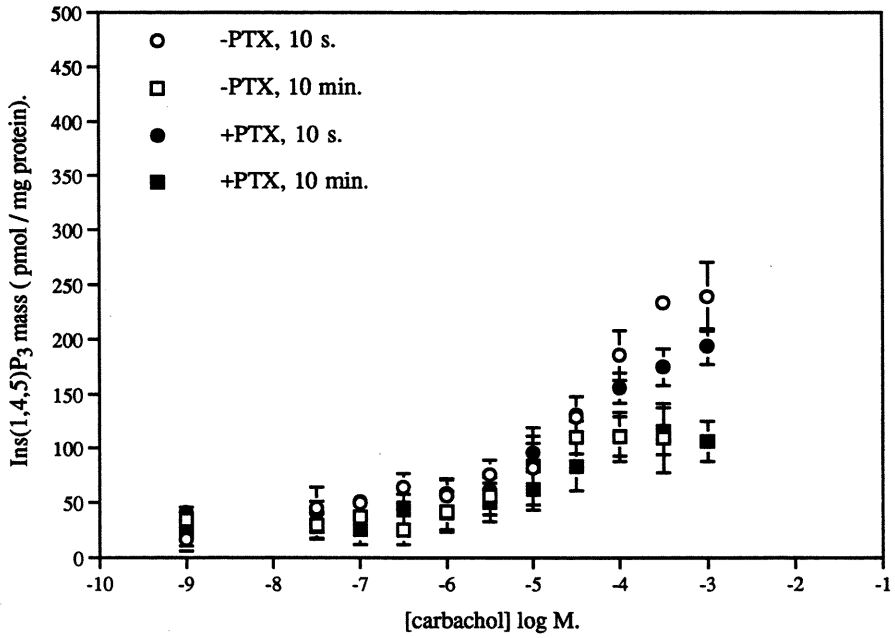

Experiments were performed in a waterbath at 37 °C and incubations were terminated by the addition of 1M TCA. Samples were prepared and assayed as described in 6.1 Methods. **Figure 6.2.8.** shows the mean ± standard error values for points derived from 4 individual experiments in untreated and PTX pretreated CHO-vt9 cell suspensions. **Table 6.2.3.** shows the mean ± standard error values resulting from analysis of individual dose response curves . Min. and max. represent minimum (basal) and maximal carbachol-stimulated $Ins(1,4,5)P_3$ mass response, respectively. EC_{50} values represent the molar concentration of carbachol which produced 50 % of the maximium response. (n) represents the number of individual experiments performed. * represents $p \leq 0.05$ for unpaired T-test analysis of data at the 10 min point compared with data at the 10 s time point.

Table 6.2.3.		**- PTX**	**+ PTX**
10 s	min.(pmol / mg protein)	47 ± 12	41 ± 10
	max.(pmol / mg protein)	224 ± 32	193 ± 6
	EC_{50} (log M values)	-4.49 ± 0.05	-4.63 ± 0.16
	(n)	(4)	(4)
10 min	min.(pmol / mg protein)	31 ± 12	28 ± 11
	max.(pmol / mg protein)	124 ± 25 *	119 ± 19 *
	EC_{50} (log M values)	-5.05 ± 0.18 *	-4.86 ± 0.26
	(n)	(4)	(4)

Figure 6.2.9.a. Time course of carbachol-stimulated Ins(1,4,5)P_3 mass accumulation in permeabilized CHO-m1 cell suspensions.

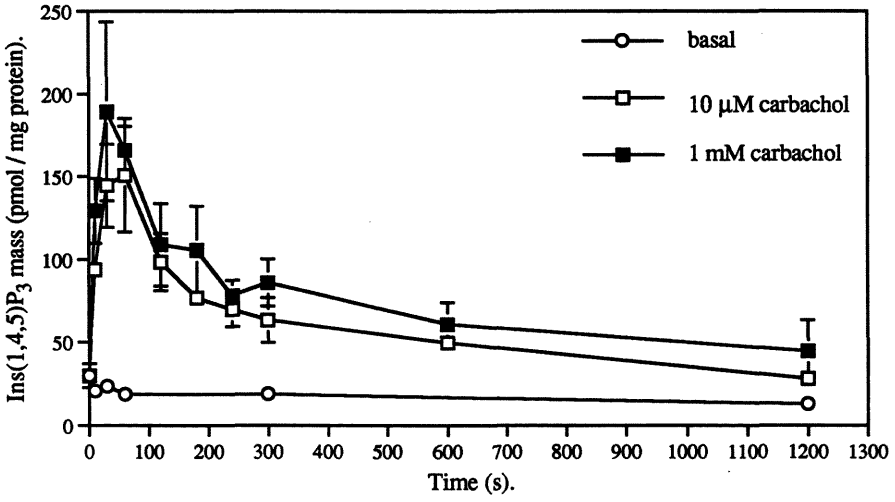

Figure 6.2.9.b. Time course of carbachol-stimulated Ins(1,4,5)P_3 mass accumulation in PTX pretreated, permeabilized CHO-m1 cell suspensions.

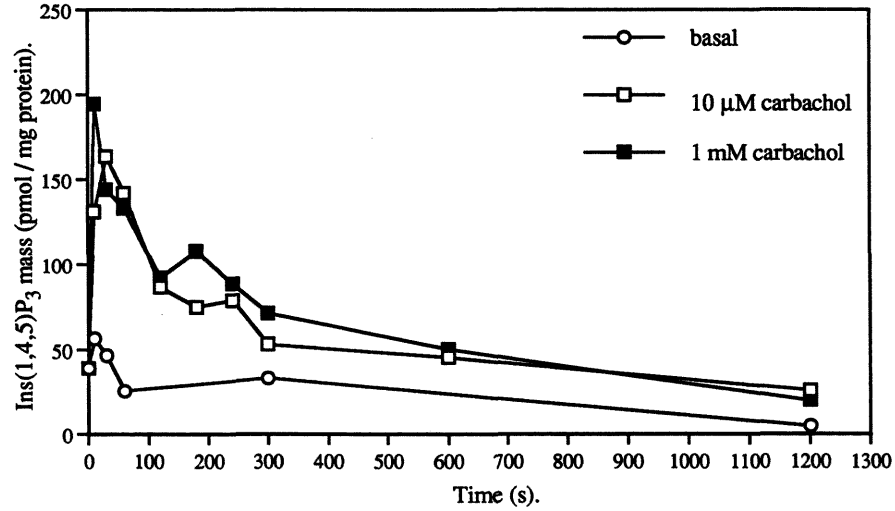

Permeabilized CHO-m1 and PTX pretreated permeabilized CHO-m1 cell suspensions were incubated with 10 µM and 1 mM carbachol in a waterbath at 37 °C, in cytosol-like buffer, pH 7.2. Incubations were terminated by the addition of 1 M TCA. Sample preparation and Ins(1,4,5)P_3 binding assays were performed as described in 6.1 Methods. **Figure 6.2.9.a.** shows mean ± standard error values of 3 independent experiments performed using untreated, permeabilized CHO-m1 cell suspensions. **Figure 6.2.9.b** shows the results of a single experiment performed in PTX pretreated, permeabilized CHO-m1 cell suspensions. The profiles of Ins(1,4,5)P_3 mass accumulation with time were almost identical before and after PTX pretreatment.

Figure 6.2.10. Carbachol dose-response curves for Ins(1,4,5)P_3 accumulation after a 30 s incubation, in untreated and PTX pretreated, permeabilized CHO-m1 cell suspensions.

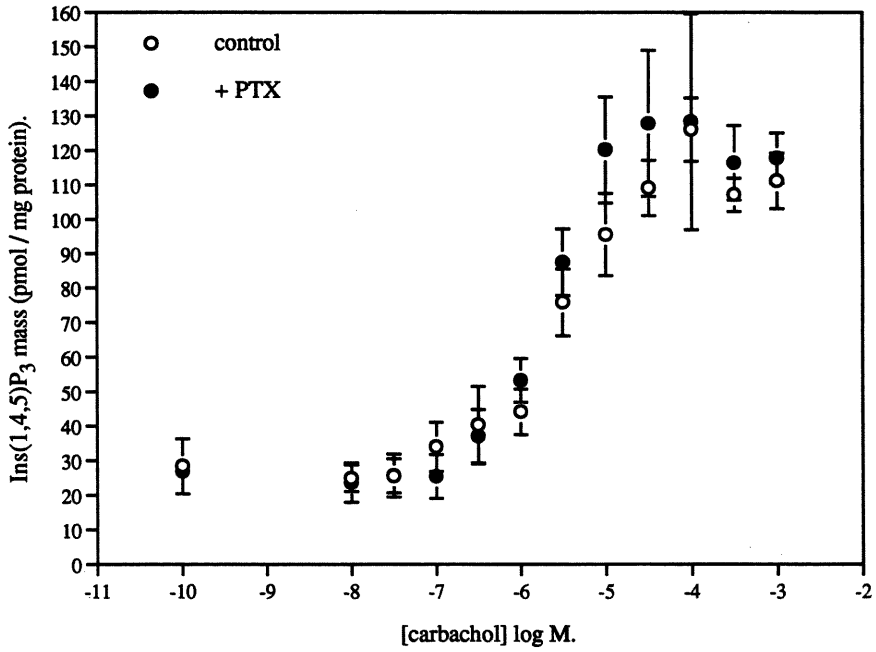

Experiments were performed in cytosol-like buffer at 37 °C, and incubations were terminated by the addition of 1M TCA. Samples were prepared and assayed as described in 6.1 Methods. **Figure 6.2.10.** shows the mean ± standard error values for points derived from 3 individual experiments. **Table 6.2.4.** shows the mean ± standard error values resulting from analysis of individual dose-response curves . Min. and max. represent minimum (basal) and maximal carbachol-stimulated Ins(1,4,5)P_3 mass response, respectively. EC_{50} values represent the molar concentration of carbachol which produced 50 % of the maximium response. (n) represents the number of individual experiments performed.

30 s

Table 6.2.4.	**- PTX**	**+ PTX**
min.(pmol / mg protein)	28 ± 7	26 ± 5
max.(pmol / mg protein)	120 ± 5	125 ± 14
EC_{50} (log M values)	-5.46 ± 0.14	-5.71 ± 0.10
(n)	(3)	(3)

CHAPTER SEVEN.

CARBACHOL AND INS(1,4,5)P_3-INDUCED $^{45}Ca^{2+}$ RELEASE FROM PERMEABILIZED CHO CELL CLONES EXPRESSING RECOMBINANT MUSCARINIC RECEPTOR SUBTYPES.

7.0 Introduction.

Agonist stimulation of PLC-linked receptors mediates the hydrolysis of PIP_2 by PLC, resulting in the production of $Ins(1,4,5)P_3$ and DAG (see chapter 1 for references). DAG is known to activate PKC resulting in phosphorylation events regulating cellular functions including cell growth and differentiation (Azzi *et al*, 1992). $Ins(1,4,5)P_3$, on the other hand, mediates Ca^{2+} release from intracellular vesicles via $Ins(1,4,5)P_3$ receptors which contain an intrinsic channel through which Ca^{2+} ions can cross vesicular membranes (see chapter 1 for references).

Free cytosolic Ca^{2+} in most cells is low (between 60 and 200 nM) accounting for only a minute fraction of the total cellular Ca^{2+} content (approximately 1-2 mM) (Meldolesi *et al,* 1990). The remaining Ca^{2+} appears to be localized within membrane-bound organelles which contain Ca^{2+}-binding proteins such as annexins (Klee, 1988) and proteins which share the typical EF-hand structure indicative of Ca^{2+} binding properties (Carafoli, 1987). *In vitro* measurements of Ca^{2+} uptake, storage and release, under carefully controlled experimental conditions have been useful in establishing roles for important protein molecules *i.e.* Ca^{2+}-ATPases, $Ins(1,4,5)P_3$ and ryanodine receptors and storage proteins.

More recently, fluorescent indicators (*e.g.* fura-2) along with computerized imaging techniques have provided information about the intracellular sites where changes in cytosolic Ca^{2+} concentration occur as a consequence of appropriate cell stimulation (Tsien, 1989).

10 years ago, it was still widely believed that mitochondria played a key role in Ca^{2+} homeostasis. These organelles can accumulate large amounts of Ca^{2+} via a transporter system driven by the highly negative membrane potential maintained across the inner membrane by electron transport along the respiratory chain (Carafoli, 1987). Antiport exchange with Na^+ was also thought to efficiently mediate the release of mitochondrial Ca^{2+} to the cytosol in some cell types (Carafoli, 1987). Other studies showed, however, that the mitochondrial Ca^{2+} uptake mechanism had a relatively low affinity for Ca^{2+} (in the micromolar range). Basal and stimulated cytosolic Ca^{2+} levels generally occur within the sub-micromolar range and, therefore, a significant involvement of mitochondria in Ca^{2+} homeostasis is expected to occur only when levels of Ca^{2+} may cause cell damage (Meldolesi *et al*, 1990).

When the intracellular second messenger $Ins(1,4,5)P_3$ was shown to mediate Ca^{2+} release from non-mitochondrial intracellular stores (Streb *et al,* 1983; Gershengorn *et al,* 1984) attention was focused on the microsomal fraction, particularly the endoplasmic reticulum (ER) or a novel organelle termed "calciosomes" (Volpe *et al,* 1988), in relation to Ca^{2+} homeostasis. The precise location of $Ins(1,4,5)P_3$-sensitive Ca^{2+} storage organelles within the cell is still unknown.

Generally, receptor-activated Ca^{2+} mobilization via the inositol phosphate-Ca^{2+} signalling pathway occurs in two phases; an initial transient release of Ca^{2+} from intracellular stores; and a prolonged phase of elevated cytosolic free Ca^{2+} mediated via Ca^{2+} entry across the plasma membrane. As described above, Ca^{2+} release from the intracellular stores is strongly believed to be mediated by Ins(1,4,5)P_3 opening an intrinsic Ca^{2+} channel on Ins(1,4,5)P_3 receptors. However, the mechanism for the Ca^{2+} entry phase of receptor-activated Ca^{2+} mobilization, although dependent on the presence of Ins(1,4,5)P_3, remains elusive (for reviews see Berridge and Irvine, 1989; Berridge, 1993; Putney and Bird, 1993).

Ins(1,4,5)P_3-induced Ca^{2+} release from intracellular stores appears to occur in a quantal manner, *i.e.* as the level of Ins(1,4,5)P_3 rises, a fixed proportion of Ca^{2+} is released from stores (Muallem *et al*, 1989; Taylor and Potter, 1990; Meyer and Stryer, 1990; Taylor, 1992; Irvine, 1990). Two interpretations have been placed on these observations; 1) that a feedback mechanism terminates release of Ca^{2+} by Ins(1,4,5)P_3, possibly by the action of elevated cytosolic Ca^{2+} levels or the reduction in Ca^{2+} within stores, acting on the Ins(1,4,5)P_3 receptors (Nunn and Taylor, 1992; Missiaen *et al*, 1992b; see also chapter 1); or 2) that Ins(1,4,5)P_3 releases all of the Ca^{2+} from a set of stores that are differentially sensitive to Ins(1,4,5)P_3, the so-called "all or none" response (Parker and Ivorra, 1990; see also chapter 1). More recently, it has been suggested that quantal Ca^{2+} release may be an artifactual response resulting from fractionation of the ER after permeabilization of cell suspensions (Renard-Rooney *et al*, 1993).

Two scenarios exist to explain the mechanism of Ins(1,4,5)P_3-induced Ca^{2+} entry across the plasma membrane. Firstly, that a specific type of Ins(1,4,5)P_3 receptor may exist on the plasma membrane mediating Ca^{2+} influx (for review see Putney and Bird, 1993); or secondly, according to the "capacitative model" for Ca^{2+} entry, that the Ca^{2+} content of the Ins(1,4,5)P_3-sensitive pool determines the rate of Ca^{2+} entry (for review see Putney and Bird, 1993). Evidence for this second scenario comes from experiments with thapsigargin, which specifically inhibits microsomal (and not plasmalemmal) Ca^{2+}-ATPase, thereby causing depletion of intracellular Ca^{2+} stores. Thapsigargin has been shown to promote Ca^{2+} entry without elevating levels of inositol phosphates (Jackson *et al*, 1988; Takemura *et al*, 1989). Although a large body of evidence is being produced in favour of the capacitance model for Ca^{2+} entry, the signal and the route by which intracellular Ca^{2+} levels can communicate with the plasma membrane leading to Ca^{2+} entry is largely unknown. Possible molecular participants in this mechanism have recently been reviewed by Putney and Bird (1993). The influx of Ca^{2+} across the plasma membrane is thought to be rapidly sequestered by the internal stores. Thus, the influx

mechanism transforms the cytoplasm into an excitable medium, setting the stage for the generation of repetitive Ca^{2+} spikes and waves induced by release of Ca^{2+} from $Ins(1,4,5)P_3$-sensitive stores and via Ca^{2+}-induced Ca^{2+} release from $Ins(1,4,5)P_3$-insensitive stores (for reviews see Berridge, 1993; Putney and Bird, 1993; see also chapter 1).

In the present study, $Ins(1,4,5)P_3$ and carbachol-induced Ca^{2+} efflux from stores was measured in permeabilized CHO cells expressing homogeneous populations of recombinant muscarinic receptor subtypes. Permeabilization of cells in suspension were performed in a cytosol-like buffer (see appendix 1) where free Ca^{2+} was buffered (with EGTA) to the basal levels of free Ca^{2+} found in the cytosol of intact cells (approximately 100 nM). The buffer was supplemented with ATP and Mg^{2+} to allow the microsomal Ca^{2+}-ATPases of the cells to mediate the uptake of added $^{45}CaCl$ (0.5 μCi / ml) into intracellular stores. $^{45}Ca^{2+}$ release was then measured in response to added $Ins(1,4,5)P_3$ or carbachol.

The aims of the present study were to characterize the $Ins(1,4,5)P_3$-sensitive Ca^{2+} pool in permeabilized CHO cells and to determine the ability of $Ins(1,4,5)P_3$, generated by the stimulation of different subtypes of muscarinic receptors, to mediate Ca^{2+} release from intracellular stores. This was done to elucidate the relationship between agonist-mediated $Ins(1,4,5)P_3$ generation and Ca^{2+} release in the CHO cell clones, *i.e.* does carbachol have a greater potency for releasing Ca^{2+} from stores compared to $Ins(1,4,5)P_3$ generation signifying an apparent receptor-reserve of $Ins(1,4,5)P_3$ receptors? Alternatively, does carbachol-stimulated $^{45}Ca^{2+}$ release increase with carbachol-stimulated $Ins(1,4,5)P_3$ generation in a linear manner?

Carbachol-stimulated $^{45}Ca^{2+}$ release was also compared between CHO cells expressing m1 receptors (CHO-m1) and CHO cells expressing m3 receptors (CHO-m3), both at similar receptor densities, to determine whether stimulation of these two receptor subtypes releases Ca^{2+} in an identical manner. The effects of reducing m3 muscarinic receptor expression in CHO cells were also compared in terms of $^{45}Ca^{2+}$ release from stores to help to elucidate the relationship between $Ins(1,4,5)P_3$ generation and $^{45}Ca^{2+}$ release in CHO-vt9 cells (expressing a lower density of m3 muscarinic receptors) compared with CHO-m3 cells (expressing a higher density of m3 muscarinic receptors). If there was an amplification step between $Ins(1,4,5)P_3$ generation and $^{45}Ca^{2+}$ release then, perhaps, the reduced maximal response for carbachol-stimulated $Ins(1,4,5)P_3$ generation (at 10 s) seen in CHO-vt9 cells compared with CHO-m3 cells (see chapter 6) might be expected to result in a carbachol-stimulated $^{45}Ca^{2+}$ release which had a similar maximal response in both CHO-vt9 cells and CHO-m3 cells.

Finally, the PTX-sensitivity of carbachol-stimulated $^{45}Ca^{2+}$ release was determined in

each of the CHO clones to see whether PTX-sensitive G proteins play a role in muscarinic receptor-mediated $^{45}Ca^{2+}$ release.

7.1 Methods.

7.1.1 Experimental Procedure.

Cells were harvested, permeabilized and resuspended in ice-cold, cytosol-like buffer (CLB) containing 2 mM ATP and 5-10 μM EGTA, pH 7.2 (see chapter 2 and appendix 1). The final free $[Ca^{2+}]$ in the buffer was between 75-150 nM. Permeabilized cell suspensions were kept on ice while protein assays were performed. Permeabilized cell suspensions were then diluted (if necessary) to appropriate protein concentrations in 3ml of ice-cold buffer.

Experiments showed that permeabilized cell suspensions could be left on ice for a period of one hr without any apparent affect on % $^{45}Ca^{2+}$ release induced by $Ins(1,4,5)P_3$ or carbachol (data not shown). Permeabilized cell suspensions were left for 15 min at room temperature to warm up before adding 0.5 μCi / ml of $^{45}CaCl$ (1000 Ci / mmol). The suspensions were then mixed gently and left for 15 min at room temperature with periodic mixing. This time period (determined by $^{45}Ca^{2+}$ uptake time course studies) was sufficient for $^{45}Ca^{2+}$ uptake to reach equilibrium (Figure 7.2.1).

100 μl aliquots of the permeabilized cell suspensions loaded with $^{45}Ca^{2+}$ were then added to 10 μl of drug or buffer in decapped, 1.5 ml microcentrifuge tubes. Cell pellets were separated from supernatant by centrifugation (16000 g for 4 min) through 500 μl of a silicon oil mixture (Dow Corning (BDH) silicon fluids 556 and 550 (1 : 1)).

$Ins(1,4,5)P_3$-induced $^{45}Ca^{2+}$ release experiments were stopped by centrifugation 1 min after addition of the permeabilized cell suspension (0.5 mg of protein / ml) to the drug. Centrifugation caused cells to separate from the supernatant (containing the drug) after a few seconds, but to achieve a firm cell pellet, centrifugation was continued for 4 min.

Carbachol-stimulated $^{45}Ca^{2+}$ release studies were carried out with 2 min incubations of permeabilized cell suspensions (3 mg of protein / ml) with carbachol, as deduced from time course studies (Figure 7.2.5). In dose-response studies, cells were incubated with concentrations of $Ins(1,4,5)P_3$ from 10^{-9} M up to 10^{-5} M. Carbachol dose-response studies were performed over a range of carbachol concentrations from $3x10^{-8}$ M up to 10^{-3} M.

Cells were pretreated with PTX by adding 100 ng / ml of PTX to the growth media of cells 20 hr prior to cell harvesting. Ionomycin was added to experiments at 10 μM final concentration, when required.

The aqueous phase and most of the silicon oil was removed carefully without disturbing the pellet by suction. The microcentrifuge tubes containing the cell pellets were inverted for 30-60 min to remove the remaining silicon oil. 1 ml of scintillation cocktail was added to each microcentrifuge tube which were then capped, vortex mixed and left for 24 hr allowing the radioactivity in the pellet to be dispersed. Radioactivity was then measured by liquid scintillation spectrometry.

7.1.2. Data Analysis.

Experiments were performed using duplicate concentrations of drug including two tubes which contained buffer instead of drug. The radioactivity in these two tubes were then taken as the total $^{45}Ca^{2+}$ content incorporated into intracellular stores. Duplicate values were averaged and compared as a percentage of this value to give % $^{45}Ca^{2+}$ release induced by either Ins(1,4,5)P_3 or carbachol. Dose-response curves to Ins(1,4,5)P_3 and carbachol were analysed by the curve fitting program GraphPAD INPLOT (GraphPAD Software Inc., San Diego, CA) to determine EC_{50} values.

7.2 Results.

$^{45}Ca^{2+}$ uptake into saponin (100 μg / ml)-permeabilized CHO cell clones (0.5 mg of protein / ml) occurred in two phases (Figure 7.2.1). There was an initial, rapid uptake of $^{45}Ca^{2+}$ into stores, in the presence of ATP, which was completed after 30 s. The second phase of $^{45}Ca^{2+}$ uptake was at a much slower rate and was maintained for 30 min. $^{45}Ca^{2+}$ uptake experiments were not performed in the absence of ATP. A 15 min incubation of permeabilized cell suspensions with $^{45}CaCl$ was used in all further studies.

Ionomycin (10 μM) released 90 % of the $^{45}Ca^{2+}$ taken up by cells suggesting that the majority of added $^{45}Ca^{2+}$ accumulated in vesicular stores.(Figure 7.2.4).

Ins(1,4,5)P_3-induced $^{45}Ca^{2+}$ release experiments were performed using saponin permeabilization of cell suspensions. Carbachol-induced $^{45}Ca^{2+}$ release experiments were performed later using electroporation of cell suspensions. Both permeabilization techniques evoked the same release of $^{45}Ca^{2+}$ in the presence of 10 μM Ins(1,4,5)P_3 (70-80 %) (Figure 7.2.4 and 7.2.6) suggesting that the results produced from both permeabilization techniques were comparable. In trypan blue exclusion studies, permeabilization of CHO cell suspensions by either method rendered greater than 90 % of cells permeable to the dye (data not shown).

Ins(1,4,5)P_3-induced $^{45}Ca^{2+}$ release dose-response curves were performed after 1 min incubation using protein concentrations of 0.5 mg / ml. This concentration of cell suspensions produced maximal % $^{45}Ca^{2+}$ release in the presence of 10 μM Ins(1,4,5)P_3

while keeping metabolism of added Ins(1,4,5)P_3 to a relatively low level (Figure 7.2.2). A lower concentration of Ins(1,4,5)P_3 (100 nM), using permeabilized cell suspensions at a protein concentration of 3 mg / ml, induced a transient release of $^{45}Ca^{2+}$ probably due to the faster rate of metabolism of added Ins(1,4,5)P_3 due to the increased protein concentration and, therefore, increased concentration of Ins(1,4,5)P_3 metabolizing enzymes (Figure 7.2.3). In both cases, Ins(1,4,5)P_3-induced $^{45}Ca^{2+}$ release was rapid, reaching maximal release after approximately 10 s (Figure 7.2.2 and 7.2.3).

Dose response curves for Ins(1,4,5)P_3-induced $^{45}Ca^{2+}$ release were identical in each of the permeabilized CHO cell clone suspensions (Figure 7.2.4 and Table 7.2.1) suggesting that Ins(1,4,5)P_3 receptors and calcium stores were not affected by the transfection of different muscarinic receptor genes into CHO cells. PTX pretreatment of CHO-m1 and CHO-m2 cells also had no significant effect on Ins(1,4,5)P_3-induced $^{45}Ca^{2+}$ release. Generally, maximal Ins(1,4,5)P_3-induced $^{45}Ca^{2+}$ release was achieved with 10 μM Ins(1,4,5)P_3, releasing 70-80 % of stored $^{45}Ca^{2+}$. The EC_{50} value for Ins(1,4,5)P_3-induced $^{45}Ca^{2+}$ release ranged from (in log M values) -7.21 to -7.48 between CHO cell clones (Table 7.2.1).

Carbachol-induced $^{45}Ca^{2+}$ release experiments were conducted using 3 mg / ml of protein which produced a maximal carbachol-stimulated $^{45}Ca^{2+}$ release after 2-3 min of incubation (Figure 7.2.5). Lowering the protein concentration in experiments caused rightward shifts and finally reduced maximal responses in dose-response curves for carbachol-stimulated $^{45}Ca^{2+}$ release (data not shown). Therefore, protein concentrations were maintained at 3 mg / ml in all of the CHO cell clones. This protein concentration range produced maximal carbachol-stimulated $^{45}Ca^{2+}$ release in electroporated CHO-m1 and CHO-m3 cell suspensions (reaching similar levels of $^{45}Ca^{2+}$ release elicited by 10 μM Ins(1,4,5)P_3) (Figure 7.2.6 and 7.2.7) and responses of the different CHO-cell clones could be directly compared as the protein concentrations used were identical.

Permeabilized CHO-m2 and CHO-slm2 cell suspensions did not produce any significant carbachol-stimulated $^{45}Ca^{2+}$ release (Figure 7.2.6) both before and after pretreatment of the cells with PTX. Permeabilized CHO-m1 cells, in the presence of 1 mM carbachol, produced a 70 % release of $^{45}Ca^{2+}$ which was marginally less than that evoked by 10 μM Ins(1,4,5)P_3. PTX-pretreatment of CHO-m1 cells had no effect on EC_{50} or maximal response values for carbachol-stimulated $^{45}Ca^{2+}$ release (Figure 7.2.6 and Table 7.2.2). Carbachol-stimulated $^{45}Ca^{2+}$ release in permeabilized CHO-m3 cell suspensions was identical to that seen in permeabilized CHO-m1 cell suspensions, in the absence of PTX-pretreatment (Figure 7.2.7 and Table 7.2.2). PTX-pretreatment of CHO-m3 cells resulted in a small, but significant, reduction in the maximal response induced by

carbachol without effecting the EC_{50} value for carbachol-stimulated $^{45}Ca^{2+}$ release.

Carbachol stimulation of $^{45}Ca^{2+}$ release in permeabilized CHO-vt9 cell suspensions was markedly less than $^{45}Ca^{2+}$ release in permeabilized CHO-m3 cell suspensions. The EC_{50} for carbachol-stimulated $^{45}Ca^{2+}$ release was shifted 35-fold to the right and the maximal response was reduced by 65 % (Figure 7.2.7 and Table 7.2.2). PTX-pretreatment of CHO-vt9 cells resulted in a further reduction in the maximal response elicited by carbachol. It was not possible to curve fit such a small response but the maximal $^{45}Ca^{2+}$ release elicited by 1 mM carbachol was 8.1 ± 1.5 %.

7.3. Discussion.

The present study shows that CHO-cells expressing recombinant muscarinic receptor subtypes can be permeabilized, either by saponin or electroporation, resulting in the uptake of $^{45}Ca^{2+}$ into intracellular stores. 90 % of loaded $^{45}Ca^{2+}$ could subsequently be released by ionomycin (10 μM). The remaining 10 % may represent the high affinity binding of $^{45}Ca^{2+}$ to calcium-binding proteins within the cell and/or a proportion of $^{45}Ca^{2+}$ from the buffer that had become trapped with the cell pellet during centrifugation.

$Ins(1,4,5)P_3$ maximally released 70-80 % of loaded $^{45}Ca^{2+}$ with a similar potency in each of the CHO cell clones indicating that the transfection of muscarinic receptor genes into CHO cells did not affect either the Ca^{2+} stores or the responsiveness of endogenously expressed $Ins(1,4,5)P_3$ receptors among the different CHO cell clones.

One controversy that exists from this data is that basal levels of $Ins(1,4,5)P_3$ (calculated from basal $Ins(1,4,5)P_3$ mass accumulation studies) are thought to be approximately 1-3 μM in many intact cells (Challiss *et al*, 1990; Shears, 1991). However, addition of 3 μM $Ins(1,4,5)P_3$ to permeabilized CHO cells and indeed in other cell types, *e.g.* SH-SY5Y cells (Wojcikiewicz *et al*, 1990) and rat cerebellar granule cells (Whitham *et al*, 1991), resulted in a maximal release of loaded $^{45}Ca^{2+}$ from stores. Therefore, either the $Ins(1,4,5)P_3$ measured in intact cells is compartmentalized where it cannot come into contact with $Ins(1,4,5)P_3$ receptors gating Ca^{2+} flux from stores, or, permeabilization of cells results in an increased sensitivity of $Ins(1,4,5)P_3$ receptors to $Ins(1,4,5)P_3$, possibly by releasing an inhibitory constraint on $Ins(1,4,5)P_3$ receptor sensitivity. These clear discrepancies between basal $Ins(1,4,5)P_3$ levels in intact cells and the responses to added $Ins(1,4,5)P_3$ in permeabilized cells have not really been investigated but deserve further research.

Pretreatment of CHO cells with PTX (100 ng / ml for 20 hr) had no significant effect on $Ins(1,4,5)P_3$-induced $^{45}Ca^{2+}$ release suggesting that any possible subsequent effects of PTX pretreatment on muscarinic receptor agonist-mediated $^{45}Ca^{2+}$ release would be at a level prior to $Ins(1,4,5)P_3$ receptor activation.

m2 Muscarinic receptor activation did not induce any $^{45}Ca^{2+}$ release from permeabilized CHO cells, at relatively low expression levels of receptor (CHO-m2 cells = 76 ± 11 fmol / mg protein) or at a higher receptor expression levels (CHO-slm2 = 366 ± 68 fmol / mg protein), both before and after PTX pretreatment. This lack of carbachol-stimulated $^{45}Ca^{2+}$ release in CHO-m2 cells corresponds with the lack of carbachol-stimulated Ins(1,4,5)P_3 accumulation in intact CHO-m2 cells (see chapter 6), suggesting that m2 muscarinic receptors expressed at relatively low expression levels in CHO cells do not couple to the activation of PLC. The lack of carbachol-stimulated $^{45}Ca^{2+}$ release in CHO-slm2 cells also suggests that m2 muscarinic receptors expressed at a level 4 to 5-fold higher than in CHO-m2 cells were still unable to couple to the activation of PLC. Other studies have found that G protein-coupled receptors that predominantly couple to G_i, expressed at high levels in CHO cells, can lead to elevations in total inositol phosphate accumulation, *e.g.* m2 receptors (Ashkenazi *et al*, 1987) and 5-HT_{1A} receptors (Raymond *et al*, 1992) in a PTX-sensitive manner. In CHO cells, m2 muscarinic receptor-mediated PLC activity appears to be driven via $G\alpha_{i2}$ and/or $G\alpha_{i3}$ or possibly their associated $\beta\gamma$ subunits (Dell'Acqua *et al*, 1993). Perhaps at higher expression levels in CHO cells, m2 muscarinic receptors may generate enough $\beta\gamma$ subunits to subsequently activate PLC isoforms (Park *et al*, 1993).

Carbachol stimulated $^{45}Ca^{2+}$ release in CHO-m1 and CHO-m3 cells reaching a maximal release slightly less than that reached by added Ins(1,4,5)P_3 (10 μM). The extent of carbachol-stimulated $^{45}Ca^{2+}$ release in CHO-m1 and CHO-m3 permeabilized cell suspensions was found to vary when different protein concentrations were used. Presumably, increasing cell number resulted in a greater overall concentration of generated Ins(1,4,5)P_3 in the suspensions, on addition of carbachol, which subsequently was capable of releasing $^{45}Ca^{2+}$ from stores. Increasing cell number resulted in an increased maximal response (up to the levels achieved by added Ins(1,4,5)P_3 (10 μM)) and the dose-response curve for carbachol was shifted to the left (*i.e.* carbachol appeared to become more potent at releasing $^{45}Ca^{2+}$ from stores). Experiments performed in this way in permeabilized cells may inherently create difficulties in comparing these responses with other responses observed in intact cells. For instance, direct comparisons between carbachol-stimulated Ins(1,4,5)P_3 generation in intact CHO cell clones with $^{45}Ca^{2+}$ release in permeabilized cells will differ depending on the protein concentration of cells used in permeabilized cell suspensions and hence the subtle changes in apparent carbachol potency for the response. Therefore, apparent potency differences between carbachol-stimulated Ins(1,4,5)P_3 generation (in intact cells, see chapter 6) and $^{45}Ca^{2+}$ release (in permeabilized cells) may simply be a reflection of the protein concentration used in $^{45}Ca^{2+}$ studies as well as the other possibility, *i.e.* an amplification step in the signal

transduction pathway between Ins(1,4,5)P_3 generation and Ca^{2+} release from stores. In order to compare agonist-stimulated Ins(1,4,5)P_3 generation with Ca^{2+} release from stores in a more comparable manner, measurements of cytosolic Ca^{2+} levels in intact cells can be measured using fluorescent indicators *i.e.* fura-2 (Willars and Nahorski, submitted for publication).

Valid comparisons can, however, be made in the present study between carbachol-stimulated $^{45}Ca^{2+}$ release in each of the CHO cell clones expressing different muscarinic receptor subtypes, as experiments were performed at identical protein concentrations (3 mg / ml).

Carbachol-stimulated $^{45}Ca^{2+}$ release from permeabilized CHO-m1 and CHO-m3 cell suspensions (expressing m1 and m3 muscarinic receptors, respectively, at similar receptor densities) was identical in terms of both the maximal release of $^{45}Ca^{2+}$ from stores and the potency with which carbachol elicited the response. Carbachol-stimulated $^{45}Ca^{2+}$ release was not significantly affected by PTX-pretreatment, although small rightward shifts in the carbachol dose-response curves were apparent in both CHO-m1 and CHO-m3 cell clones. The PTX-insensitivity of the carbachol-stimulated $^{45}Ca^{2+}$ release response in CHO-m1 and CHO-m3 cells was largely expected considering the PTX-insensitivity of carbachol-stimulated Ins(1,4,5)P_3 generation observed in these cells in the previous chapter (chapter 6).

Carbachol-stimulated Ins(1,4,5)P_3 generation was measured in both intact and permeabilized CHO-m1 cell suspensions in the previous chapter (chapter 6) yielding very similar EC_{50} values for carbachol, suggesting that Ins(1,4,5)P_3 accumulation in intact and permeabilized CHO cells can be readily compared in terms of their carbachol potency. Carbachol-stimulated Ins(1,4,5)P_3 accumulation in permeabilized CHO-m1 cell suspensions were achieved using identical assay conditions to the $^{45}Ca^{2+}$ release experiments. Carbachol had a 5-fold greater potency for inducing $^{45}Ca^{2+}$ mobilization in permeabilized CHO-m1 cells than for generating Ins(1,4,5)P_3 mass. Such a response is indicative of an amplification step between Ins(1,4,5)P_3 generation and $^{45}Ca^{2+}$ release from stores, elicited by the Ins(1,4,5)P_3 generated. As discussed above, such comparisons of different responses to carbachol in relation to $^{45}Ca^{2+}$ release in permeabilized cell preparations will be affected by the cell concentration used, and therefore, by the levels of Ins(1,4,5)P_3 generated by agonist stimulation. However, it would appear that 3 mg / ml of protein in $^{45}Ca^{2+}$ release assays produces a maximal carbachol-stimulation of $^{45}Ca^{2+}$ release almost equivalent to that produced by a maximally effective concentration of added Ins(1,4,5)P_3. Any further reduction in the protein concentration used in these experiments, might be expected to decrease the carbachol-stimulated maximal response, relative to that observed in response to 10 μM Ins(1,4,5)P_3. Any further increase in

protein concentration, on the other hand, would be expected to increase the carbachol potency of $^{45}Ca^{2+}$ release, whilst maintaining the same maximal response, thus increasing the apparent amplification step between carbachol-stimulated Ins(1,4,5)P_3 generation and $^{45}Ca^{2+}$ release. The amplification step between these two responses may, therefore, cause a greater than 5-fold increase in the potency of carbachol for $^{45}Ca^{2+}$ release compared to Ins(1,4,5)P_3 generation in CHO-m1 cells.

Carbachol was approximately 3-fold more potent for inducing $^{45}Ca^{2+}$ release from permeabilized CHO-m3 cells than for stimulating Ins(1,4,5)P_3 accumulation in intact CHO m3 cells. These results suggest that both m1 and m3 muscarinic receptors couple to the activation of PLC, inducing similar profiles of Ins(1,4,5)P_3 accumulation in intact CHO cells and $^{45}Ca^{2+}$ release from permeabilized CHO cells.

The nature of the amplification step between Ins(1,4,5)P_3 generation and $^{45}Ca^{2+}$ release from stores may lie with the population of Ins(1,4,5)P_3 receptors present. Ins(1,4,5)P_3 will release Ca^{2+} from stores with a potency that depends on the number of Ins(1,4,5)P_3 receptors present, *e.g.* a large reserve of Ins(1,4,5)P_3 receptors would be expected to increase the potency of Ins(1,4,5)P_3-induced Ca^{2+} release compared to a system which lacked an Ins(1,4,5)P_3 receptor reserve. Alternatively, the amplification step between carbachol-stimulated Ins(1,4,5)P_3 generation and Ca^{2+} release may result from a positive feedback pathway, whereby Ca^{2+} may increase the sensitivity of Ins(1,4,5)P_3 receptors to activation by Ins(1,4,5)P_3 (Bezprozvanny *et al*, 1991; Pietri *et al*, 1990; Berridge, 1993). Such a theory is also hypothesized to explain Ca^{2+} spiking and oscillations in cells (Berridge, 1993; Putney and Bird, 1993).

Carbachol stimulation of CHO-vt9 cells (which express m3 muscarinic receptors at a density of approximately 300-400 fmol / mg protein) resulted in a significant reduction in % $^{45}Ca^{2+}$ release compared to CHO-m3 cells (expressing m3 muscarinic receptors at a density of approximately 1-2 pmol / mg protein). The reduction in maximal response in CHO-vt9 cells compared with CHO-m3 cells suggests that too few m3 muscarinic receptors are expressed in CHO-vt9 cells to maintain a maximal response to carbachol and this was accompanied by an apparent reduction in potency of carbachol to elicit $^{45}Ca^{2+}$ release. A similar response profile was observed with carbachol-stimulated Ins(1,4,5)P_3 generation (at 10 s) in CHO-vt9 cells compared with CHO-m3 cells, in which case the maximal Ins(1,4,5)P_3 accumulation in response to carbachol was reduced by approximately 50 % in CHO-vt9 cells compared with CHO-m3 cells (see chapter 6). However, as discussed above, the maximal carbachol-stimulated $^{45}Ca^{2+}$ release response in permeabilized CHO-vt9 cell suspensions may well increase with increases in cell number present, until a maximal response may be produced which is similar to that seen in permeabilized CHO-m3 cell suspensions, though with a different apparent potency for carbachol. Therefore, although it appears that there is little or no amplification between

carbachol-induced Ins(1,4,5)P_3 generation and $^{45}Ca^{2+}$ release in CHO-vt9 cells, such conclusions cannot be drawn using $^{45}Ca^{2+}$ release measurements from permeabilized cells in suspension.

In summary, the present study has shown that Ins(1,4,5)P_3 can enter permeabilized CHO cells resulting in the release of a large proportion (70-80 %) of $^{45}Ca^{2+}$ from vesicular stores. Similarly, Ins(1,4,5)P_3 generated by recombinant m1 and m3 muscarinic receptor activation produced a similar release of $^{45}Ca^{2+}$ from intracellular stores in permeabilized CHO cells. The release of $^{45}Ca^{2+}$ mediated by m1 and m3 muscarinic receptor activation was identical and PTX-insensitive, when receptors were expressed at a similar receptor density. Recombinant m2 receptor activation did not produce any $^{45}Ca^{2+}$ release in permeabilized CHO cells, either in the presence and absence of PTX pretreatment.

Carbachol-stimulated $^{45}Ca^{2+}$ release from permeabilized cells was affected by the cellular concentration of permeabilized cells used and, therefore, made comparisons of the potency of carbachol to elicit this response compared with other carbachol-mediated responses, difficult to interpret. The results do, however, suggest that an amplification step may exist between carbachol-stimulated Ins(1,4,5)P_3 generation and $^{45}Ca^{2+}$ release in permeabilized CHO-m1 cell suspensions. Further studies using fluorescent indicators (*i.e.* fura-2) in intact cells could be used to determine, with greater confidence, this apparent amplification step in the signalling cascade.

Figure 7.2.1. Time course for $^{45}Ca^{2+}$ uptake in permeabilized CHO cell clone suspensions.

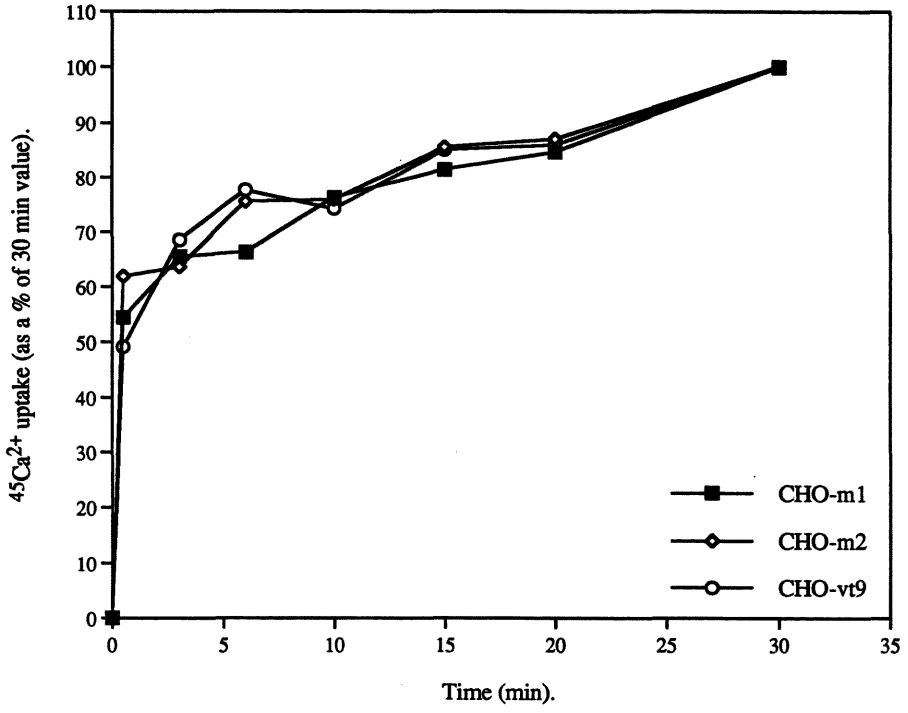

0.5 μCi / ml of $^{45}CaCl_2$ was added at time zero, to 3 ml of saponin permeabilized cells in suspension (0.5 mg of protein / ml), in cytosol-like buffer (CLB). Experiments were terminated by centrifugation through silicon oil mixture (see 7.1 Methods). Data is expressed as the % $^{45}Ca^{2+}$ uptake compared with the 30 min time point. Values represent the mean of two individual experiments.

Figure 7.2.2. Ins(1,4,5)P_3 (3 μM) stimulated $^{45}Ca^{2+}$ release time course in permeabilized CHO cell suspensions (0.5 mg protein / ml).

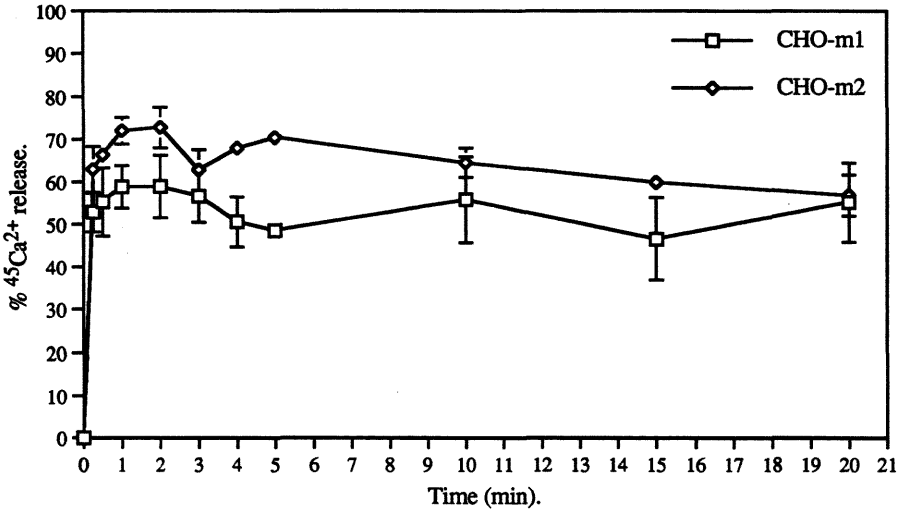

Figure 7.2.3. Ins(1,4,5)P_3 (100 nM) stimulated $^{45}Ca^{2+}$ release time course in permeabilized CHO cell suspensions (3 mg protein / ml).

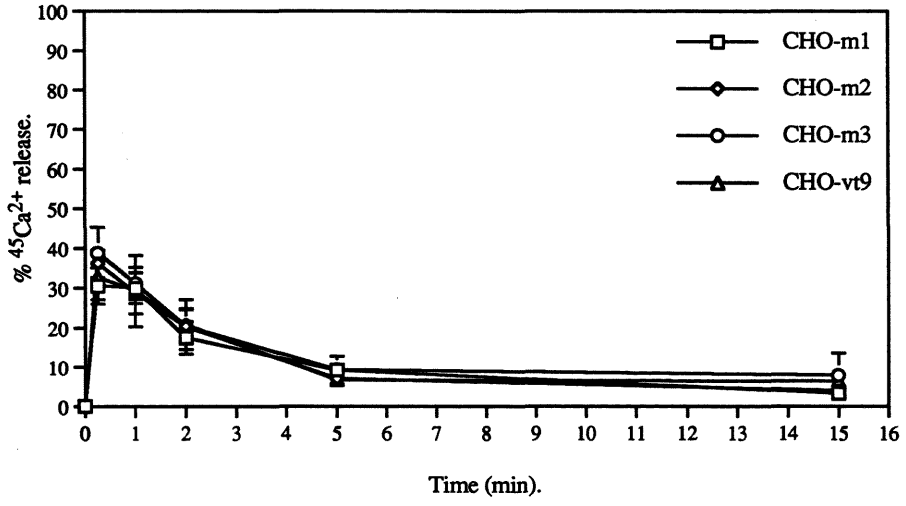

Saponin-permeabilized cell suspensions were loaded with $^{45}Ca^{2+}$ (0.5 μCi / ml) for 15 min prior to time zero. **Figure 7.2.2.** shows the $^{45}Ca^{2+}$ release profile in the presence of 3 μM Ins(1,4,5)P_3 in suspensions at a protein concentration of 0.5 mg / ml. **Figure 7.2.3.** shows the $^{45}Ca^{2+}$ release profile in the presence of 100 nM Ins(1,4,5)P_3 at a higher protein concentration of 3 mg / ml. Values represent the mean ± standard error of 3 individual experiments.

Figure 7.2.4. Ins(1,4,5)P_3-stimulated $^{45}Ca^{2+}$ release in permeabilized CHO cell suspensions (0.5 mg protein / ml).

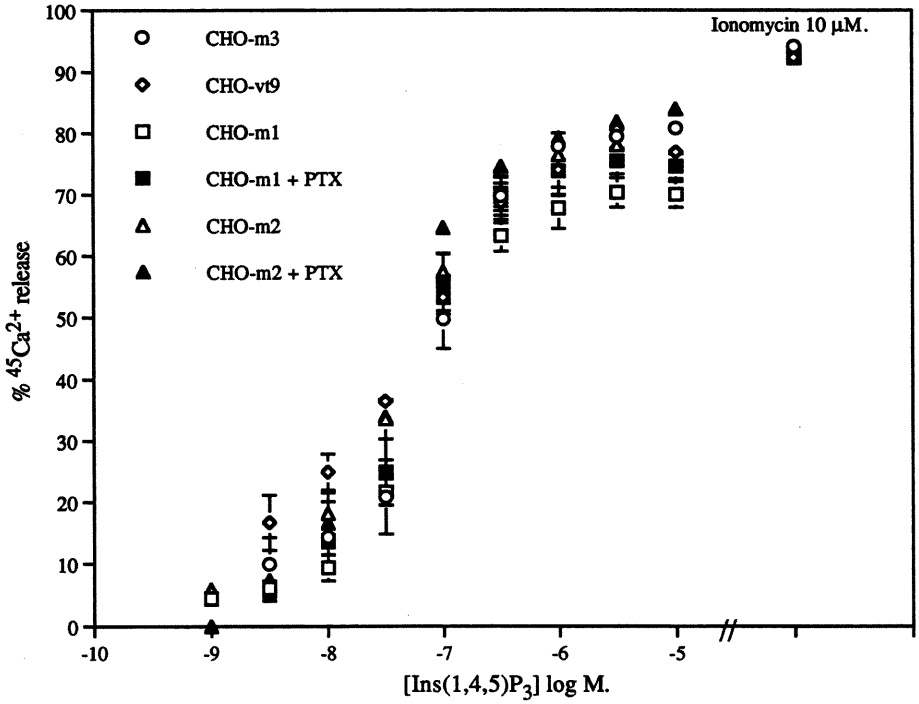

Figure 7.2.4. shows Ins(1,4,5)P_3 dose-response curves for $^{45}Ca^{2+}$ release after 1 min in saponin-permeabilized CHO cells which had been prelabelled with 0.5 µCi / ml $^{45}Ca^{2+}$ for 15 min. CHO-m1 and CHO-m2 cells were also pretreated with 100 ng / ml PTX for 20 hr prior to permeabilization of the cells with saponin. 10 µM Ionomycin released approximately 91 % of loaded $^{45}Ca^{2+}$ in each cell type. The graph shows mean ± standard error values of the individual points from a number of experiments (shown in parenthesis in **Table 7.2.1**).
Table 7.2.1 shows the maximal $^{45}Ca^{2+}$ release induced by Ins(1,4,5)P_3 and the EC_{50} (log M) derived from curve fitting of the data shown in **Figure 7.2.4.** Values are expressed as mean ± standard error of the number of experiments shown in parenthesis.

Table 7.2.1.	Max.response	EC_{50}(log molar values)	(n)
CHO-m3	80.3 ± 1.7	-7.21 ± 0.10	(4)
CHO-vt9	80.6 ± 1.2	-7.48 ± 0.03	(3)
CHO-m1	71.6 ± 2.0	-7.28 ± 0.05	(8)
CHO-m1 + PTX	76.0 ± 2.2	-7.33 ± 0.09	(3)
CHO-m2	78.1 ± 0.7	-7.42 ± 0.09	(5)
CHO-m2 + PTX	82.6	-7.42	(2)

Figure 7.2.5. Time course for (1 mM) carbachol-stimulated $^{45}Ca^{2+}$ release in electroporated CHO cell suspensions.

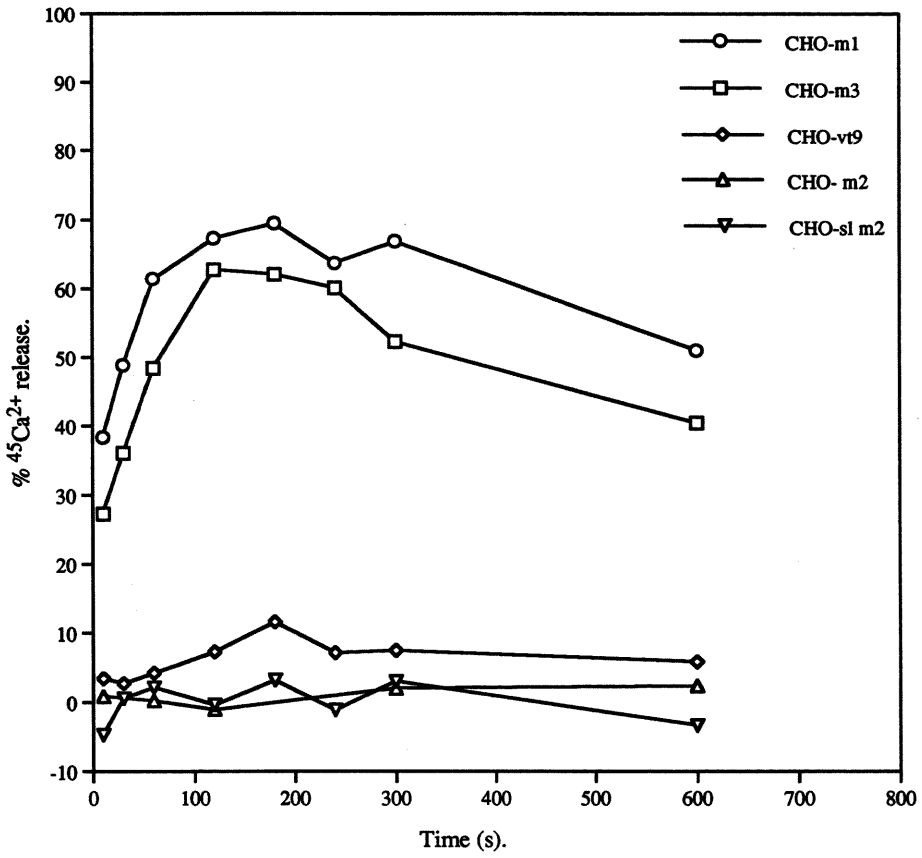

Figure 7.2.5. shows (1 mM) carbachol-stimulated $^{45}Ca^{2+}$ release in electroporated CHO cell suspensions (3 mg protein / ml). Time zero was set 15 min after cell suspensions were loaded with 0.5 μCi / ml $^{45}Ca^{2+}$. Data is expressed as the mean of two independent experiments performed in duplicate.

Figure 7.2.6. Carbachol-stimulated $^{45}Ca^{2+}$ release from electroporated CHO-m1, CHO-m2 and CHO-slm2 cell suspensions, in the presence and absence of PTX pretreatment.

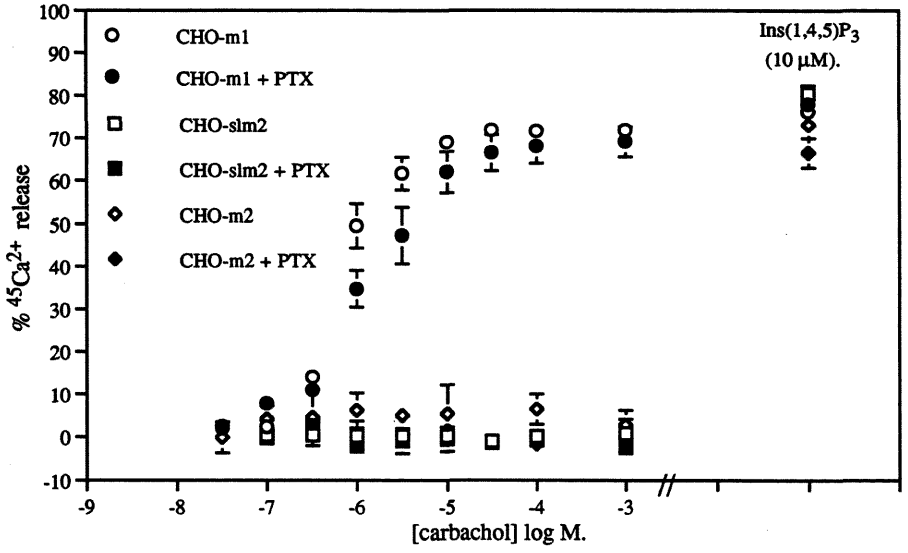

Figure 7.2.7. Carbachol-stimulated $^{45}Ca^{2+}$ release from electroporated CHO-m3 and CHO-vt9 cell suspensions, in the presence and absence of PTX pretreatment.

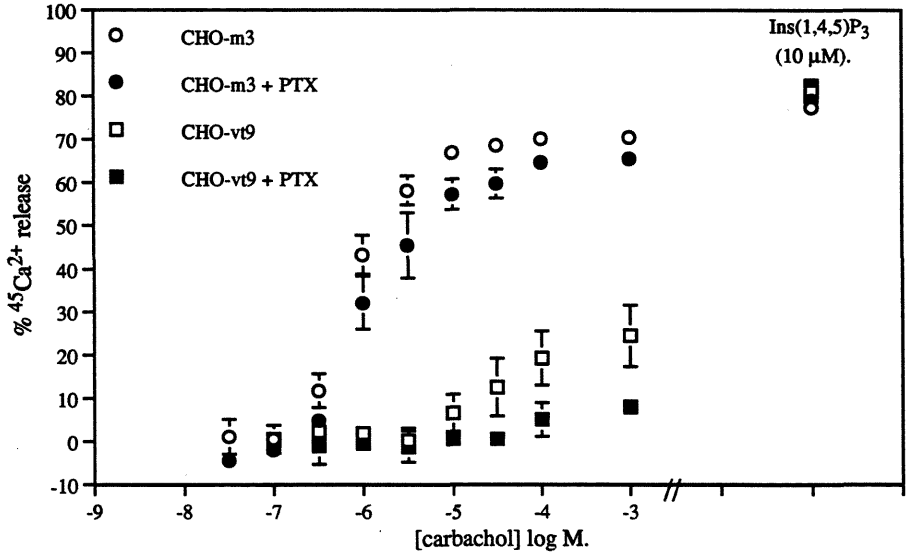

Figures 7.2.6 and 7.2.7 represent the mean ± standard error values of points from 3 individual experiments. Maximal $^{45}Ca^{2+}$ release and EC_{50} values were obtained from curve fitting analysis of the data and are shown in **Table 7.2.2.** 10 μM $Ins(1,4,5)P_3$ released $^{45}Ca^{2+}$ in electroporated CHO cell suspensions, to the same extent as in saponin permeabilized cells (see **Table 7.2.1**).

Table 7.2.2.

Values for maximal, carbachol-stimulated $^{45}Ca^{2+}$ release and EC_{50}s derived from curve fitting analysis of data from electroporated CHO cell suspensions, in the presence and absence of PTX pretreatment (shown in **Figure 7.2.6** and **Figure 7.2.7**).The table shows mean ± standard error values of 3 independent experiments.

* represents $p \leq 0.05$ for unpaired T-test analysis, between values from permeabilized CHO-m3 and PTX pretreated permeabilized CHO-m3 cell suspensions.

† represents $p \leq 0.05$ for unpaired T-test analysis between values obtained in permeabilized CHO-vt9 cell suspensions compared with values obtained in permeabilized CHO-m3 cell suspensions.

	maximal carbachol-stimulated % $^{45}Ca^{2+}$ release	**EC_{50} for carbachol (log molar values)**	**(n)**
CHO-m1	70.68 ± 2.03	-6.16 ± 0.04	(3)
CHO-m1 + PTX	69.17 ± 3.48	-5.88 ± 0.10	(3)
CHO-m3	69.46 ± 0.63	-6.11 ± 0.05	(3)
CHO-m3 + PTX	64.56 ± 1.08 *	-5.94 ± 0.14	(3)
CHO-vt9	23.94 ± 6.61 †	-4.57 ± 0.14 †	(3)

It was not possible to curve fit data from CHO-vt9 cell suspensions after PTX pretreatment, or CHO-m2, or CHO-slm2 cell suspensions in the presence and absence of PTX pretreatment, due to the absence of responses, or due to the relatively small responses, produced in these cell types.

CHAPTER EIGHT.

CARBACHOL-STIMULATED cAMP ACCUMULATION IN CHO CELL CLONES EXPRESSING RECOMBINANT MUSCARINIC RECEPTOR SUBTYPES.

8.0 Introduction.

Adenosine 3':5'-cyclic monophosphate (cAMP) accumulation in CHO cell clones expressing recombinant muscarinic receptor subtypes was initially studied in order to determine whether the recombinant m2 muscarinic receptors expressed in these cells coupled to adenylate cyclase (AC). PTX modification of agonist binding (see chapter 4) and carbachol-stimulated [^{35}S]GTPγS binding (see chapter 5) in CHO-m2 membranes suggested that these receptors were at least coupling to PTX-sensitive G proteins. It was also of interest to see whether m1 and m3 muscarinic receptors, expressed in CHO cells, also coupled to AC due to the partial PTX-sensitivity of carbachol-stimulated [^{35}S]GTPγS binding (see chapter 5) observed in CHO-m1 and CHO-m3 cell clones.

m2-Transformed CHO cells have been shown to couple to the inhibition of AC, attenuating forskolin-stimulated cAMP levels in a PTX-sensitive manner (Ashkenazi *et al*, 1987; Jones *et al*, 1991). Forskolin stimulates AC in membranes and in intact cells (Metzger and Lindner, 1981; Seamon *et al*, 1981). Forskolin was used in the present study to elevate cAMP levels so that receptor-stimulated inhibition of forskolin-stimulated cAMP accumulation could be assessed.

Muscarinic receptor-mediated increases in cAMP accumulation have also been observed in many studies and three hypotheses have been proposed to explain this phenomenon. Some groups (Baron and Siegal, 1989; Jansson *et al*, 1991; Felder *et al*, 1989) have suggested that the mechanism of activation of cAMP accumulation, via m1 and m3 receptors, is secondary to activation of PLC. PLC activation results in increases in Ca^{2+}/ calmodulin and PKC activation which can stimulate AC activity (Iyengar, 1993). Other groups have shown that receptors which do not primarily couple to G_s can do so at high levels of receptor expression (Eason *et al*, 1992). Alternatively, βγ subunits of G proteins may mediate muscarinic receptor-stimulated increases in cAMP accumulation (Tang and Gilman, 1991; Federman *et al*, 1992).

8.1. Methods.

8.1.1. Experimental Procedure.

CHO cells were harvested (as previously described in Chapter 2) and finally resuspended in Krebs-HEPES buffer, pH 7.4 (appendix 2) at a concentration of 1 flask of cells / 2 ml of buffer. Samples were taken, pelleted (16 000 g) and resuspended in 0.1 M NaOH. These samples were then stored at 4 °C for 24 hours at which time protein assays were performed.

Cell suspensions were warmed to 37 °C in a water bath, for 15 min, before

experiments were performed to allow cAMP levels in cells to reach a stable basal level. 85 µl of cell suspensions (approximately 500 µg of protein / tube) were added to decapped, 1.5 ml microcentrifuge tubes in a water bath, at 37 °C, in a final assay volume of 100 µl. Cells were incubated in the presence or absence of carbachol (10^{-3}M -10^{-8}M), forskolin (10 µM) and atropine (1µM) which were added to the reaction mixture in volumes of 5 µl. Incubations were terminated by the addition of 1 M TCA, after which, sample tubes were vortex mixed gently and kept on ice until samples were prepared for the cAMP assay. Carbachol dose-response curves were generated using a 3 min incubation of cells with increasing carbachol concentrations. Carbachol and atropine concentrations were prepared in Krebs-HEPES buffer, pH 7.4. Forskolin (200 µM stock) was prepared in Krebs-HEPES buffer, pH 7.4 containing 10 % DMSO. 5 µl aliquots of forskolin (10 µM final) were added to the final incubation volume of 100 µl so that DMSO comprised only 0.5% of the total volume.

8.1.2. Sample Preparation.

Samples generated from experiments were centrifuged at 16 000 g for 4 min and 160 µl of supernatant was removed and added to tubes containing 40 µl of (10 mM) EDTA and 200 µl of a mixture of 1,1,2-Trichlorotrifluoroethane (Freon) and Tri-n-octylamine (1:1). The Freon / Tri-n-octylamine was used to extract the TCA from the samples. The resulting mixture was vortex mixed and left for 15 min before being centrifuged at 16 000 g for 4 min. This resulted in the separation of two phases; the lower phase consisted of the Freon /Tri-n-octylamine plus the extracted TCA; the upper phase consisted of the water soluble fraction containing cAMP. 100 µl of the upper phase was removed from each sample and added to tubes containing 50 µl of (25 mM) $NaHCO_3$ which corrected the pH of the sample to pH 7.8. The prepared samples were then kept at 4 °C until cAMP binding assays were performed.

8.1.3. Preparation of Standards.

Unlabelled cAMP was diluted in ice-cold buffer consisting of 50 mM Tris base, 4 mM EDTA, pH 7.5, to a range of concentrations ranging from 200 nM cAMP (250 pmol / 50 µl) to 2.5 nM cAMP (0.125 pmol / 50 µl). 5 µM cAMP (250 pmol / 50 µl) was used to define non-specific binding.

8.1.4. Preparation of cAMP Binding Protein from Bovine Adrenal Cortical Membranes.

12-15 Bovine adrenal glands were collected fresh from the abattoir and placed on large petri dishes, on ice. Fat and connective tissue was removed from the glands which were then halved, demedullated and the cortex scraped into a pre-weighed beaker, on ice. 2 volumes of ice-cold buffer (50 mM Tris, 4 mM EDTA, pH7.4) were added and the mixture homogenized using a polytron tissue disrupter (level 6 for 10 x 5 second bursts). The homogenate was then filtered through 2 layers of muslin cloth and spun at 15 000 g for 15 min at 4 °C, in a refrigerated centrifuge. The supernatant was collected (avoiding fatty layer and pellet) and 500 µl aliquots were stored at -20 °C until use.

8.1.5. cAMP Binding Assay.

The cAMP binding assay is a competition assay between a single concentration of radiolabelled cAMP and unlabelled cAMP generated in the samples or present in the standards. Radiolabelled and unlabelled cAMP compete for binding to sites in the binding protein. These sites are probably the regulatory binding sites of protein kinase A. Each assay tube contained 50 µl of standard / sample, 100 µl of [^{3}H]cAMP (0.33 µCi / ml) and 150 µl of binding protein (diluted 30-fold in ice-cold buffer (50 mM Tris, 4 mM EDTA, pH 7.5).The assay tubes were then vortex mixed gently and left for > 90 min at 4 °C. Reactions were terminated by the addition of 250 µl of ice-cold charcoal / BSA mix (0.25 g of activated charcoal and 0.1 g BSA / 50 ml of buffer (50 mM Tris, 4 mM EDTA, pH 7.5)). Samples were immediately vortex mixed and left for exactly 7 min before being spun at 16 000 g for 4 min. The charcoal / BSA mix bound the free cAMP which was then pelleted after centrifugation. The supernatant contained the portion of cAMP which was bound to the binding protein. 500 µl of supernatant was taken and added to 5 ml of scintillant. Samples were then vortex mixed and left for 24 hours before being counted for radioactivity by liquid scintillation spectrometry.

8.1.6. Data Analysis.

Sample data (in dpm) were converted to cAMP mass (pmol / tube) by comparison with the standard curve. cAMP Mass was then converted to pmol / mg protein using the protein concentrations deduced from protein assays. These values were then multiplied by the dilution factor (7.5) which resulted from preparation of the samples, to give the concentration of cAMP generated in the experiments. EC_{50}, maximum and minimum values for carbachol dose-response curves were derived by computer-assisted curve fitting

(GraphPAD Software Inc. San Diego, CA). Data is expressed as the mean ± standard error of 3 individual experiments. Significant differences were assessed by T-test analysis where significance was set at $P \leq 0.05$.

8.2. Results

Carbachol (1 mM) produced no stimulation of cAMP accumulation above basal levels in CHO-m2, CHO-slm2 and CHO-vt9 cells (data not shown). Basal cAMP levels remained constant at approximately 2-5 pmol / mg protein for the 20 min incubation period.

10 μM Forskolin stimulated cAMP levels in the absence of carbachol in each of the CHO cell clone suspensions. Maximal, forskolin-stimulated cAMP accumulation occurred between 3 and 5 min incubation causing a 10-40 fold elevation in basal cAMP levels. This variability in the forskolin response made it difficult to analyze the effects of carbachol when co-incubated with forskolin, in time course experiments. Data from paired experiments were, therefore, normalized to the level of cAMP accumulation in the presence of 10 μM forskolin after 5 min incubation, in the absence of carbachol, in cells which were not pretreated with PTX.

Carbachol dose-response curves for cAMP accumulation, performed in CHO cell clone suspensions in the presence of forskolin, were also normalized to the forskolin-stimulated basal level of cAMP accumulation in the absence of PTX pretreatment, after 3 min incubation. In these experiments, PTX pretreatment of CHO cell clones resulted in an attenuation of forskolin-stimulated cAMP accumulation when compared, in paired experiments, with levels of forskolin-stimulated cAMP accumulation in cells which were not pretreated with PTX. Therefore, it was deemed more suitable to normalize the carbachol dose-response data in this way rather than simply express the data as the percentage stimulation of each forskolin-stimulated basal level.

CHO-m2 and CHO-slm2 Cells.

Carbachol (1 mM) attenuated forskolin-stimulated cAMP accumulation in CHO-m2 and CHO-slm2 cell suspensions, in the absence of PTX pretreatment (Figures 8.2.6 and 8.2.7). It was not possible to ascertain the time point at which the carbachol-mediated attenuation of forskolin-stimulated cAMP accumulation was maximal due to the coincidental elevation of cAMP accumulation induced by co-incubation with forskolin.

Carbachol dose-response curves for the attenuation of forskolin-stimulated cAMP accumulation were performed in CHO-m2 and CHO-slm2 cell suspensions after 3 min incubation (Figures 8.2.13 and 8.2.14). Maximal, carbachol-mediated attenuation of

forskolin-stimulated cAMP accumulation was 20-30% and approximately 90% in CHO-m2 and CHO-slm2 cell suspensions, respectively. EC_{50} values were not significantly different between CHO-m2 and CHO-slm2 cell clones (approximately 100-200 nM).

Co-incubation of CHO-slm2 cell suspensions with forskolin, 1 mM carbachol and 1 μM atropine still produced a significant attenuation of forskolin-stimulated cAMP accumulation (Figure 8.2.14). Carbachol may be a highly efficacious agonist in terms of its ability to attenuate forskolin-stimulated cAMP accumulation and, therefore, may produce a maximal response at very low levels of receptor occupancy. Atropine (1 μM) may reversibly deplete the number of receptors to which carbachol can bind by greater than 90% whilst having relatively little effect on the response produced.

Forskolin-stimulated cAMP accumulation in CHO-m2 and CHO-slm2 cells was attenuated after pretreatment of cells with PTX. In contrast to the attenuation of forskolin-stimulated cAMP accumulation induced by carbachol in untreated CHO-m2 and CHO-slm2 cells, carbachol (1 mM) potentiated forskolin-stimulated cAMP accumulation in PTX pretreated CHO-m2 and CHO-slm2 cells (Figures 8.2.6 and 8.2.7). Again it was not possible to define the time point at which the peak carbachol stimulation of cAMP accumulation occurred due to the coincidental elevations in cAMP accumulation induced by co-incubated forskolin.

Carbachol dose-response curves for cAMP accumulation, in PTX pretreated CHO-m2 and CHO-slm2 cells, after 3 minutes incubation, produced a maximal potentiation of forskolin-stimulated cAMP accumulation of approximately 1.5-fold and 3-fold above forskolin-stimulated basal levels, respectively (Figures 8.2.13 and 8.2.14). EC_{50} values were approximately 6 μM and 8 μM in CHO-m2 cells and CHO-slm2 cells, respectively.

Co-incubation of PTX pretreated CHO-m2 and CHO-slm2 cell suspensions with 1 mM carbachol and 1 μM atropine produced no significant potentiation of forskolin-stimulated cAMP accumulation above basal levels (Figures 8.2.13 and 8.2.14).

CHO-m1 and CHO-m3 Cells.

Carbachol (1 mM) stimulated cAMP accumulation in CHO-m1 and CHO-m3 cell suspensions, even in the absence of forskolin. Peak stimulation occurred after 3 min incubation (Figures 8.2.1 and 8.2.2) and was followed by a gradual attenuation of cAMP accumulation which still remained above basal levels after 20 min incubation, in the continued presence of carbachol. This apparent attenuation of carbachol-stimulated cAMP accumulation with time may have been produced by receptor desensitization (Tobin *et al*, 1992), down-regulation of AC activity via cAMP-dependent protein kinase (Iyengar, 1993), or via an increased activation of phosphodiesterases (PDEs).

PTX pretreatment of CHO-m1 and CHO-m3 cells resulted in similar time course

profiles for carbachol-stimulated cAMP accumulation.

Carbachol dose-response curves for cAMP accumulation, after a 3 min incubation with CHO-m1 and CHO-m3 cell suspensions, were performed and stimulations of cAMP accumulation of 199 ± 28 pmol / mg protein and 110 ± 24 pmol / mg protein, respectively, were achieved with 1mM carbachol (Figures 8.2.8 and 8.2.9). The comparative stimulations of cAMP accumulation induced by carbachol in CHO-m1 and CHO-m3 cells were not significantly different (by paired T-test analysis where significance was set at $p \leq 0.05$). EC_{50} values were greater than or equal to approximately 100 μM in both CHO-m1 and CHO-m3 cell suspensions.

Co-incubation of CHO-m1 and CHO-m3 cell suspensions with 1 mM carbachol and 1 μM atropine did not produce any significant stimulation of cAMP accumulation above basal levels. Carbachol-stimulated cAMP accumulation in CHO-m1 and CHO-m3 cell suspensions was not significantly affected by PTX pretreatment of the cells (Figure 8.2.8 and 8.2.9).

Incubation of CHO-m1 or CHO-m3 cell suspensions with either 1 mM carbachol or 10 μM forskolin increased cAMP accumulation to levels of approximately 50-200 pmol / mg protein from a basal level of approximately 2-5 pmol / mg protein (Figures 8.2.3, 8.2.4, 8.2.10 and 8.2.11). Co-incubation of CHO-m1 or CHO-m3 cell suspensions with carbachol and forskolin produced elevations of cAMP accumulation that were more than additive, especially after pretreatment of the cells with PTX (approximately 1000 pmol / mg protein in CHO-m1 cells; approximately 600 pmol / mg protein in CHO-m3 cells) (Figures 8.2.10 and 8.2.11). Pretreatment of CHO-m1 and CHO-m3 cells with PTX, also reduced the basal level of forskolin-stimulated cAMP accumulation by approximately 50 %.

EC_{50} values (of approximately 14-26 μM) and maximal responses for carbachol-mediated potentiation of forskolin-stimulated cAMP accumulation were not significantly different between CHO-m1 cells and CHO-m3 cells, in the presence or absence of PTX pretreatment (by paired T-test analysis where significance was set at $p \leq 0.05$). Higher concentrations of carbachol produced large variations in the cAMP response between experiments resulting in large standard error values. Although not significantly different, the trend of the data suggests that carbachol responses in CHO-m1 cells were greater than in CHO-m3 cells and that responses in PTX pretreated CHO-m1 and CHO-m3 cells were greeter than in untreated CHO-m1 and CHO-m3 cells (Figures 8.2.10 and 8.2.11).

Co-incubation of CHO-m1 and CHO-m3 cell suspensions with 1 mM carbachol and 1 μM atropine produced no significant potentiation of forskolin-stimulated cAMP accumulation.

CHO-vt9 Cells.

Carbachol (1 mM) was shown to slightly potentiate forskolin-stimulated cAMP accumulation in CHO-vt9 cell suspensions (Figure 8.2.5). Carbachol dose-response curves in CHO-vt9 cells produced only a small potentiation of forskolin-stimulated cAMP accumulation in the absence of PTX pretreatment and the EC_{50} value for this response could not be determined by curve fitting (Figure 8.2.12). In PTX pretreated CHO-vt9 cells, forskolin-stimulated cAMP accumulation was attenuated by approximately 50%. Carbachol maximally potentiated the forskolin-stimulated cAMP response in PTX pretreated CHO-vt9 cells by 2-fold with an EC_{50} of approximately 65 μM. Co-incubation of PTX pretreated CHO-vt9 cell suspensions with 1 mM carbachol and 1 μM atropine produced no potentiation of forskolin-stimulated cAMP accumulation (Figure 8.2.12).

8.3 Discussion.

Stimulation of m2 and m4 muscarinic receptors, has been shown to attenuate AC activity in cells (Ashkenazi *et al*, 1987; Jones *et al*, 1991). However, it is becoming increasingly apparent that m1 and m3 muscarinic receptors, which couple primarily to the activation of PLC, can also modulate AC activity (Baron and Siegal, 1989; Jansson *et al*, 1991; Fraser *et al*, 1989; see reviews by Caulfield, 1994; Hulme *et al*, 1984). The effects of m1, m2 and m3 muscarinic receptor stimulation were studied in CHO cell clones to investigate possible modulation of AC activity via these muscarinic receptor subtypes.

Carbachol was equally potent at inhibiting forskolin-stimulated cAMP accumulation in CHO-m2 and CHO-slm2 cells, which express m2 muscarinic receptors. These inhibitory responses were abolished after pretreatment of cells with PTX, strongly suggesting that the cAMP attenuation was mediated by G_i family G proteins, inhibiting AC activity. Gerhardt and Neubig (1991) have shown that activation of recombinant α_2-adrenergic receptors expressed in CHO-K1 cells can inhibit AC via at least two subtypes of G_i proteins and they provided the first evidence of functional involvement of $G\alpha_{i3}$ in the inhibition of AC. Similarly, Peralta's group have shown that recombinant m2 muscarinic receptors expressed in CHO cells can couple with $G\alpha_{i2}$ and $G\alpha_{i3}$ (Dell'Acqua *et al*, 1993).

The intrinsic activity of carbachol to produce inhibition of AC was dependent on the expression level of m2 receptors in these two cell clones. CHO-m2 cells (which express approximately 100 fmol of receptor / mg protein), produced a 20% maximal attenuation of forskolin-stimulated cAMP accumulation. CHO-slm2 cells (which express approximately 300-400 fmol of receptor / mg protein), produced a 90% maximal

attenuation of forskolin-stimulated cAMP accumulation. Classical receptor theory dictates that a decrease in the number of receptors should be accompanied by a decrease in potency and, when the receptor reserve has been exhausted, by a subsequent decrease in the maximal responsiveness of the agonist, with no further shift in potency. In the absence of receptor reserve, receptor inactivation should lead to a gradual decrease in the maximal response to the agonist without affecting its potency. Therefore, according to classical receptor theory, there appears to be no receptor reserve in CHO-m2 and CHO-slm2 cells. However, at the point where full receptor occupancy is required to produce a maximal response, the occupancy and response curves for the full agonist should overlap. In chapter 4, carbachol binding curves were generated in CHO-m2 cell membranes by displacement [^{3}H]NMS binding, in the presence of guanine nucleotides. Although this experiment can only be used to estimate the carbachol-occupancy curve, it is clear that the occupancy curve lies approximately two log units to the right of the response curve shown in this study. In contrast, m3 muscarinic receptors coupled to PLC activation have very similar potency, occupancy-response curves for carbachol, in the absence of receptor reserve (compare CHO-vt9 binding curves in chapter 4 with Ins(1,4,5)P_3 mass generation curves in CHO-vt9 cells in chapter 6). It would appear that classical receptor theory cannot explain the response curves generated by G_i-coupled m2 receptors in CHO cells.

Many studies, which have used different expression levels of recombinant 5-HT_{1A} receptors in transfected cell lines, have found similar anomalies whereby occupancy-response curves for agonists could not be explained by classical receptor theory (Hoyer *et al*, 1993). Varrault *et al* (1992) using NIH-3T_3 cells expressing a range of densities of recombinant, human 5-HT_{1A} receptors showed that agonist stimulation also resulted in an inhibition of forskolin-stimulated cAMP accumulation. This group showed that the full agonist 5-HT produced larger maximal responses in cells expressing higher densities of 5-HT_{1A} receptors. However, they also observed no apparent change in potency of this response. They similarly concluded that their results could not be explained by the classical model of drug-receptor action.

PTX-pretreatment of CHO-m2 and CHO-slm2 clones abolished the receptor-mediated attenuation of forskolin-stimulated cAMP accumulation and resulted in a receptor-mediated potentiation of forskolin-stimulated cAMP accumulation. Carbachol stimulation of CHO-slm2 cells produced a maximal 3-fold increase in forskolin-stimulated cAMP accumulation compared with a maximal 1.5-fold increase in CHO-m2 cells. This suggests that the level of cAMP accumulation induced by carbachol was proportional to the increased expression levels of m2 receptors in CHO-slm2 compared with CHO-m2 cells. The changes in receptor expression did not significantly effect the potency of carbachol to elicit these responses in CHO-slm2 and CHO-m2 cells. The decrease in the maximal response to carbachol with decreasing receptor expression, without having a significant

affect on the potency of carbachol, is indicative of a system which lacks an apparent receptor reserve.

Other groups have observed similar attenuation and potentiation of cAMP accumulation via agonist stimulation of recombinant m4 muscarinic receptors (Jones *et al*, 1991) and recombinant α_2 adrenoceptors (Eason *et al*, 1992; Fraser *et al*, 1989) expressed in CHO cells. In each case, biphasic cAMP accumulation dose-response curves were produced. At lower concentrations of agonist, forskolin-stimulated cAMP accumulation was dose-dependently attenuated, but at higher concentrations of agonist, forskolin-stimulated cAMP accumulation was potentiated. In each case, PTX pretreatment abolished the agonist-mediated attenuation of forskolin-stimulated cAMP accumulation revealing the agonist-mediated potentiation of forskolin-stimulated cAMP accumulation.

The biphasic nature of these responses were due to the relatively higher potency of the agonists to induce attenuation of cAMP accumulation compared with potentiation of cAMP accumulation. Similar potency differences were observed in the present study with CHO-m2 cells (approximately 30-fold) and with CHO-slm2 (approximately 80-fold).

In the present study, however, carbachol-mediated potentiation of forskolin-stimulated cAMP accumulation was only observed after PTX pretreatment (*i.e.* no biphasic response was seen in the absence of PTX pretreatment). A possible explanation for this discrepancy comes from studies by Eason *et al* (1992) and Jones *et al* (1991) who found that the agonist-mediated potentiation of cAMP accumulation was dependent on the expression levels of receptors in CHO cells, whereas the agonist-mediated attenuation of cAMP accumulation was relatively unaffected by receptor expression levels. Perhaps the expression levels of m2 muscarinic receptors expressed in CHO-m2 and CHO-slm2 cells were not sufficiently high to induce the level of agonist-mediated potentiation of cAMP accumulation necessary to observe a biphasic response. Alternatively, m4 receptors may differ from m2 receptors in terms of their ability to stimulate cAMP levels in CHO cells.

The mechanism by which carbachol stimulation of PTX pretreated CHO-m2 and CHO-slm2 cells potentiates forskolin-stimulated cAMP accumulation, can only be speculated at the present time. One possibility is that the m2 receptors in CHO cells may couple weakly to G_s proteins which then activate AC.

No significant carbachol-stimulated [^{35}S]GTPγS binding was observed in CHO-m2 membranes after PTX pretreatment (see chapter 5), suggesting that the small carbachol potentiation of forskolin-stimulated cAMP accumulation, after PTX pretreatment, in CHO-m2 cells was not mediated by a G_α subunit. Alternatively, it may be argued that a weak association of G_s with m2 muscarinic receptors in CHO-m2 cells may not have been resolved against the relatively high basal [^{35}S]GTPγS binding observed in these

experiments (chapter 5). It is also possible that a weak association of G_s with m2 receptors was lost during membrane preparation in [^{35}S]GTPγS binding experiments.

From the literature, there is evidence that single receptor subtypes may couple to more than one G protein (Paulssen *et al*, 1992; Yamada *et al*, 1993; Dai *et al*, 1991; Richards, 1991; Mohuczy-Dominiak and Garg, 1992; Fargin *et al*, 1989; Ashkenazi *et al*, 1987).

For instance, Eason *et al* (1992) have shown that recombinant α_2-adrenoceptors, in membrane preparations from transfected CHO cells, can couple simultaneously to G_i and G_s producing biphasic agonist (UK-14304) dose-response curves for AC activity. Pretreatment of the cells (expressing α_2-adrenoceptors) with PTX abolished the inhibition of AC activity whereas CTX pretreatment abolished the stimulation of AC activity. This suggested that the former event was mediated by $G\alpha_i$ and the latter by $G\alpha_s$. UK-14304-stimulated AC activity was also reduced in the presence of antisera directed against the carboxy-terminal portion of Gs_α. Agonist-receptor-Gs_α complex was immunoprecipitated with a specific α_2 antibody and the Gs_α component was recognized by western blots using Gs_α antibody, and CTX-mediated ADP-ribosylation.

The dependency of the agonist-mediated potentiation of cAMP accumulation on receptor expression levels suggested that α_2-adrenoceptors were becoming more promiscuous with G_s proteins as receptor expression levels were increased (Eason *et al*, 1992).

A second possible mechanism for m2 receptor-mediated potentiation of cAMP accumulation, observed in the present study in PTX pretreated CHO-m2 and CHO-slm2 cells, might be via crosstalk with activation of other effector systems. For instance, PLC activation results in increased concentrations of intracellular Ca^{2+} and DAG which can in turn lead to activation of AC via Ca^{2+}/calmodulin and PKC (Iyengar, 1993). However, $^{45}Ca^{2+}$ release studies in permeabilized CHO-m2 and CHO-slm2 cells (chapter 7) showed no agonist-stimulated $^{45}Ca^{2+}$ release from these permeabilized cells. Also, no Ins(1,4,5)P_3 mass accumulation was detected in CHO-m2 cells (chapter 6). Similarly, Jones *et al* (1991) suggested that the agonist-mediated elevations in cAMP accumulation observed in PTX pretreated m4-transformed CHO cells did not occur as a consequence of PLC activation due to the lack of PI-hydrolysis observed.

Fraser *et al* (1989) found that the agonist-mediated potentiation of cAMP accumulation observed in CHO cells expressing recombinant α_2 adrenoceptors could be inhibited by the PLA_2 inhibitor, quinocrine. They suggested that the agonist-mediated potentiation of cAMP accumulation was a consequence of PLA_2 activation. The mechanism by which PLA_2 activation can lead to AC activation is not known.

Carbachol-stimulation of recombinant m1 and m3 muscarinic receptors expressed in CHO cells, at relatively high receptor densities (1-2 pmol / mg protein), led to large increases in cAMP accumulation, in intact cells, with an EC_{50} value of $\geq$ 100 μM. Elevations in cAMP accumulation were PTX-insensitive and could be detected in the absence of forskolin. Carbachol stimulation of CHO-vt9 cells, which express m3 receptors at approximately 300 fmol / mg protein, did not produce any detectable increase in cAMP accumulation in the absence of forskolin. These results are similar to those obtained in another study (Jones *et al*, 1991) where, in the presence of 1mM IBMX (a phosphodiesterase inhibitor), CHO cells expressing m3 receptors (between 0.9-2 pmol / mg protein) produced a PTX-insensitive, greater than 10-fold, carbachol stimulation of cAMP accumulation with an EC_{50} value of > 200μM. Surprisingly, m5 receptor stimulation (at a similar expression level to the m3 receptors) resulted in only a 2-fold stimulation of cAMP accumulation despite similar carbachol-stimulated activation of PI hydrolysis and a K^+ conductance (Jones *et al*, 1991).

Co-incubation of CHO-m1 and CHO-m3 cells with carbachol, in the presence of 10 μM forskolin, increased the potency and maximal responsiveness of carbachol to increase cAMP accumulation. One possible explanation for this apparent synergy between receptor- and forskolin-activation of AC might be that receptor activation results in activation of Gs_α. Many studies have shown that stimulation of AC activity by forskolin and Gs_α is synergistic (Seamon and Daly, 1986). Activated Gs_α increases the proportion of high affinity forskolin binding sites (Nelson and Seamon, 1985; Seamon and Daly, 1985), and increases the potency and maximal responsiveness of forskolin-stimulated AC activity (Seamon and Daly, 1986; Daly, 1984). Similarly, forskolin has also been shown to markedly potentiate hormonal-activation of AC (Daly *et al*, 1982). Forskolin, in many systems, can increase the potency and maximal responsiveness of the receptor agonist to stimulate AC activity (Daly, 1984; Seamon and Wetzel, 1984). Evidence to date suggests that the co-operative interaction between Gs_α and forskolin occurs at, or closely associated with, the catalytic site of AC. This has been shown in solubilized preparations where GppNHp-activated Gs_α and forskolin produced a markedly synergistic activation of the catalytic subunit of AC (Bender and Neer, 1983). There is relatively little evidence to suggest that forskolin potentiates receptor-mediated AC activity by an interaction at the receptor level though Darfler *et al* (1982) did show an increase in the proportion of high affinity agonist binding sites for β-adrenoceptors, in the presence of forskolin, in intact lymphoma cells.

Receptor activation of Gs_α might explain the shift in potency and maximal responsiveness of carbachol, in the presence of forskolin, seen in this study. This view could be extended to suggest that the "factor" which activates AC via m1 and m3 receptor activation in this study (whether it be Gs_α or not), may be more potent and/or efficient at

activating AC, in the presence of forskolin.

PTX pretreatment of all the cell clones attenuated forskolin-stimulated cAMP accumulation (discussed in more detail later in this section). PTX pretreatment also increased the sensitivity of AC to receptor stimulation by carbachol, in the presence of forskolin. This was most clearly seen in the CHO-vt9 clone and suggests that AC activity is tonically under inhibition by G_i. However, carbachol stimulation of CHO-m1 and CHO-m3 cells, in the absence of forskolin, produced large, PTX-insensitive increases in cAMP accumulation, suggesting that tonic inhibition of AC activity by G_i was either not present or was overwhelmed by receptor-mediated stimulation of AC activity.

Alternatively, an unknown interaction between AC, forskolin and PTX might mediate the initial attenuation of forskolin-stimulated AC activity and the subsequent sensitivity of AC to receptor activation.

In the present study there appears to be a correlation between levels of expression of the m3 muscarinic receptor subtype and maximal cAMP accumulation in the presence of forskolin and after PTX pretreatment. CHO-m3 cells (expressing receptors at $\geq$ 1 pmol / mg protein) produced large increases in cAMP accumulation (>10-fold), in response to carbachol. Lowering the expression level of m3 receptors, as in CHO-vt9 cells (approximately 300 fmol / mg protein), resulted in a 2-fold increase in carbachol-stimulated cAMP accumulation.

Jones *et al* (1991) suggested that the receptor density expressed in CHO cells was an important factor in determining the extent of carbachol-stimulated cAMP levels. Relatively low expression m1-transformed CHO cells (0.1-0.2 pmol / mg protein) produced a less than 2-fold stimulation of cAMP accumulation in the presence of carbachol. Identical stimulation of high expression m1-transformed CHO cells (2 pmol / mg protein) resulted in a >10-fold increase in cAMP levels (EC_{50} > 200 μM).

The differential effects of m3 and m5 receptor stimulation on cAMP accumulation in CHO cells observed by Jones *et al* (1991) suggests that m1, m3 and m5 receptors may activate multiple effector systems differentially, explaining the existence of three receptor subtypes all seemingly producing an identical activation of PLC.

In the present study, comparisons can be made between the cAMP accumulation responses evoked by carbachol stimulation of m2 muscarinic receptors, in CHO-slm2 cells, and m3 muscarinic receptors, in CHO-vt9 cells. These cell clones express similar densities of muscarinic receptors, but, in the presence of PTX pretreatment, the m2 muscarinic receptor stimulation evoked a 3-fold potentiation of forskolin-stimulated cAMP accumulation, whilst m3 muscarinic receptor activation resulted in a 2-fold

potentiation of forskolin-stimulated cAMP accumulation. This suggests that m2 muscarinic receptors may couple more efficiently to the potentiation of forskolin-stimulated cAMP accumulation than m3 muscarinic receptors.

One possible mechanism for the receptor-mediated increase in cAMP accumulation observed in the present study could be that m1 and m3 muscarinic receptors are able to couple to G_s as well as to G_q. The thyrotrophin-releasing hormone (TRH) receptor expressed by rat pituitary tumour GH_3 cells activates PLC-β via the G_q family of G proteins (Aragay *et al*, 1992). However, TRH is also able to stimulate AC activity in membranes of GH_3 cells. Paulssen *et al* (1992) have shown that antisera directed against Gs_α causes a substantial inhibition of TRH-stimulated AC activity, suggesting that a receptor is capable of coupling to G_q and G_s. Furthermore, recombinant neurotensin receptors expressed in CHO cells couple primarily to PI hydrolysis but have also been shown to activate AC, even in membrane preparations (Yamada *et al*, 1993). Therefore, a number of receptor types which couple primarily to G_q may also be able to couple (less efficiently) to G_s.

M_3 muscarinic receptors expressed endogenously in rat parotid gland (Dai *et al*, 1991) and in Madin-Darby canine kidney (MDCK) cells (Mohuczy-Dominiak and Garg, 1992) have been shown to couple to PI hydrolysis and to inhibit forskolin-stimulated AC activity. The inhibition of AC activity was PTX-sensitive and the potencies of various antagonists to block agonist-induced inhibition of AC activity were consistent with the agonist acting via M_3 receptors. These results suggest that M3 receptors, endogenously expressed in these tissues, can couple to both PTX-sensitive and PTX-insensitive G proteins.

Agonist stimulation of m1 or m3 receptors (in CHO-m1 and CHO-m3 cells, respectively) in the present study, did not result in any inhibition of forskolin-stimulated cAMP accumulation despite the fact that carbachol-stimulated [^{35}S]GTPγS binding in these cell membranes showed some degree of PTX-sensitivity (see chapter 5). It remains a possibility that the fraction of PTX-sensitive G proteins that couple with m1 and m3 receptors may not modulate AC activity (*e.g.* G_o).

Another possible mechanism for the elevation of cAMP accumulation seen in this study is one involving the βγ subunits of G proteins. βγ subunits can activate type 2 and type 4 AC in the presence of activated Gs_α (Tang and Gilman,1991; Federman *et al*,1992), and inhibit activity of type 1 AC (Clapham and Neer, 1993). Similarly, βγ subunits have also been found to mediate PLC-β activation (Park *et al*, 1993) in an isozyme-selective manner, and in the absence of activated Gq_α. G protein βγ subunits were approximately 20-fold less potent at stimulating types 2 and 4 AC than was Gs_α (Tang and Gilman, 1991). Similar potency differences exist between Gq_α and βγ

stimulation of PLC-β activity.(Park *et al*, 1993).

The isoforms of AC present in CHO cells is not known but types 2 and 4 AC have been detected in peripheral tissues (Iyengar, 1993). βγ subunits, released from PTX-insensitive G proteins upon agonist stimulation , may therefore mediate the low potency stimulation of cAMP accumulation seen in this study. Again, a high degree of receptor occupancy would be required to release sufficient βγ subunits to stimulate AC activity and may explain the lack of response in CHO-vt9 cells compared with CHO-m3 cells.

The similarities in experimental methods between the present study and the detection of $Ins(1,4,5)P_3$ accumulation (see Chapter 6) allows data from these two studies to be compared. Maximal $Ins(1,4,5)P_3$ accumulation occurred, in CHO-m1 and CHO-m3 cells, in the presence of approximately 30 μM carbachol. This suggests that cytosolic calcium concentrations would also be maximal in the presence of this concentration of carbachol. The $^{45}Ca^{2+}$ release studies in permeabilized CHO-m1 and CHO-m3 cells (see Chapter 7) suggest that this is the case, with maximal $^{45}Ca^{2+}$ release occurring in the presence of 10 μM carbachol. Although the $^{45}Ca^{2+}$ release studies were performed using totally different buffers and permeabilized cells in the absence of added guanine nucleotides, an increased potency of carbachol-stimulated Ca^{2+} release would be expected compared to carbachol-stimulated $Ins(1,4,5)P_3$ accumulation as found in permeabilized SH-SY5Y cells (Wojcikiewicz *et al*, 1990). $^{45}Ca^{2+}$-release studies in the presence of guanine nucleotides (Safrany and Nahorski, 1994) produced an increase in potency of carbachol to elicit $^{45}Ca^{2+}$ release in permeabilized SH-SY5Y cells. Fura-2 studies of changes in cytosolic Ca^{2+} concentration upon stimulation of CHO-m3 cells with carbachol (Willars and Nahorski, submitted for publication) resulted in a maximal, plateaux Ca^{2+} response in the presence of approximately 10 μM carbachol.

Incubations of CHO-m1 and CHO-m3 cells with 30 μM carbachol produced only a threshold stimulation of cAMP accumulation, although this concentration of carbachol produced maximal increases in $Ins(1,4,5)P_3$ accumulation and Ca^{2+} flux. This suggests that a crosstalk mechanism involving elevations in cytosolic Ca^{2+} concentration is unlikely to be the mechanism by which m1 and m3 receptor stimulation leads to increases in cAMP accumulation. In m3-transformed CHO cells (Jones *et al* , 1991), carbachol stimulation produced dose-response relationships for PI metabolism and cAMP accumulation that differed by greater than 100-fold again suggesting that cAMP accumulation could not have been mediated via PLC activation. Furthermore, only type 1 and type 3 AC are stimulated by Ca^{2+}/calmodulin (Tang *et al*, 1991; Choi *et al*, 1992); type 1 AC is thought to be localized in neuronal tissue and is, therefore, unlikely to be found in these fibroblast cell clones. Type 3 AC is abundantly found in olfactory epithelia but has also been detected in lung and is, therefore, a possible candidate for Ca^{2+}/calmodulin activation of AC in peripheral tissues.

Stimulation of pharmacologically characterized M_3 muscarinic receptors endogenously expressed in SK-N-SH cells (Baron and Siegal, 1989) and M_1 receptors endogenously expressed in SH-SY5Y neuroblastoma cells (Jansson *et al*, 1991) has also been shown to induce elevations in cAMP accumulation. Receptor densities in these two cell lines were 0.1-0.3 pmol / mg protein and the stimulation of cAMP accumulation was relatively small (less than two-fold). In both cases, EC_{50} values for carbachol-stimulated cAMP accumulation were between 1-20 μM, similar to the K_i for carbachol binding (Baron and Siegal, 1989), or similar to the EC_{50} value for carbachol-stimulated increases in intracellular Ca^{2+} (Jansson *et al*, 1991). Many studies have shown that m1 and/or m3 muscarinic receptor stimulation can potentiate cAMP accumulation in a manner whereby agonist dose-response curves for cAMP accumulation were similar to agonist-stimulated increases in intracellular Ca^{2+} (Jansson *et al,* 1991), or inositol phosphate accumulation (Felder *et al*, 1989; Peralta *et al*, 1988). In these studies, cAMP accumulation was shown to be secondary to an increase in Ca^{2+} / calmodulin and/or PKC activation resulting from receptor-mediated activation of PLC.

This hypothesis has been challenged by Baumgold (Baumgold *et al*, 1992; Baumgold, 1992) who found that carbachol-stimulated cAMP accumulation in SK-N-SH cells was not effected in the presence of BAPTA which was shown to abolish carbachol-stimulated elevations in intracellular Ca^{2+}. Similarly, pre-exposure of the cells to a dose of carbachol in a low Ca^{2+}-containing medium, depleted Ca^{2+} stores so that a further dose of carbachol did not increase intracellular levels of Ca^{2+}. However, both challenges with carbachol produced a stimulation of cAMP accumulation. Baumgold (1992) also suggested that the carbachol-stimulated cAMP response was unlikely to be mediated via PKC activation because in SK-N-SH cells, PKC can be completely down-regulated without significantly affecting the receptor-mediated increase in cAMP accumulation (Baumgold and Fishman, 1989).

The present study has shown that high concentrations of carbachol (>30 μM) can induce large elevations in cAMP accumulation in intact CHO-m1 and CHO-m3 cells. Increased activation of PKA resulting from elevated cAMP levels may modulate other effector pathways. For instance, cAMP-dependent phosphorylation of a brain inositol trisphosphate receptor has been shown to decrease its release of Ca^{2+} (Supattapone *et al,* 1988). Similarly, elevated cAMP levels has been shown to attenuate histamine-induced release of intracellular Ca^{2+} in the hamster vas deferens smooth muscle cell line DDT_1MF-2 (Dickenson *et al*, 1993). These 'crosstalk' activities induced by elevated cAMP levels should be taken into account when investigating effector mechanisms in CHO-m1 and CHO-m3 cells. Elevated cAMP levels in these CHO clones only occurs at

high concentrations of carbachol, so any 'crosstalk' activity will only be observed at concentrations of carbachol above 30 μM. This concentration of carbachol is sufficient to induce maximal Ins(1,4,5)P_3 accumulation and $^{45}Ca^{2+}$ release in CHO-m1 and CHO-m3 cells (see chapters 6 and 7) which appeared to be unaffected by further increases in carbachol concentration.

The variability in forskolin-stimulated cAMP accumulation seen in this study between cell clones and between experiments cannot be explained and requires further investigation. Assuming that G-protein and effector systems are unaffected by the transfection of cDNA encoding muscarinic receptor subtypes (which has not been established), into CHO cells, then the only reason for changes in the level of the forskolin response can be the differences in expression levels of the different muscarinic receptors found in these cell clones.

Forskolin-stimulated cAMP accumulation is highly sensitive to inputs from both G_s and G_i (Seamon and Daly, 1986). In the absence of agonist, these receptors would have to have some constitutive activity in order to affect AC activity (Lefkowitz *et al*, 1993). Constitutive activity of m2 receptors and hence activation of G_i proteins should, if anything, lead to a reduction in forskolin-stimulated cAMP accumulation as receptor number was increased. This was not the case in the present study, where CHO-slm2 cells produced larger elevations of forskolin-stimulated cAMP accumulation than did CHO-m2 cells.

An additional problem with interpretation of the data from this study, was the consistent attenuation of forskolin-stimulated cAMP accumulation after PTX pretreatment, seen in all of the CHO clones studied. Data from paired experiments (in the presence and absence of PTX pretreatment) were, therefore, expressed as the % of forskolin-stimulated cAMP accumulation in the absence of PTX pretreatment. If each experimental result was expressed as a % of its own forskolin-stimulated cAMP level, then this would have resulted in clear differences between agonist-stimulated cAMP responses in forskolin-stimulated CHO-m1 and CHO-m3 cells in the presence and absence of PTX pretreatment. This deduction was not found to be the case when results from paired experiments were expressed as the % of forskolin-stimulated cAMP accumulation in the absence of PTX pretreatment. Carbachol-stimulated cAMP accumulation in the absence of forskolin, in CHO-m1 and CHO-m3 cells, was insensitive to PTX pretreatment supporting this interpretation of these results.

One, purely speculative explanation for the attenuation of forskolin-stimulated cAMP accumulation, after PTX pretreatment is that PTX pretreatment, via removal of

constitutively active Gi_α may lead to small elevations of cAMP accumulation in the CHO-cell clones, especially if AC is under tonic inhibition by Gi_α. Elevations in cAMP accumulation over the 20 hrs of incubation with PTX may result in a slight desensitization of AC, possibly via cAMP-dependent protein kinase phosphorylation of AC (Iyengar, 1993). Similarly, it is possible that 20 hrs incubation of these cells with PTX may lead to changes in G protein levels within the cells. For instance, small elevations in cAMP accumulation, after ADP-ribosylation of Gi_α, may lead to a subsequent lowering of Gs_α molecules. Extrapolating this view, it has been shown that long term (24 hrs) stimulation of S49 mouse lymphoma cells with 10 μM forskolin resulted in a 3-fold increase in $G\alpha_{i2}$ steady state levels and a 25% decline in $G\alpha_s$ (Hadcock *et al*, 1990). The problem with these theories is that cAMP accumulation in CHO-m1 and CHO-m3 cells , in the absence of forskolin, is not sensitive to PTX pretreatment.

A more simple explanation is that PTX interferes in some way with forskolin binding, thereby shifting the dose-response curve for forskolin activation of AC. Credence for this hypothesis could be gained by performing forskolin dose-response curves in the presence and absence of PTX pretreatment.

In many systems, AC activity seems to be under tonic inhibition by G_i (Reisine *et al*, 1985). This has been observed as a potentiation of forskolin-stimulated cAMP accumulation after PTX pretreatment. However, Johnson and Aguilera (1992) have also observed an attenuation of forskolin-stimulated cAMP accumulation after pretreatment of foetal and adult mouse skin fibroblasts with PTX. They suggested that the attenuation of the cAMP response was not due to increased activation of phosphodiesterases (PDEs) as experiments were carried out in the presence of high concentrations of the PDE inhibitor IBMX. Interestingly, the inactivation of G_i by PTX resulted in the expected potentiation of forskolin-stimulated AC activity in broken cell preparations of these cells, indicating that AC was tonically inhibited by G_i. They suggested that PTX-dependent ADP-ribosylation activated some unknown factor(s) which inhibits AC in intact cells. This response also appeared to be species-selective as PTX pretreatment of human skin fibroblasts resulted in potentiation rather than attenuation of forskolin-stimulated cAMP production.

In summary, agonist stimulation of recombinant m2 receptors expressed in CHO cells led to a PTX-sensitive attenuation of forskolin-stimulated cAMP accumulation. Changing expression levels of m2 muscarinic receptors affected the maximal inhibitory response to carbachol, but had relatively little affect on the potency of the agonist. The potency of the response lay approximately two log units to the left of the carbachol occupancy curve, suggesting that classical receptor theory could not adequately explain this phenomenon.

Carbachol stimulation of m1, m2 and m3 receptors (in CHO cells) produced a potentiation of cAMP accumulation which was PTX-insensitive. The agonist-mediated potentiation of cAMP accumulation observed in the present study was unlikely to be a consequence of elevated cytosolic Ca^{2+} levels. The size of the maximal increase in cAMP accumulation, induced by receptor activation, appeared to correlate with the expression level of the particular muscarinic receptor subtype in CHO cells. At similar receptor densities, m2 muscarinic receptors were found to be more efficiently coupled to the potentiation of forskolin-stimulated cAMP accumulation (after PTX pretreatment), compared with m3 muscarinic receptors.

The nature of the agonist-mediated potentiation of cAMP accumulation requires further investigation. It would be interesting to see whether the response is maintained in a permeabilized CHO cell preparation where pharmacological tools such as inhibitors or activators of Ca^{2+} release, PKC or PLA_2 could be used to deduce the mechanism. Similarly, agonist mediated potentiation of cAMP accumulation could be performed in a permeabilized cell preparation, in the presence and absence of guanine nucleotides to deduce whether the mechanism is mediated via G proteins such as G_s.

Figure 8.2.1. Time course for carbachol-stimulated (1 mM) cAMP accumulation in the presence and absence of PTX pretreatment, in CHO-m1 cell suspensions (approximately 500 µg of protein / ml). Carbachol-stimulated cAMP responses after 3 min incubation were 177 and 196 pmol / mg protein in untreated and PTX pretreated cells, respectively. Data is expressed as the mean of two individual experiments.

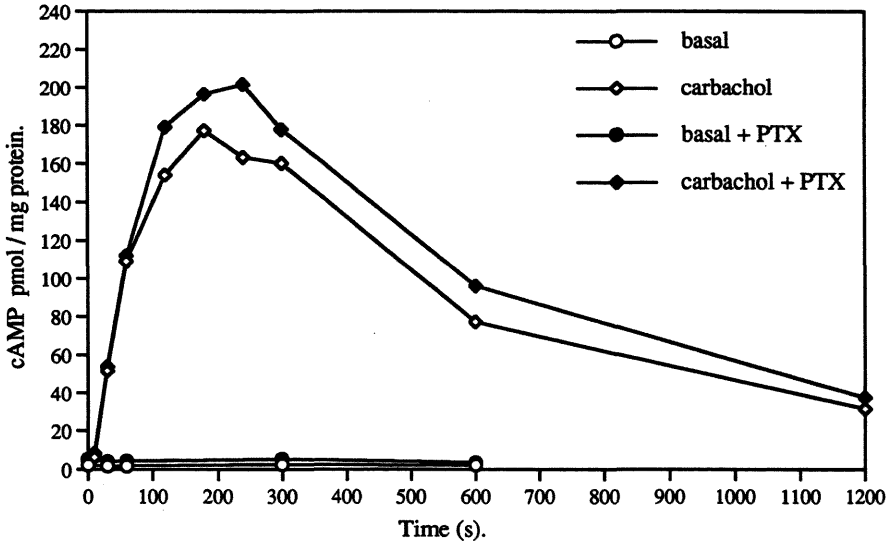

Figure 8.2.2. Time course for carbachol-stimulated (1 mM) cAMP accumulation in the presence and absence of PTX pretreatment, in CHO-m3 cell suspensions (approximately 500 µg of protein / ml). Carbachol-stimulated cAMP responses after 3 min incubation were 93 and 222 pmol / mg protein in untreated and PTX pretreated cells, respectively. Data is expressed as the mean of two individual experiments.

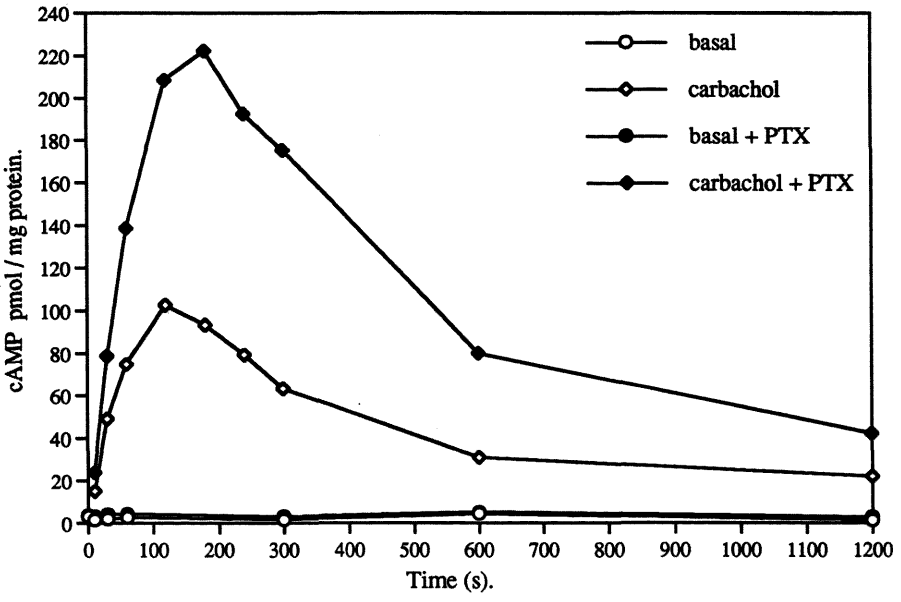

Figure 8.2.3. Time course for (1 mM) carbachol-stimulated cAMP accumulation in the presence of 10 μM forskolin, in the presence and absence of PTX pretreatment, in CHO-m1 cell suspensions. Data is expressed as the mean of two independent experiments. Forskolin-stimulated cAMP accumulation at 300 s (in untreated cells) was 83 pmol / mg protein. All data from paired experiments were normalized to this value. Peak stimulation of cAMP accumulation occurred at 5 min and was 681 % and 1253 % in untreated and PTX pretreated CHO-m1 cells, respectively.

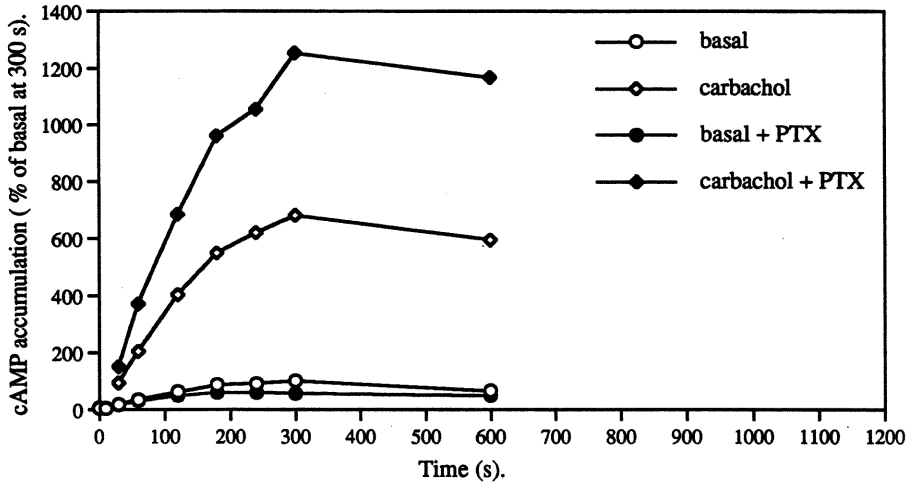

Figure 8.2.4. Time course for (1 mM) carbachol-stimulated cAMP accumulation in the presence of 10 μM forskolin, in the presence and absence of PTX pretreatment, in CHO-m3 cell suspensions. Data is expressed as the mean of two independent experiments. Forskolin-stimulated cAMP accumulation at 300 s (in untreated cells) was 57 pmol / mg protein. All data from paired experiments were normalized to this value. Peak stimulation of cAMP accumulation occurred at 5 min and was 598 % and 1783 % in untreated and PTX pretreated CHO-m3 cells, respectively.

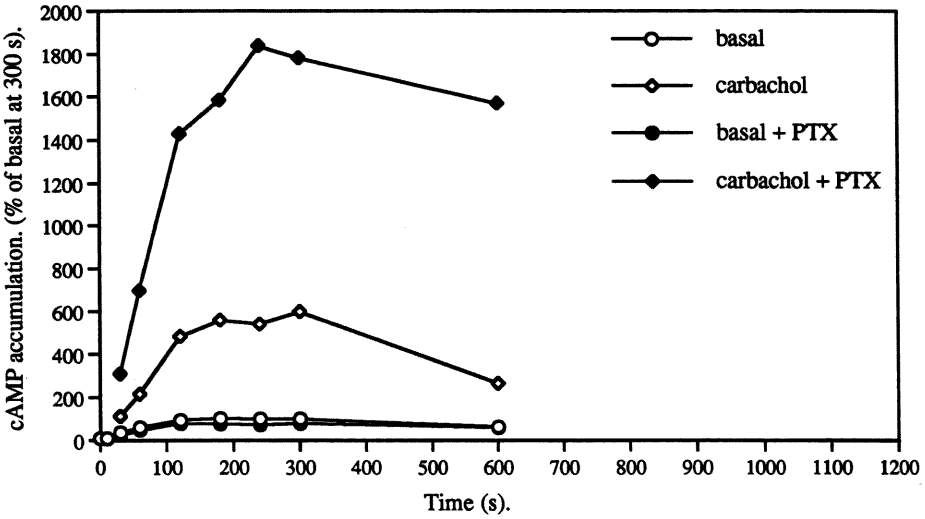

Figure 8.2.5. Time course for (1 mM) carbachol-stimulated cAMP accumulation in the presence of 10 μM forskolin, in the presence and absence of PTX pretreatment, in CHO-vt9 cell suspensions. Data is expressed as the mean of two independent experiments. Forskolin-stimulated cAMP accumulation at 300 s (in untreated cells) was 42 pmol / mg protein. All data from paired experiments were normalized to this value. Peak stimulation of cAMP accumulation occurred at 5 min and was 131 % and 163 % in untreated and PTX pretreated CHO-vt9 cells, respectively.

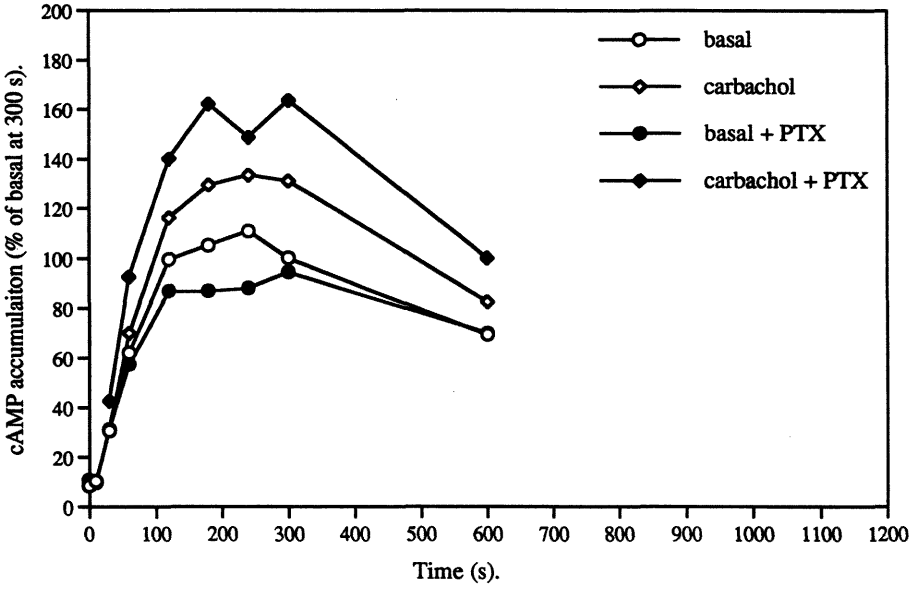

Figure 8.2.6. Time course for (1 mM) carbachol stimulation and inhibition of 10 μM forskolin-stimulated cAMP accumulation in the absence and presence of PTX pretreatment, in CHO-m2 cell suspensions. Data is expressed as the mean of two independent experiments. Forskolin-stimulated cAMP accumulation at 300 s (in untreated cells) was 62 pmol / mg protein. All data from paired experiments were normalized to this value. Peak, carbachol responses (both inhibition and stimulation) occurred at 5 min and were 84 % and 147 % in untreated and PTX pretreated CHO-m2 cells, respectively.

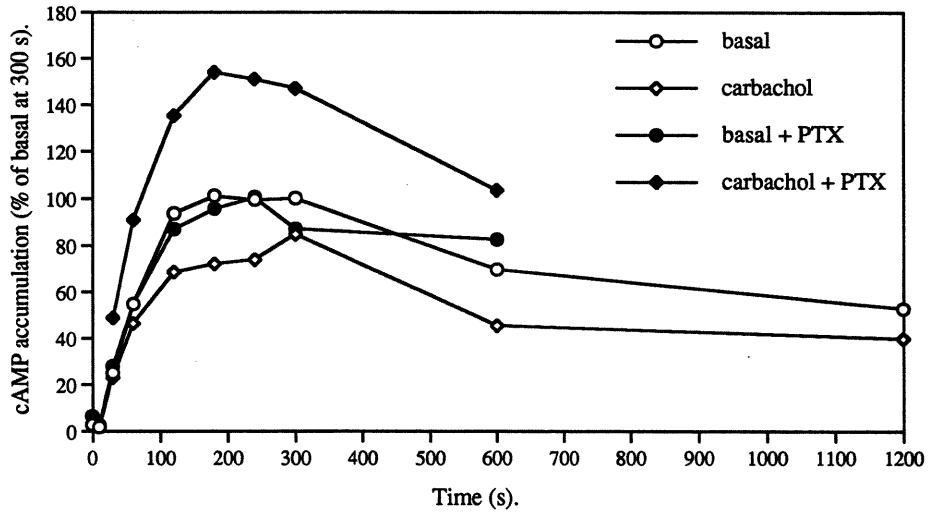

Figure 8.2.7. Time course for (1 mM) carbachol stimulation and inhibition of 10 μM forskolin-stimulated cAMP accumulation in the absence and presence of PTX pretreatment, in CHO-slm2 cell suspensions. Data is expressed as the mean of two independent experiments. Forskolin-stimulated cAMP accumulation at 300 s (in untreated cells) was 221 pmol / mg protein. All data from paired experiments were normalized to this value. Peak, carbachol responses (both inhibition and stimulation) occurred at 5 min and were 9 % and 171 % in untreated and PTX pretreated CHO-slm2 cells, respectively.

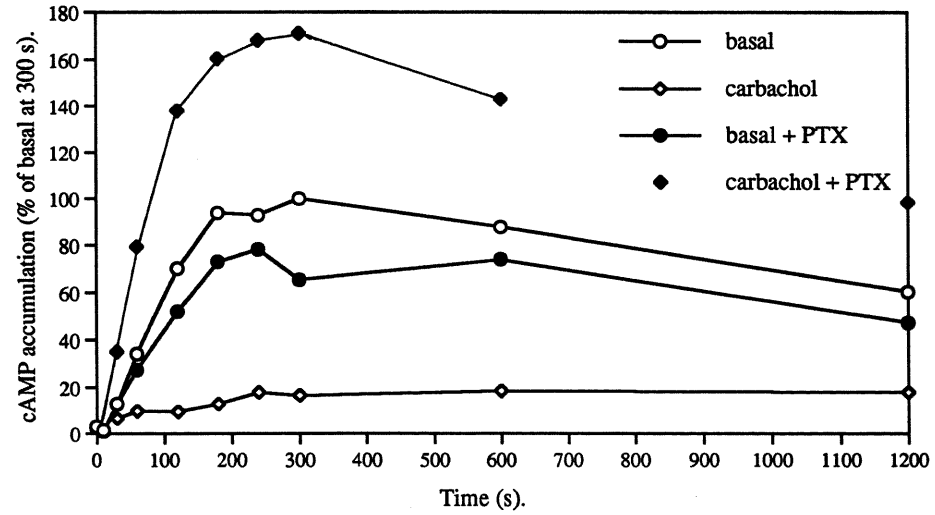

Figure 8.2.8. Carbachol stimulation of cAMP accumulation after a 3 min incubation with CHO-m1 cell suspensions, in the absence and presence of PTX pretreatment. Data is expressed as the mean ± standard error of 3 independent experiments. cAMP accumulation stimulated by 1 mM carbachol was 199 ± 28 and 232 ± 63 pmol / mg protein in untreated and PTX pretreated CHO-m1 cells, respectively. EC_{50} values were greater than or equal to approximately 100 µM.

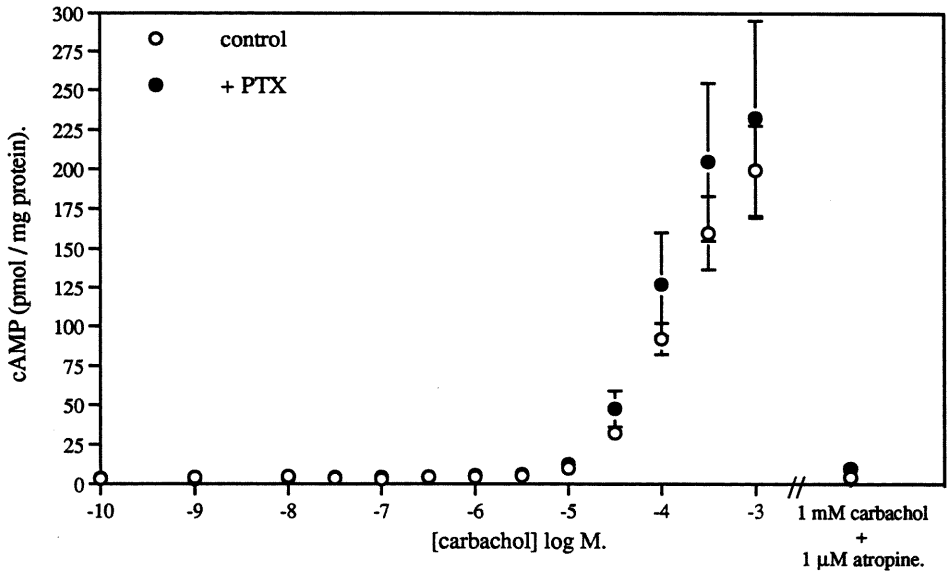

Figure 8.2.9. Carbachol stimulation of cAMP accumulation after a 3 min incubation with CHO-m3 cell suspensions, in the absence and presence of PTX pretreatment. Data is expressed as the mean ± standard error of 3 independent experiments. cAMP accumulation stimulated by 1 mM carbachol was 110 ± 24 and 144 ± 32 pmol / mg protein in untreated and PTX pretreated CHO-m3 cells, respectively. EC_{50} values were greater than or equal to approximately 100 µM.

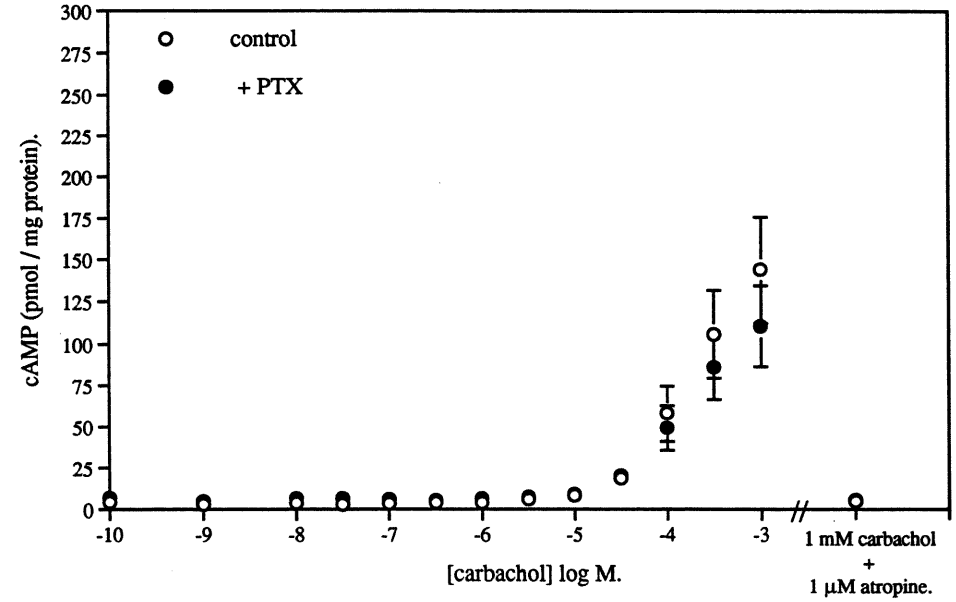

Figure 8.2.10. Effect of carbachol on forskolin (10 μM)-stimulated cAMP accumulation in untreated and PTX pretreated CHO-m1 cell suspensions. Data is expressed as the mean ± standard error of 3 independent experiments. Forskolin-stimulated cAMP accumulation (in untreated cells) was 111 ± 58 pmol / mg protein. All data from paired experiments were normalized to this value. Forskolin-stimulated cAMP accumulation was reduced, after PTX pretreatment of cells, to 31 ± 13 %. Maximal, carbachol-stimulated cAMP accumulation (in the presence of forskolin) was 599 ±126 % and 942 ± 279 % in untreated and PTX pretreated cells, respectively. EC_{50} log values were -4.86 ± 0.11 and -4.67 ± 0.08 in untreated and PTX pretreated cells, respectively.

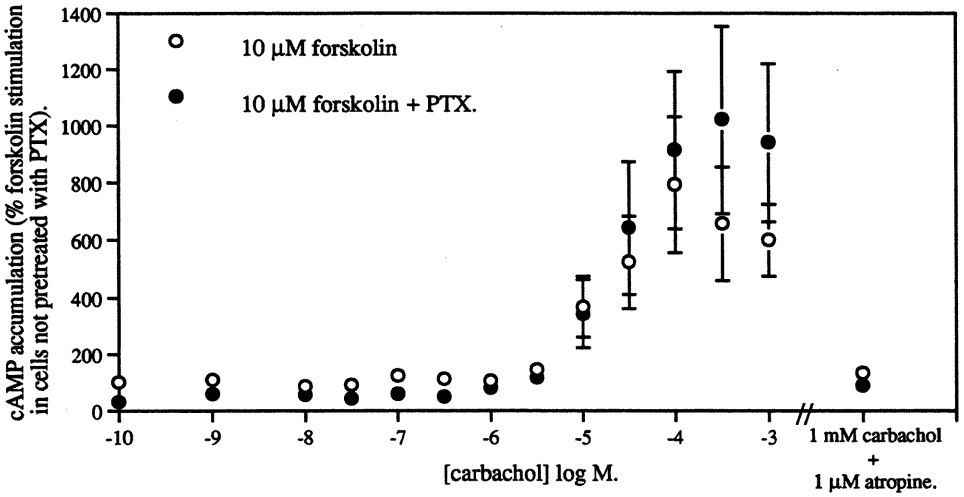

Figure 8.2.11. Effect of carbachol on forskolin (10 μM)-stimulated cAMP accumulation in untreated and PTX pretreated CHO-m3 cell suspensions. Data is expressed as the mean ± standard error of 3 independent experiments. Forskolin-stimulated cAMP accumulation (in untreated cells) was 123 ± 23 pmol / mg protein. All data from paired experiments were normalized to this value. Forskolin-stimulated cAMP accumulation was reduced, after PTX pretreatment of cells, to 38 ± 18 %. Maximal, carbachol-stimulated cAMP accumulation (in the presence of forskolin) was 222 ± 41 % and 475 ± 114 % in untreated and PTX pretreated cells, respectively. EC_{50} log values were -4.92 * and -4.58 ± 0.14 in untreated and PTX pretreated cells, respectively. * represents the mean of two EC_{50} determinations because the third experiment could not be accurately curve-fitted.

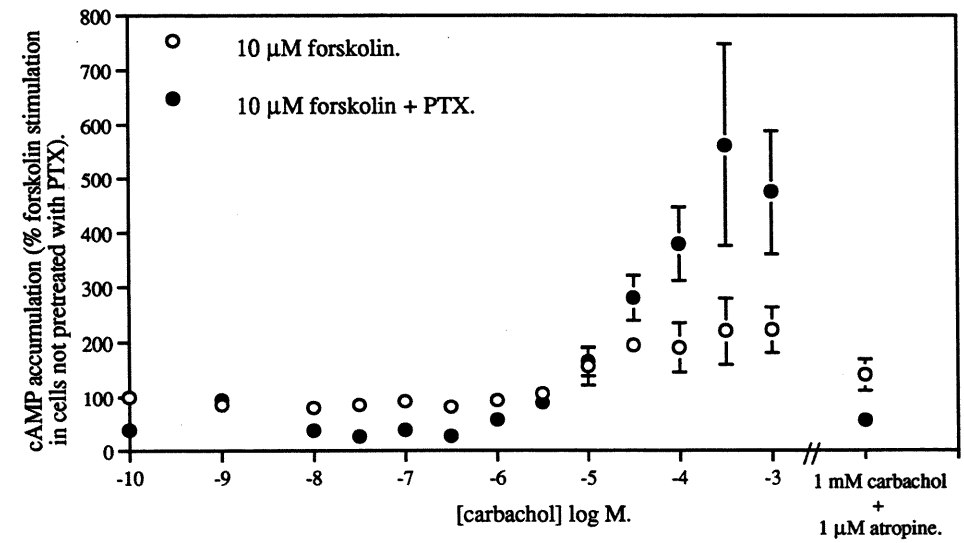

Figure 8.2.12. Effect of carbachol on forskolin (10 μM)-stimulated cAMP accumulation in untreated and PTX pretreated CHO-vt9 cell suspensions. Data is expressed as the mean ± standard error of 3 independent experiments. Forskolin-stimulated cAMP accumulation (in untreated cells) was 28 ± 5 pmol / mg protein. All data from paired experiments were normalized to this value. Forskolin-stimulated cAMP accumulation was reduced, after PTX pretreatment of cells, to 56 ± 4 %. Maximal, carbachol-stimulated cAMP accumulation (in the presence of forskolin) was 121 ±7 % and 110 ± 9 % in untreated and PTX pretreated cells, respectively. EC_{50} log values could not be determined in untreated cells. The EC_{50} (log values) for carbachol-stimulated cAMP accumulation in the presence of PTX pretreatment was -4.19 ± 0.06.

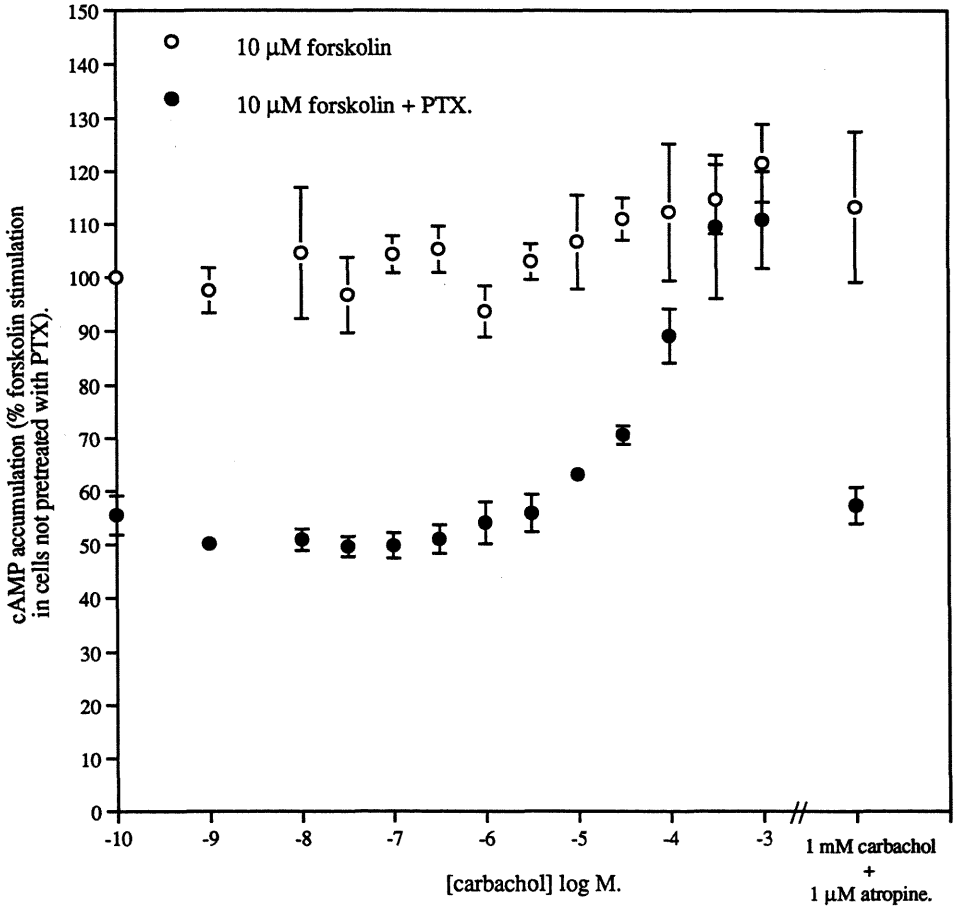

Figure 8.2.13. Effect of carbachol on forskolin (10 μM)-stimulated cAMP accumulation in untreated and PTX pretreated CHO-m2 cell suspensions. Data is expressed as the mean ± standard error of 3 independent experiments. Forskolin-stimulated cAMP accumulation (in untreated cells) was 25 ± 4 pmol / mg protein. All data from paired experiments were normalized to this value. Forskolin-stimulated cAMP accumulation was reduced after PTX pretreatment of cells to 77 ± 11 %. Maximal, carbachol-induced inhibition of forskolin-stimulated cAMP accumulation was 79 ± 4 % in untreated cells (a 20 % reduction). Maximal, carbachol stimulation of forskolin-stimulated cAMP accumulation was 108 ± 12 % in PTX pretreated cells (a 50 % increase). EC_{50} log values were -6.68 * and -5.22 ± 0.16 in untreated and PTX pretreated cells, respectively. * represents the mean of two EC_{50} determinations because the third experiment could not be accurately curve-fitted.

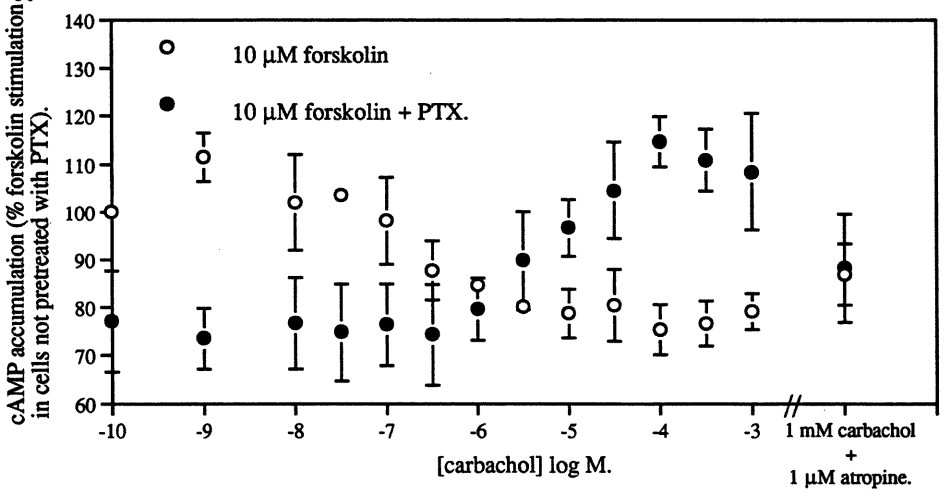

Figure 8.2.14. Effect of carbachol on forskolin (10 μM)-stimulated cAMP accumulation in untreated and PTX pretreated CHO-slm2 cell suspensions. Data is expressed as the mean ± standard error of 3 independent experiments. Forskolin-stimulated cAMP accumulation (in untreated cells) was 208 ± 66 pmol / mg protein. All data from paired experiments were normalized to this value. Forskolin-stimulated cAMP accumulation was reduced after PTX pretreatment of cells to 54 ± 10 %. Maximal, carbachol-induced inhibition of forskolin-stimulated cAMP accumulation was 9 ± 2 % in untreated cells (a 90 % reduction). Maximal carbachol stimulation of forskolin-stimulated cAMP accumulation was 181 ± 27 % in PTX pretreated cells (a 300 % increase). EC_{50} log values were -6.93 ± 0.03 and -5.09 ± 0.07, in untreated and PTX pretreated cells, respectively.

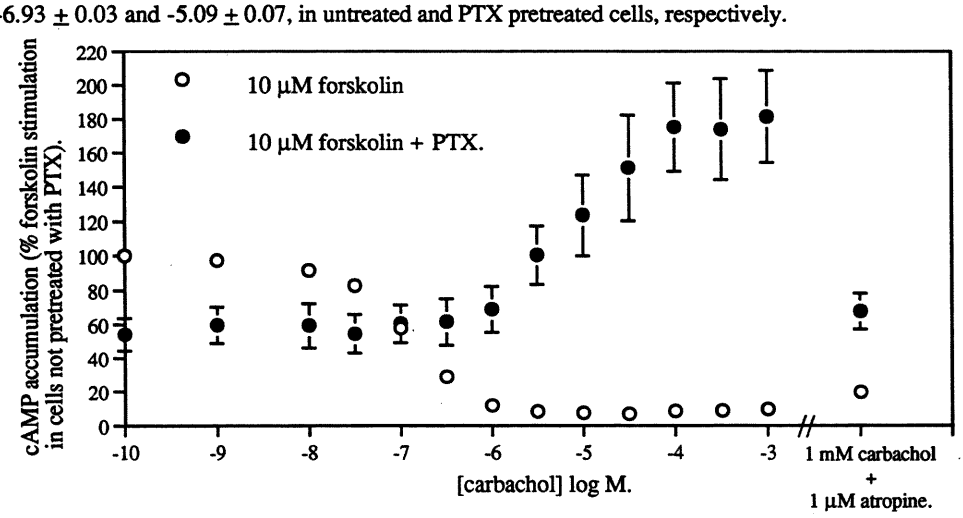

CHAPTER 9.
SUMMARY AND CONCLUDING DISCUSSION.

The original aims of this study were to compare and contrast the responses to agonist stimulation of different muscarinic receptor subtypes, expressed as homogeneous populations in CHO cells. Concurrently it was hoped that the coupling of the recombinant muscarinic receptor subtypes to endogenously expressed G proteins, and subsequently to effector systems might yield insights into the mechanism of agonist-receptor-G protein interactions and whether the data produced could be described by the ternary complex model (DeLean *et al*, 1980) and/or more recently by the allosteric ternary complex model (Lefkowitz *et al*, 1993; Samama *et al*, 1993). The effect of changing muscarinic receptor expression levels on agonist-mediated responses were also investigated to determine whether agonist potency and intrinsic activity (*i.e.* maximal responses) were modulated by changes in receptor density in a manner described by classical receptor theory. Finally, the possible promiscuous coupling of muscarinic receptors (when expressed at high levels) with multiple G proteins was investigated to see whether increasing expression of m3 receptors led to an increased promiscuous coupling of these receptors with PTX-sensitive G proteins.

The major advantage of using recombinant muscarinic receptors expressed in CHO cells is that tissues generally possess mixed populations of muscarinic receptors. This complicates interpretation of agonist-mediated responses where the muscarinic receptor agonists used are relatively non-selective. Furthermore, comparisons of responses between single populations of muscarinic receptors expressed in two different tissues may be complicated by the different levels of expression of the receptors, the level of expression and the subtypes of G proteins expressed, and the expression level and subtypes of effector molecules present. Therefore, by expressing recombinant muscarinic receptor subtypes in CHO cells, the G protein and effector pools, in theory, should be identical. Furthermore, by expressing similar densities of muscarinic receptor subtypes in different CHO cell clones, agonist-mediated responses could be directly compared between receptor subtypes.

One disadvantage of this system is that CHO cells do not normally express muscarinic receptor subtypes and, therefore, it could be argued that the responses elicited by muscarinic receptor stimulation in CHO cells may not be physiologically relevant. Furthermore, expression levels of muscarinic receptors in cell clones can be high compared with expression of these receptors in certain tissues. However, the variety of expression levels of various muscarinic receptor subtypes in tissues which, in turn, have heterogeneous pools of G proteins and effector proteins, suggests that muscarinic receptor agonist-mediated responses may vary from tissue to tissue with no single response encompassing the activity of a particular muscarinic receptor subtype. Therefore, although not ideal, CHO cells expressing recombinant muscarinic receptor subtypes offer several advantages over tissues for comparing agonist-mediated responses between the different

muscarinic receptor subtypes. Furthermore, this system can be used to investigate agonist-receptor-G protein interactions.

The muscarinic receptor subtypes expressed in the different CHO cell clones were pharmacologically characterized and compared with the muscarinic receptors expressed endogenously in SH-SY5Y cells. Antagonist affinity values were determined by competition studies, whereby unlabelled selective antagonists displaced radiolabelled [^{3}H]NMS (a non-selective muscarinic receptor antagonist) binding. The rank order of affinity of a series of selective antagonists for the different muscarinic receptor subtypes, expressed in CHO cell clones, correlated well with those observed by many other groups (see review by Caulfield, 1993). Furthermore, the antagonist affinity profile of the SH-SY5Y cells closely correlated with the antagonist affinity profile obtained in CHO cells expressing m3 muscarinic receptors. It was, therefore, concluded that SH-SY5Y cells expressed a predominant population of M_3 muscarinic receptors.

m1 and m3 Muscarinic Receptors Expressed in CHO Cells.

In the present study, carbachol-stimulation of m1 and m3 muscarinic receptors, expressed at similar receptor densities in different CHO cell clones, coupled, via G proteins, to the stimulation of PLC resulting in the accumulation of Ins(1,4,5)P_3, both in intact CHO cells and in electrically permeabilized CHO cells in suspension. The Ins(1,4,5)P_3 liberated was capable of releasing pre-loaded $^{45}Ca^{2+}$ from vesicular stores of permeabilized CHO cell suspensions. Therefore, electroporation of cell suspensions, while making the cells "leaky", did not prevent receptor-G protein-PLC coupling. Ins(1,4,5)P_3 accumulation in response to m1 and m3 muscarinic receptor stimulation is thought to be mediated via the $G_{q/11}$ family of PTX-insensitive G proteins (Berstein *et al*, 1992). Carbachol stimulation of m1 and m3 muscarinic receptors also produced a relatively large accumulation of cAMP, suggesting that m1 and m3 muscarinic receptors modulate AC activity. The Ins(1,4,5)P_3 response and the cAMP accumulation response, induced by carbachol-stimulation of m1 and m3 muscarinic receptors, were both mediated via PTX-insensitive G proteins in CHO cells.

Carbachol-stimulated Ins(1,4,5)P_3 accumulation in CHO-m1 and CHO-m3 cells reached a rapid peak accumulation after about 10 s incubation. Carbachol-stimulated Ins(1,4,5)P_3 levels then fell to a lower, but sustained phase of Ins(1,4,5)P_3 accumulation after 1 min. This sustained phase of carbachol-stimulated Ins(1,4,,5)P_3 accumulation remained significantly above basal levels of Ins(1,4,5)P_3 accumulation for at least a further 19 min. Two explanations have been hypothesized to account for the profile of this receptor-mediated response. The first hypothesis comes from the observation that, in CHO-m3 cells, levels of PIP_2 are rapidly depleted in response to agonist stimulation, with

a profile that closely mirrors that of agonist-stimulated Ins(1,4,5)P_3 accumulation (Wojcikiewicz *et al*, 1993). Therefore, rapid substrate depletion may change the rate at which PLC activity operates, producing two phases of agonist-stimulated Ins(1,4,5)P_3 accumulation. The second hypothesis comes from the observation that a rapid, serine kinase-mediated phosphorylation of m3 muscarinic receptors expressed in CHO cells occurs, in response to carbachol, with a time course that appears to mimic what could be a rapid, partial desensitization of m3 muscarinic receptor-mediated PLC activation (Tobin and Nahorski, 1993).

The results from the present study suggested that m1 and m3 muscarinic receptors, expressed at similar receptor densities in CHO cell clones, produced similar profiles of carbachol-stimulated Ins(1,4,5)P_3 accumulation.

The mechanism by which m1 and m3 muscarinic receptor-stimulation leads to increased AC activity remains elusive. One possible mechanism may be via a coupling of m1 and m3 muscarinic receptors with G_s which, in turn, activates AC. Alternatively, some of the AC isozymes can be stimulated by Ca^{2+}-calmodulin activity (types I and III) and others by PKC activation (type II and smaller responses in I and III). Therefore, m1 and m3 muscarinic receptor-stimulated cAMP accumulation may result from the increased levels of Ca^{2+} and/or in PKC activity resulting from PLC activation. Future studies may be able to determine the mechanism of this response. For instance, carbachol-stimulated cAMP accumulation could be assessed in permeabilized CHO-m1 or CHO-m3 cell suspensions, in a Ca^{2+}-free buffer. Ca^{2+} mobilization from vesicular stores could also be abolished by preincubating the permeabilized cell suspensions with thapsigargin, a blocker of the microsomal Ca^{2+}-ATPase. If carbachol-stimulated cAMP accumulation was still apparent, then the mechanism for this response would be unlikely to involve increased free Ca^{2+} levels within the cells. The role of PKC activation in agonist-stimulated cAMP accumulation in CHO-m1 or CHO-m3 cells, could be assessed by preincubating the cells with phorbol esters (activators of PKC) or PKC inhibitors. The present study has suggested that neither PKC nor intracellular free Ca^{2+} levels may be involved in the activation of AC in CHO cells due to the clear differences in potency between carbachol-stimulated PLC activation (evoking increased intracellular free Ca^{2+} levels and PKC activity) and the potency with which carbachol stimulated cAMP accumulation. G protein $\beta\gamma$ subunits can also activate specific isoforms of AC (types II and IV). Generally, much larger concentrations of $\beta\gamma$ subunits are required to activate AC compared with Gs_α subunits. The PTX-insensitivity of the cAMP accumulation response suggests that the $\beta\gamma$ subunits would have to be derived from $G_{q/11}$ G proteins or an as yet undefined, PTX-insensitive G protein. It is, therefore, unlikely that enough $\beta\gamma$ subunits could be made available to produce such large elevations in cAMP accumulation in CHO cells. The most plausible mechanism, therefore, is one where the m1 and m3 muscarinic

receptors, expressed at high receptor densities in CHO cells, couple with G_s proteins as well as with $G_{q/11}$-family G proteins and with PTX-sensitive G proteins (G_i/G_o) (see below). A definitive experiment to determine the nature of the G proteins that couple with m1 and m3 muscarinic receptors, in CHO cells, would be to use muscarinic receptor subtype-specific antibodies and antibodies for specific G proteins to solubilize and purify the agonist-stimulated receptors with G proteins attached, and then to determine the nature of these attached G proteins, as has been previously described in the literature (Matesic and Luthin, 1991).

Carbachol-stimulated [^{35}S]GTPγS binding to G proteins in CHO-m1 and CHO-m3 cell membranes showed that both m1 and m3 muscarinic receptors coupled to G proteins less efficiently than did m2 muscarinic receptors in CHO-m2 cell membranes. Although expressing at least 10-fold fewer muscarinic receptors than CHO-m1 and CHO-m3 cell membranes, CHO-m2 cell membranes produced equivalent or higher levels of carbachol-stimulated [^{35}S]GTPγS binding. However, this data must be viewed with a certain amount of caution as it is not known whether the assay conditions preferentially detected [^{35}S]GTPγS binding to specific G proteins (*i.e.* G_i). Somewhat surprisingly, both m1 and m3 muscarinic receptors, expressed at relatively high levels in CHO cell membranes, were found to couple with both PTX-sensitive and PTX-insensitive G proteins, as observed from the [^{35}S]GTPγS binding experiments. The functional significance of the coupling of m1 and m3 muscarinic receptors to PTX-sensitive G proteins in CHO cell membranes could not be determined from this study. By increasing the protein concentration used in these experiments and optimizing carbachol-stimulated [^{35}S]GTPγS binding conditions for PI-linked receptors, it may be possible to produce carbachol dose-response curves for [^{35}S]GTPγS binding in the different CHO cell clones, so that the efficiency of the different muscarinic receptor subtypes to activate their respective G proteins could be assessed.

PTX pretreatment of CHO cells, in [^{35}S]GTPγS binding experiments, resulted in a 70-80 % reduction in basal [^{35}S]GTPγS binding, in each of the CHO cell clones. PTX-catalyzed ADP-ribosylation of certain G proteins is thought to prevent these G proteins from coupling with receptors, without affecting the intrinsic functions of the G protein, *i.e.* the binding affinity of GTPγS or GTPase activity (Haga *et al,* 1985; Enomoto and Asakawa, 1986; Huff and Neer, 1986; Katada *et al*, 1986). This study, therefore, suggests that G proteins are coupled to receptors, even in the absence of receptor-agonist, in CHO cells. These results, therefore, fit with the allosteric ternary complex model of agonist-receptor-G protein interactions, which suggests that receptors can couple to, and activate, G proteins in the absence of receptor agonist (Samama *et al*, 1993). Alternatively, in disagreement with the literature, PTX pretreatment may affect the intrinsic properties of G proteins, affecting [^{35}S]GTPγS binding affinity.

PI-linked muscarinic receptors have generally shown relatively small GTP shifts in agonist binding studies when compared to m2 muscarinic receptors coupled to the inhibition of AC (see chapter 4 introduction). A similar finding was observed in the present study where GTP shifts in CHO-m1 and CHO-m3 cell membranes were much smaller, or absent, compared to those produced in CHO-m2 cell membranes. All agonist binding curves, in the presence of GTP, produced slope factors of unity indicating the presence of a homogeneous population of low affinity binding sites. Therefore, the relative lack of GTP shifts observed in CHO-m1 and CHO-m3 cells could be explained by one or both of two features; 1) that the relative differences between the affinity of the high and low affinity agonist binding states in m1 and m3 muscarinic receptors were relatively small compared to the affinity state difference of the m2 muscarinic receptors; and 2) a smaller percentage of m1 and m3 muscarinic receptors were found to have a high affinity for carbachol under the assay conditions used. Indeed, CHO-m1 cell membranes produced no high affinity agonist binding sites in the absence of added guanine nucleotides. The case that there was a general lack of high affinity agonist binding sites observed in the PI-linked muscarinic receptors, was further strengthened by the observation that a proportion of the high affinity agonist binding sites observed in CHO-m3 cell membranes were PTX-sensitive. Therefore, whilst the m1 and m3 muscarinic receptors expressed in CHO-m1 and CHO-m3 cells, respectively, were shown to couple efficiently to the activation of PLC (see figure 9.1), membrane preparations of either CHO cell clones showed very little apparent high affinity agonist binding sites. Coupling of m1 and m3 muscarinic receptors to $G_{q/11}$-family G proteins, unlike coupling of m2 muscarinic receptors to PTX-sensitive G proteins, may be lost in membrane preparations of the CHO cell clones. This theory is probably not correct, however, due to the proportion of PTX-insensitive carbachol-stimulated [^{35}S]GTPγS binding that was observed in CHO-m1 and CHO-m3 cell membranes. It may also have been expected that the PTX-sensitive element of carbachol-stimulated [^{35}S]GTPγS binding to CHO-m1 cell membranes, should have yielded some PTX-sensitive high agonist affinity binding sites. This was not the case.

GTP shifts in agonist binding curves to PI-linked muscarinic receptors may not correspond with the apparent intrinsic activity of the agonist used. In AC-linked receptors, the intrinsic activity of agonists correlates well with the proportion of high affinity agonist binding sites present (Ehlert, 1985). The ternary complex model describes this high affinity agonist binding component as being the "activated" receptor, *i.e.* one where the receptor is coupled to a G protein with no guanine nucleotide bound to the α subunit (the ternary complex). The greater the intrinsic activity of the agonist, the greater will be its ability to transform the receptor into a conformation whereby it activates an associated G protein, exchanging GDP for GTP (Tota and Schimerlik, 1990). In the absence of guanine

nucleotides, GDP dissociation will result in the formation of the ternary complex, and thereby a proportion of high affinity agonist binding sites would be detected. The lack of PTX-insensitive high affinity agonist binding to m1 and m3 muscarinic receptors, expressed in CHO cell membranes, despite the high intrinsic activity of the agonist, suggests that high affinity agonist binding and agonist intrinsic activity may not correlate, in PI-linked muscarinic receptors, with the view hypothesized by the ternary complex model of agonist-receptor-G protein interactions. Recently, a new model to explain agonist-receptor-G protein interactions has been devised to account for other results which do not fit with the traditional ternary complex model. The allosteric ternary complex model (Lefkowitz *et al*, 1993) suggests that the receptor can exist in two conformations, the rate of isomerization from the inactive form to the active form being governed by the intrinsic activity of the agonist used. This new theory accounts for the presence of high affinity agonist binding to constitutively active mutant receptors in the absence of G proteins (*i.e.* after solubilization and purification of the receptor) suggesting that the receptor does not need to be coupled to G proteins in order to form high affinity agonist binding sites. Furthermore, the constitutively active mutant receptors, expressed in cloned cell lines, increased cellular responses even in the absence of agonist. The allosteric ternary complex model thereby separates high affinity agonist binding from G protein activation and may open the way to explaining the results obtained in the present study.

When comparing the affinity of carbachol for the low affinity binding sites of m1, m2 and m3 muscarinic receptors in CHO cell membranes, carbachol bound with greater affinity to the m2 muscarinic receptors. Carbachol also bound with a slightly higher affinity for m3 muscarinic receptors compared with m1 muscarinic receptors. The potency of carbachol to generate Ins(1,4,5)P_3 in m3 muscarinic receptors was slightly higher compared with m1 muscarinic receptors, expressed at similar receptor densities in CHO cells, probably due to the slight variations in carbachol affinity for these two muscarinic receptor subtypes (see figure 9.1). The potency of carbachol to stimulate Ins(1,4,5)P_3 accumulation in CHO-m1 and CHO-m3 cells was approximately 37-fold greater than the affinity of carbachol for m1 and m3 muscarinic receptors, respectively, with both receptor subtypes eliciting the same maximal Ins(1,4,5)P_3 response.

Carbachol stimulated $^{45}Ca^{2+}$ release from permeabilized CHO cell clones expressing similar densities of m1 or m3 muscarinic receptors, with an identical maximal release and identical potency, at similar protein concentrations of permeabilized CHO cell clones. Comparisons of carbachol potency for $^{45}Ca^{2+}$ release with carbachol occupancy curves could not be drawn due to the variations in carbachol potency that could be produced by changing the protein concentration (cell number) of permeabilized cells used in suspensions. The only conclusions that can be drawn is that, at similar receptor densities

and at similar numbers of cells used in suspensions, m1 and m3 muscarinic receptors in CHO-m1 and CHO-m3 cells, respectively, produced identical carbachol-stimulated $^{45}Ca^{2+}$ release from vesicular stores. To obtain comparable potency ratios for the carbachol-stimulated responses in CHO-m1 and CHO-m3 cell clones, carbachol-stimulated Ca^{2+} mobilization and carbachol-stimulated $Ins(1,4,5)P_3$ accumulation should be performed under identical assay conditions *i.e.* in intact cells. Ca^{2+} mobilization could be detected by loading the cells with fura-2, prior to receptor stimulation. Ca^{2+} release and Ca^{2+} entry phases could be dissociated by performing the experiments in the presence and absence of extracellular Ca^{2+}. Furthermore, possible Ca^{2+} entry-induced PLC activation could be determined by measuring $Ins(1,4,5)P_3$ accumulation in the presence and absence of extracellular Ca^{2+}. In this way, possible amplification between carbachol-stimulated $Ins(1,4,5)P_3$ accumulation and Ca^{2+} mobilization could be determined and compared between CHO-m1 and CHO-m3 cell clones.

Carbachol-stimulated cAMP accumulation in CHO-m1 and CHO-m3 cell clones were very similar in terms of both the maximal response and the potency of the response produced. The occupancy-response curves for carbachol-stimulated cAMP accumulation in CHO-m1 and CHO-m3 cells were very similar indicating that there was very little amplification of the signal, *i.e.* very little, if any, receptor reserve for this response (see figure 9.1).

m2 Muscarinic Receptors Expressed in CHO Cells.

The present study showed that carbachol bound to CHO-m2 cell membranes, with more than one affinity state for the m2 muscarinic receptors. The high affinity state of the m2 receptors were sensitive to both guanine nucleotides and PTX pretreatment, resulting in a conversion of the high affinity binding sites to low affinity binding sites. Furthermore, carbachol-stimulated $[^{35}S]GTP\gamma S$ binding to G proteins in CHO-m2 cell membranes was completely abolished after pretreatment of the cells with PTX. m2 Receptors expressed in CHO cell membranes, therefore, appear to couple with only PTX-sensitive G proteins, at relatively low receptor expression levels.

The relatively large proportion of carbachol-stimulated $[^{35}S]GTP\gamma S$ binding in CHO-m2 cell membranes, compared with the more highly expressed PI-linked m1 and m3 muscarinic receptors, suggested that m2 muscarinic receptors coupled more efficiently with G proteins in CHO cell membranes than either m1 or m3 muscarinic receptors. However, carbachol stimulation of m2 muscarinic receptors in CHO cells did not appear to stimulate PLC activation due to the absence of any $Ins(1,4,5)P_3$ accumulation or mobilization of $^{45}Ca^{2+}$ from permeabilized cells. Carbachol stimulation of m2 muscarinic receptors in CHO-m2 and CHO-slm2 cells attenuated forskolin-stimulated cAMP

accumulation, a response which was abolished after PTX pretreatment of cells. The results suggest a coupling of m2 muscarinic receptors to the inhibition of AC via PTX-sensitive G_i-family G proteins.

After PTX pretreatment of CHO-m2 and CHO-slm2 cells, carbachol actually mediated a small, dose-dependent potentiation of forskolin-stimulated cAMP accumulation. The potency of carbachol to elicit this response was much lower than that required to observe attenuation of forskolin-stimulated cAMP accumulation, closely correlating with the apparent affinity of carbachol for the low affinity state of the m2 muscarinic receptors (see figure 9.2). Interpretation of the data produced in these experiments was complicated by an apparent interaction of forkolin-stimulated cAMP accumulation with PTX pretreatment. PTX pretreatment consistantly reduced the amount of forskolin-stimulated cAMP accumulation observed in each of the CHO cell clones, when compared with cells that were not incubated with PTX.

The mechanism whereby m2 muscarinic receptor activation leads to stimulation of AC activity, via PTX-insensitive G proteins is not yet known. The most likely candidate for this response is a relatively weak coupling of m2 muscarinic receptors to G_s-family G proteins. It should be noted, however, that an association of m2 muscarinic receptors in CHO-m2 cell membranes, with PTX-insensitive G proteins, was not observed in [^{35}S]GTPγS binding experiments. An association of m2 muscarinic receptors with G_s may have been lost in preparation of CHO cell membranes. Alternatively, the [^{35}S]GTPγS binding assay may not have been sufficiently sensitive to detect a relatively weak association of m2 muscarinic receptors with G_s.

m2 Muscarinic receptors, in CHO-slm2 cells, and m3 muscarinic receptors, in CHO-vt9 cells, were expressed at similar receptor densities. However, maximal carbachol potentiation of forskolin-stimulated cAMP accumulation (after PTX pretreatment) was greater in CHO-slm2 cells than in CHO-vt9 cells. This suggests that m2 muscarinic receptors appeared to couple more efficiently to the stimulation of AC activity compared with m3 muscarinic receptors.

The Effects of Manipulating Expression Levels of Muscarinic Receptors in CHO Cells.

Increasing m2 muscarinic receptor expression in CHO cells led to an increased maximal carbachol-stimulated attenuation of forskolin-stimulated cAMP accumulation. Classical receptor theory dictates that the maximal response to an agonist will begin to decrease when the number of receptors present are not sufficient to produce the same maximal response, *i.e.* the system lacks an apparent receptor reserve. At this point the potency of the response to the receptor agonist should be similar to the apparent affinity

of the agonist for the low affinity state of the receptor. Clearly, in the present study, this was not the case. As m2 muscarinic receptor expression was lowered in CHO-m2 cells compared with CHO-slm2 cells, the maximal response to carbachol was greatly reduced, but the potency of carbachol to elicit the response in CHO-m2 cells was approximately two orders of magnitude to the left of the carbachol occupancy curve (see figure 9.2) suggesting that a substantial receptor reserve was apparent. Similar conclusions drawn from other studies on AC-linked receptors (*e.g.* 5-HT_{1A} receptors; α_2-adrenoceptors) in cloned cell lines, suggest that the classical view of receptor theory may not account for these results (Hoyer *et al*, 1993; Varrault *et al*, 1992). In this respect it would be very interesting to compare carbachol-stimulated [^{35}S]GTPγS binding dose-response curves in CHO-m2 and CHO-slm2 cell membranes to see whether the potency and/or the maximal responsiveness of carbachol to activate G proteins is affected in a similar manner to that of inhibition of forskolin-stimulated cAMP accumulation.

The maximal carbachol-mediated potentiation of forskolin-stimulated cAMP accumulation, in PTX pretreated CHO-m2 and CHO-slm2 cells, was also affected by changes in m2 muscarinic receptor expression. Increasing m2 muscarinic receptor expression produced an increased maximal response to carbachol without significantly affecting the potency of the response to carbachol. However, in this situation, the carbachol potency was similar to the apparent affinity of carbachol for the low affinity state of the m2 muscarinic receptors, suggesting that the system lacked an apparent receptor reserve. In the absence of an apparent receptor reserve, changes in the maximal response to carbachol would be expected by classical receptor theory.

Increasing m2 muscarinic receptor density in CHO-slm2 cells compared with CHO-m2 cells did not produce any $^{45}Ca^{2+}$ release from permeabilized CHO-slm2 cell suspensions suggesting that this increase in expression of m2 muscarinic receptors in CHO cells did not lead to a promiscuous coupling of these receptors to PLC activation. Furthermore, abolishing the coupling of PTX-sensitive G proteins to m2 muscarinic recpectors, in CHO cells, with PTX pretreatment, did not produce any carbachol-stimulated PLC activation, suggesting that PTX preteatment did not induce a promiscuous coupling of m2 muscarinic receptors with PTX-insensitive $G_{q/11}$ family G proteins.

Changes in m3 muscarinic receptor expression were found to markedly affect both the potency and the maximal responsiveness of the CHO cell clones in response to carbachol. The differences in potency between the CHO cell clones expressing relatively low levels of m3 muscarinic receptors (CHO-vt9) and high levels of m3 muscarinic receptors (CHO-m3) (see figure 9.3) clearly indicate that comparisons of responses between muscarinic receptor subtypes must be performed at identical levels of receptor expression. This is why comparisons of m1 and m3 muscarinic receptor responses to carbachol were valid, as the receptors were expressed at similar receptor densities in CHO-m1 and CHO-m3 cells,

respectively.

Lowering m3 muscarinc receptor expression in CHO-vt9 cells resulted in the loss of the PTX-sensitive high affinity carbachol binding component, observed in CHO-m3 cell membranes. Furthermore, PTX-sensitive carbachol-stimulated [^{35}S]GTPγS binding in CHO-vt9 cell membranes was reduced compared with the proportion of PTX-sensitive carbachol-stimulated [^{35}S]GTPγS binding observed in CHO-m3 cell membranes. These results suggested that as m3 muscarinic receptor expression was increased, the receptors coupled promiscuously with PTX-sensitive as well as PTX-insensitive G proteins.

Lowering m3 muscarinic receptor expression in CHO-vt9 cells compared with CHO-m3 cells resulted in rightward shifts in carbachol dose-response curves for Ins(1,4,5)P_3 generation (at 10 s) and for $^{45}Ca^{2+}$ release from permeabilized cell suspensions. The maximal responses to carbachol were also reduced in CHO-vt9 cells compared with CHO-m3 cells. Such effects are indicative of the CHO-vt9 cells lacking a receptor reserve for these carbachol responses, *i.e.* the m3 muscarinic receptor number was lowered beyond the point where it could sustain a maximal response to the agonist. Comparisons of the carbachol response curves with the carbachol occupancy curve in CHO-vt9 cells shows that the response curve for Ins(1,4,5)P_3 accumulation lies marginally, but significantly to the left of the occupancy curve (see figure 9.3). However, when evaluating these occupancy-response curves, the differences in assay conditions must be taken into consideration. Occupancy curves were evaluated in membrane preparations whereas Ins(1,4,5)P_3 accumulation studies were carried out in intact cell suspensions.

Reducing m3 muscarinic receptor expression levels, in CHO-vt9 cells compared with CHO-m3 cells, resulted in a greater attenuation of the peak phase of carbachol-stimulated Ins(1,4,5)P_3 accumulation compared with the plateau phase of carbachol-stimulated Ins(1,4,5)P_3 accumulation. These results were of interest, particularly in terms of deducing a possible mechanism for the two distinct phases of receptor-mediated Ins(1,4,5)P_3 accumulation. In the case of the PIP_2 depletion theory, if PIP_2 levels were depleted at a slower rate, in CHO-vt9 cells (due to the lower m3 muscarinic receptor density) compared with CHO-m3 cells, then a lower maximal response, but more prolonged, peak phase of receptor-mediated Ins(1,4,5)P_3 accumulation might have been expected. Indeed, (1 mM) carbachol-stimulated Ins(1,4,5)P_3 accumulation in CHO-vt9 cells produced responses at 10 s and at 20 s which were not significantly different. However, in CHO-m1 and CHO-m3 cells, (1mM) carbachol-stimulated Ins(1,4,5)P_3 accumulation at 20 s was significantly reduced compared with the response at 10 s. Similarly, stimulation of CHO-m3 and CHO-m1 cells with lower concentrations of carbachol, might also be expected to slow the rate of PIP_2 depletion and thereby prolong the peak phase of receptor-mediated Ins(1,4,5)P_3 accumulation. More detailed time course studies using a range of carbachol concentrations are required to investigate this

possibility further.

The results obtained in this study, between CHO-m3 and CHO-vt9 cells, may also provide evidence for the other possible hypothesis for explaining the two phases of receptor-mediated Ins(1,4,5)P_3 accumulation. By reducing the expression level of m3 muscarinic receptors in CHO cells, the relative stimulation of G proteins may also be reduced following agonist stimulation (as was observed in [^{35}S]GTPγS binding studies). $\beta\gamma$ subunits of G proteins are possible candidates for co-ordinating the agonist-mediated phosphorylation of the m3 muscarinic receptors (Kameyama *et al*, 1993). Therefore, by reducing receptor number and, therefore, reducing G protein activation, the levels of free $\beta\gamma$ subunits available to co-ordinate agonist-mediated phosphorylation of the m3 muscarinic receptors, may be reduced, thereby, reducing the level of phosphorylation of the receptors. If this phosphorylation event mediates the partial desensitization of receptor-mediated PLC activation, then perhaps, the desensitization of the receptors in CHO-vt9 cells may be less than that observed in CHO-m3 cells. This theory may explain why reducing m3 muscarinic receptor number appeared to have proportionally less effect on the sustained phase of carbachol-stimulated Ins(1,4,5)P_3 accumulation compared with the peak phase. Further work is, therefore, necessary to deduce the apparent phosphorylation of m3 muscarinic receptors expressed in CHO-vt9 cells compared with CHO-m3 cells, to see whether the levels and/or sites of agonist-mediated phosphorylation differ. Further studies could also investigate the possible role of free $\beta\gamma$ subunits in co-ordinating the agonist-stimulated phosphorylation of the m3 muscarinic receptors in CHO cells.

In CHO-m3 cells, the carbachol-stimulated cAMP response overlapped the occupancy curve for carbachol binding, suggesting that very little, if any, receptor reserve was apparent. Reduction of m3 muscarinic receptor expression in CHO-vt9 cells, abolished carbachol-stimulated cAMP accumulation, presumably because the receptor level was reduced below a threshold which could sustain this response. A small carbachol-stimulated cAMP accumulation response was observed in CHO-vt9 cells when experiments were performed in the presence of forskolin and after PTX pretreatment. Forskolin appeared to increase both the potency and maximal responsiveness of the carbachol-stimulated cAMP response in CHO-m1, CHO-m3 and CHO-vt9 cells.

The general lack of carbachol-stimulated cAMP accumulation in CHO-vt9 cells compared with CHO-m3 cells suggests that cells may, or may not, activate this cellular response, depending on the levels of muscarinic receptors expressed in cells. Levels of muscarinic receptors expressed in physiological tissues are thought to range between 30-3000 fmol / mg protein (Venter *et al*, 1988). This poses the question as to whether muscarinic receptor-mediated cAMP accumulation occurs in tissues. Of course, the

presence or absence of this particular response in tissues will depend on a number of other factors as well as muscarinic receptor number. The levels and subtypes of G proteins will vary in tissues, as will the levels and isoforms of AC. These factors will markedly affect the responsiveness of the tissues to receptor stimulation. Indeed, muscarinic receptor-mediated potentiation of AC has been observed in a number of tissues, *e.g.* mouse parotid cells (Watson *et al*, 1990), rat brain olfactory bulb (Olianas and Onali, 1990), cultured sympathetic neurons (Suidan *et al*, 1991) and in rat adrenal gland slices (Regunathan *et al*, 1990). Similarly, M_3 muscarinic receptors have been found to couple via PTX-sensitive G proteins, to the inhibition of AC in Madin-Darby canine kidney cells (Mohuczy-Dominiak and Garg, 1992) and in rat parotid gland (Dai *et al*, 1991). Agonist-stimulated PLC activation has also been observed in CHO cells expressing high levels of m2 muscarinic receptors (Ashkenazi *et al*, 1987). Therefore, stimulation of a particular muscarinic receptor subtype may elicit a variety of cellular responses depending on the level of receptor expression, G protein expression, and the effector isoforms present. The expression level of the receptors may affect, not only the potency and maximal responsiveness of the agonist response, but also the ability of the receptors to couple promiscuously with G proteins, thereby modulating different effector systems.

The present study, therefore, provides evidence for the idea that physiological responses to pharmacological agents acting on muscarinic receptors, and other G protein-coupled receptors, have the potential to be extremely varied depending on the cells or tissue involved. Detailed knowledge of the receptors, G proteins and effectors involved in the signal transduction mechanism within a particular tissue, may be necessary before specific therapeutic strategies can be devised.

Figure 9.1.

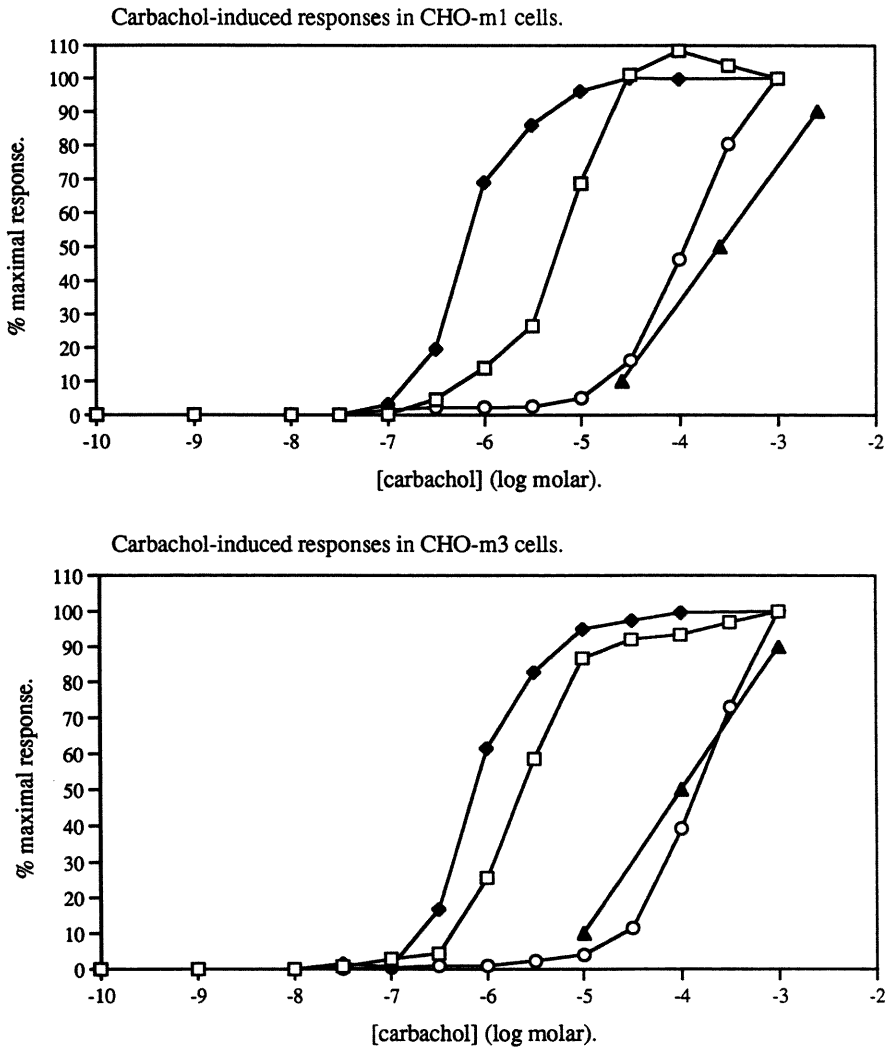

—□— $Ins(1,4,5)P_3$ mass (peak response at 10 s in intact cells).

—◆— $^{45}Ca^{2+}$ release (peak response at 2 min in permeabilized cell suspensions).

—○— cAMP mass (peak response at 3 min in intact cells).

—▲— Binding affinity in the presence of GTP in membrane preparations.

Figure 9.2.

Carbachol-induced responses in CHO-m2 and CHO-slm2 cells.

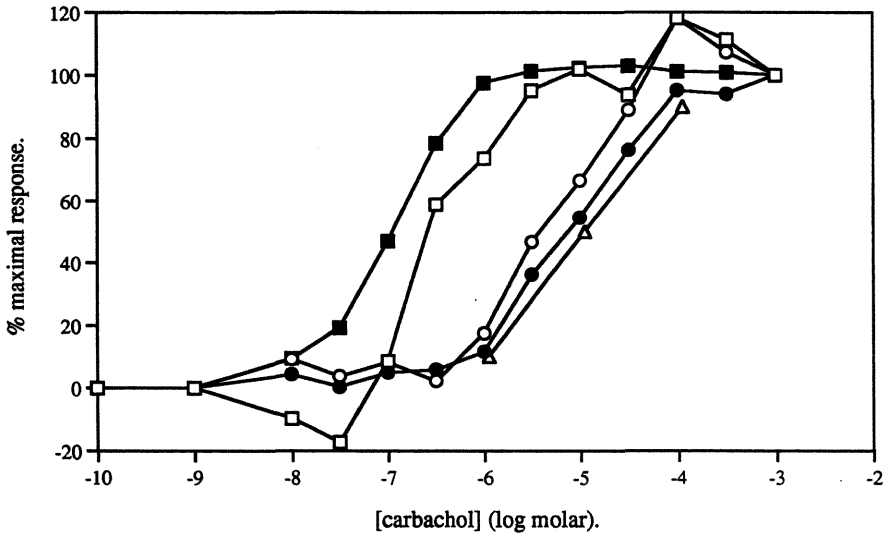

—□— CHO-m2 (intact cells). Inhibition of forskolin-stimulated cAMP mass (response at 5 min).

—○— CHO-m2 (intact cells). Potentiation of forskolin-stimulated cAMP mass after PTX pretreatment (response at 5 min).

—■— CHO-slm2 (intact cells). Inhibition of forskolin-stimulated cAMP mass (response at 5 min).

—●— CHO-slm2 (intact cells). Potentiation of forskolin-stimulated cAMP mass after PTX pretreatment (response at 5 min).

—△— CHO-m2 (membranes). Binding affinity in the presence of GTP

Figure 9.3.

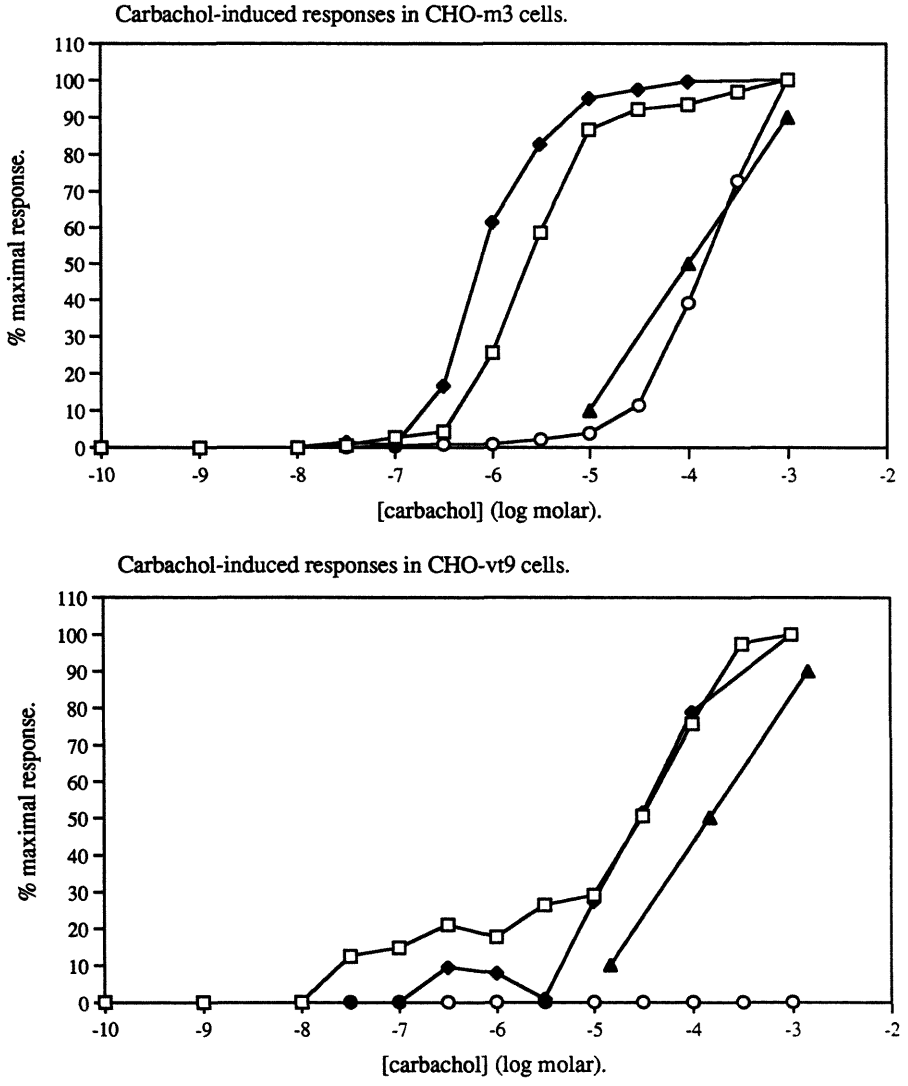

—□— $Ins(1,4,5)P_3$ mass (peak response at 10 s in intact cells).

—◆— $^{45}Ca^{2+}$ release (peak response at 2 min in permeabilized cells).

—○— cAMP mass (peak response at 3 min in intact cells).

—▲— binding affinity in the presence of GTP (in membrane preparations).

APPENDICES.

Appendix 1.

Preparation of Cytosol-Like Buffer (CLB)

CLB was prepared fresh just prior to use due to the relative instability of adenosine 5'-triphosphate (disodium salt, grade 1, 99 % pure) (ATP) in neutral pH solutions. CLB (minus ATP) was prepared at 5 x stock using nominally calcium-free distilled water and stored in plastic containers (not glass) to avoid calcium contamination of the buffer. The ingredients for CLB are listed below.

Table 1.

chemical name	chemical formula	stock concentration in CLB (mM).
Potassium chloride	KCl	120
Potassium dihydrogen orthophosphate	KH_2PO_4	2
Sodium succinate hexahydrate	$(NaH_2COONa)_2.6H_2O$	5
Magnesium chloride hexahydrate	$MgCl_2.6H_2O$	2.4
HEPES (free acid)	$C_8H_{18}N_2O_4S$	20

10 ml of 5 x stock CLB was added to 40 ml of distilled water. 2 mM ATP was added resulting in a Mg^{2+} / ATP ratio of 6:5. ATP exists in two forms: ATP^{2-} and ATP^{4-}. ATP^{2-} is the active form in terms of its ability to drive Ca^{2+}-ATPase activity and thus allow Ca^{2+} uptake into pools within the cell. This Mg^{2+} / ATP ratio preferentially shifts the equilibrium of the two forms of ATP in favour of the ATP^{2-} form thus optimizing the uptake of Ca^{2+}.

30 µl of EGTA (10 mM in KOH (20 mM)) was added to the CLB + ATP (2-5 µM EGTA final concentration) and the pH was corrected to 7.2 with 20 % (w / v) KOH and 1 mM HCl. This concentration of EGTA buffered $[Ca^{2+}]$ to between 80-150 nM.

$[Ca^{2+}]$ in CLB was checked before each experiment by fura-2 studies in a fluorimeter

and more EGTA was added if required.

Determination of CLB Free [Ca^{2+}].

A sample of EGTA-buffered CLB (2 ml) was placed in a fluorimeter cuvette with 5 µl of fura-2 free acid (100 µM stock). The fluorescent intensity (F) of the buffer was determined at excitation and emission wavelengths of 340 nm and 480 nm, respectively. Values for F_{max} were determined by the further addition of 5 µl of $CaCl_2$ solution (200 mM stock). F_{min} values were obtained by further addition of 50 µl of EGTA (200 mM stock made up in 400 mM KOH) to sequester all free [Ca^{2+}]. Free [Ca^{2+}] in the EGTA-buffered CLB was determined using the following equation:

$$\text{free}[Ca^{2+}]\ (nM) = (F - F_{min} / F_{max} - F) \times K_D$$

where the K_D = 139 nM at 25 °C and represents the dissociation constant for Ca^{2+} binding to fura-2. Care was taken to check and adjust the free [Ca^{2+}] of the CLB before each experiment due to the variations in [Ca^{2+}] found in the distilled water from week to week.

Appendix 2.

Preparation of Krebs-HEPES Buffer.

Krebs-HEPES buffer consisted of the following ingredients:

chemical name	**chemical formula**	**concentration**	
		(mM)	**(g / l)**
Sodium chloride	NaCl	118.6	6.74
Potassium chloride	KCl	4.7	0.35
Magnesium sulphate hexahydrate	$MgSO_4.6H_2O$	1.2	0.29
Potassium dihydrogen orthophosphate	KH_2PO_4	1.2	0.16
Sodium hydrogen carbonate	$NaHCO_3$	4.2	0.35
D-Glucose	$C_6H_{12}O_6$	11.7	2.10
Calcium chloride dihydrate	$CaCl_2.2H_2O$	1.3	0.19
HEPES (free acid)	$C_8H_{18}N_2O_4S$	10.0	2.38

p.H. was adjusted to 7.4 with 1 M NaOH.

Appendix 3.
List of reagents.

from Sigma Chemical Company Limited, Poole, Dorset, England.

Adenosine-5'-triphosphate (ATP)
Atropine sulphate
Bordetella Pertussis Toxin (PTX)
Bovine Serum Albumin (B.S.A).
Calcium chloride dihydrate ($CaCl_2.2H_2O$)
Carbamylcholine chloride (carbachol)
Dithiothreitol (DTT)
Ethylene glycol-bis(β-aminoethyl ether)-N,N,N',N'-tetraacetic acid (EGTA)
($C_{14}H_{24}N_2O_{10}$)
Forskolin
Guanosine-5'-diphosphate (GDP)
Guanosine-5'-O-(3-thiotriphosphate) (GTPγS)
HEPES ($C_8H_{18}N_2O_4S$) (N-[2-Hydroxyethyl]piperazine-N'-[2-ethanesulfonic acid
Pirenzepine dihydrochloride
Saponin
Sigmacote
1,1,2-Trichlorotrifluoroethane (Freon)
Tri-n-octylamine

from Fisons Scientific Equipment, Loughborough, Leics, England.

Cupric sulphate ($CuSO_4.5H_2O$)
D-Glucose ($C_6H_{12}O_6$)
Hydrochloric acid (HCl)
Potassium chloride (KCl)
Potassium dihydrogen orthophosphate (KH_2PO_4)
Potassium hydroxide (KOH)
Potassium sodium tartrate ($KNaC_4H_4O_6.4H_2O$)
Sodium chloride (NaCl)
Sodium carbonate (Na_2CO_3)
Sodium hydrogen carbonate ($NaHCO_3$)
Sodium hydroxide (NaOH)
Sodium succinate hexahydrate ($(NaH_2COONa)_2.6H_2O$)

Trichloroacetic acid (TCA) ($CCl_3.COOH$)
Tris-(hydroxymethyl)-methylamine ($NH_2.C(CH_2OH)_3$)

from GIBCO. BRL, Paisley, Scotland.

Growth media and supplements

from B.D.H. Limited, Poole, Dorset, England.

Ethylenediaminetetra-acetic acid (EDTA) ($[CH_2N(CH_2.COOH)_2]_2$)
Folin-Ciocalteu's phenol reagent
Magnesium chloride hexahydrate ($MgCl_2.6H_2O$)

from Amersham International PLC, Aylesbury, Bucks, England.

$^{45}CaCl$ (calcium chloride)
D-myo-[^{3}H] Inositol-1,4,5-triphosphate ([^{3}H]Ins(1,4,5)P_3)
[^{3}H] N-methyl scopolamine chloride ([^{3}H]NMS)

from Research Biochemicals International. Semet Technical (U.K.) Ltd, St. Albans, Herts, England.

Methoctramine tetrahydrochloride

from Boehringer Corporation Limited,Lewes, East Sussex.

Guanosine-5'-triphosphate (dilithium salt) (GTP)
Guanylyl-imidodiphosphate (tetralithium salt) (GppNHp)

from Calbiochem. Novabiochem. Ltd, Nottingham, England.

Fura-2

from New England Nuclear (N.E.N. Ltd), Du Pont (U.K.) Ltd, Stevenage, Herts, England.

Adenosine 3',5'-cyclic monophosphate (cAMP)
[^{3}H]Adenosine 3',5'-cyclic monophosphate ([^{3}H]cAMP)
[^{35}S] Guanosine-5'-O-(3-thiotriphosphate) ([^{35}S]GTPγS)

from the University of Rhode Island Foundation Chemistry Group, U.S.A.

D-myo-inositol 1,4,5,-triphosphate ($Ins(1,4,5)P_3$).

from Dr. R. Barlow, University of Bristol, Avon, England.

4-Diphenylacetoxy-N-methyl piperidine methiodide (4-DAMP)

from Aldrich Chemical Company, Gillingham, Dorset, England.

Dimethylsulphoxide (DMSO)

Appendix 4.

A typical standard curve for displacement of [^{3}H]Ins(1,4,5)P_3 (0.8 nM) (specific activity 34 Ci / mmol) with increasing amounts of cold Ins(1,4,5)P_3.

The assay contained 30 µl of standard / sample, 30 µl Tris / EDTA, pH 8.0, 30 µl of [^{3}H]Ins(1,4,5)P_3 and 30 µl of Ins(1,4,5)P_3 binding protein.

Incubations were started by the addition of the binding protein at 4 ^{o}C for 60 min. Incubations were terminated by vacuum filtration onto Whatman GF/B filters as described in chapter 6 methods.

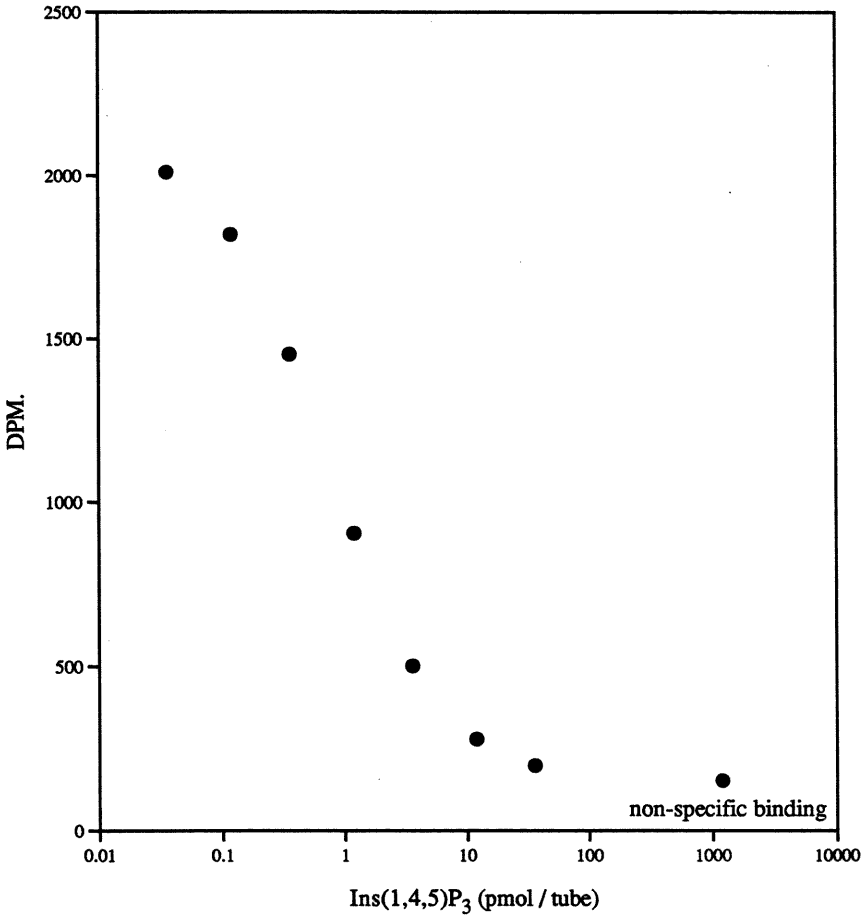

Appendix 5.

Example of a typical standard curve showing displacement of [^{3}H]cAMP (approximately 4 nM) (specific activity 28.9 Ci / mmol) with increasing amounts of cold cAMP. Each assay tube contained 50 µl of standard / sample, 100 µl of [^{3}H]cAMP and 150 µl of binding protein. Incubations were for greater than 90 min at 4 °C and were terminated by the addition of 250 µl of ice-cold charcoal / BSA mix as explained in chapter 8 methods.

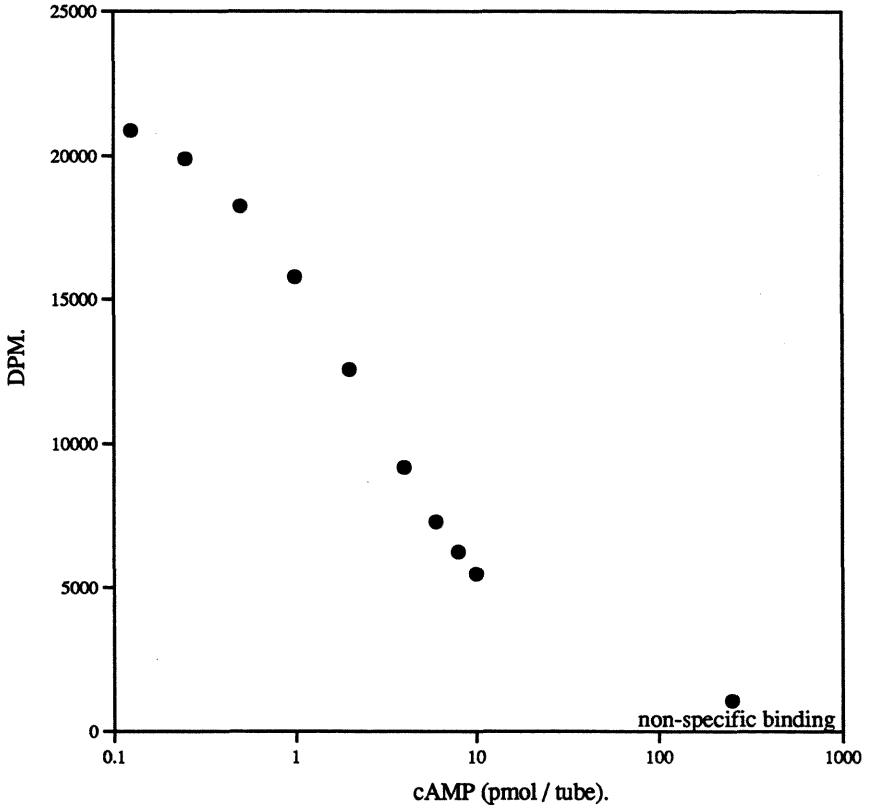

Appendix 6.

Abbreviations List.

AC	Adenylate cyclase
ADP	Adenosine 5'-diphosphate
AFDX-116	(11[[2-[(diethylamino)methyl]-1-piperidinyl]acetyl]-5,11- dihydro-6H-pyrido[2,3-b][1,4]benzodiazepine-6-one).
ATP	Adenosine 5'-triphosphate
βARK	β-adrenergic receptor kinase
B_{max}	Maximal specific binding capacity
BSA	Bovine serum albumin
cAMP	Adenosine 3',5'-cyclic monophosphate.
cDNA	Complementary Deoxyribose nucleic acid
CHO cells	Chinese Hamster Ovary cells.
CLB	Cytosol-like buffer
CNS	Central Nervous System
CTX	cholera toxin
DAG	*sn*-1,2-Diacylglycerol
4-DAMP	4-Diphenylacetoxy-N-methyl piperidine methiodide
DMSO	Dimethylsulphoxide
DPM	Disintegrations per minute
EC_{50}	The concentration of an agonist which produces 50% of the maximum possible response for that agonist
EDTA	Ethylenediaminetetra-acetic acid
EGTA	Ethylene glycol-bis(β-aminoethyl ether)-N,N,N',N'-tetraacetic acid
FMLP	Formyl-methionyl-leucyl-phenylalanine
GAP	Guanine nucleotide binding protein-activating protein
GDP	Guanosine 5'-diphosphate
GDPβS	Guanosine 5'-O-(2-thiodiphosphate)
G protein	Guanine nucleotide binding protein
GppNHp	Guanylyl-imidodiphosphate
GTP	Guanosine 5'-triphosphate.
GTPγS	Guanosine 5'-O-(3-thiotriphosphate)
HHSiD	Hexahydro-sila-difenidol
IBMX	3-Isobutyl-1-methylxanthine
IC_{50}	The concentration of competing ligand which displaces 50% of the

	specific binding of the radioligand
$Ins(1)P_1$	D-myo-Inositol 1-monophosphate
$Ins(3)P_1$	D-myo-Inositol 3-monophosphate
$Ins(4)P_1$	D-myo-Inositol 4-monophosphate
$Ins(1,4)P_2$	D-myo-Inositol 1,4-bisphosphate
$Ins(1,3)P_2$	D-myo-Inositol 1,3-bisphosphate
$Ins(3,4)P_2$	D-myo-Inositol 3,4-bisphosphate
$Ins(1,4,5)P_3$	D-myo-Inositol 1,4,5-trisphosphate
$Ins(1,3,4)P_3$	D-myo-Inositol 1,3,4-trisphosphate
$Ins(1,3,4,5)P_4$	D-myo-Inositol 1,3,4,5-tetrakisphosphate.
$Ins(1,3,4,5,6)P_5$	D-myo-Inositol 1,3,4,5,6-pentakisphosphate
$InsP_6$	D-myo-Inositol 1,2,3,4,5,6-hexakisphosphate
K_D	Equilibrium dissociation constant
K_i	Inhibition constant
K_{50}	The inhibition constant when the slope factor is significantly less than unity
mAChR	Muscarinic acetylcholine receptor.
McN-A-343	(4-Hydroxy-2-butynyl)-1-trimethylammonium-m-chlorocarbinilate chloride).
mRNA	Messenger ribose nucleic acid.
NAD^+	β-nicotinamide-adenine-dinucleotide
nH	Hill coefficient
NMS	N-methyl scopolamine
NSB	Non-specific binding
PDE	Phosphodiesterase
PI	Phosphatidylinositol
PI-linked	Phosphoinositide-linked
PIP	Phosphatidylinositol 4-phosphate
PIP_2	Phosphatidylinositol 4,5-bisphosphate
PKC	Protein kinase C
PKA	Protein kinase A
PLA_2	Phospholipase A_2
PLC	Phospholipase C
PLD	Phospholipase D
PTX	pertussis toxin (from *Bordetella pertussis*)
TCA	Trichloroacetic acid
TM	Trans-membrane

Publication list.

Refereed Abstracts.

Burford, N.T., Tobin, A.B. and Nahorski, S.R.
Agonist binding and G protein activation in CHO cells expressing m1, m2 or m3 muscarinic receptors.
Brit. J. Pharmacol. (1992). **106**: C.92.

Burford, N.T., Tobin, A.B. and Nahorski, S.R.
Agonist-stimulated Ins(1,4,5)P_3 accumulation and Ca^{2+} mobilization from intact and permeabilized CHO cells expressing recombinant muscarinic receptor subtypes.
Brit. J. Pharmacol. (1994). April edition (to be published).

Posters.

Burford, N.T., Wojcikiewicz, R.J.H. and Nahorski, S.R.
Guanine nucleotide-sensitive agonist binding to recombinant m3 muscarinic receptors.
Thirty-sixth Harden conference on GTP-binding proteins, Wye College, Kent. (September 1991).

Burford, N.T., Tobin, A.B. and Nahorski, S.R.
Agonist binding to recombinant m2 and m3 muscarinic receptors in CHO-K1 cells: Guanine nucleotide and PTX-sensitivity.
8th International Conference on Second Messengers and Phosphoproteins, Glasgow, Scotland. (August 1992).

Burford, N.T., Tobin, A.B. and Nahorski, S.R.
Promiscuous coupling of m1 and m3 muscarinic receptors, expressed in CHO cells, with PTX-sensitive and PTX-insensitive G proteins.
Mechanism and analysis of agonist action: The influence of receptor structure, Wadham College, Oxford. (September 1993).

Reviews.

Wojcikiewicz, R.J.H., Burford, N.T. and Nahorski, S.R.
Coupling of pharmacological receptors to polyphosphoinositide turnover.
In: Topics in Pharmaceutical Sciences, 1991. (eds) Crommelin, D.J.A. and Midha, K.K.

Medpharm Scientific Publishers, Stuttgart (1992) pp 575-582.

Lambert, D.G., Burford, N.T. and Nahorski, S.R.
Muscarinic receptor subtypes: inositol phosphates and intracellular calcium.
Biochem. Soc. Trans. (1992) **20**: 130-135.

BIBLIOGRAPHY.

Adem, A., Mattsson, M.E.K., Nordberg, A. and Pahlman, S. (1987). Dev. Brain. Res. **33**: 235-242.

Aragay, A.M., Katz, A. and Simon, M.I. (1992). J. Biol. Chem. **267**: 24983-24988.

Arunlakshana, O. and Schild, H.O. (1959). Brit. J. Pharmacol. **14**: 48-58.

Ashkenazi, A., Winslow, J.W., Peralta, E.G., Peterson, G.L., Schimerlik, M.I., Capon, D.J. and Ramachandran, J. (1987). Science. **238**: 672-674.

Azzi, A., Boscoboinik, D. and Hensey, C. (1992). Eur. J. Biochem. **208**: 547-557.

Bakalyer, H.A. and Reed, R.R. (1990). Science. **250**: 1403-1406.

Barlow, R.B., Berry, K.J., Glenton, P.A.M., Nikolaou, N.M. and Soh, K.S. (1976). Br. J. Pharmacol. **58**: 613-620.

Baron, B.M. and Siegal, B.W. (1989). J. Neurochem. **53**: 602-609.

Bauer, P.H., Muller, S., Puzicha, M., Pippig, S., Obermaier, B., Helmreich, E.J.M. and Lohse, M.J. (1992). Nature. **358**: 73-76.

Baumgold, J. (1992). TiPS. **13**: 339-340.

Baumgold, J. and Fishman, P.H. (1989). Biochem. Biophys. Res. Commun. **154**: 1137-1143.

Baumgold, J., Paek, R. and Fiskum, G. (1992). J. Neurochem. **58**: 1754-1759.

Bender, J.L. and Neer, E.J. (1983). J. Biol. Chem. **258**: 2432-2439.

Berlot, C.H. and Bourne, H.R. (1992). Cell. **68**: 911-922.

Berridge, M.J. (1993). Nature. **361**: 315-324.

Berridge, M.J. and Irvine, R.F. (1984). Nature. **312**: 315-321.

Berridge, M.J. and Irvine, R.F. (1989). Nature. **341**: 197-205.

Berstein, G., Blanks, J.L., Smrcka, A.V., Higashijima, T., Sternweis, P.C., Exton, J.H. and Ross, E.M. (1992). J. Biol. Chem. **267**: 8081-8088.

Bezprozvanny, I., Watras, J. and Ehrlich, B.E. (1991). Nature. **351**: 751-754.

Bigay, J., Deterre, P., Pfister, C. and Chabre, M. (1985). FEBS Lett. **191**: 181-185.

Bird, G.ST.J., Rossier, M.F., Hughes, A.R., Shears, S.B., Armstrong, D.L. and Putney, Jr.J.W. (1992). Nature. **352**: 162-165.

Birdsall, N., Buckley, N., Doods, K., Fukuda, A., Giachetti, A., Hammer, R., Kilbinger, H., Lambrecht, G., Mutschler, E., Nathanson, N., North, A. and Schwarz, R. (1989). TiPS. **4**: VII.

Birdsall, N.J.M., Burgen, A.S.V., Hulme, E.C. and Wells, J.W. (1979). Br. J. Pharm. **67**: 371-377.

Birnbaumer, L., Abromowitz, J. and Brown, A.M. (1990). Biochim. Biophys. Acta. **1031**: 163-224.

Bitensky, M.W., Wheeler, G.L., Yamazaki, A., Rasenick, M.M. and Stein, P.J. (1981). Curr. Top. Membr. Transp. **15**: 237-271.

Bokoch, G.M. Katada, T., Northup, J.K., Ui, M. and Gilman, A.G. (1984). J. Biol. Chem. **259**: 3560-3567.

Bonner, T.I., Buckley, N.J., Young, A,C. and Brann, M.R. (1987). Science. **237**: 527-532.

Bonner, T.I., Young, A.C., Brann, M.R. and Buckley, N.J. (1988). Neuron. **1**: 403-410.

Bourne, H.R. (1989). Nature. **337**: 504-505.

Bourne, H.R., Coffino, P. and Tomkins, G.M. (1975). Science. **187**: 750-752.

Bourne, H.R. and Stryer, L. (1992). Nature. **358**: 541-543.

Bradford, P.G. and Irvine, R.F. (1987). Biochem. Biophys. Res. Commun. **148**: 1283-1289.

Brann, M.R., Buckley, N.J., Jones, S.V.P. and Bonner, T.I. (1987). Mol. Pharmacol. **32**: 450-455.

Buck, M.A. and Fraser, C.M. (1990). Biochem. Biophys. Res. Commun. **173**: 666-672.

Buckley, N.J. (1990) Intracelluler Messengers and Implications for Drug Development. Ed. Nahorski, S. Wiley, New York. pp 11-30.

Buckley, N.J., Bonner, T.I., Buckley, C.M. and Brann, M.R. (1989). Mol. Pharmacol. **35**: 469-476.

Camps, M., Carozzi, A., Schnabel, P., Scheer, A., Parker, P.J. and Gierschik, P. (1992). Nature. **360**: 684-689.

Carafoli, E. (1987). Annu. Rev. Biochem. **56**: 395-433.

Carozzi, A., Camps, M., Gierschik, P. and Parker, P.J. (1993). FEBS Lett. **315**: 340-342.

Caulfield, M.P. (1993). Pharmacol. Thera. **58**: 319-379.

Caulfield, M.P. and Brown, D.A. (1991). Br. J. Pharmacol. **104**: 39-45.

Cerione, R.A., Codina, J., Benovic, J.L., Lefkowitz, R.J. (1984). Biochemistry. **23**: 4519.

Chabre, M. and Deterre, P. (1989). Eur. J. Biochem. **179**: 255.

Challiss, R.A.J., Batty, I.H. and Nahorski, S.R. (1988). Biochem. Biophys. Res. Commun. **157**: 684-691.

Challiss, R.A.J., Chilvers, E.R., Willcocks, A.L. and Nahorski, S.R. (1990). Biochem. J. **265**: 421-427.

Chen, C. and Okayama, H. (1987). Mol. Cell. Biol. **7**: 2745-2752.

Cheng, Y.C. and Prusoff, W.H. (1973). Biochem. Pharmacol. **22**: 3099.

Cheung, A.H., Huang, R-R.C. and Strader, C.D. (1992). Mol. Pharmacol. **41**: 1061-1065.

Chinkers, M., and Garbers, D.L. (1991). Annu. Rev. Biochem. **60**: 553-575.

Choi, E.J., Xia, Z. and Storm, D.R. (1992). Biochemistry. **31**: 6492-6498.

Clapham, D.E. and Neer, E.J. (1993). Nature. **365**: 403-406.

Clark, J.D., Lin, L-L, Kriz, R.W., Rannesha, C.S., Sultzman, L.A., Lin, A.Y., Milona, N. and Knopf, J.W. (1991). Cell. **65**: 1043-1051.

Cockcroft, S. (1987). TiBS. **12**: 75-78.

Cockcroft, S. and Thomas, G.M.H. (1992). Biochem. J. **288**: 1-14.

Conklin, B.R. and Bourne, H.R. (1993). Cell. **73**: 631-641.

Conklin, B.R., Farfel, Z., Lustig, K.D., Julius, D. and Bourne, H.R. (1993). Nature. **363**: 274-276.

Dai, Y., Ambudkar, I.S., Horn, V.J., Yeh, C-K., Kousvelari, E.E., Wall, S.J., Li, M., Yashuda, R.P., Wolfe, B.B. and Baum, B.J. (1991). Am. J. Physiol. **261** (Cell Physiol. 30): C1063-C1073.

Dale, H.H. (1914). Proc. Physiol. Soc. London. p iii.

Dale, H.H. and Ewin, A.J. (1914). Proc. Physiol. Soc. London. p xxiv.

Daly, J.W. (1984). Adv. Cyc. Nuc. Res. **17**: 81-90.

Darfler, F.J., Mohan, L.C., Koachman, A.M. and Insel, P.A. (1982). J. Biol. Chem. **257**: 11901-11907.

Decker, S.J., Ellis, C., Pawson, T. and Velu, T. (1990) J. Biol. Chem. **265**: 7009-7015.

De Lean, A., Munson, P.J. and Rodbard, D. (1978). Am. J. Physiol. **235**: E97.

De Lean, A., Stadel, J.M. and Leftkowitz, R.J. (1980) J. Biol. Chem. **255**: 71108-71117.

Dell'Acqua, M.L., Carroll, R.C. and Peralta, E.G. (1993). J. Biol. Chem. **268**: 5676-5685.

DeLisle, S. and Welsh, M.J. (1992). J. Biol. Chem. **267**: 7963-7966.

Dickenson, J.M., White, T.E. and Hill, S.J. (1993). Biochem. J. **292**: 409-417.

Doods, H.N., Mathy, M-J, Davidesko, D., Charldorp, K.J. VAN, Jonge, A. DE. and Zweitoen, P.A. VAN. (1987). J. Pharm. Exp. Thera. **242(1)**: 257-262.

Dorje, F., Levey, A.I. and Brann, M.R. (1991b), Mol. Pharmacol. **40**: 459-462.

Dorje, F., Wess, J., Lambrecht, G., Tacke, R., Mutschler, E. and Brann, M.R. (1991). J. Pharm. Exp. Thera. **256**: 727-733.

Downes, C.P. and MacPhee, C.H. (1990). Eur. J. Biochem. **193**: 1-18.

Downward, J. (1990). TiBS. **15**: 469-472.

Eason, M.G., Kurose, H., Holt, B.D., Raymond, J.R., and Liggett, S.B. (1992). J. Biol. Chem. **267**: 15795-15801.

Ehlert, F.J. (1985). Mol. Pharmacol. **28**: 410-421.

Eltze, M. (1988). Eur. J. Pharmacol. **151**: 205-221.

Enomoto, K. and Asakawa, T. (1986). FEBS. Letts. **202**: 63.

Enyedi, P. and William, G.H. (1988). J. Biol. Chem. **263**: 7940-7942.

Evans, T., Martin, M.W., Hughes, A.R. and Harden, T.K. (1985a). Mol. Pharmacol. **27**: 32-37.

Evans, T., Hepler, J.R., Masters, S.B., Brown, J.H. and Harden, T.K. (1985b). Biochem. J. **232**: 751-757.

Fain, J.N. (1990). Biochim. Biophys. Acta. **1053**: 81-88.

Fargin, A., Raymond, J.R., Regan, J.W., Cotecchia, S., Lefkowitz, R.J. and Caron, M.G. (1989) J. Biol. Chem. **264**: 14848-14852.

Federman, A.D., Conklin, B.R., Schrader, K.A., Reed, R.R. and Bourne, H.R. (1992).

Nature. **356**: 159-161.

Feinstein, P.G., Schrader, K.A., Bakalyer, H.A., Tang, W-J., Krupinski, J., Gilman, A.G. and Reed, R.R. (1991). Proc. Natl. Acad. Sci. USA. **88**: 10173-10177.

Felder, C.C., Kanterman, R.Y., Ma, A.L. and Axelrod, J. (1989). J. Biol. Chem. **264**: 20356-20362.

Ferris, C.D., Huganir, R.L. and Snyder, S.H. (1990). Proc. Natl. Acad. Sci. USA. **87**: 2147-2151.

Florio, V.A. and Sterweis, P.C. (1989). J. Biol. Chem. **264**: 3909-3915.

Flynn, D.D., Palermo, N. and Suarez, A. (1989). Eur. J. Pharmacol. Mol. Pharmacol. Section. **172**: 363-372.

Fraser, C.M., Arakawa, S., McCombie, W.R. and Venter, J.C. (1989). J. Biol. Chem. **264**: 11754-11761.

Fraser, C.M., Wang, C.D., Robinson, D.A., Gocayne, J.D. and Venter, J.C. (1989), Mol. Pharmacol. **36**: 840-847.

Furuichi, T., Yoshikawa, S., Miyawaki, A., Wada, K., Maeda, N. and Mikoshiba, K. (1989). Nature. **342**: 32-38.

Gao, B. and Gilman, A.G. (1991). Proc. Natl. Acad. Sci. USA. **88**: 10178-10182.

Gerhardt, M.A. and Neubig, R.R, (1991). Mol. Pharmacol. **40**: 707-711.

Gershengorn, M.C., Geras, G., Purrella, V.S. and Rebecchi, M.J. (1984). J. Biol. Chem. **259**: 10675-10681.

Gierschik, P. (1992). Current Topics in Microbiology and Immunology. **175**: 69-96.

Gierschik, P., Sidiropoulos, D., Steisslinger, M. and Jakobs, K.H. (1989). Eur. J. Pharm.-Mol. Pharmacol. Sec. **172**: 481-492.

Gierschik, P., Moghtader, R., Straub, C., Dieterich, K. and Jakobs, K.H. (1991).Eur. J. Biochem. **197**:725-732.

Giraldo, E., Micheletti, R., Montagna, E., Giachetti, A., Vigano, M., Ladinsky, H. and Melchiorre, C. (1988). J. Pharm. Exp. Thera. **244**: 1016-1020.

Godchaux, W., III and Zimmerman, W.F. (1979). J. Biol. Chem. **254**: 7874-7884.

Graziano, M.P., Casey, P.J. and Gilman, A.G. (1987). J. Biol. Chem. **262**: 11375.

Guerrant, R.L., Brunton, L.L., Schnaitman, T.C., Rebhun, L.I. and Gilman, A.G. (1974). Infect. Immunol. **10**: 320-327.

Gurwitz, D., Kloog, Y. and Sokolovsky, M. (1985). Mol. Pharmacol. **28**: 297-305.

Gurwitz, D. Haring, R., Heldman, E., Fraser, C.M., Manor, D. and Fisher, A. (1994). Eur. J. Pharmacol. (Mol. Pharm. Sec.). **267**: 21-31.

Gusovsky, F., Lueders, J.E., Kohn, E.C. and Felder, C.C. (1993). J. Biol. Chem. **268**: 7768-7772.

Gutowski, S., Smrcka, A., Nowak, L., Wu, D., Simon, M. and Sternweis, P.C. (1991). J. Biol. Chem. **266**: 20519-20524.

Hadcock, J.R. and Malbon, C.C. (1993). J. Neurochem. **60**: 1-9.

Haga, T., Haga, K., Kameyama, K. and Nakata, H. (1993). Life Sciences. **52**: 421-428.

Haga, K., Haga, T., Ichijama, A., Katada, T., Kurose, H. and Ui, M. (1985). Nature. **316**: 731.

Hall, A. (1992). Cell. **69**: 389-391.

Hamm, H.E. (1990). The Biology and Medicine of Signal Transduction. ed. Nishizuka, Y. Raven Press. New York. pp. 76-82.

Hamm, H.E., Deretic, D., Arendt, A., Hargrove, P.A., Koenig, B. and Hofmann, K.P. (1988). Science. **241**: 832-835.

Hammer, R., Berrie, C.P., Birdsall, N.J.M., Burgen, A.S.V. and Hulme, E.C. (1980). Nature. **283**: 90-92.

Hammer, R. and Giachetti, A. (1982). Life Sciences. **31**: 2991-2999.

Hanski, E., Sternweis, P.C., Northup, J.K., Dramerick, A.W. and Gilman, A.G. (1981). J. Biol. Chem. **256**: 12911-12919.

Harden, T.K., Meeker, R.B. and Martin, M.W. (1983). J. Pharm. Exp. Thera. **227**: 570-577.

Harden, T.K., Hawkins, P.T., Stephens, L., Boyer, J.C. and Downes, C.P. (1988). Biochem. J. **252**: 583-593.

Hausdorff, W.P., Hnatowich, M., O'Dowd, B.F., Caron, M.G. and Lefkowitz, R.J. (1990). J. Biol. Chem. **265**: 1388-1393.

Higashijima, T., Burnier, J. and Ross, E.M. (1990). J. Biol. Chem. **265**: 14176-14186.

Higashijima, T., Ferguson, K.M., Sternweis, P.C., Smigel, M.D. and Gilman, A.G. (1987). J. Biol. Chem. **262(2)**: 762-766.

Hilf, G., Gierschik, P. and Jakobs, K.H. (1989). Eur. J. Biochem. **186**: 725-731.

Hilf, G. and Jakobs, K.H. (1992). Eur. J. Pharm.- Mol. Pharmacol. Sec. **225**: 245-252.

Hokin, M.R. and Hokin, L.E. (1953) J. Biol. Chem. **203**: 967-977.

Horstman, D.A., Brandon, S., Wilson, A.L., Guyer, C.A., Cragoe, E.J.Jr. and Limbird, L.E. (1990). J. Biol. Chem. **265(35)**: 21590-21595.

Hosey, M.M. (1983). Biochim. et Biophys. ACTA. **757**:119-127.

Hoyer, D. and Boddeke, H.W.G.M. (1993) TiPS. **14**: 270-275.

Hu, J. and El-Fakahany, E.E. (1990). Mol. Pharmacol. **38**: 895-903.

Hu, J., Wang, S-Z. and El-Fakahany, E.E. (1991). J. Pharm. Exp. Thera. **257**: 938-945.

Huff, R.M. and Neer, E.J. (1986). J. Biol. Chem. **261**: 1105.

Hughes, A.R., Martin, M.W. and Harden, T.K. (1984). Proc. Natl. Acad. Sci. USA. **81**: 5680-5684.

Hulme, E.C., Berrie, C.P., Birdsall, N.J.M., Jameson, M. and Stockton, J.M. (1983). Eur. J. Pharmacol. **94**: 59-72.

Hulme, E.C., Birdsall, N.J.M. and Buckley, N.J. (1990). A. Rev. Pharmacol. Toxicol. **30**: 633-673.

Irvine, R.F. (1990). FEBS Lett. **263**: 5-9.

Irvine, R.F., Moor, R.M., Pollock, W.K., Smith, P.M. and Wreggett, K.A. (1988). Philos. Trans. R. Soc. Lond. **B320**: 281-298.

Irvine, R.F. (1992). Putney, Jr.J.W. (ed). Inositol Polyphosphates and Calcium Signalling: Advances in Second Messenger and Phosphoprotein Research. Raven Press, New York. **26**: 161-185.

Ishikawa, Y., Katsushika, S., Chen, L., Halnon, N.J., Kawabe, J-I. and Homcy, C.J. (1992). J. Biol. Chem. **267**: 13553-13557.

Iyengar, R. and Birnbaumer, L. (1982). Proc. Natl. Acad. Sci. U.S.A. **79**: 5179-5183.

Iyengar, R., Rich, K.A., Herberg, J.T., Premont, R.T. and Codina, J. (1988). J. Biol. Chem. **263**: 15348-15353.

Iyengar, R. (1993). FASEB J. **7**: 768-775.

Jackson, T.R., Patterson, S.I., Thastrup, O.and Hanley, M.R. (1988). Biochem J. **253**: 81-86.

Jakobs, K.H., Aktories, K. and Schultz, G. (1979). Naunyn-Schmiederberg's Arch. Pharmacol. **310**: 113-119.

Jakobs, K.H., Aktories, K. and Schultz, G. (1981). Adv. Cyclic. Nuc. Res. **14**: 173-187.

Jansson, C.C., Kukkonen, J. and Akerman, K.E.O. (1991). Biochim. Biophys. Acta. **1095**: 255-260.

Johnson, M.C. and Aguilera, G. (1992). Endocrinology. **131**: 2404-2412.

Jones, S.V.P., Heilman, C.J. and Brann, M.R. (1991). Mol. Pharmacol. **40**: 242-247.

Jones, S.V.P., Levey, A.I., Weiner, D.M., Ellis, J., Novotny, E., Yu, S.H., Dorje, F., Wess, J. and Brann, M.R. (1992). Molecular Biology of G Proterin Coupled Receptors. Ed. Brann, M.R., Birkhauser, Boston. pp 170-197.

Jurnak, F. (1985). Science. **230**: 32-36.

Kameyama, K., Haga, K., Haga, T., Kontani, K., Katada, T. and Fukada, Y. (1993). J. Biol. Chem. **268(11)**: 7753-7758.

Katada, T., Bokoch, G.M., Northup, J.K., Ui, M. and Gilman, A.G. (1984). J. Biol. Chem. **259**: 3568.

Katada, T., Northup, J.K., Bokoch, G.M., Ui, M. and Gilman, A.G. (1984b). J. Biol. Chem. **259**: 3578-3585.

Katada, T., Oinuma, M. and Ui, M. (1986). J. Biol. Chem. **261**: 5215.

Katz. B. and Miledi, R. (1965). Proc. R. Soc. Lodon. Ser. B. **161**: 483-495.

Katz, A., Wu, D. and Simon, M.I. (1992). Nature. **360**: 686-689.

Keen, M. and Nahorski, S.R. (1988). Mol. Pharmacol. **34**: 769-778.

Kim, D., Lewis, D.L., Graziadei, L., Neer, E.J., Bar-Sagi, D. and Clapham, D.E. (1989). Nature. **337**: 557-560.

Kim, H.K., Kim, J.W., Zilberstein, A., Margolis, B., Kim, C.K., Schlessinger, J. and Rhee, S.G. (1991). Cell. **65**: 435-441.

Klee, C.B. (1988). Biochemistry. **27**: 6645-6653.

Kobilka, B.K., Kobilka, T.S., Daniel, K., Regan, J.W., Caron, M.G. and Leftkowitz, R.J. (1988). Science. **240**: 1310-1316.

Koch, A.C., Anderson, D.A., Moran, M.F., Ellis, C. and Pawson, T. (1991). Science. **252**:

668-674.

Korn, S.J., Martin, M.W. and Harden, T.K. (1983). J. Pharm. Exp. Thera. **224**: 118-126.

Krupinski, J., Coussen, F., Bakalyer, H.A., Tang, W.T., Feinstein, P.G., Orth, K., Slaughter, C., Reed, R.R. and Gilman, A.G. (1989). Science. **244**: 1558-1564.

Kubo, T., Fukuda, K., Mikami, A., Maeda, A., Takahashi, H., Mishina, M., Haga, T., Haga, K., Ichiyama, A., Kangawa, K., Kajima, M., Matsuo, H., Hirose, T. and Numa, S. (1986a). Nature. **323**: 411-416.

Kubo, T., Maeda, A., Sugimoto, K., Akiba, I., Mikami, A., Takahashi, H., Haga, T., Haga, K., Ichiyama, A., Kangawa, K., Matsuo, H., Hirose, T. and Numa, S. (1986b). FEBS Lett. **209**: 367-372.

Kuhn, H. (1980). Nature. **283**: 587-589.

Kukkonen, J., Ojala, P., Nasman, J., Hamalainen, H., Heikkila, J. and Akerman, K.E.O. (1992). J. Pharm. Exp. Thera. **263**: 1487-1493.

Kurose, H., Katada, T., Haga, T., Haga, K., Ichiyama, A. and Ui, M. (1986). J. Biol. Chem. **261**: 6423-6428.

Lambert, D.G. and Nahorski, S.R. (1990a). Biochem J. **265**: 555-562.

Lambert, D.G. and Nahorski, S.R. (1990b). Progress in Brain Research. vol 84. Eds. Aquilonius, S-M and Gillberg, P-G. pp31-42.

Lambert, D.G. and Nahorski, S.R. (1990c). Biochemical Pharmacology. **40**: 2291-2295.

Lambert, D.G., Ghataorre, A.S. and Nahorski, S.R. (1989). Eur. J. Pharm. **165**: 71-77.

Lambert, D.G., Challiss, R.A.J. and Nahorski, S.R. (1991). Biochem. J. **273**: 791-794.

Lambrecht, G., Fiefel, R., Forth, B., Strohmann, C., Tacke, R. and Mutschler, E. (1988). Eur. J. Pharmacol. **152**: 193-194.

Lameh, J., Philip. M., Sharma, Y.K., Moro, O., Ramachandran, J. and Sadee, W. (1992). J. Biol. Chem. **267**: 13406-13412.

Lai, J., Mei, L., Roeske, W.R., Chung, F-Z., Yamamura, H.I. and Venter, J.C. (1988). Life Sci. **42**: 2489-2502.

Lai, J., Waite, S.L., Bloom, J.W., Yamamura, H.I. and Roeske, W.R. (1991). J. Pharm. Exp. Ther. **258**: 938-944.

Lazareno, S., Buckley, N.J. and Roberts, F.F. (1990). Mol. Pharmacol. **38**: 805-815.

Lazareno, S., Farries, T. and Birdsall, N.J.M. (1993). Life Sciences. **52**: 449-456.

Lechleiter, J.D. and Clapham, D.E. (1992). Cell. **69**: 1-20.

Lee, N.H. and Fraser, C.M. (1993). J. Biol. Chem. **268**: 7949-7957.

Lee, C.H., Park, D.J., Wu, D., Rhee, S.G. and Simon, M.I. (1992). J. Biol. Chem. **267(33)**: 16044-16047.

Leftkowitz, R.J., Cotecchio, S., Samama, P. and Costa, T. (1993). TiPS. **14**: 303-307.

Levey, A.J., Kitt, C.A., Simonds, W.F., Price, D.L. and Brann, M. (1991), J. Neoroscience. **11**: 3218-3226.

Limbird, L.E., Speck, J.L. and Smith, S.K. (1982). Mol. Pharmacol. **21**: 609-617.

Linder, M.E., Pang, I-H., Duronio, R.J., Gordon, J.I., Sternweis, P.C. and Gilman, A,G, (1991). J. Biol. Chem. **266**: 4654-4659.

Logothetis, D.E., Kurachi, Y., Galper, J., Neer, E.J. and Clapham, D.E. (1987). Nature. **325**: 321-326.

Lorenzen, A., Fuss, M., Vogt, H. and Schwabe, U. (1993). Mol. Pharmacol. **44**: 115-123.

Lowry, O.H., Rosenbough, A.L., Farr, A.L. and Randall, R.J. (1951). J. Biol. Chem. **193**: 265-275.

Maeda, N., Kawasaki, T., Nakade, S., Yokota, N., Taguchi, T., Kasai, M. and Mikoshiba, K. (1991). J. Biol. Chem. **266**:1109-1116.

Maeda, N., Niinobe, M., Nakahira, K. and Mikoshiba, K. (1988). J. Neurochem. **51**: 1724-1730.

Maeda, N., Niinobe, M. and Mikoshiba, K. (1990). EMBO J. **9**: 61-67.

Maggio, R., Vogal, Z. and Wess, J. (1993). FEBS Lett. **319**: 195-200.

Marchi, M., Augliera, A., Codignola, A., Lunardi, G., Fedele, E., Fontana, G. and Raiteri, M. (1991). Arch. Pharmacol. **344**: 275-280.

Masters, S.B., Stroud, R.M. and Bourne, H.R. (1986). Protein Engineering. **1**: 47-54.

Matesic, D.F. and Luthin, G.R. (1991). FEBS. Lett. **284**: 184-186.

Matesic, D.F., Manning, D.R. and Luthin, G.R. (1991). Mol. Pharmacol. **40**: 347-353.

Matesic, D.F., Manning, D.R., Wolfe, B.B. and Luthin, G.R. (1989). J. Biol. Chem. **264**: 21638-21645.

Mazzoni, M.R. and Hamm, H.E. (1989). Biochemistry. **28**: 9873-9880.

McMahon, K.K. and Hosey, M.M. (1985). Mol. Pharmacol. **28**: 400-409.

Mei, L., Lai, J., Yamamura, H.I. and Roeske, W.R. (1989). J. Pharm. Exp. Thera. **251**: 90-97.

Mei, L., Lai, J., Yamamura, H.I. and Roeske, W.R. (1991). J. Pharm. Exp. Thera. **256**: 689-694.

Meldolesi, J., Madeddu, L. and Pozzan, T. (1990). Biochim. et Biophys. Acta. **1055**: 130-140.

Meldolesi, J., Clementi, E., Fasolato, C. Zacchetti, D. and Pozzan, T. (1991). TiPS. **12**: 289-292.

Metzger, H. and Lindner, E. (1981). IRCS Med. Sci. Biochem. **9**: 99.

Meyer, T., Holowka, D. and Stryer, L. (1988). Science. **240**: 653-656.

Meyer, T. and Stryer, L. (1990). Proc. Natl. Acad. Sci. USA. **87**: 3841-3845.

Michel, A.D. and Whiting, R.L. (1988). Eur. J. Pharmacol. **145**: 61-66.

Michel, R.H. (1982). Cell Calcium. **3**: 285-294.

Mignery, G.A., Johnson, P.A. and Sudhof, T.C. (1992). J. Biol. Chem. **267**: 7450-7455.

Mignery, G.A. and Sudhof, T.C. (1990). EMBO J. **9**:3893-3898.

Mikoshiba, K. (1993). TiPS. **14**: 86-89.

Mikoshiba, K., Huchet, M. and Changeux, J.P. (1979). Dev. Neurosci. **2**: 254-275.

Milburn, M.V., Tong, L., deVos, A.M., Brunger, A., Yamaizumi, Z., Nishimura, S. and Kim, S-H. (1990). Science. **247**: 939-945.

Missiaen, L., De Smedt, H., Droogmans, G. and Casteels, R. (1992a). J. Biol. Chem. **267**: 22961-22966.

Missiaen, L., De Smedt, H., Droogmans, G. and Casteels, R. (1992b). Nature. **357**: 599-602.

Mitchelson, F., Choo, L.K. and Darroch, S. (1989). Clin. Exp. Pharmacol. Physiol. **16**: 523-528.

Miyawaki, A., Furuichi, T., Maeda, N. and Mikoshiba, K. (1990). Neuron. **5**: 11-18.

Mohuczy-Dominiak, D. and Garg, L.C. (1992). Am. J. Physiol. **263** (Cell Physiol. 32): C1289-C1294.

Moolenar, W.H., Kruijer, W., Tilly, B.C., Verlaan, I., Bierman, A.J. and de Laat, S.W. (1986). Nature. **323**: 171-173.

Morris, A.P., Gallacher, D.V., Irvine, R.F. and Peterson, O.H. (1987). Nature. **330**: 653-655.

Moro, O., Lameh, J. and Sadee, W. (1993). J. Biol. Chem. **268**: 6862-6865.

Muallem, S., Pandol, S.J., Beeker, T.G. (1989). J. Biol. Chem. **264**: 205-212.

Mullaney, I., Dodd, M.W., Buckley, N. and Milligan, G. (1993). Biochem. J. **289**: 125-131.

Mumby, S.M., Heukeroth, R.O., Gordon, J.I. and Gilman, A.G. (1990). Proc. Natl. Acad. Sci. U.S.A. **87**: 728-732.

Nahorski, S.R. and Potter, B.V.L. (1989). TiPS. **10**: 139-144.

Nahorski, S.R., Ragan, I. and Challiss, R.A. (1991). TiPS. **12**: 297-303.

Neer, E.J., Echeverria, D. and Knox, S. (1980). J. Biol. Chem. **255**: 9782-9789.

Nelson, C.A. and Seamon, K.B. (1985). FEBS Lett. **183**: 349-352.

Neve, K.A., Cox, B.A., Henningsen, R.A., Spanoyannis, A. and Neve, R.L. (1991). Mol. Pharmacol. **39**: 733-739.

Nishizuka, Y. (1992). Science. **258**: 607-614.

Northup, J.K., Smigel, M.D. and Gilman, A.G. (1982). J. Biol. Chem. **257**: 11416-11423.

Nunn, D.L. and Taylor, C.W. (1992). Mol. Pharmacol. **41**: 115-119.

Okayama, H. and Berg, P. (1983). Mol. Cell. Biol. **3**: 280-289.

Olianas, M.R. and Onali, P. (1990). J. Neurochem. **55**: 1083-1086.

Parenti, M., Vigano, M.A., Newman, C.M.H., Milligan, G. and Magee, A. (1993). Biochem. J. **291**: 349-353.

Park, D., Jhon, D-Y., Lee, C-W., Lee, K-H. and Rhee, S.G. (1993). J. Biol. Chem. **268**(7): 4573-4576.

Park, D., Jhon, D-Y., Kriz, R., Knopf, J. and Rhee, S.G. (1992). J. Biol. Chem. **267(33)**: 16048-16055.

Parker, E.M., Kameyama, K., Higashijima, T. and Ross, E.M. (1991). J. Biol. Chem. **266**:

519-527.

Parker, I. and Ivorra, I. (1990). Science. **250**: 977-979.

Parker, I. and Yao, Y. (1991). Proc. R. Soc. Lond. **B246**: 269-274.

Paulssen, R.H., Paulssen, E.J., Gautvik, K.M. and Gordeladze, J.O. (1992). Eur. J. Biochem. **204**: 413-418.

Pedder, E.K., Eveleigh, P., Poyner, D., Hulme, E.C. and Birdsall, N.J.M. (1991). Br. J. Pharmacol. **103**: 1561-1567.

Peralta, E.G., Ashkenazi, A., Winslow, J.W., Smith, D., Ramachandran, J. and Capon, D.J. (1987a). EMBO. J. **6**: 3923-3929.

Peralta, E.G., Winslow, J.W., Peterson, G., Smith, D.H., Ashkenazi, A., Ramachandran, J., Schimerlik, M. and Capon, D.J. (1987b). Science. **236**: 600-605.

Peralta, E.G., Ashkenazi, A., Winslow, J.W., Ramachandran, J. and Capon, D.J. (1988). Nature. **334**: 434-437.

Peterson, J.W., Reitmeyer, J.C., Jackson, C.A. and Ansari, G.A.S. (1991). Biochim. et Biophys. Acta. **1092**: 79-84.

Pietri, F., Hilly, M. and Mauger, J-P. (1990). J. Biol. Chem. **265**: 17478-17485.

Premont, R.J., Chen, J., Ma, H-W., Ponnapalli, M. and Iyengar, R. (1992). Proc. Natl. Acad. Sci. USA. **89**: 9808-9813.

Putney, J.W.Jnr. (1986). Cell Calcium. **7**: 1-12.

Putney, J.W.Jnr. and Bird, G.S T.J. (1993). Endocrine Reviews. **14(5)**: 610-631.

Raymond, J.R., Albers, F.J. and Middleton, J.P. (1992). Naunyn Schmiedeberg's Arch. Pharmacol. **346**: 127-137.

Regunathan, S., Meeley, M.P. and Reis, D.J. (1990). Life. Sci. **47**: 2127-2133.

Reisine, T., Zhang, Y.L. and Sekura, R. (1985). J. Pharm. Exp. Thera. **232**: 275-282.

Renard-Rooney, D.C., Hajnoczky, G., Seitz, M.B., Schneider, T.G. and Thomas, A.P. (1993). J. Biol. Chem. **268**: 23601-23610.

Rhee, S.G. and Choi, K.D. (1992). J. Biol. Chem. **267**: 12393-12396.

Rhee, S.G., Suh, P.G., Ryu, S.H. and Lee, S.Y. (1989). Science. **244**: 546-550.

Richards, M. (1991). Biochem. Pharmac. **42(9)**: 1645-1653.

Rodbell, M., Birnbaumer, L., Pohl, S.L. and Krans, H.M.J. (1971). J. Biol. Chem. **246**: 1877-1992.

Rodbell, M., Krans, H.M.M., Pohl, S.L. and Birnbaumer, L. (1971), J. Biol. Chem. **246**: 1872-1876.

Ross, C.A., Danoff, S.K., Schell, M.J., Snyder, S.H. and Ullrich, A. (1992). Proc. Natl. Acad. Sci. USA. **89**: 4265-4269.

Ross, R.A. and Biedler, J.L. (1985). Cancer. Res. **45**: 1628-1632.

Ross, E.M. and Berstein, G. (1993). Life Sciences. **52**: 413-419.

Ross, E.M. and Gilman, A.G. (1977). J. Biol. Chem. **252**: 6966-6969.

Ryu, S.H., Kim, U.H., Wahl, M.I., Brown, A.B., Carpenter, G., Huang, K-P. and Rhee, S.G. (1990). J. Biol. Chem. **265**: 17941-17945.

Safrany, S.T. and Nahorski, S.R. (1994). Neuropharmacology (in press).

Samama, P., Cotecchia, S., Costa, T. and Leftkowitz, R.J. (1993). J. Biol. Chem. **268**: 4625-4636.

Sambrook, J., Fritsch, E.F. and Maniatis, T. (1989). Molecular Cloning, A Laboratory Manual. 2nd edition. ed. Nolan, C. pp: 16.33-16.38.

Scatchard, G. (1949). Ann. N. Y. Acad. Sci. **51**: 660.

Schutz, W. and Freissmuth, M. (1992). TiPS. 13: 376-380.

Schwarz, R.D., Davis, R.E., Jaen, J.C., Spencer, C.J., Tecle, H. and Thomas, A.J. (1993). Life Sciences. **52**: 465-472.

Seamon, K.B. and Daly, J.W. (1985). Adv. Cyc. Nuc. Res. **19**: 125-135.

Seamon, K.B. and Daly, J.W. (1986). Adv. Cyc. Nuc. Res. **20**: 1-152.

Seamon, K.B., Padgett, W. and Daly, J.W. (1981). Proc. Natl. Acad. Sci. USA. **78**: 3363-3367.

Seamon, K.B. and Wetzel, B. (1984). Adv. Cyc. Nuc. Res. **17**: 91-99.

Serra, M., Mei, L., Roeske, W.R., Lui, G.K., Watson, M. and Yamamura, H.I. (1988). J. Neurochem. **50**: 1513-1521.

Shears, S.B. (1991). Pharmac. Ther. **49**: 79-104.

Shiozaki, K. and Haga, T. (1992). Biochemistry. **31**: 10634-10642.

Simon, M.I., Strathmann, M.P. and Gautum, N. (1991). Science. **252**: 802-808.

Smrcka, A.V., Hepler, J.R., Brown, K.O. and Sternweis, P.C. (1991). Science. **251**: 804-807.

Spat, A., Bradford, P.G., McKinney, J.S., Rubin, R.P. and Putney, J.W. Jnr. (1986). Nature. **319**: 514-516.

Spiegal, A.M., Backlund, P.S.Jr., Butrynski, J.E., Jones, T.L.Z. and Simonds, W.F. (1991). TiBS. **16**: 338-341.

Strader, C.D., Sigal, I.S., Candelore, M.R., Rands, E., Hill, W.S. and Dixon, R.A.F. (1988). J. Biol. Chem. **263**: 10267-10271.

Strader, C.D., Sigal, I.S. and Dixon, R.A.F. (1989). FASEB J. **3**: 1825-1832.

Streb, H., Irvine, R.F., Berridge, M.J. and Schulz, I. (1983). Nature. **306**: 67-69.

Sternweis, P.C., Northup, J.K., Smigel, M.D. and Gilman, A.G. (1981). J. Biol. Chem.

256: 11517-11526.

Sternweis, P.C. and Smrcka, A.V. (1992). TiBS. 17: 502-506.

Stryer, L., Hurley, J.B. and Fung, B.K. (1981). Curr. Top. Membr. Transp. 15: 93-108.

Sudhof, T.C., Newton, C.L., Archer III, B.T., Ushkaryov, Y.A. and Mignery, G.A. (1991). EMBO J. 10: 3199-3206.

Suidan, H.S., Murrel, R.D. and Tolkovsky, A.M. (1991). Cell. Regul. 2:13-25.

Supattapone, S., Danoff, S.K., Theibert, A., Joseph, S.K., Steiner, J. and Snyder, S.H. (1988). Proc. Natl. Acad. Sci. USA. 85: 8747-8750.

Supattapone, S., Worley, P.F., Baraban, J.M. and Snyder, S.H. (1988). J. Biol. Chem. 263: 1530-1534.

Takemura, H., Hughes, A.R., Thastrup, O. and Putney, Jr.J.W. (1989). J. Biol. Chem. 264: 12266-12271.

Tang, W-J., Krupinski, J. and Gilman, A.G. (1991). J. Biol. Chem. 266: 8595-8603.

Tang, W.J. and Gilman, A.G. (1991). Science. 254: 1500-1503.

Tang, W-J. and Gilman, A.G. (1992). Cell. 70: 869-872.

Taussig, R., Iniguez-Lluhi, J.A. and Gilman, A.G. (1993). Science. 261: 218-221.

Taylor, C.W. (1990). Biochem. J. 272: 1-13.

Taylor, S.J., Chae, H.Z., Rhee, S.G. and Exton, J.H. (1991). Nature. 350: 516-518.

Taylor, C. and Potter, B.V.L. (1990). Biochem. J. 266: 189-194.

Taylor, C.W. (1992). Putney, Jr.J.W. (ed). Inositol Polyphosphates and Calcium Signalling: Advances in Second Messenger and Phosphoprotein Research. Raven Press, New York. 26: 109-142.

Tobin, A.B., Lambert, D.G. and Nahorski, S.R. (1992). Mol. Pharmacol. 42: 1042-1048.

Tobin, A.B. and Nahorski, S.R. (1993). J. Biol. Chem. **268**: 9817-9823.

Tobin, A.B., Keys, B. and Nahorski, S.R. (1993). FEBS Lett. **335**: 353-357.

Tota, M.R. and Schimerlik, M.I. (1990). Mol. Pharmacol. 7: 996-1004.

Tsien, R.Y. (1989). Annu. Rev. Neurosci. **12**: 227-253.

Varrault, A., Journot, L., Audigier, Y. and Bockaert, J. (1992). Mol. Pharmacol. **41**: 999-1007.

Venter, J.C., di Porzio, U., Robinson, D.A., Shreeve, S.M., Lai, J., Kerlavage, A.R., Fracek, S.P.Jr., Lentes, K-U. and Fraser, C.M. (1988). Prog. Neurobiol. **30**: 105-169.

Vickroy, T.W., Yamamura, H.I. and Roeske, W.R. (1983). Biochem. Biophys. Res. Commun. **116**: 284-290.

Vilaro, M.T., Palacios, J.M. and Mengod, G. (1990). Neurosci. Lett. **114**: 154-159.

Vilaro, M.T., Wielderhold, K.H., Palacios, J.M. and Mengod, G. (1991). Neuroscience. **40**: 159-167.

Volpe, P., Krause, K-H., Hashimoto, S., Zorzato, F., Pozzan, T., Meldolesi, J. and Lew, D.P. (1988). Proc. Natl. Acad. Sci. USA. **85**: 1091-1095.

Waelbreck, M., Robberecht, P., Chatelain, P. and Christophe, J. (1982). Mol. Pharmacol. **21**: 581-588.

Waelbroeck, M., Tastenoy, M., Camus, J. and Christophe, J. (1990). Mol. Pharmacol. **38**: 267-273.

Wakamatsu, K., Higashijima, T., Fujino, M., Nakajima, T. and Miyazawa, T. (1983). FEBS Lett. **162**: 123-126.

Wall, S.J., Yasuda, R.P., Li, M. and Wolfe, B.B. (1991). Mol. Pharmacol. **40**: 783-789.

Wang, C-D., Buck, M.A. and Fraser, C.M. (1991). Mol. Pharmacol. **40**: 168-179.

Watras, J., Bezprozvanny, I. and Ehrlich, B.E. (1991). J. Neurosci. **11**: 3239-3245.

Watson, E.L., Singh, J.C., McPhee, C., Beavo, J. and Jacobson, K.L. (1990). Mol. Pharmacol. **38**: 547-553.

Watson, M., Yamamura, H.I. and Roeske, W.R. (1986). J. Pharm. Exp. Thera. **237**: 411-418.

Wei, J.W. and Sulakhe, P.V. (1980). Eur. J. Pharmacol. **62**: 345-347.

Weiner, D.M., Levey, A.I. and Brann, M.R. (1990). Proc. Natl. Acad. Sci. USA. **87**: 7050-7054.

Wess, J. (1993). TiPS. **14**: 308-313.

Wess, J., Bonner, T.I. and Brann, M.R. (1990b) Mol. Pharmacol. **38**: 872-877.

Wess, J., Bonner, T.I., Dorje, F. and Brann, M.R. (1990a). Mol. Pharmacol. **38**: 517-523.

Wess, J., Brann, M.R. and Bonner, T.I. (1989). FEBS Lett. **258**: 133-136.

Wess, J., Gdula, D. and Brann, M.R. (1991b). EMBO J. **10**: 3729-2734.

Wess, J., Lambrecht, G., Mutschler, E., Brann, M.R. and Dorje, F. (1991a). Br. J. Pharmacol. **102**: 246-250.

Wess, J., Nanavati, S., Vogel, Z. and Maggio, R. (1993). EMBO J. **12**: 331-338.

West, R.E., Moss, J., Vaughan, M., Liu, T. and Liu, T.Y. (1985). J. Biol. Chem. **260**: 14428-14430.

Wheeler, G.L. and Bitensky, M.W. (1977). Proc. Natl. Acad. Sci. U.S.A. **74**: 4238-4242.

White, M.F. and Kahn, C.R. (1994). J. Biol. Chem. **269**: 1-4.

Whiteway, M., Hougan, L., Dignard, D., Thomas, D.Y., Bell, L., Saari, G.C., Grant, F.J., O'Hara, P. and MacKay, V.L. (1989). Cell. **56**: 467-477.

Whitham, E.M., Challiss, R.A.J. and Nahorski, S.R. (1991). Eur. J. Pharm.- Mol. Pharm.

Sec. **206**: 181-189.

Wieland, T., Kreiss, J., Gierschik, P. and Jacobs, K.H. (1992). Eur. J. Biochem. **205**: 1201-1206.

Wilcox, R.A., Challiss, R.A.J., Baudin, G., Vasella, A., Potter, B.V.L. and Nahorski, S.R. (1993). Biochem. J. **294**: 191-194.

Willcocks, A.L., Cooke, A.M., Potter, B.V.L. and Nahorski, S.R. (1987). Biochem. Biophys. Res. Commun. **146**: 1071.

Wojcikiewicz, R.J.H., Nakade, S., Mikoshiba, K. and Nahorski, S.R. (1992). J. Neurochem. **59**: 383.

Wojcikiewicz, R.J.H., Safrany, S.T., Challiss, R.A.J., Strupish, J. and Nahorski, S.R. (1990a). Biochem. J. **272**: 269-272.

Wojcikiewicz, R.J.H., Lambert, D.G. and Nahorski, S.R. (1990b). J. Neurochem. **54**: 676-685.

Wojcikiewicz, R.J.H., Tobin, A.B. and Nahorski, S.R. (1993). TiPS. **14**: 279-285.

Wojcikiewicz, R.J.H. and Nahorski, S.R. (1993). J. Exp. Biol. **184**: 145-159.

Wojcikiewicz, R.H., Tobin, A.B. and Nahorski, S.R. (1994). J. Neurochem. (in press).

Wong, Y.H., Conklin, B.R. and Bourne, H.R. (1992). Science. **255**: 334-342.

Wong, Y.H., Federman, A., Pace, A.M. Zachary, I., Evans, T., Pouyssegur, J. and Bourne, H.R. (1991). Nature. **351**: 63-65.

Wu, D., Katz, A. and Simon, M.I. (1993). Proc. Natl. Acad. Sci. U.S.A. **90**: 5297-5301.

Wu, D., Lee, C.H., Rhee, S.G. and Simon, M.I. (1992). J. Biol. Chem. **267(3)**: 1811-1817.

Yatini, A., Codina, J., Imoto, Y., Reeves, J.P., Birnbaumer, L. and Brown, A.M. (1987). Science. **238**: 1288-1292.